The Mathematics of Ship Slamming

by

Stephen Kenneth Wilson

St. Peter's College, Oxford.

Thesis submitted for the Degree
of Doctor of Philosophy at the
University of Oxford.

Trinity Term 1989

The Mathematics of Ship Slamming

Stephen K. Wilson
St. Peter's College, Oxford.
D. Phil. Thesis, Trinity Term 1989.

Abstract

Motivated by the motion of a ship in a heavy sea, a mathematical model for the vertical impact of a two-dimensional solid body onto a half-space of quiescent, inviscid, incompressible fluid is formulated. No solutions to the full problem are known, but in the case when the impacting body has small *deadrise angle* (meaning that the angle between the tangent to the profile and the horizontal is everywhere small) a uniformly valid solution is obtained by using the method of matched asymptotic expansions. The pressure on the body is calculated and is in fair agreement with experimental results. The model is generalised for more complicated impacts and the justifications for the model are discussed.

The method is extended to three-dimensional bodies with small deadrise angle and solutions are obtained in some special cases. A variational formulation of the leading order outer problem is derived, which gives information about the solution and leads to an fixed domain scheme for calculating solutions numerically. A partial linear stability analysis of the outer problem is given which indicates that entry problems are stable but exit problems are unstable to small perturbations.

A mathematical model for the effect of a cushioning air layer between the body and the fluid is presented and analysed both numerically and in appropriate asymptotic limits.

Finally, the limitations of the models are discussed and directions for future work indicated.

Acknowledgements

This work would not have been possible without the advice and encouragement of my supervisor Dr. J.R. Ockendon over the last two years. I would also like to thank Dr. S.D. Howison and Dr. J.N. Dewynne for their invaluable assistance.

I am indebted to Dr. D.W. Chalmers of the Admiralty Procurement Executive, Foxhill, Bath for bringing the problem to Oxford and to Mr. J.D. Clarke of the Admiralty Procurement Executive, St. Leonard's Hill, Dunfermline for acting as my industrial supervisor.

Special thanks to my colleagues Jonathan Evans, Ken Louie, Louise Terrill, Steve Williams and Bruce van-Brunt for all the help and encouragement they have given me.

I am also very grateful to Dr. M. Greenhow of Imperial College for helping me locate some of the more obscure papers on ship slamming, and for providing the photograph in Chapter 1.

The financial support of the Science and Engineering Research Council and the Admiralty Procurement Executive, through the C.A.S.E. scheme, and St. Peter's College, Oxford, in the form of a Graduate Award, is gratefully acknowledged.

To Ruth, Kenneth and Rachel.

Contents

List of Figures

Chapter 1

Introduction

1.1 Ship Slamming

A ship travelling in a heavy sea experiences a continuous buffeting from the waves, which can cause violent motions of the hull. For certain combinations of ship speed, course, loading and sea state, the bows can leave the waves and impact back onto the water, generating large pressures on the hull. This phenomenon is known as *ship slamming*, and is the motivation for the research in this thesis. The transient loading experienced during a slam can cause localised damage to the plates of the hull near the keel. Not only are these plates expensive to repair, but sensitive devices such as sonar domes are often located on the keel and are especially vulnerable to damage. A more serious problem is the whipping vibration of the hull that is excited by the transient impact force, which causes a characteristic shudder throughout the ship. The resulting stresses can be larger than those induced by the waves, and dramatically reduce the fatigue life of the hull. In extreme cases they have even caused hulls to fracture. In order to reduce the damage to the ship (and discomfort to the occupants) caused by slamming, the Master is usually compelled to slow the vessel down. Indeed, in heavy seas this is the primary reason for speed reduction for ships of frigate and destroyer size.

Slamming first came to the attention of naval architects more than fifty years ago with the introduction of the diesel engine. Recently, interest in the subject has been revived by the advent of new types of vessels, such a hydrofoils and Small Waterplane Area Twin Hull (S.W.A.T.H.) ships, for which the traditional

theoretical and empirical methods for predicting the occurrence of slamming and the resulting fluid loadings are inappropriate.

1.2 The Background of the Problem

The ship slamming problem was first brought to the Oxford Applied Mathematics Group by Dr. D.W. Chalmers from the Admiralty Procurement Executive in Bath, and was discussed during the 1986 Oxford Study Group with Industry. Following the interest in the problem expressed at this meeting, the author wrote an M.Sc. dissertation concerning a simple model for the response of a ship hull to transient loading, and the problem became the subject of a C.A.S.E. studentship. The award was funded jointly by S.E.R.C. and the Admiralty Procurement Executive in Dunfermline through Mr. J.D. Clarke, and began in October 1987.

1.3 Aim and Structure of Thesis

The aim of this thesis is to formulate and analyse mathematical models for solid-fluid impact problems which are relevant to ship slamming. The chief theoretical aims are to identify the important physical effects and predict the pressure distribution on an impacting body.

The remainder of Chapter 1 consists of a review of the mathematical literature about fluid entry problems. The majority of the papers discuss approximate methods of varying rigour and usefulness, but there are also a number of analytical and numerical results concerning the full nonlinear free boundary problem.

Chapter 2 concerns the vertical entry at constant velocity of a two-dimensional rigid body into a half-space of quiescent, inviscid, incompressible fluid. In the case when the body has small deadrise angle (i.e. when angle made between the tangent to the profile of the body and the horizontal is small), we show that the flow field can be analysed in three distinct regions. In each region we seek solutions in the form of asymptotic series in the deadrise angle and derive the appropriate leading order problem. Using the method of matched asymptotic expansions the unknown parameters are determined by matching the solutions appropriately, and the uniformly valid composite pressure is constructed. The

model is generalised to include the effects of variable impact velocity, surface tension and gravity. Solutions are obtained for a number of simple body shapes, and the theoretically predicted pressure distributions are found to be in fair agreement with experimental observations.

In Chapter 3 the approach of the previous chapter is extended to three-dimensional bodies with small deadrise angle. Less analytical progress is possible, but solutions are obtained in a number of special cases. A variational formulation of the leading order outer problem is derived, which leads to a 'fixed domain' numerical scheme for computing solutions. Simple finite element programs which implement the scheme in two and in three dimensions are described.

Chapter 4 contains a local linear stability analysis of the outer problem, and the results lead to a discussion of the fundamental differences between entry and exit problems.

The major discrepancy between the theoretically predicted pressures and experimental observations on the keel is due to the presence of a cushioning air layer between the body and the fluid, an effect which reduces the large pressures generated in the initial stages of an impact. In Chapter 5 a coupled model for the flow in the air and the fluid before the body reaches the fluid is formulated. The leading order problem is examined in various asymptotic limits, and numerical solutions obtained which predict the formation of an air pocket between the body and the fluid.

Finally, in Chapter 6 conclusions are drawn from the work presented and directions for future work are indicated.

1.4 Review of Previous Work

The literature concerning ship slamming reviewed in this section consists of three basic kinds; theoretical papers about idealised solid-fluid impact problems, those which report the results of experiments, and those that try to make predictions about the effect of slamming on real ships, their cargoes and their crews.

1.4.1 Fluid Impact Problems

The large body of literature about fluid impact problems falls into two broad categories, viz. solely mathematical papers and those which attempt to combine approximate theories with experimental results. Those in the first group concentrate on exact mathematical analysis of the simplest impact problems. The subject of most of those in the much larger second group is a variety of approximate and asymptotic theories, of varying complexity, rigour and usefulness, and their comparison with experimental data.

Numerical and Analytical Studies of the Full Problem

(a) The Wedge Entry Problem

Mathematically, the simplest fluid impact problem is that of an infinite two-dimensional *wedge*, with opening angle 2α, entering a half-space of quiescent, inviscid, incompressible fluid. This situation is called the *wedge entry problem* and is summarised in Figure (1.1). Since, in the absence of gravity and surface tension, there is no length scale in the problem, the solution is *self-similar* and the number of independent variables can be reduced from three, viz. x, y and t, to two by introducing the similarity variables X and Y defined by $X = x/Vt$ and $Y = y/Vt$. As a result of this simplification most of the analytical and numerical studies have concentrated on the wedge entry problem. Although several authors have studied this problem, no closed form solutions are known, and no existence/uniqueness theory has been developed.

As in classical jet theory, substantial progress has been made by employing complex variable techniques, beginning with the pioneering paper by Wagner (1932). In a footnote to this paper the author introduced the so-called *Wagner function*, $h(z)$, defined by

$$h(z) = \int_{\infty}^{z} \sqrt{w''(\zeta)}\, \mathrm{d}\zeta$$

where $z = X + iY$, $\zeta = \xi + i\eta$ and $w(\zeta)$ is the complex potential. Subsequently, a number of workers have corrected a mistake in Wagner's work which prevented him from exploiting the properties of this function, and have shown that it maps

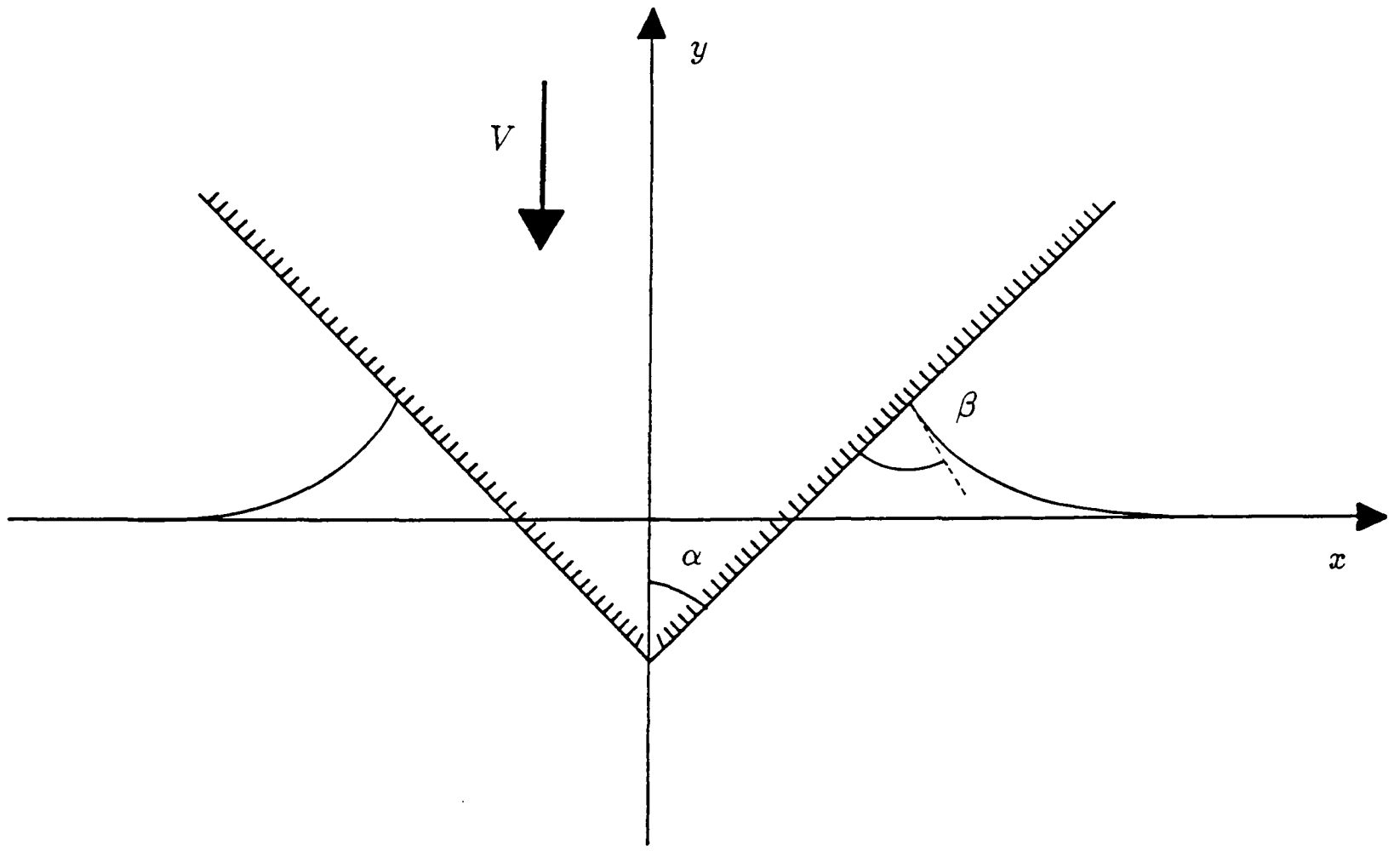

Figure 1.1: Wedge entry geometry.

the unknown fluid domain to a finite region in the h-plane bounded by straight lines.

Wagner (1932) also showed that the arc length measured along the free surface between any two fluid particles remains constant throughout the motion, and this was subsequently confirmed by Garabedian (1953) using complex variable methods. A direct proof of this property is given in Appendix A. Garabedian (1965) used the properties of the Wagner function to obtain bounds on the contact angle made between the free surface and the solid boundary, β. Under the assumption that the free boundary was convex, he showed that

$$0 < \beta < \frac{\pi}{4}.$$

Mackie (1969) proved that if the pressure on the wedge face was greater than or equal to atmospheric pressure, then the free boundary must be convex, and under this assumption improved the bounds on the contact angle by showing that

$$0 < \beta < \frac{\pi}{2} - \alpha.$$

Figure 1.2: Pressure distribution along the wedge face for different values of the half-angle α, reproduced from Dobrovol'skaya (1969). The vertical scale of the dashed curve is one quarter of that of the solid curves.

Dobrovol'skaya (1969) used the Wagner function to reduce the wedge entry problem to a non-linear singular integral equation, whose solution she computed. Her numerical calculations of the pressure on the wedge face are reproduced here in Figure (1.2), and for small opening angles are in agreement with the linearized theory of Mackie (1962). The largest half-angle she computed was $\alpha = \pi/3$, and in this case she found a large pressure maximum some distance up the wedge face above the undisturbed waterline. By performing a local analysis around the three phase contact line, Tayler (1972) reproduced Mackie's bounds on the contact angle without using complex variable methods.

Hughes (1972) developed an unusual quasi-analytical numerical method, which exploited the properties of the Wagner function and combined numerical conformal mapping with a local analysis of the singular points in the flow. Some errors in Dobrovol'skaya's (1969) calculations were pointed out, and good agreement obtained with Wagner's (1932) approximate expression for the total force for wedge in the case $\alpha = \pi/4$.

The first Lagrangian formulation of the wedge entry problem was performed by Johnstone & Mackie (1973), who neatly established the convexity of the free surface and derived an explicit formula for the contact angle. Unfortunately, their analysis depended on the invalid assumption of continuity of fluid velocity at the wedge tip, and this explains why the predicted contact angle violated Mackie's (1969) upper bound.

Greenhow (1987) reviewed some of the work on wedge impact problems, and compared a number of approximate theories with the results of his own numerical calculations, made using a boundary integral method. Particular difficulty was experienced in resolving the flow in the thin, fast-moving jet of fluid that forms close to the body, and in consequence he was unable to perform calculations for wedges with half-angle larger than about $\pi/4$. Worse, even in the absence of gravity the jet was observed to separate from the wedge, in violation of the self-similarity property. Some more complicated problems were also studied, including those of variable impact velocity, oblique entry and complete submergence of finite wedges. Yim (1986) encountered similar difficulties resolving the jet in his numerical calculations. Taking atmospheric pressure to be zero, he observed that for convex pointed bodies the pressure due to the jet was always positive and that for convex bodies it was negative, indicating that in the latter case the jet might separate from the body. In a recent paper Greenhow (1988) applied the same numerical approach as that in his earlier paper to the entry of a circular cylinder, and obtained a wide variety of free surface flows, including jet formation and cavity formation behind a fully submerged body.

(b) The Cone Entry Problem

The simplest three-dimensional impact problem is that of a semi-infinite cone entering a half-space of quiescent, inviscid, incompressible fluid. In the absence of gravity and surface tension the problem is again self-similar, but complex variable methods can no longer be used, and as a consequence less progress has been made. Tayler (1972) performed a local analysis in the region of the jet tip and showed that, in contrast the wedge entry problem, the contact angle must be zero. The Lagrangian formulation due to Johnstone & Mackie (1973) extended

easily to three-dimensions and, although unable to obtain an explicit formula for the free surface, they reproduced Tayler's (1972) result that the contact angle must be zero.

Approximate and Asymptotic Theories

(a) Incompressible Fluid Models

The earliest work was motivated not by an interest in ships, but by the desire to predict the force on the floats of a landing sea-plane. The pioneering papers were written independently by T. Von Kármán in 1929 and by H. Wagner in 1931 and 1932. Both authors propose approximate theories for simple solid-fluid impact problems based largely on intuition. Essentially, Von Kármán's approach consists of replacing the impacting body with a flat plate whose width is equal to the body cross-section at the instantaneous waterline, and neglecting the deformation of the free surface. An expression for the force is then obtained by equating the momentum of the fluid to the momentum of the plate, set instantaneously into motion normal to the undisturbed fluid surface with the impact velocity.

Wagner's approach is more sophisticated, and more closely resembles the present work. The body is again approximated by a flat plate, whose width is now determined by obtaining an approximate expression for the free surface rise around the body and requiring that it meets the body at the point corresponding to edge of the plate. The resulting pressure distribution on the plate can be integrated to give an expression for the force, but has physically unacceptable singularities at the edges of the plate. Wagner (1932) realised that to correct this singularity a new problem would have to be formulated in this region, corresponding to the spray root where the free surface turns over to form a jet, and suggested the form it should have. However, since his work pre-dates the development of the techniques of matched asymptotic expansions, his ideas lacked a formal basis and he was unable to determine the size of this region. Furthermore, he neglected the effect of the thin, fast-moving jet that forms close to the body, implicitly assuming it to be of low pressure compared to that in the main part of the flow. Both these approaches are valid only when the body has small deadrise angle, defined as the angle made between the tangent to the

body and the horizontal, but various ad hoc attempts have been made to modify them for bodies with large deadrise angles. Some of these are listed by Pierson (1951). For example, Pabst (1931) added an 'aspect ratio' correction, Mayo (1943) multiplied Wagner's result by an empirical factor of 0.82 in order improve the agreement with some experimental data, and Kreps (1943) added a 'fluid dynamic' resistance.

Pierson (1950) employed an unusual graphical method to obtain approximate solutions for the entry of a wedge with arbitrary deadrise angle. By insisting that the free surface satisfy conditions of continuity of flow, dynamic similarity and irrotationality he derived an iterative scheme for calculating the free surface shape, and hence the velocity and pressure everywhere. By measuring the thickness of the jet he then calculated the force in the region of the spray root suggested by Wagner (1932) and found it to be in reasonable agreement with his own direct calculations.

Schmieden (1953) extended Wagner's flat plate analogy to rotationally symmetric bodies by approximating the body by an equivalent disc, whose radius had to be determined.

A widely employed method of extending the early flat plate theories is that of approximating the flow by that around a simpler shape, chosen in some way to be 'equivalent' to the impacting body. Shiffman & Spencer (1953) derived an approximate theory for the impact of a cone by 'fitting' an ellipse, whose dimensions were determined by equating the depth of penetration and accounting for the free surface rise in the same way as Wagner (1932). Fabula (1957) compared ellipse fitting with the alternative approach of approximating the flow by the flow around a diamond-shaped body, like described by Ferdinande (1966). Perhaps surprisingly, he found the former to be in closer agreement with experiment, and he attributed this to the fortunate accident of a more accurate representation of the singularity in the region of the spray root.

Borg (1959) considered the impact of a wedge with small deadrise angle and, by using a crude geometrical construction of the jet, was led to approximating the body by a flat plate of width 1.5 times that of the cross-section at the instantaneous waterline. His analysis also gave approximate values of the value

of pressure at the vertex and the pressure maximum in the region of the spray root.

Fraenkel (1958) addressed the problem of the impact of a slender cone and obtained solutions to a linearized problem for $\alpha \ll 1$, representing the flow around the submerged portion of the body. He took into account the discontinuous slope of the reflected body, but the linearization of the free surface condition was invalid in a region of width $O(e^{-1/\alpha})$ near the body. Mackie (1962) adopted a similar approach for slender wedges and cones, and derived and solved the appropriate linearized problem, from which he obtained an explicit formula for the shape of the free surface. A similar approach, closely related to the distribution of singularities in aerofoil theory was taken by Moran (1961), who obtained approximate solutions to a linearized entry or exit problem for slender bodies. Recently Gonor (1986) has corrected the weak singularity at the wedge tip to obtain a solution valid everywhere away from the contact points.

Cumberbatch (1960) tackled the related impact problem of a wedge of fluid striking a rigid wall by numerically patching together solutions valid near to and far from the wall, and was able to give estimates of the free surface shape and the force on the wall.

Payne (1981) extended Von Kármán's (1929) flat plate theory and added mass calculations by calculating the added mass associated with the immersed portion of an impacting wedge, and found fair agreement between his predictions and some experiments made using wedges with small deadrise angles.

Most of the recent developments in fluid impact problems have been made by Russian researchers. Pukhnachov (1979) formulated the impact problem in Lagrangian coordinates and, when the impacting body is blunt, derived a linearized problem based on the assumption of small fluid displacement. Pukhnachov & Korobkin (1981), Korobkin & Pukhnachov (1985) and Korobkin (1985) extended this approach to three-dimensional bodies with elliptical cross-section. In the case of the impact of a two-dimensional parabolic body they derived an inner expansion to correct the singularity in the outer solution at the contact line. They employed time as their perturbation parameter and so their analysis applies is valid during the initial stages of the motion. Korobkin (1982) employed a

clever Baiocchi-type smoothing transformation to write the leading order outer problem as a variational inequality.

The modern paper closest in spirit to the present approach is that by Watanabe (1986), who sought to correct the singularity in Wagner's flat plate solution for bodies with small deadrise angle by considering an inner problem in the region of the spray root. His inner problem, however, represented the physically meaningless problem of an infinitely long planing flat plate, and expanding in the region of the stagnation point therefore gave the wrong local behaviour.

(b) Compressible Fluid Models

All of the incompressible impact theories predict an infinite pressure on a blunt body at the instant of impact which, of course, cannot occur. One possible neglected effect is that of the fluid compressibility, which is significant in the early stages of impact even when the Mach number, M, is small. Here M is defined to be V/c, where V is the impact velocity and c is the sound speed. The solution of the incompressible problem is evidently the leading term in the asymptotic expansion of the solution to the compressible problem in the limit $M \to 0$.

There are two characteristic stages of the impact onto a compressible fluid. First, there is a time interval, $0 < t < t^*$, during which the boundary of the solid-fluid contact region is expanding supersonically, and the region of disturbed fluid is bounded by a shock attached to the body and to the contact line. Second, there is a subsonic phase, $t > t^*$, during which the shock moves away from the contact line.

Von Kármán (1929) considered the one-dimensional situation of the normal impact of a flat plate onto a compressible fluid and, by making an acoustic approximation in the fluid, found the pressure on the body at the instant of impact to be the so-called *water-hammer pressure* ρcV, where ρ is the density of the water.

During the supersonic stage, the contact region is known and Korobkin (1984) obtained the solution using an acoustic approximation, based on the assumption that the disturbance of the fluid is small, which reproduces Von Kármán's result

at $t = 0$. The approximation is invalid within a small vicinity of the contact points as $t \rightarrow t^{*-}$, and this problem has been addressed by Korobkin & Pukhnachov (1985), who showed that for a parabolic body the pressure at the contact point is $O(M^{-\frac{1}{2}})$ as $M \rightarrow 0$, $t \rightarrow t^{*-}$. During the subsonic phase the contact region is unknown, and the solution has only been obtained numerically.

A different approach to the problem was taken by Lesser (1981), who used a simplification based on geometrical acoustics, and obtained good agreement with earlier theoretical and experimental work.

Despite a large body of work, there is currently no well-developed theory for the fully compressible problem.

(c) Models Including a Cushioning Fluid

The pressures and total forces predicted by both compressible and incompressible theories are, in general, overestimates of the experimental observations. The most likely mechanism for reducing the actual pressure is that a pocket of air, which cushions the impact, is trapped between the body and the fluid surface. The geometry is shown in Figure (1.3) and a number of approximate theories have been developed to account for the presence of an air layer during fluid impact.

Verhagen (1967) used a simple one-dimensional model for the compressible flow of air in the narrowing gap between a flat plate and the fluid, which he solved numerically. Motivated by the well-known theory applying to the steady flow of compressible fluid in converging and diverging channels, he assumed that as the air velocity reached the local sound speed in the throat formed between the body and the rising water surface, the flow would choke, and thereafter that the local air speed would be equal to the sound speed. The flow in this new regime was then calculated until the instant the body first touched the water. Then a model for the trapped pocket of air, in which it was assumed that the air pressure was a function of time only, was used to predict the pressure on the body. Despite incorporating a number of crude approximations, and introducing an arbitrary smoothing factor into the pressure distribution, the calculations were shown to be a good agreement with a set of experimental measurements made using a light-weight model.

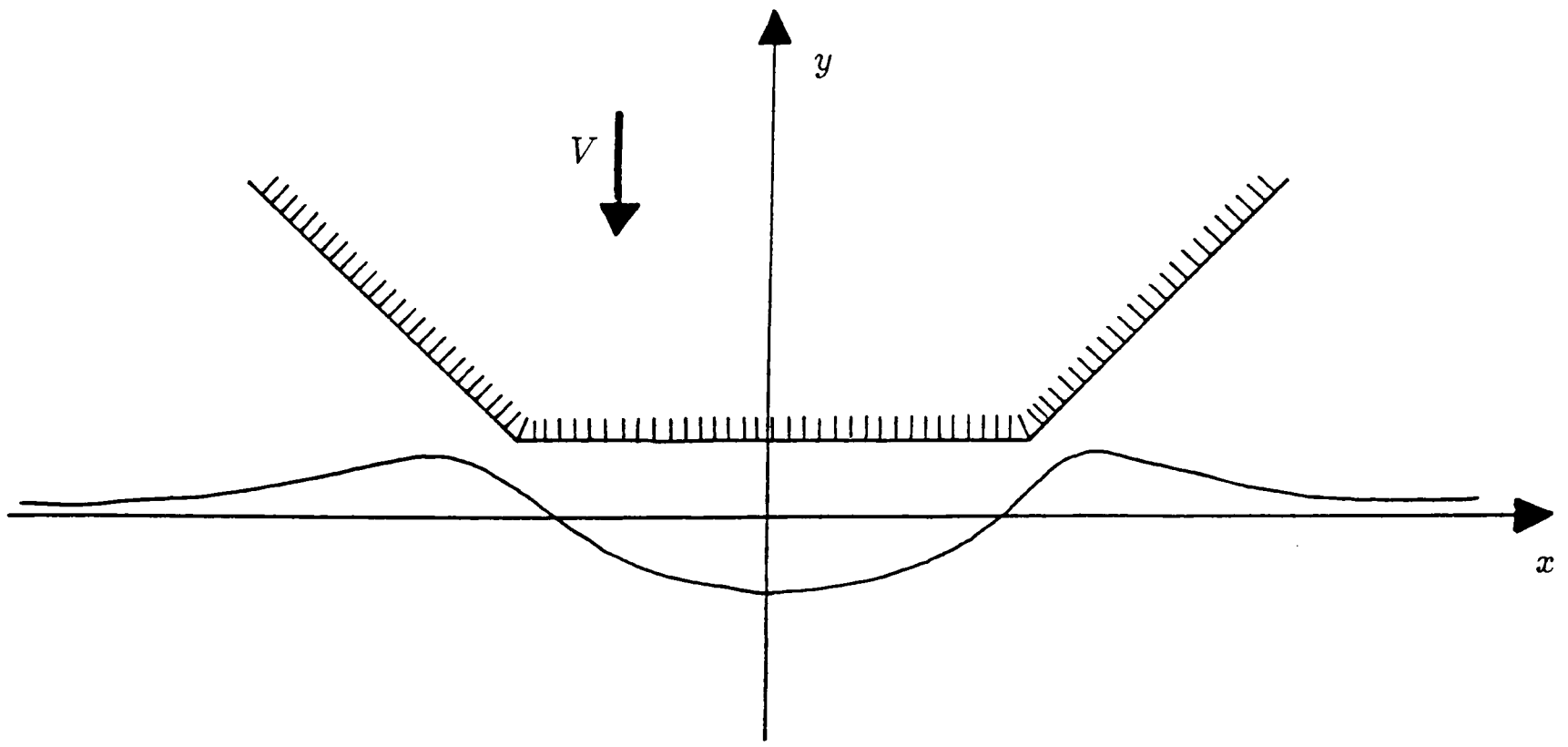

Figure 1.3: Air Cushioning Geometry.

Lewison & Maclean (1967) and Lewison (1970) reported an extensive series of drop tests of flat plates, and compared them with approximate numerical solutions to a one-dimensional model for the flow in the air which incorporated additional physical assumptions. The computed solutions were in qualitative agreement with the experiments, but displayed a marked sensitivity to the the choice of initial conditions and overestimated the pressures by roughly a factor of two. A series of experiments with ship models showed, unsurprisingly, that adding flanges to the keel to encourage air entrapment reduced the measured impact pressures.

Apparently working without reference to the earlier work, Asryan (1972) derived averaged equations for the flow of air beneath a plate, modelled first as an incompressible and then as a compressible fluid. Approximate solutions were obtained numerically and in both cases estimates for the time of first contact between the plate and the water were calculated.

(d) Review Papers

A number of review papers have appeared in the last fifty years. Among them Chu & Abramson (1961) discussed the various flat plate, diamond, circle and

ellipse fitting theories and compared them with experimental results. A broader ranging survey by Moran (1965) included sections on slender body theories and more complicated impact problems, including variable entry speed, water compressibility and the effect of a cushioning air layer. Recent developments are reviewed in Korobkin & Pukhnachov (1988), who placed particular emphasis on their Lagrangian formulation of the problem. This latter paper includes a number of valuable references to the work of other Russian authors, and incorporates sections on the impact of elastic shells and impact onto compressible fluids.

1.4.2 Experimental Papers

There is a large body of literature reporting experimental data from drop tests and full scale measurements, and many compare their findings with the various approximate theories outlined above.

Chuang (1967) described a series of drop tests performed with flat-bottomed and small deadrise wedges. His experiments indicated that only the flat body and 1^o deadrise wedge entrapped a significant quantity of air, and he derived a sequence of empirical correction factors to Wagner's (1932) simple flat plate theory to give better agreement with observations. Hagiwara & Yuhara (1974a,b) conducted experiments to measure the impact forces and resulting stress distributions in a number of one-third scale bow models. They too observed the effects of air-entrapment for angles of less than about 3^o, and were able to produce pressures roughly equal to the water hammer pressure for large impact velocities.

Results of experimental impacts made using a variety of different bodies and compressible fluids were reported by Eroshin *et al.* (1980). Figure (1.4) is reproduced from their paper, and shows that the dependence of the total force on the body on the Mach number in the fluid, M, is strongly influenced by the shape of the body. Whereas the force on a flat disc rises sharply as $M \rightarrow 0$, that on a cone with a semi-angle of 75^o is only weakly dependent on M, while that on a hemisphere is effectively independent of M.

Moghisi & Squire (1981) performed drop test experiments using a hemisphere and measured the resulting total force on the body, which they found to be proportional to the square root of the depth of immersion. Two typical force

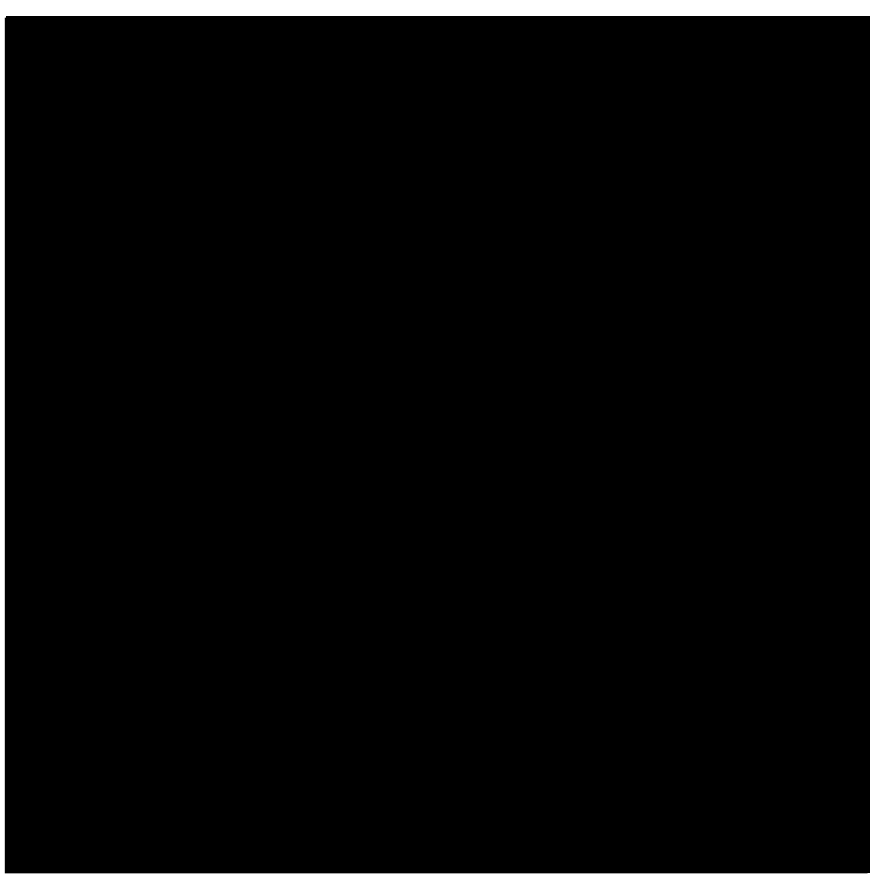

Figure 1.4: Maximum values of the force on (1) a disc, (2) a cone with half-angle $\alpha = 25°$, and (3) a hemisphere plotted as a function of the Mach number, M. Reproduced from Eroshin *et al.* (1980). S denotes the midsection area of the body.

Figure 1.5: Typical relations between drag force and time for a hemisphere. Reproduced from Moghisi & Squire (1981).

histories are shown in Figure (1.5).

Driscoll & Lloyd (1982) reported a series of drop tests using flat bottomed wedges of varying keel size and deadrise angle, and made measurements of the speed and magnitude of the maximum pressure pulse. First contact was usually made at the edge of the keel, and for larger keels a smaller secondary, inward travelling pressure pulse due to air entrapment was recorded.

Eroshin *et al.* (1984) reported a series of drop test experiments onto a compressible fluid using flat bodies in the presence of various types of cushioning fluid layers, and found them to be in good agreement with numerical solutions to a simple one-dimensional model.

Nethercote *et al.* (1986) conducted an extensive series of drop tests using representative hull sections and ship models and performed numerical calculations using a commercially available finite difference code. The numerical results were very noisy, and even after extensive smoothing were only approximately in agreement with the experimental results.

Greenhow (1987) included a number of photographs of small scale experiments, one of which is reproduced here in Figure (1.6). They clearly show jet separation does occur during wedge impacts, probably due to the effect of gravity.

1.4.3 Applications to Ship Loading and Dynamics

There are a large number of numerically and empirically based papers which seek to apply approximate predictions of impact pressures to realistic ship models, and hence make useful predictions about the resulting stresses set up in the hull, as well as the effect on the dynamics of the motion of a ship in a seaway. A full review is not attempted here but we should record that a series of papers combining an elastic beam model for the ship hull with empirical approximations for the impact force are due to Bishop with various co-workers, and are summarised in the recent paper by Belick, Bishop & Price (1987). A more mathematical presentation is given in Bishop, Price & Wu (1986), in which the ideas are extended to other floating structures. In both cases extensive finite element

Figure 1.6: High speed impact of a wedge with half-angle $\alpha = \pi/6$ into water. Photograph courtesy of Dr. M. Greenhow, Brunel University, London.

calculations are performed and a large number of empirical factors have to be estimated.

There are also a large group of research papers and technical reports detailing experimental and real life observations of sea trials, such those made on two frigates on rough weather by Bishop, Clarke & Price (1984). Recently attention has been focused on new types of vessel, and a recent paper by Graham (1988) reports a series on slamming trials made using a scale model of a SWATH destroyer.

Other authors seek to draw conclusions directly from the experimental data without using mathematics, or by employing the techniques of statistics and probabilistic modelling.

Chapter 2

Two-Dimensional Fluid Impact Problems

In this chapter, we consider the problem of a two-dimensional rigid body impacting onto an inviscid, incompressible fluid. When the body has small deadrise angle, the flow field decomposes into three regions. In the outer region, the problem is the normal impact of a flat plate of unknown width, whilst in the inner region, a free streamline problem is obtained. In the third region there is a thin, fast-moving jet close to the body. In each region we formulate and solve the leading order problem, and obtain the corresponding leading order pressure distribution on the body. We construct solutions for a number of simple body profiles, and consider the effect of additional physical phenomena, such as gravity and surface tension, neglected in the simple model. Finally we compare our asymptotic results with the work of other authors and with some of the experimental data available in the literature.

2.1 Physical Motivation

We wish to construct a mathematical model for the impact of the forward part of a ship hull onto the sea, with the principal aim of predicting the resulting pressure distribution on the hull. The first step of the modelling procedure is to identify the most important physical phenomena, and we shall do this crudely by evaluating the orders of magnitude of the relevant non-dimensional parameters.

Consider a 'typical' ship with characteristic width, l, of 10m impacting onto the ocean with a relative speed, V, of 30ms^{-1}. Since the kinematic viscosity of

water, ν, is roughly $10^{-6}\mathrm{m}^2\mathrm{s}^{-1}$ the *Reynolds number*, R_e, for the flow is

$$\mathrm{R}_e = \frac{Vl}{\nu} \sim 10^8.$$

The square of the *Froude number*, F_r^2, is given by

$$\mathrm{F}_r^2 = \frac{V^2}{gl} \sim 10,$$

where $g \simeq 9.8\mathrm{ms}^{-2}$ is the acceleration due to gravity and the *Weber number*, W_e, is defined as

$$\mathrm{W}_e = \frac{\rho l V^2}{\gamma} \sim 10^4,$$

where $\gamma \simeq 7.5 \times 10^{-4}\mathrm{Nm}^{-1}$ is the surface tension at a water-air interface and ρ is the density of water. Finally the *Mach number in the water*, M_w, is

$$\mathrm{M}_w = \frac{V}{c_w} \sim 10^{-2},$$

where $c_w \simeq 1400\mathrm{ms}^{-2}$ is the local sound speed.

Since $\mathrm{R}_e \gg 1$ and $\mathrm{M}_w \ll 1$ our first model will be of an inviscid, incompressible fluid and since $\mathrm{F}_r^2 \gg 1$ and $\mathrm{W}_e \gg 1$ we shall neglect the effects of gravity and surface tension.

The air present between the ship and the sea before the impact occurs may play an important rôle in the impact process, and we will consider it more carefully in Chapter 5. Typical magnitudes of the air and water pressures are $\rho_a V_a^2$ and $\rho_w V_w^2$ respectively, where ρ_a is the air density, V_a is a characteristic air speed and ρ_w, V_w are the corresponding quantities for the water. The air pressure will, therefore, be negligible compared to the water pressure provided

$$\left(\frac{v_a^2}{v_w^2}\right)^2 \ll \frac{\rho_w}{\rho_a},$$

where

$$\frac{\rho_w}{\rho_a} \sim 10^3.$$

Since this density ratio is large, we expect the air pressure to be negligible except just before impact occurs, when the air velocity may become sufficiently large for the air pressure to be significant. This stage of the impact is analysed in Chapter 5, but in this first model we can assume that the impacting body moves through a vacuum before striking the fluid.

Clearly, all these intuitively evident assumptions must be reviewed when the calculation is completed and some or all of these effects may have to be re-introduced to reproduce the observed physical phenomena.

2.2 Problem Formulation

Consider the impact of a two-dimensional rigid body onto a half-space of quiescent, inviscid and incompressible fluid. In this simple model we assume that the body is symmetric and take cartesian coordinates (x, y) with the y-axis vertically upwards along the axis of symmetry of the body and the x-axis along the undisturbed fluid surface. The fluid initially fills $y \leq 0$ and the region $y > 0$ is assumed to be a vacuum. The effects of gravity and surface tension are ignored. The body has profile $y = f(x)$, where $f(0) = 0$, $f(x) = f(-x)$ and $f(x) > 0$ for $|x| > 0$, and moves vertically downwards with constant speed V throughout the impact. We choose the origin of time $t = 0$ to correspond to the moment when the body first touches the undisturbed fluid surface, and so the position of the body at time t is given by

$$y = f(x) - Vt.$$

The fluid flow is described by the fluid velocity $\mathbf{u}(x, y, t)$ and pressure $p(x, y, t)$. The governing equations, which are derived from the principles of conservation of mass and of momentum, are Euler's equations,

$$\nabla \cdot \mathbf{u} = 0, \tag{2.1}$$

$$\frac{D\mathbf{u}}{Dt} = -\frac{1}{\rho}\nabla p + \mathbf{F}, \tag{2.2}$$

where ρ is the constant fluid density. The body force $\mathbf{F}$ is assumed to be conservative and consequently can be written in the form $\mathbf{F} = -\nabla\Omega$, where $\Omega(x, y, t)$ is a scalar potential function. D/Dt denotes the convective derivative which can be expressed in terms of derivatives at a fixed point as

$$\frac{D}{Dt} = \frac{\partial}{\partial t} + (\mathbf{u} \cdot \nabla).$$

A fluid flow is said to be *irrotational* if $\nabla \times \mathbf{u} = \mathbf{0}$. Since the fluid is incompressible and inviscid, Kelvin's Theorem applies, and so the circulation around any closed

curve moving with the flow is constant. Hence, since the flow is initially at rest and therefore irrotational, it will remain irrotational throughout the motion. We can therefore define a *velocity potential* $\phi(x, y, t)$ such that

$$\mathbf{u} = \nabla\phi,$$

and hence, from equation (2.1), the potential ϕ satisfies Laplace's equation

$$\nabla^2\phi = 0. \tag{2.3}$$

When ϕ has been determined the pressure, p, is calculated from the equation of motion (2.2) which can be integrated to give the unsteady form of Bernoulli's equation,

$$\frac{\partial\phi}{\partial t} + \frac{1}{2}|\nabla\phi|^2 + \frac{p}{\rho} + \Omega = g(t), \tag{2.4}$$

in which $g(t)$ is a function of time t only.

For $t > 0$ the surface of the fluid will be divided into two parts, the *wetted body surface* and the *free surface*.

On the wetted body surface the appropriate boundary condition for an inviscid fluid is that there should be continuity of normal velocity between the body and the fluid. This means that

$$\frac{D}{Dt}(y - f(x) + Vt) = 0,$$

and so

$$\frac{df}{dx}\frac{\partial\phi}{\partial x} - \frac{\partial\phi}{\partial y} = V \quad \text{on} \quad y = f(x) - Vt. \tag{2.5}$$

The shape of the free surface is denoted by $y = h(x, t)$ and, since it is to be determined as part of the solution, we require that two boundary conditions are imposed on it. The first comes from the kinematic condition that fluid particles originally in the free surface always remain so. Consequently for a fluid particle in the surface

$$\frac{D}{Dt}(y - h(x, t)) = 0,$$

which gives the condition

$$\frac{\partial h}{\partial t} + \frac{\partial h}{\partial x}\frac{\partial\phi}{\partial x} - \frac{\partial\phi}{\partial y} = 0 \quad \text{on} \quad y = h(x, t). \tag{2.6}$$

The second relation is the pressure matching condition that the pressure on the free surface is equal to the zero pressure in the vacuum above, and so from Bernoulli's equation (2.4) in the absence of gravity and surface tension we have

$$\frac{\partial \phi}{\partial t} + \frac{1}{2}\left[\left(\frac{\partial \phi}{\partial x}\right)^2 + \left(\frac{\partial \phi}{\partial y}\right)^2\right] = 0 \quad \text{on} \quad y = h(x,t). \tag{2.7}$$

We must also specify initial conditions at the instant of impact $t = 0$ and the far-field behaviour of the solution. Without loss of generality we can choose the potential so that

$$\phi(x, y, 0) = 0, \tag{2.8}$$

and since the fluid filling $y \leq 0$ is initially at rest, we have that

$$h(x, 0) = 0. \tag{2.9}$$

Physically we insist that the fluid velocity must tend to zero at large distances from the body and so

$$|\nabla \phi(x, y, t)| \to 0 \quad \text{as} \quad (x^2 + y^2)^{\frac{1}{2}} \to \infty, \tag{2.10}$$

with the consequence that $h(x,t) \to 0$ as $|x| \to \infty$.

Laplace's equation (2.3) together with the boundary conditions (2.5), (2.6), (2.7), the initial conditions (2.8), (2.9) and the far field condition (2.10) are an unsteady, nonlinear free boundary problem for $\phi(x,y,t)$ and $h(x,t)$ in the geometry shown in Figure (2.1). No solutions of this set of equations are known for arbitrary shaped bodies and there is no existence/uniqueness theory for the problem.

2.3 Bodies with Small Deadrise Angle

In order to make progress we restrict our attention to bodies whose *deadrise angle* β, defined to be the angle made between the tangent to the profile and the horizontal, is everywhere 'small'. By 'small' in this context we mean that β is much less than $\pi/2$.

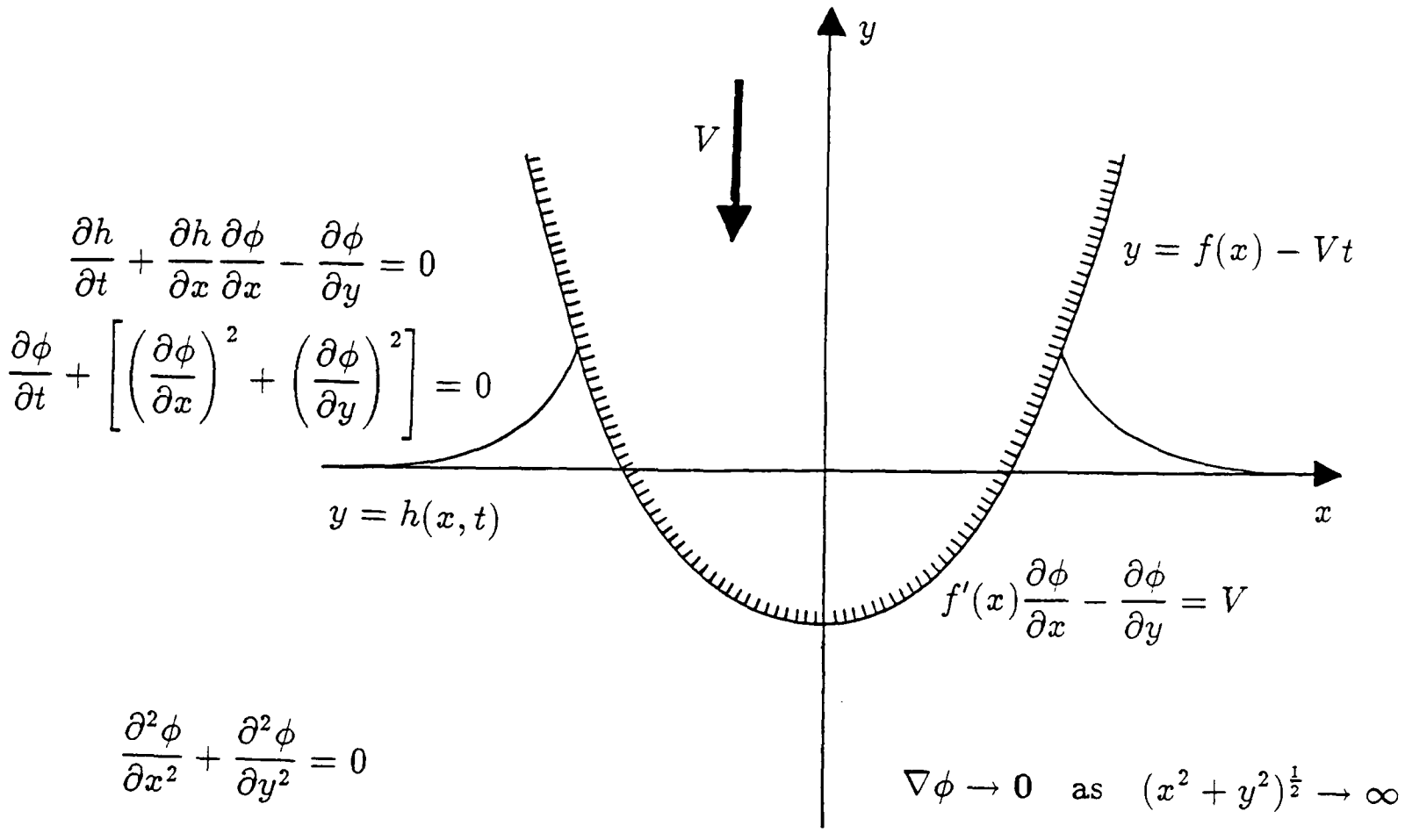

Figure 2.1: Rigid body impact geometry.

First we *non-dimensionalize* the problem by introducing suitably scaled non-dimensional variables x^*, y^* and t^*, based on a typical length scale l and impact velocity V, in the form

$$x^* = \frac{x}{l}, \qquad y^* = \frac{y}{l}, \qquad t^* = \frac{Vt}{l}.$$

In a similar way we define a non-dimensional velocity potential $\phi^*(x^*, y^*, t^*)$, pressure $p^*(x^*, y^*, t^*)$ and free surface elevation $h^*(x^*, t^*)$ by

$$\phi^*(x^*, y^*, t^*) = \frac{1}{lV}\phi(x, y, t), \quad p^*(x^*, y^*, t^*) = \frac{1}{\rho V^2}p(x, y, t), \quad h^*(x^*, t^*) = \frac{1}{l}h(x, t).$$

We now introduce the small dimensionless parameter $\epsilon \ll 1$ in such a way that the position of the impacting body is given by

$$y^* = f^*(\epsilon x^*) - t^*,$$

where the function $f^*(\cdot)$ describes the profile of the body. We immediately drop the cumbersome starred notation, but hereafter all quantities will be non-dimensional unless otherwise stated. Non-dimensionalizing equations (2.3), (2.5),

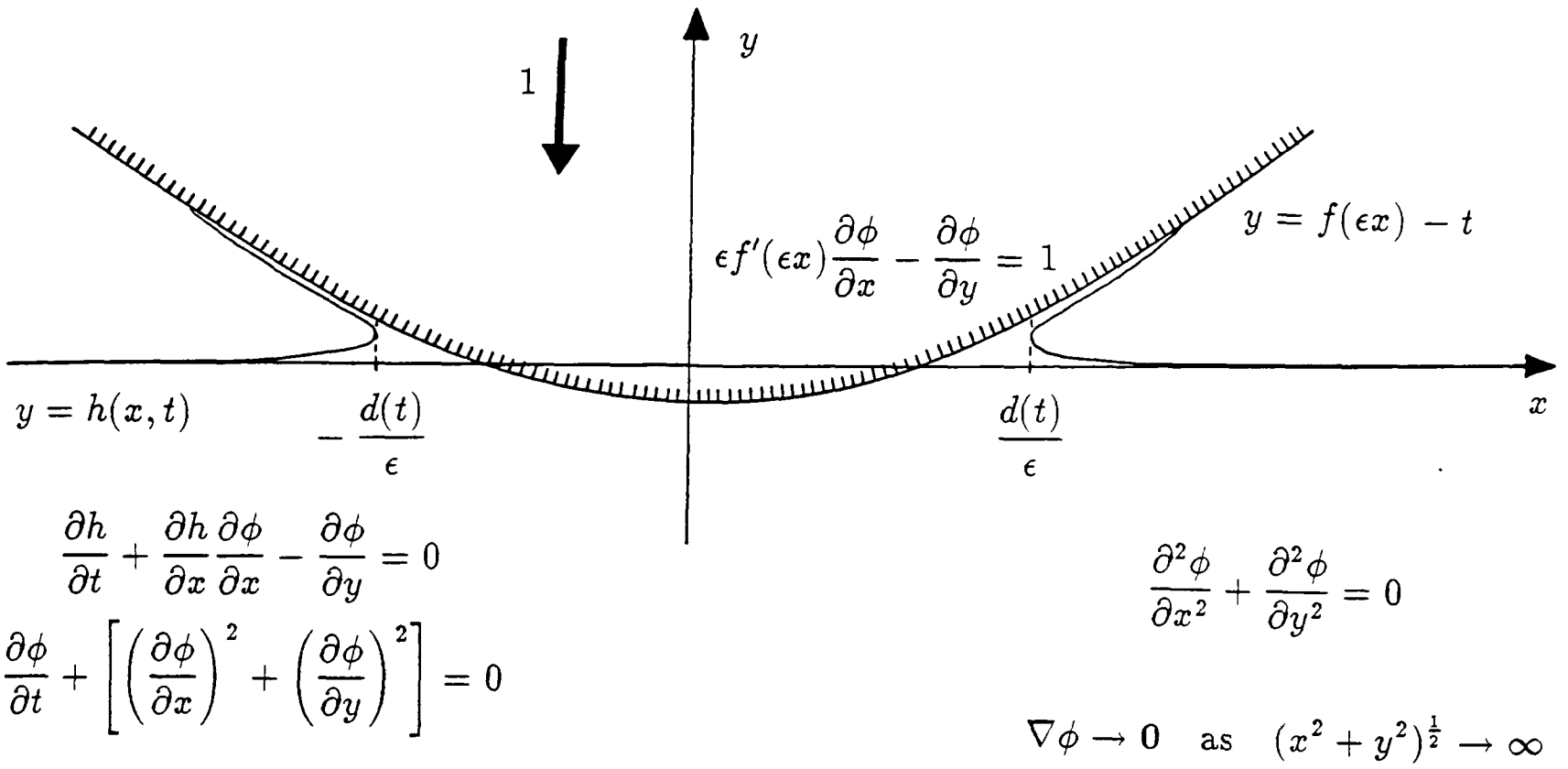

Figure 2.2: Impact of a body with small deadrise angle.

(2.6) and (2.7), we obtain the full impact problem,

$$\frac{\partial^2 \phi}{\partial x^2} + \frac{\partial^2 \phi}{\partial y^2} = 0 \quad \text{in the fluid,} \tag{2.11}$$

$$\epsilon f'(\epsilon x)\frac{\partial \phi}{\partial x} - \frac{\partial \phi}{\partial y} = 1 \quad \text{on} \quad y = f(\epsilon x) - t, \tag{2.12}$$

$$\frac{\partial h}{\partial t} + \frac{\partial h}{\partial x}\frac{\partial \phi}{\partial x} - \frac{\partial \phi}{\partial y} = 0 \quad \text{on} \quad y = h(x,t), \tag{2.13}$$

$$\frac{\partial \phi}{\partial t} + \frac{1}{2}\left[\left(\frac{\partial \phi}{\partial x}\right)^2 + \left(\frac{\partial \phi}{\partial y}\right)^2\right] = 0 \quad \text{on} \quad y = h(x,t), \tag{2.14}$$

together with the initial conditions from (2.8) and (2.9),

$$\phi(x,y,0) = 0, \quad h(x,0) = 0, \tag{2.15}$$

and the far-field condition from (2.10),

$$\frac{\partial \phi}{\partial x}, \quad \frac{\partial \phi}{\partial y} \to 0 \quad \text{as} \quad (x^2+y^2)^{\frac{1}{2}} \to \infty, \tag{2.16}$$

which is summarised in Figure (2.2).

A natural way to approach the equation (2.11) together with the boundary conditions (2.12), (2.13) and (2.14) is as a perturbation problem in the small parameter ϵ, which we do by introducing suitably scaled variables and seeking a

solution in the form of an asymptotic series in ϵ. As we shall see, this approach yields a description of the flow which is valid in an *outer region* but fails in an *inner region* near the body where it is singular. In order to correct the singularity in the *outer problem*, we must rescale the variables, then formulate and solve the appropriate *inner problem* in that region. Once the inner solution is known a uniformly valid solution can be obtained by first *matching* the two expansions, and then constructing a uniformly valid composite expansion. This technique is known as the method of Matched Asymptotic Expansions and has been applied to many singular perturbation problems, especially in fluid mechanics, and is described in detail in the classic book by Van Dyke (1975).

2.4 The Outer Problem

The profile of the body changes by an $O(1)$ quantity over a length of $O(1/\epsilon)$. The length scale of the outer region is, therefore, $O(1/\epsilon)$, and so we introduce scaled *outer variables* X and Y defined by

$$X = \epsilon x, \qquad Y = \epsilon y.$$

Since the velocities in the outer region will be $O(1)$, we introduce a scaled outer velocity potential $\Phi(X, Y, t)$ defined by

$$\Phi(X, Y, t) = \epsilon\phi(x, y, t),$$

and, since the free surface deformation will also be $O(1)$, we define an outer free surface elevation $H(X, t)$ by $h(x, t) = H(X, t)$ so that

$$Y = \epsilon H(X, t)$$

describes the position of the fluid surface. Writing (2.11), (2.12), (2.13) and (2.14) in outer variables we obtain the full outer problem:

$$\frac{\partial^2\Phi}{\partial X^2} + \frac{\partial^2\Phi}{\partial Y^2} = 0 \quad \text{in the fluid,} \tag{2.17}$$

$$\epsilon f'(X)\frac{\partial\Phi}{\partial X} - \frac{\partial\Phi}{\partial Y} = 1 \quad \text{on} \quad Y = \epsilon(f(X) - t), \tag{2.18}$$

$$\frac{\partial H}{\partial t} + \epsilon\frac{\partial H}{\partial X}\frac{\partial\Phi}{\partial X} - \frac{\partial\Phi}{\partial Y} = 0 \quad \text{on} \quad Y = \epsilon H(X, t), \tag{2.19}$$

$$\frac{\partial\Phi}{\partial t} + \frac{\epsilon}{2}\left[\left(\frac{\partial\Phi}{\partial X}\right)^2 + \left(\frac{\partial\Phi}{\partial Y}\right)^2\right] = 0 \quad \text{on} \quad Y = \epsilon H(X, t), \tag{2.20}$$

together with the initial conditions from (2.15),

$$\Phi(X,Y,0) = 0, \quad H(X,0) = 0, \tag{2.21}$$

and far-field condition from (2.16),

$$\frac{\partial \Phi}{\partial X}, \quad \frac{\partial \Phi}{\partial Y} \to 0 \quad \text{as} \quad (X^2+Y^2)^{\frac{1}{2}} \to \infty. \tag{2.22}$$

In order to carry out a systematic expansion the boundary conditions on the body and on the free surface, they must be expressed in terms of quantities evaluated on the undisturbed position of the free surface $Y = 0$, corresponding to setting $\epsilon = 0$. This is accomplished by expanding the boundary conditions in Taylor series about their values at $Y = 0$. This procedure presents no difficulties for the boundary condition on the body $Y = \epsilon(f(X) - t)$, but when applied to those on the free surface $Y = \epsilon H(X,t)$ it does if the free surface becomes double valued. Indeed, we would expect this to be the case since many experimental and numerical investigations note the formation of a long, thin, fast-moving jet of fluid close to the body during small deadrise impacts. For example, Figure (1.6) is a photograph of a small scale experiment reproduced from Greenhow (1987) which clearly shows such a jet. Motivated by these observations and by the assumption, to be verified a posteriori, that the volume of fluid in the jet is small compared to a typical volume measured on the outer length scale, we neglect the effect of the jet in the outer problem. Hence when performing the linearization of the boundary conditions we apply the wetted body condition on $Y = 0$, $|X| < d(t)$ and the free surface conditions on $Y = 0$, $|X| > d(t)$ where $d(t)$ is an unknown function of t which represents the position of the point where the free surface turns over to form the jet.

We now seek regular perturbation solutions for Φ and H as power series in ϵ in the form

$$\begin{aligned} \Phi &= \Phi_0 + \epsilon\Phi_1 + \epsilon^2\Phi_2 + O(\epsilon^3), \\ H &= H_0 + \epsilon H_1 + \epsilon^2 H_2 + O(\epsilon^3). \end{aligned}$$

The leading order outer problem is, therefore,

$$\frac{\partial^2 \Phi_0}{\partial X^2} + \frac{\partial^2 \Phi_0}{\partial Y^2} = 0 \quad \text{in} \quad Y < 0, \tag{2.23}$$

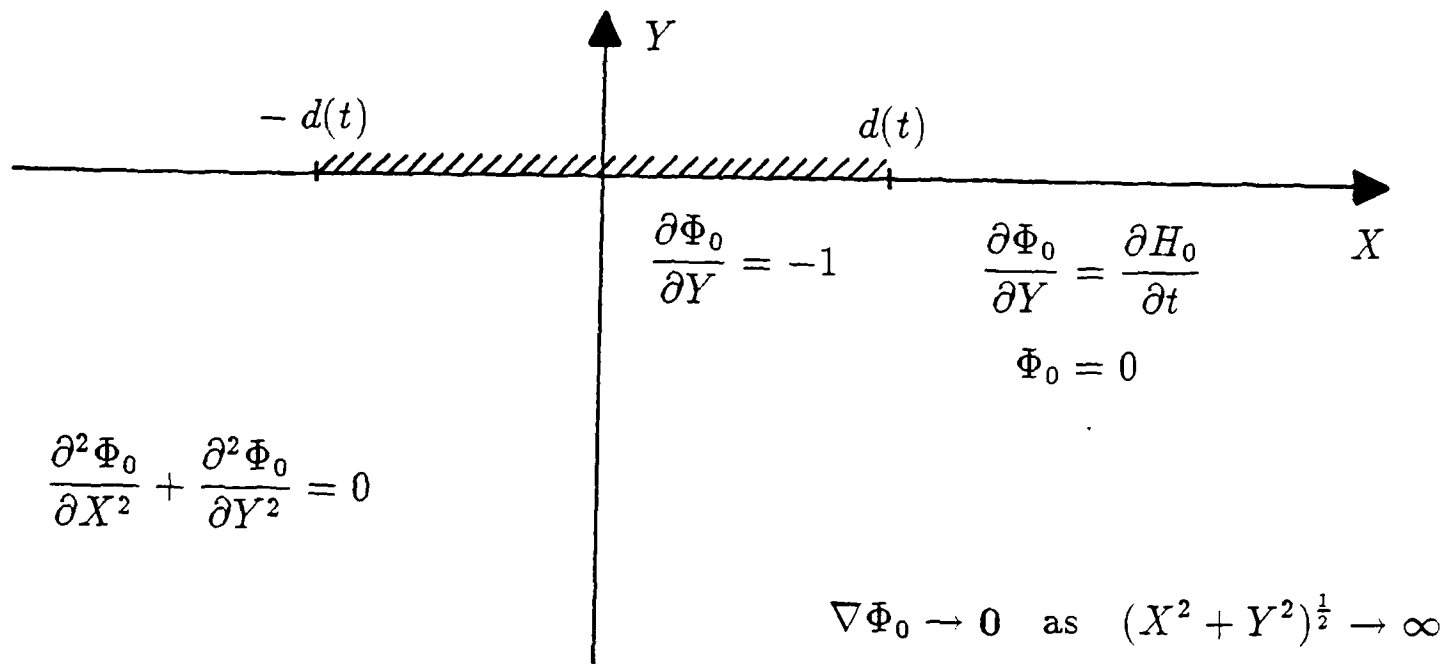

Figure 2.3: Leading order outer problem.

$$\frac{\partial \Phi_0}{\partial Y} = -1 \quad \text{on} \quad Y = 0, \quad |X| < d(t), \tag{2.24}$$

$$\frac{\partial \Phi_0}{\partial Y} = \frac{\partial H_0}{\partial t} \quad \text{on} \quad Y = 0, \quad |X| > d(t), \tag{2.25}$$

$$\frac{\partial \Phi_0}{\partial t} = 0 \quad \text{on} \quad Y = 0, \quad |X| > d(t), \tag{2.26}$$

with initial conditions

$$\Phi_0(X, Y, 0) = 0, \quad H_0(X, 0) = 0, \tag{2.27}$$

and far-field conditions

$$\frac{\partial \Phi_0}{\partial X}, \quad \frac{\partial \Phi_0}{\partial Y} \to 0 \quad \text{as} \quad (X^2 + Y^2)^{\frac{1}{2}} \to \infty. \tag{2.28}$$

Integrating (2.26) with respect to time and using the initial condition (2.27a) we obtain

$$\Phi_0 = 0 \quad \text{on} \quad Y = 0, \quad |X| > d(t). \tag{2.29}$$

The equation (2.23), together with the boundary conditions (2.24), (2.25) and (2.29), form a mixed boundary value problem for Φ_0, which is summarised in Figure (2.3). It is mathematically equivalent to the problem of the normal impact, with speed 1, of a flat plate of width $2d(t)$ onto a half-space of fluid $Y \leq 0$. Because of this analogy, first drawn by Wagner (1932), we shall call

$d(t)$ the *semi-width of the equivalent flat plate*, which will be determined by an appropriate matching condition.

For completeness, we note that the second order outer problem is

$$\frac{\partial^2\Phi_1}{\partial X^2}+\frac{\partial^2\Phi_1}{\partial Y^2} = 0 \quad \text{in the fluid,} \tag{2.30}$$

$$f'(X)\frac{\partial\Phi_0}{\partial X}-\frac{\partial\Phi_1}{\partial Y}-(f(X)-t)\frac{\partial^2\Phi_0}{\partial Y^2} = 0 \quad \text{on} \quad Y=0, \quad |X|<d(t), \tag{2.31}$$

$$\frac{\partial H_1}{\partial t}+\frac{\partial H_0}{\partial X}\frac{\partial\Phi_0}{\partial X}-\frac{\partial\Phi_1}{\partial Y}-H_0\frac{\partial^2\Phi_0}{\partial Y^2} = 0 \quad \text{on} \quad Y=0, \quad |X|>d(t), \tag{2.32}$$

$$\frac{\partial\Phi_1}{\partial t}+H_0\frac{\partial^2\Phi_0}{\partial t\partial Y}+\frac{1}{2}\left[\left(\frac{\partial\Phi_0}{\partial X}\right)^2+\left(\frac{\partial\Phi_0}{\partial Y}\right)^2\right] = 0 \quad \text{on} \quad Y=0, \quad |X|>d(t), \tag{2.33}$$

with

$$\Phi_1(X,Y,0)=0, \quad H_1(X,0)=0, \tag{2.34}$$

and

$$\frac{\partial\Phi_1}{\partial X}, \quad \frac{\partial\Phi_1}{\partial Y}\to 0 \quad \text{as} \quad (X^2+Y^2)^{\frac{1}{2}}\to\infty. \tag{2.35}$$

2.4.1 Solution of the Leading Order Outer Problem

The nature of the singularity at the edge of the plate in the leading order outer problem can be determined in a straightforward way by taking local polar coordinates (R,Θ) about $X=d(t)$ and obtaining the local form of the solution. If we insist, on physical grounds, that the spatially integrated fluid energy remains bounded, then it is easy to show that the worst possible singularity in the velocity is $R^{-\frac{1}{2}}$ and so the velocity potential behaves locally like $R^{\frac{1}{2}}$. The solution for Φ_0 is then obtained by observing that the complex function

$$W_0(Z)=iZ-(d(t)^2-Z^2)^{\frac{1}{2}}, \quad \text{where} \quad Z=X+iY,$$

is holomorphic in the cut Z-plane if we make branch cuts along the X-axis between $(-\infty,0)$ and $(-d(t),0)$ and between $(d(t),0)$ and $(+\infty,0)$. Moreover, $W_0(Z)$ evidently satisfies

$$W_0(X+i0)=iX-(d(t)^2-X^2)^{\frac{1}{2}},$$

with

$$\frac{\partial W_0}{\partial X}(X+i0) = i + \frac{X}{(d(t)^2 - X^2)^{\frac{1}{2}}}, \quad \frac{\partial W_0}{\partial Y}(X+i0) = -1 + \frac{iX}{(d(t)^2 - X^2)^{\frac{1}{2}}},$$

and the far behaviour

$$W_0(Z) \to 0 \quad \text{and} \quad \frac{dW_0}{dZ} \to 0 \quad \text{as} \quad |Z| \to \infty.$$

If we now write the complex potential $W_0(Z)$ in terms of its real and imaginary parts thus : $W_0(Z) = \Phi_0 + i\Psi_0$, then, since $W_0(Z)$ is holomorphic in Z, the function $\Phi_0 = \Re(W_0)$ is harmonic in $Y < 0$ and satisfies the correct boundary and far field conditions. The appropriate solution for Φ_0 is, therefore,

$$\Phi_0(X, Y, t) = -\left[Y + \Re(d(t)^2 - Z^2)^{\frac{1}{2}}\right], \tag{2.36}$$

where $\Re(\cdot)$ denotes the real part of a complex quantity. Once Φ_0 is known we can determine H_0 by integrating (2.25) with respect to time for $|X| > d(t)$ and use the initial condition (2.27b) to obtain

$$H_0(X, t) = \int_0^t \frac{\partial \Phi_0}{\partial Y}(X, 0, \tau)\, \mathrm{d}\tau. \tag{2.37}$$

Hence, substituting from (2.36), the leading order solution for the profile of the free surface for $|X| > d(t)$ is given by

$$H_0(X, t) = -t + \int_0^t \frac{X}{(X^2 - d(\tau)^2)^{\frac{1}{2}}}\, \mathrm{d}\tau. \tag{2.38}$$

2.4.2 The Pressure in the Outer Region

Once the outer velocity field is known, we can evaluate the outer pressure distribution $P(X, Y, t)$ from Bernoulli's equation (2.4), which, when written in outer variables, gives

$$\frac{1}{2}\left[\left(\frac{\partial \Phi}{\partial X}\right)^2 + \left(\frac{\partial \Phi}{\partial Y}\right)^2\right] + \frac{1}{\epsilon}\frac{\partial \Phi}{\partial t} + P = 0.$$

Expanding $P(X, Y, t)$ as an asymptotic series in powers of ϵ in the form,

$$P = \frac{1}{\epsilon}P_0 + P_1 + \epsilon P_2 + O(\epsilon^2),$$

and substituting for Φ, we obtain the leading order terms

$$-P_0 = \frac{\partial \Phi_0}{\partial t}, \tag{2.39}$$

$$-P_1 = \frac{\partial \Phi_1}{\partial t} + \frac{1}{2}\left[\left(\frac{\partial \Phi_0}{\partial X}\right)^2 + \left(\frac{\partial \Phi_0}{\partial Y}\right)^2\right], \tag{2.40}$$

and we can, therefore, easily evaluate the leading order outer pressure to be,

$$P_0(X,Y,t) = \Re\left[\frac{d(t)d'(t)}{(d(t)^2 - Z^2)^{\frac{1}{2}}}\right]. \tag{2.41}$$

The pressure on the body is given in terms of quantities evaluated on the plate $Y = 0$, $|X| < d(t)$, and its leading order terms are

$$-P_0(X,0,t) = \frac{\partial \Phi_0}{\partial t}, \tag{2.42}$$

$$-P_1(X,0,t) = \frac{\partial \Phi_1}{\partial t} + (f(X) - t)\frac{\partial^2 \Phi_0}{\partial t \partial Y} + \frac{1}{2}\left[\left(\frac{\partial \Phi_0}{\partial X}\right)^2 + \left(\frac{\partial \Phi_0}{\partial Y}\right)^2\right]. \tag{2.43}$$

In particular, the leading order pressure on the body is given by

$$P_0(X,0,t) = \frac{d(t)d'(t)}{(d(t)^2 - X^2)^{\frac{1}{2}}}, \tag{2.44}$$

which has square root singularities at the points $|X| = d(t)$. A typical leading order outer pressure distribution is shown in Figure (2.4).

2.5 The Matching Condition to Determine $d(t)$

The matching condition to determine the semi-plate width $d(t)$ was first suggested by Wagner (1932), and requires that the leading order free surface elevation in the outer problem as $X \to d(t)^+$ should be equal to the position of the body at $X = d(t)$, viz.

$$H_0(d(t),t) = f(d(t)) - t \quad \text{for all} \quad t \geq 0. \tag{2.45}$$

In Appendix B we show that this condition follows from the assumption that the volume of fluid in the jet is small on the length scale of the outer problem, and we will be able to justify this assumption a posteriori once the jet solution has been determined. $H_0(X,t)$ is already known in terms of $d(t)$, and so we can

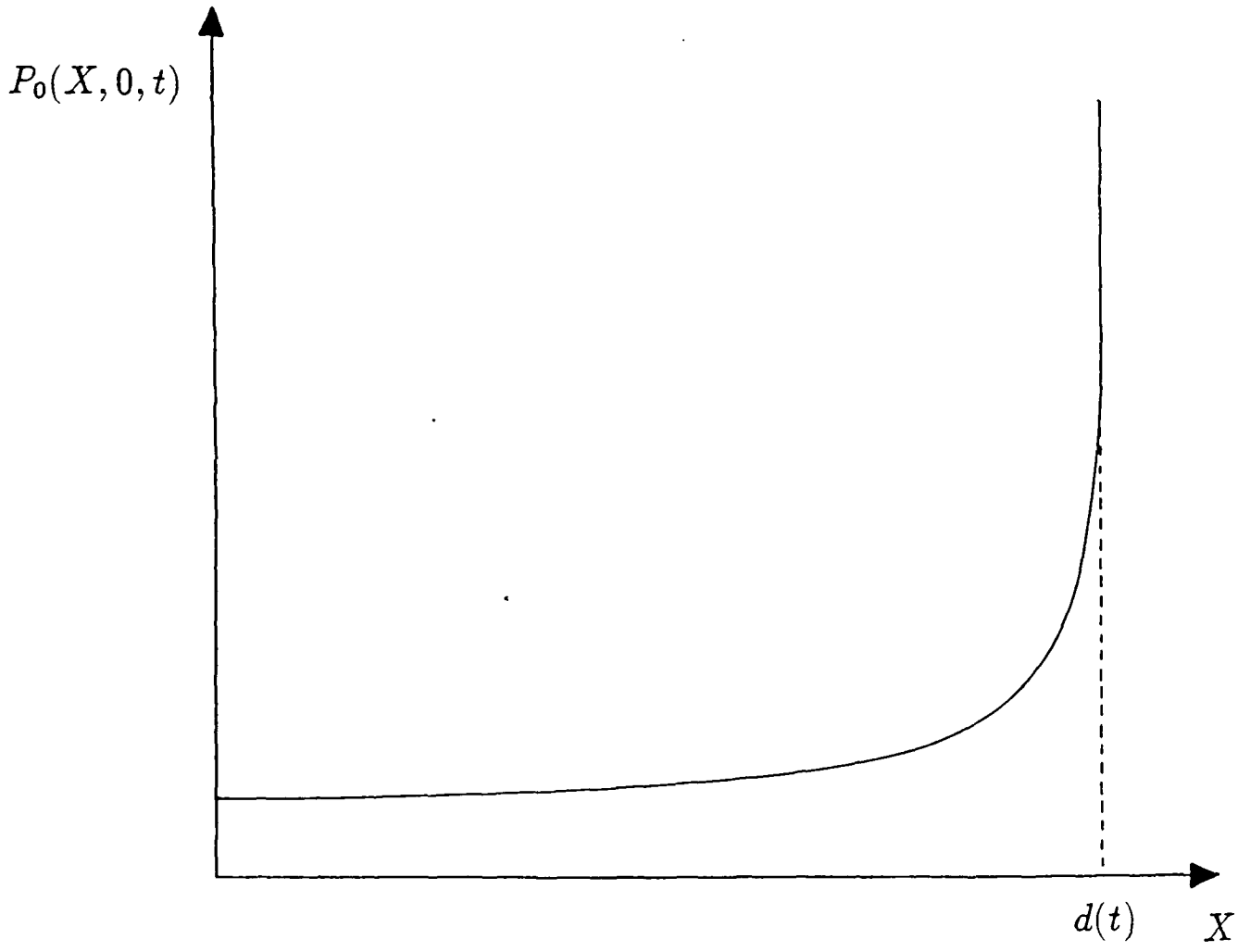

Figure 2.4: Typical leading order outer pressure on the body.

substitute from equation (2.38) into this matching condition to obtain a singular integral equation for the plate semi-width $d(t)$, namely

$$d(t)\int_0^t \frac{d\tau}{(d(t)^2 - d(\tau)^2)^{\frac{1}{2}}} = f(d(t)). \tag{2.46}$$

2.5.1 Solution of the Singular Integral Equation for $d(t)$

Confronted with the singular integral equation (2.46), Wagner (1932) attempted to solve it for $d(t)$ by writing t as a function of d and expanding $t'(d)$ as a power series in d. After expanding the body shape $f(d)$ in powers of d he equated the coefficients of the powers of d and obtained expressions for the coefficients in the power series expansion of $t(d)$. In practice inverting the power series for $d(t)$ is too difficult for all but the simplest bodies and the method, copied by a number of authors since including Fabula (1957), Watanabe (1986) and Greenhow & Yanbao (1987), fails to provide a useful closed form solution. The integral equation can in fact be solved simply in a closed form. First we write t as a function of d, then introduce the new integration variable σ and write $\tau = t(\sigma)$ so that $d\tau = t'(\sigma)d\sigma$ and hence equation (2.46) becomes

$$\int_0^d \frac{t'(\sigma)}{(d^2 - \sigma^2)^{\frac{1}{2}}}\,\mathrm{d}\sigma = \frac{f(d)}{d}.$$

This is an Abel integral equation, as described in Sneddon (1966), and has the solution

$$t'(\sigma) = \frac{2}{\pi}\frac{d}{d\sigma}\int_0^\sigma \frac{f(\xi)}{(\sigma^2 - \xi^2)^{\frac{1}{2}}}\,\mathrm{d}\xi,$$

provided the that integral exists. In this thesis, the function $f(\cdot)$ describing the body shape will always be continuous, and this is a sufficient condition for the existence of the integral. Integrating this expression once with respect to σ, $t(d)$ is given by

$$t(d) = \frac{2}{\pi}\int_0^d \frac{f(\xi)}{(d^2 - \xi^2)^{\frac{1}{2}}}\,\mathrm{d}\xi. \tag{2.47}$$

Given any body shape, the corresponding semi-width function can be calculated simply by evaluating (2.47), and then inverting for $d(t)$.

2.6 The Inner Problem

The leading order solution of the outer problem is singular at $x = \pm d(t)/\epsilon$ and hence fails to accurately represent the flow near these two points. Since the problem is symmetric in x, it is sufficient to analyse the flow in the neighbourhood of just one of them. In order to obtain the correct *inner problem* in the neighbourhood of $x = d(t)/\epsilon$ and $y = f(d(t)) - t$, we introduce scaled *inner variables* $\hat{x}$ and $\hat{y}$ defined by

$$x = \frac{d(t)}{\epsilon} + \epsilon^n \hat{x}, \qquad y = f(d(t)) - t + \epsilon^n \hat{y}.$$

The exponent $n > -1$, which determines the scale of the inner region, is unknown and will be determined by matching the inner solution with the outer solution. Since the entire inner region is moving with the positive x-direction with speed $d'(t)/\epsilon$ we deduce that the fluid velocity in the inner region must be of $O(1/\epsilon)$ and therefore the velocity potential must be $O(\epsilon^{n-1})$. Hence, we define a scaled inner velocity potential $\hat{\phi}(\hat{x}, \hat{y}, t)$ so that

$$\phi(x, y, t) = \epsilon^{n-1} \left[d'(t)\hat{x} + \hat{\phi}(\hat{x}, \hat{y}, t) \right],$$

where the factor of $d'(t)\hat{x}$ has been subtracted out to simplify the algebra. Written in inner variables, the position of the body is given by

$$\hat{y} = \frac{1}{\epsilon}(f(d(t) + \epsilon^{n+1}\hat{x}) - f(d(t))) = \epsilon \hat{x} f'(d(t)) + \epsilon^{n+2} \frac{\hat{x}^2}{2} f''(d(t)) + O(\epsilon^{2n+3}).$$

Since the $O(1)$ term in this expansion is zero whatever the value of n, the body is flat to leading order, and so we can write the position of the body as

$$\hat{y} = \epsilon \hat{f}(\hat{x}, t).$$

Similarly, the profile of the free surface is given by

$$\hat{y} = \frac{1}{\epsilon^n}(h(x, t) - f(d(t)) + t). \tag{2.48}$$

Written in outer variables and expanded about $X = d(t)$ in powers of ϵ, the leading order term in (2.48) is

$$\frac{1}{\epsilon^n} \left(H_0(d(t), t) - f(d(t)) + t \right),$$

which, because of the matching condition defining $d(t)$, is identically zero. The second order term is $O(1)$ whatever the value of n, and we can therefore define an inner free surface profile $\hat{h}(\hat{x},t)$ so that

$$\hat{y} = \hat{h}(\hat{x},t)$$

describes the position of the fluid surface.

Writing the impact problem (2.11), (2.12), (2.13) and (2.14) in inner variables we obtain the full inner problem,

$$\frac{\partial^2\hat{\phi}}{\partial\hat{x}^2} + \frac{\partial^2\hat{\phi}}{\partial\hat{y}^2} = 0 \quad \text{in the fluid,} \tag{2.49}$$

$$f'(d(t)+\epsilon^{n+1}\hat{x})\left[d'(t)+\frac{\partial\hat{\phi}}{\partial\hat{x}}\right] - \frac{1}{\epsilon}\frac{\partial\hat{\phi}}{\partial\hat{y}} = 1 \quad \text{on} \quad \hat{y} = \epsilon\hat{f}(\hat{x},t), \tag{2.50}$$

$$f'(d(t))d'(t) - 1 + \epsilon^n\frac{\partial\hat{h}}{\partial t} + \frac{1}{\epsilon}\left[\frac{\partial\hat{\phi}}{\partial\hat{x}}\frac{\partial\hat{h}}{\partial\hat{x}} - \frac{\partial\hat{\phi}}{\partial\hat{y}}\right] = 0$$

$$\text{on} \quad \hat{y} = \hat{h}(\hat{x},t), \tag{2.51}$$

$$\frac{1}{2\epsilon^2}\left[\left(\frac{\partial\hat{\phi}}{\partial\hat{x}}\right)^2 + \left(\frac{\partial\hat{\phi}}{\partial\hat{y}}\right)^2 - d'(t)^2\right] + \frac{1}{\epsilon}\left[1 - f'(d(t))d'(t)\right]\frac{\partial\hat{\phi}}{\partial\hat{y}} + \epsilon^{n-1}\left[d''(t)\hat{x} + \frac{\partial\hat{\phi}}{\partial t}\right] = 0$$

$$\text{on} \quad \hat{y} = \hat{h}(\hat{x},t). \tag{2.52}$$

We now seek regular perturbation solutions for $\hat{\phi}$ and $\hat{h}$ as power series in ϵ,

$$\hat{\phi} = \hat{\phi}_0 + \epsilon\hat{\phi}_1 + \epsilon^2\hat{\phi}_2 + O(\epsilon^3),$$
$$\hat{h} = \hat{h}_0 + \epsilon\hat{h}_1 + \epsilon^2\hat{h}_2 + O(\epsilon^3).$$

After expressing quantities in terms of their values on their basic positions corresponding to $\epsilon = 0$, the leading order inner problem is found to be

$$\frac{\partial^2\hat{\phi}_0}{\partial\hat{x}^2} + \frac{\partial^2\hat{\phi}_0}{\partial\hat{y}^2} = 0 \quad \text{in the fluid,} \tag{2.53}$$

$$\frac{\partial\hat{\phi}_0}{\partial\hat{y}} = 0 \quad \text{on} \quad \hat{y} = 0, \tag{2.54}$$

$$\frac{\partial\hat{\phi}_0}{\partial\hat{x}}\frac{\partial\hat{h}_0}{\partial\hat{x}} - \frac{\partial\hat{\phi}_0}{\partial\hat{y}} = 0 \quad \text{on} \quad \hat{y} = \hat{h}_0(\hat{x},t), \tag{2.55}$$

$$\left(\frac{\partial\hat{\phi}_0}{\partial\hat{x}}\right)^2 + \left(\frac{\partial\hat{\phi}_0}{\partial\hat{y}}\right)^2 = d'(t)^2 \quad \text{on} \quad \hat{y} = \hat{h}_0(\hat{x},t). \tag{2.56}$$

Since the leading order problem is steady, there are no initial conditions imposed on it.

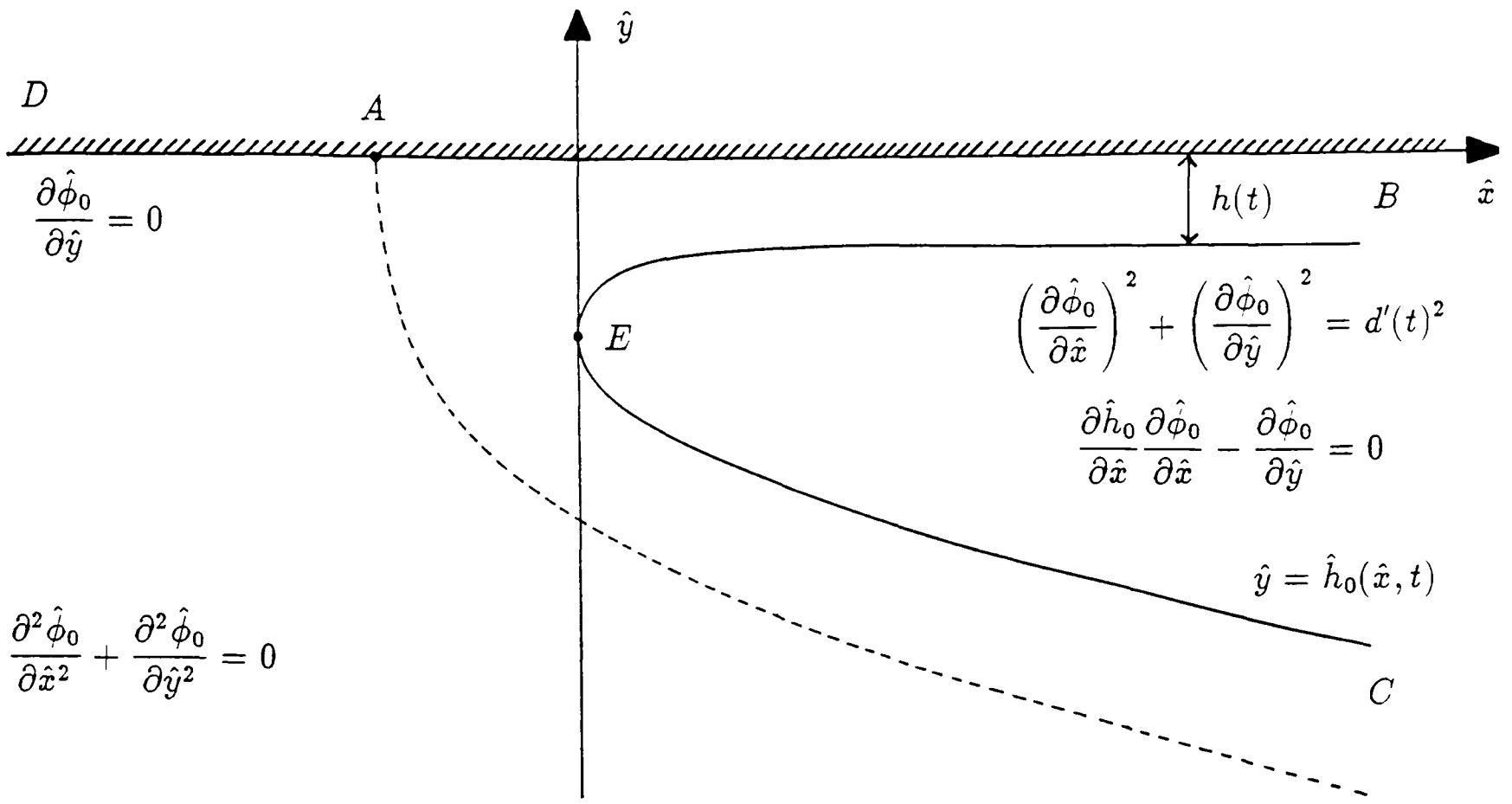

Figure 2.5: Leading order inner problem.

2.6.1 Solution of the Leading Order Inner Problem

The geometry of the leading order inner problem is shown in Figure (2.5). It is a Helmholtz cavity flow with a jet whose asymptotic thickness, denoted by $h(t)$, is unknown. To leading order the body is flat and, since no time derivatives appear in the problem, it is steady with time, t, only entering as a parameter. The most well-known steady, inviscid free streamline problem is the 'Borda Mouthpiece', and we can apply the same conformal mapping techniques, as described in Birkhoff & Zarantonello (1957) and Milne-Thomson (1968), to solve the present problem.

First we construct the scaled *complex potential plane* defined by

$$\hat{w}(\hat{z}) = \frac{1}{U}(\hat{\phi} + i\hat{\psi}),$$

where $\hat{\phi}$ and $\hat{\psi}$ are the velocity potential and stream function respectively and so $\hat{w}$ is an analytic function of $\hat{z} = \hat{x} + i\hat{y}$. U is a typical reference velocity and, since equation (2.56) tells us that the speed everywhere on the free streamline is $d'(t)$, this is the natural choice for U. We denote the image of the point A in

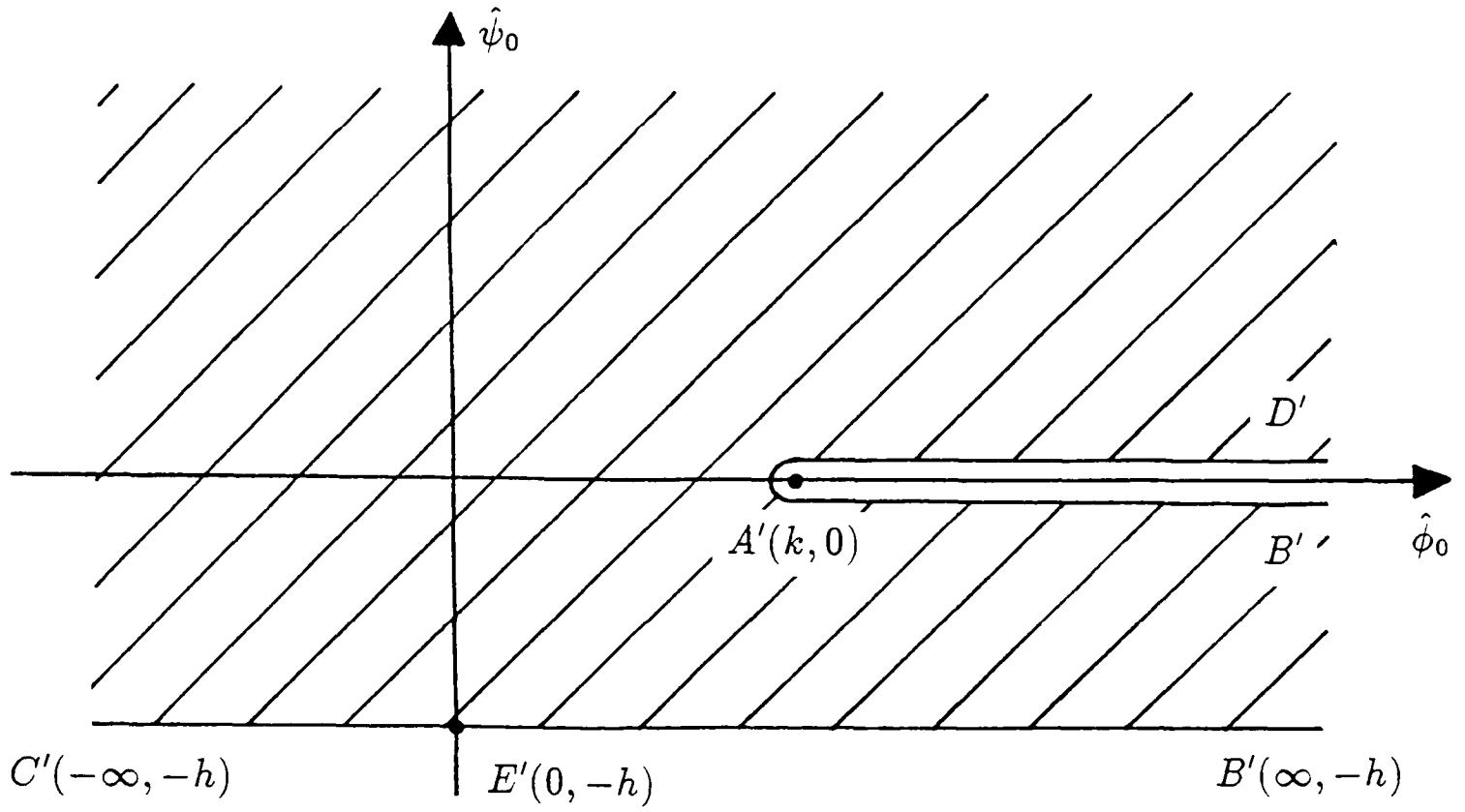

Figure 2.6: $\hat{w}$-plane.

the physical z-plane by A' in the $\hat{w}$-plane and so on. Since the rigid boundary and the free surface are streamlines they correspond to straight lines on which $\hat{\psi}$ is constant in the $\hat{w}$-plane. CA denotes the separating streamline of the flow and therefore A is the stagnation point on DB. Without loss of generality we take $\hat{\psi} = 0$ on the rigid boundary DB and choose $\hat{\phi} = k(t)d'(t)$, where $k(t)$ is unknown, at the stagnation point A. AB now maps to the upper side of a branch cut in the $\hat{w}$-plane from B' at $(k, 0)$ to A' at $(\infty, 0)$ and similarly AD maps to the lower side. Far down the jet there is a uniform parallel flow with velocity $d'(t)$ and thickness $h(t)$, and so $\hat{\psi} = -h(t)d'(t)$ on the free surface CEB, and $\hat{\phi}$ varies from $-\infty$ at C' to $+\infty$ at B'. The region occupied by fluid is, therefore, mapped to the fixed region in the $\hat{w}$-plane shown in Figure (2.6).

Now we construct the *hodograph plane* defined by

$$Q(\hat{w}) = \log\left(\frac{d\hat{z}}{d\hat{w}}\right),$$

where $\hat{w}(\hat{z})$ is the scaled complex velocity potential. Q is an analytic function of

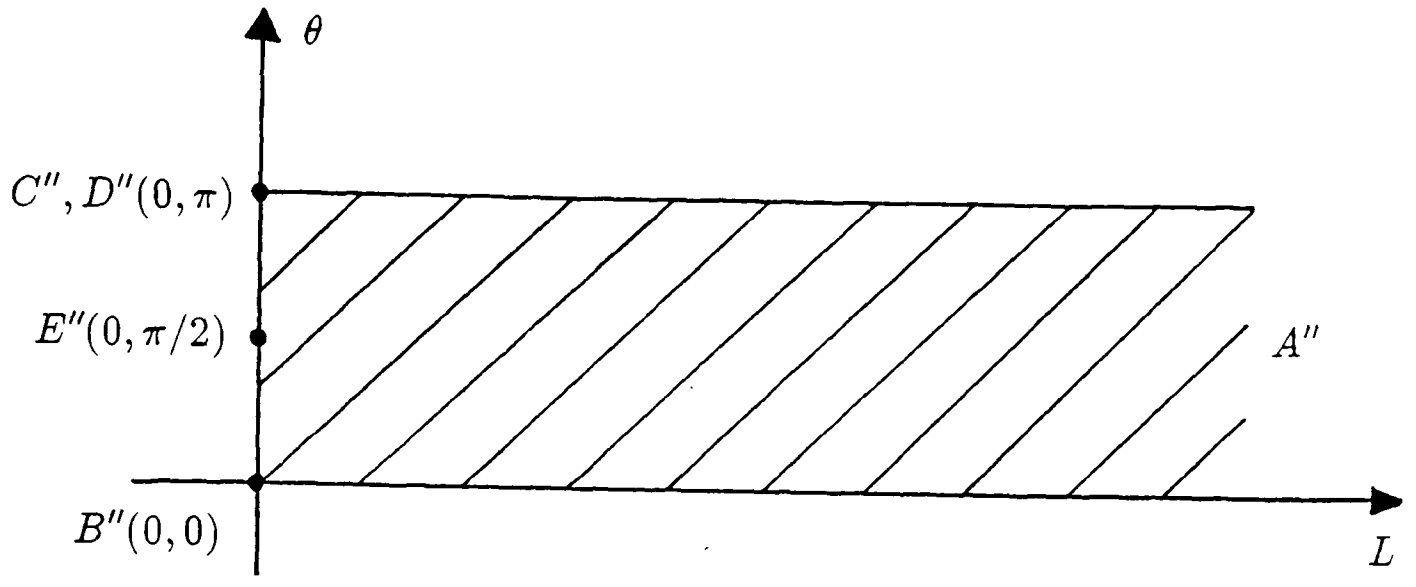

Figure 2.7: $Q(\hat{w})$-plane.

z and hence also of $\hat{w}(\hat{z})$. We motivate this definition by observing that

$$Q = L + i\theta,$$

where $L = \log |d\hat{z}/d\hat{w}|$ and θ is the direction of the fluid velocity, and so along a free streamline the fluid speed is constant and therefore L is constant, while on a fixed straight body the fluid velocity coincides with the direction of the body and so θ is constant. Hence we can determine the boundary of the region occupied by fluid in the hodograph plane. We construct the hodograph plane $Q(\hat{w})$ for the present problem, denoting the image of the point A by A''. The free surface CEB then maps to the line $L = 0$. At C θ equals π and moving along CEB θ decreases to $\pi/2$ at E and 0 at B. On AB θ is equal to zero and since the velocity is also zero at A, it maps to the point A'' at $(\infty, 0)$. Moving along AB towards B the fluid velocity increases towards its asymptotic value of $d'(t)$ and so L decreases towards zero at B'' while θ remains zero. Similarly moving along DA θ equals π and L decreases from infinity at A'' to zero at D''. The region occupied by fluid in the physical plane is therefore mapped to a region bounded by straight lines in the $Q(\hat{w})$-plane, viz. the semi-infinite strip shown in Figure (2.7).

The problem can now be solved if a conformal transformation can be found from the fluid region in the Q-plane onto the fluid region in the $\hat{w}$-plane, since then we can eliminate $Q(\hat{w})$ and, in theory, solve for $\hat{w}(\hat{z})$. To accomplish this

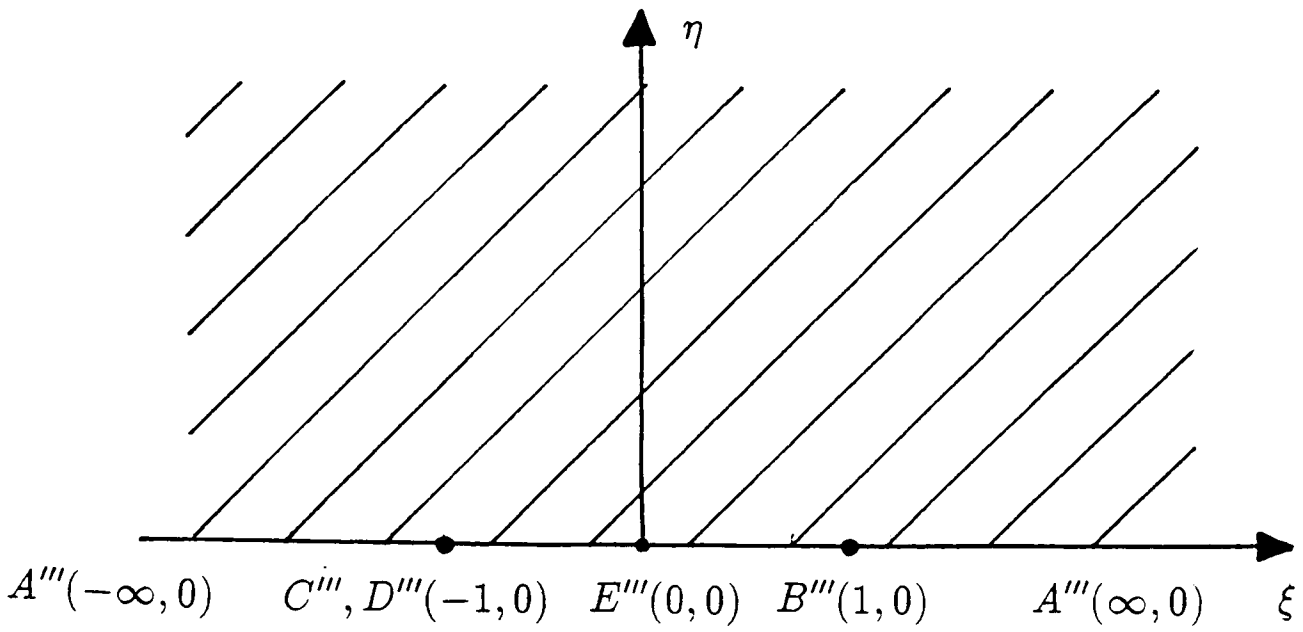

Figure 2.8: ζ-plane.

transformation we introduce an intermediate variable $\zeta = \xi + i\eta$ and map the fluid region in the Q-plane into the upper half of the ζ-plane, which is shown in Figure (2.8). E corresponds to E''' at the origin, D and C correspond to D''' and C''' at $(-1,0)$ and B maps to B''' at $(1,0)$. The well-known conformal mapping fixing these points is

$$\zeta = \cosh(Q(\hat{w})) = \frac{1}{2}\left[\hat{w}' + \frac{1}{\hat{w}'}\right], \tag{2.57}$$

where $\hat{w}'$ denotes $d\hat{w}/d\hat{z}$.

We must now find a conformal transformation from the fluid region in the $Q(\hat{w})$-plane onto the upper half of the ζ-plane. The required mapping is provided by the well-known Schwartz-Christoffel Transformation, from which we obtain

$$\frac{d\hat{w}}{d\zeta} = \frac{K}{(\zeta+1)^2(\zeta-1)}, \tag{2.58}$$

where K is a complex constant which is determined by the orientation in the fluid region to be $-h/\pi$. Integrating with respect to $\hat{z}$ we have

$$\hat{w} = k - \frac{h}{\pi}\left[\frac{2}{(\zeta+1)} + \log\left|\frac{\zeta-1}{\zeta+1}\right|\right], \tag{2.59}$$

where the constant of integration has been chosen appropriately. We can now eliminate ζ between (2.57) and (2.59) to obtain a nonlinear differential equation

for $\hat{w}(\hat{z})$, namely

$$\hat{w} = k - \frac{2h}{\pi}\left[\frac{2\hat{w}'}{(\hat{w}'+1)^2} + \log\left|\frac{\hat{w}'-1}{\hat{w}'+1}\right|\right]. \tag{2.60}$$

In principal, we could now integrate this equation to obtain $\hat{w}(\hat{z})$ and hence solve the problem. However, we shall not attempt to solve this equation here, since we can determine the properties of $\hat{w}(\hat{z})$ we require without deriving an explicit solution.

2.7 Matching of the Leading Order Solutions

Having derived the leading order terms in the inner and outer expansions we can now determine the scale of the inner region and the unknown asymptotic jet thickness by *matching* the two appropriately. Van Dyke (1975) discusses matching at length and states the *asymptotic matching principle* which dictates that, for all integers M and N, the M-th term inner expansion of (the N-th term outer expansion) equals the N-th term outer expansion of (the M-th term inner expansion). This rule will be sufficient for our present purposes if we take $M = N = 1$ and match the inner limit of the leading order outer solution with the outer limit of the leading order inner solution.

Written in inner variables the first term of the outer expansion of the velocity potential evaluated on the body is given by equation (2.36) as

$$-\frac{1}{\epsilon}\Re\left[d(t)^2 - \left(d(t) + \epsilon^{n+1}\hat{x}\right)^2\right]^{\frac{1}{2}}.$$

Expanding for small ϵ, and writing back in outer variables, we obtain an expression the one term inner expansion of the one term outer solution evaluated on the body,

$$-\frac{1}{\epsilon}\Re\left[-2d(t)\left(X - d(t)\right)\right]^{\frac{1}{2}}. \tag{2.61}$$

Without solving equation (2.60) we can still determine the far behaviour of the inner leading order solution. As $\hat{x} \to -\infty$ we know that $\hat{w} \sim -\hat{z}$, representing a uniform stream with speed $d'(t)$ in the negative $\hat{x}$-direction. We therefore write

$$\hat{w}(\hat{z}) = -\hat{z} + w(\hat{z})$$

and, by substituting into equation (2.60), we find that $w(\hat{z})$ satisfies the nonlinear differential equation

$$-\hat{z} + w = k - \frac{2h}{\pi}\left[2\frac{(-1+w')}{w'^2} + \log\left|\frac{-2+w'}{w'}\right|\right].$$

As $\hat{x} \to -\infty$ $w' \to 0$, and so the $1/w'^2$ term dominates the right side of the equation, which indicates that the asymptotic behaviour of $w'(\hat{z})$ is given by

$$w'^2 \sim -\frac{4h}{\pi\hat{z}} \quad \text{as} \quad \hat{x} \to -\infty.$$

Taking the appropriate square root, integrating once, and substituting back for $\hat{w}(\hat{z})$, we obtain the far behaviour of the scaled inner complex potential to be,

$$\hat{w} \sim -\hat{z} - 4i\left(\frac{h\hat{z}}{\pi}\right)^{\frac{1}{2}} \quad \text{as} \quad \hat{x} \to -\infty,$$

and so the inner velocity potential on the body is asymptotically equal to

$$\epsilon^{n-1}d'(t)\Re\left[-4i\left(\frac{h\hat{z}}{\pi}\right)^{\frac{1}{2}}\right] \quad \text{as} \quad \hat{x} \to -\infty.$$

Writing the velocity potential in outer variables we obtain

$$\epsilon^{n-1}d'(t)\Re\left[-4i\left(\frac{h(X-d(t))}{\pi\epsilon^{n+1}}\right)^{\frac{1}{2}}\right],$$

and so expanding for small ϵ and writing back in inner variables we find the one term outer expansion of the far behaviour of the one term inner expansion to be

$$\epsilon^{n-1}d'(t)\Re\left[-4i\left(\frac{h\hat{z}}{\pi}\right)^{\frac{1}{2}}\right] \quad \text{as} \quad \hat{x} \to -\infty. \tag{2.62}$$

The matching condition now requires that the outer inner limit of the outer expansion is equal to the inner limit of the outer expansion. The far behaviour of the inner is the correct quantity to match with the outer, and so, writing both (2.61) and (2.62) in original variables, we find that the one term inner of the one term outer is $O(\epsilon^{\frac{1}{2}})$ and the one term outer of the far behaviour of the inner is $O(\epsilon^{n-\frac{3}{2}})$. Evidently these orders must be the same and so $n = 1$. The scale of the inner region is, therefore, $O(\epsilon)$ and the velocity potential is $O(1)$.

Equating the coefficients of ϵ we obtain an expression for the asymptotic jet thickness $h(t)$ in terms of $d(t)$, namely

$$h(t) = \frac{\pi}{8}\frac{d(t)}{d'(t)^2}. \tag{2.63}$$

For completeness, we note that the second order inner problem is given by

$$\frac{\partial^2\hat{\phi}_1}{\partial\hat{x}^2} + \frac{\partial^2\hat{\phi}_1}{\partial\hat{y}^2} = 0 \quad \text{in the fluid,} \tag{2.64}$$

$$f'(d(t))\frac{\partial\hat{\phi}_0}{\partial\hat{x}} - \frac{\partial\hat{\phi}_1}{\partial\hat{y}} - \hat{x}f'(d(t))\frac{\partial^2\hat{\phi}_0}{\partial\hat{y}^2} = 1 \quad \text{on} \quad \hat{y} = 0, \tag{2.65}$$

$$\left[\frac{\partial\hat{\phi}_0}{\partial\hat{x}} + \hat{h}_1\frac{\partial^2\hat{\phi}_0}{\partial\hat{x}\partial\hat{y}}\right]\frac{\partial\hat{h}_0}{\partial\hat{x}} + \frac{\partial\hat{\phi}_0}{\partial\hat{x}}\frac{\partial\hat{h}_1}{\partial\hat{x}} - \frac{\partial\hat{\phi}_1}{\partial\hat{y}} - \hat{h}_1\frac{\partial^2\hat{\phi}_0}{\partial\hat{y}^2} + d'(t)f'(d(t)) - 1 = 0$$

$$\text{on } \hat{y} = \hat{h}_0(\hat{x}, t), \tag{2.66}$$

$$\frac{\partial\hat{\phi}_0}{\partial\hat{x}}\left[\frac{\partial\hat{\phi}_1}{\partial\hat{x}} + \hat{h}_1\frac{\partial^2\hat{\phi}_0}{\partial\hat{x}\partial\hat{y}}\right] + \frac{\partial\hat{\phi}_0}{\partial\hat{y}}\left[\frac{\partial\hat{\phi}_1}{\partial\hat{y}} + \hat{h}_1\frac{\partial^2\hat{\phi}_0}{\partial\hat{y}^2}\right] + (1 - d'(t)f'(d(t)))\frac{\partial\hat{\phi}_0}{\partial\hat{y}} = 0$$

$$\text{on } \hat{y} = \hat{h}_0(\hat{x}, t). \tag{2.67}$$

2.7.1 The Equations of the Streamlines

Without obtaining the solution of the leading order inner problem $\hat{w}(\hat{z})$ we can obtain implicitly the equations of the free streamline and the body. If $d\hat{z}$ is an element of a streamline parameterized by ξ then

$$d\hat{z} = \frac{d\hat{z}}{d\hat{w}}\frac{d\hat{w}}{d\xi}d\xi. \tag{2.68}$$

The free streamline CEB is mapped to the segment $-1 \leq \xi \leq 1$ of the real axis $\eta = 0$ in the ζ-plane, and so from (2.57) we obtain

$$\frac{d\hat{z}}{d\hat{w}} = \xi + i(1 - \xi^2)^{\frac{1}{2}},$$

and from equation (2.59)

$$\frac{d\hat{w}}{d\xi} = -\frac{4h}{\pi}\frac{1}{(\xi+1)^2(\xi-1)}.$$

Thus, taking a origin for $\hat{z}$ at E, corresponding to $\xi = 0$, we have

$$\hat{z} = -\frac{4h}{\pi}\int_0^{\xi}\frac{\xi + i(1-\xi^2)^{\frac{1}{2}}}{(\xi+1)^2(\xi-1)}\,\mathrm{d}\xi.$$

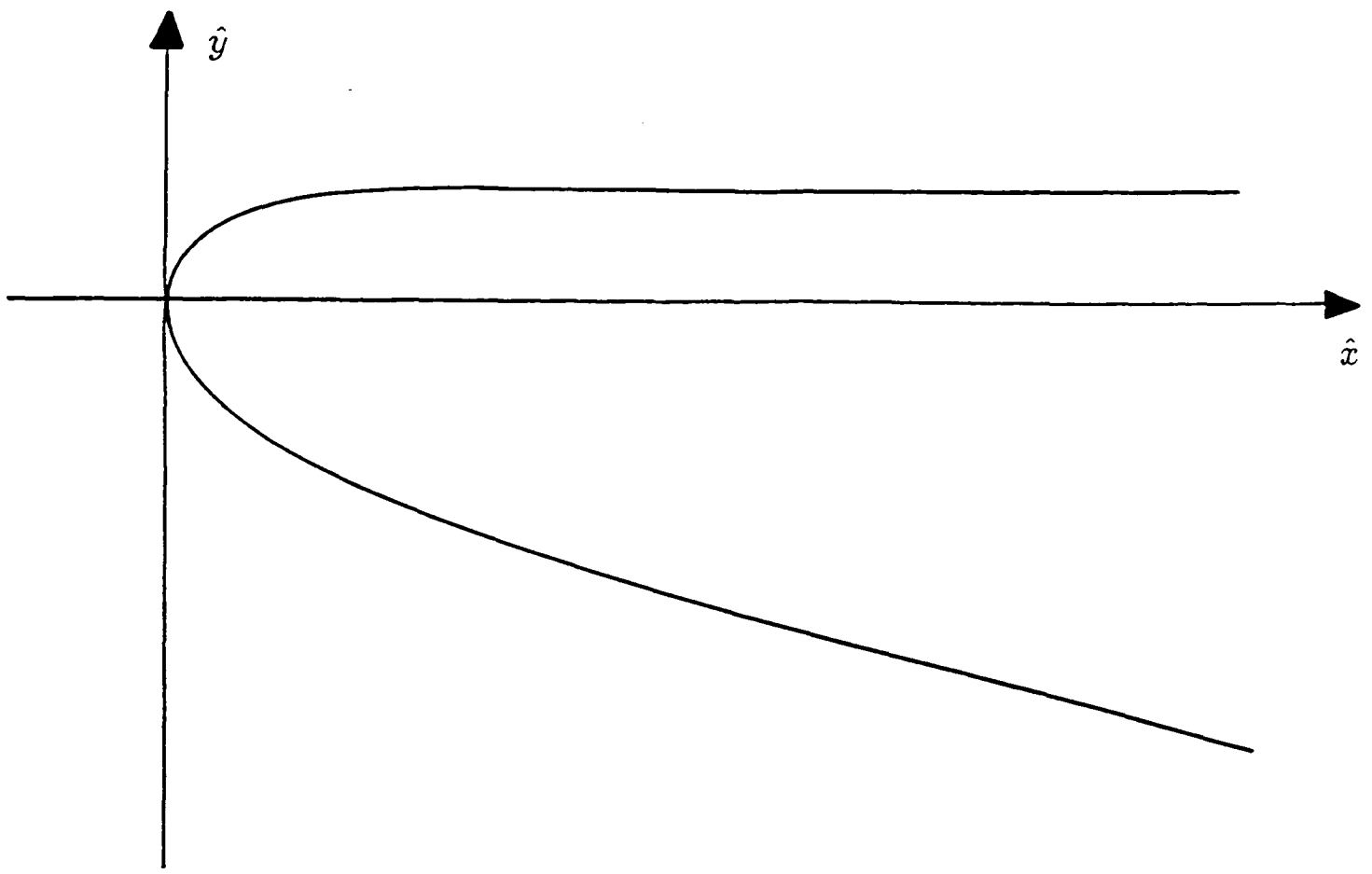

Figure 2.9: Leading order shape of inner free surface.

Performing the integration we obtain a formula for the shape of the free surface $\hat{x} = \hat{x}(\xi, t)$, $\hat{y} = \hat{y}(\xi, t)$ parameterized by ξ where $-1 \leq \xi \leq 1$, namely

$$\hat{x} = \frac{h}{\pi}\left[\log\left|\frac{1+\xi}{1-\xi}\right| - \frac{2\xi}{1+\xi}\right], \tag{2.69}$$

$$\hat{y} = \frac{4h}{\pi}\left[1 - \left(\frac{1-\xi}{1+\xi}\right)^{\frac{1}{2}}\right], \tag{2.70}$$

which is plotted in Figure (2.9).

The body DB is mapped to the regions $\xi \leq -1$ and $\xi \geq 1$ of the real axis $\eta = 0$ in the ζ-plane. From equation (2.57), and by choosing the signs to give the correct asymptotic behaviour, we obtain

$$\frac{d\hat{z}}{d\hat{w}} = \begin{cases} \xi - (\xi^2+1)^{\frac{1}{2}} & \text{for } \xi \leq -1, \\ \xi + (\xi^2+1)^{\frac{1}{2}} & \text{for } \xi \geq 1. \end{cases}$$

Thus, taking an origin for $\hat{z}$ at A, corresponding to $\xi = \pm\infty$, we have

$$\hat{z} = \begin{cases} -\dfrac{4h}{\pi}\displaystyle\int_{-\infty}^{\xi} \frac{\xi - (\xi^2-1)^{\frac{1}{2}}}{(\xi+1)^2(\xi-1)}\,\mathrm{d}\xi & \text{for } \xi \leq -1, \\ -\dfrac{4h}{\pi}\displaystyle\int_{\infty}^{\xi} \frac{\xi + (\xi^2-1)^{\frac{1}{2}}}{(\xi+1)^2(\xi-1)}\,\mathrm{d}\xi & \text{for } \xi \geq 1. \end{cases}$$

Performing the integration, we obtain a parameterization of the leading order shape of the body $\hat{x} = \hat{x}(\xi, t)$, $\hat{y} = \hat{y}(\xi, t)$ in terms of ξ, namely

$$\hat{x} = \frac{h}{\pi}\left[\log\left|\frac{\xi+1}{\xi-1}\right| - 4\left(\frac{\xi-1}{\xi+1}\right)^{\frac{1}{2}} + \frac{6+4\xi}{1+\xi}\right], \tag{2.71}$$

and of course

$$\hat{y} = 0. \tag{2.72}$$

2.7.2 The Pressure in the Inner Region

Once the velocity field is known, we can obtain the inner pressure distribution $\hat{p}(\hat{x}, \hat{y}, t)$ from Bernoulli's equation (2.4), which, when written in inner variables, gives

$$\frac{1}{2\epsilon^2}\left[\left(\frac{\partial\hat{\phi}}{\partial x}\right)^2 + \left(\frac{\partial\hat{\phi}}{\partial y}\right)^2 - d'(t)^2\right] + \frac{1}{\epsilon}\left[1 - d'(t)f'(d(t))\right]\frac{\partial\hat{\phi}}{\partial\hat{y}} + d''(t)\hat{x} + \frac{\partial\hat{\phi}}{\partial t} + \hat{p} = 0$$

Expanding $\hat{p}(\hat{x}, \hat{y}, t)$ as an asymptotic series in powers of ϵ, in the form

$$\hat{p} = \frac{1}{\epsilon^2}\hat{p}_0 + \frac{1}{\epsilon}\hat{p}_1 + \hat{p}_2 + O(\epsilon),$$

and substituting for $\hat{\phi}$, we obtain the leading order terms

$$-\hat{p}_0 = \frac{1}{2}\left[\left(\frac{\partial\hat{\phi}_0}{\partial\hat{x}}\right)^2 + \left(\frac{\partial\hat{\phi}_0}{\partial\hat{y}}\right)^2 - d'(t)^2\right] \tag{2.73}$$

$$-\hat{p}_1 = \frac{\partial\hat{\phi}_0}{\partial\hat{x}}\frac{\partial\hat{\phi}_1}{\partial\hat{x}} + \frac{\partial\hat{\phi}_0}{\partial\hat{y}}\frac{\partial\hat{\phi}_1}{\partial\hat{y}}. \tag{2.74}$$

In particular, the leading order inner pressure on the body is given in terms of quantities evaluated on $\hat{y} = 0$ as,

$$\hat{p}_0(\hat{x}, 0, t) = \frac{d'(t)^2}{2}\left[1 - (\xi \pm (\xi^2 - 1)^{\frac{1}{2}})^2\right], \tag{2.75}$$

where we take the positive square root for $\xi \leq -1$ and the negative square root for $\xi \geq 1$, and $\hat{x}$ is given as a function of ξ by equation (2.71). The maximum pressure occurs at the local stagnation point A, corresponding to $\xi = \pm\infty$, and is of magnitude

$$\frac{d'(t)^2}{2\epsilon^2},$$

which is evidently $O(1/\epsilon^2)$ compared to the $O(1/\epsilon)$ pressure in the outer region. The leading order inner pressure distribution on the body is shown in Figure (2.10).

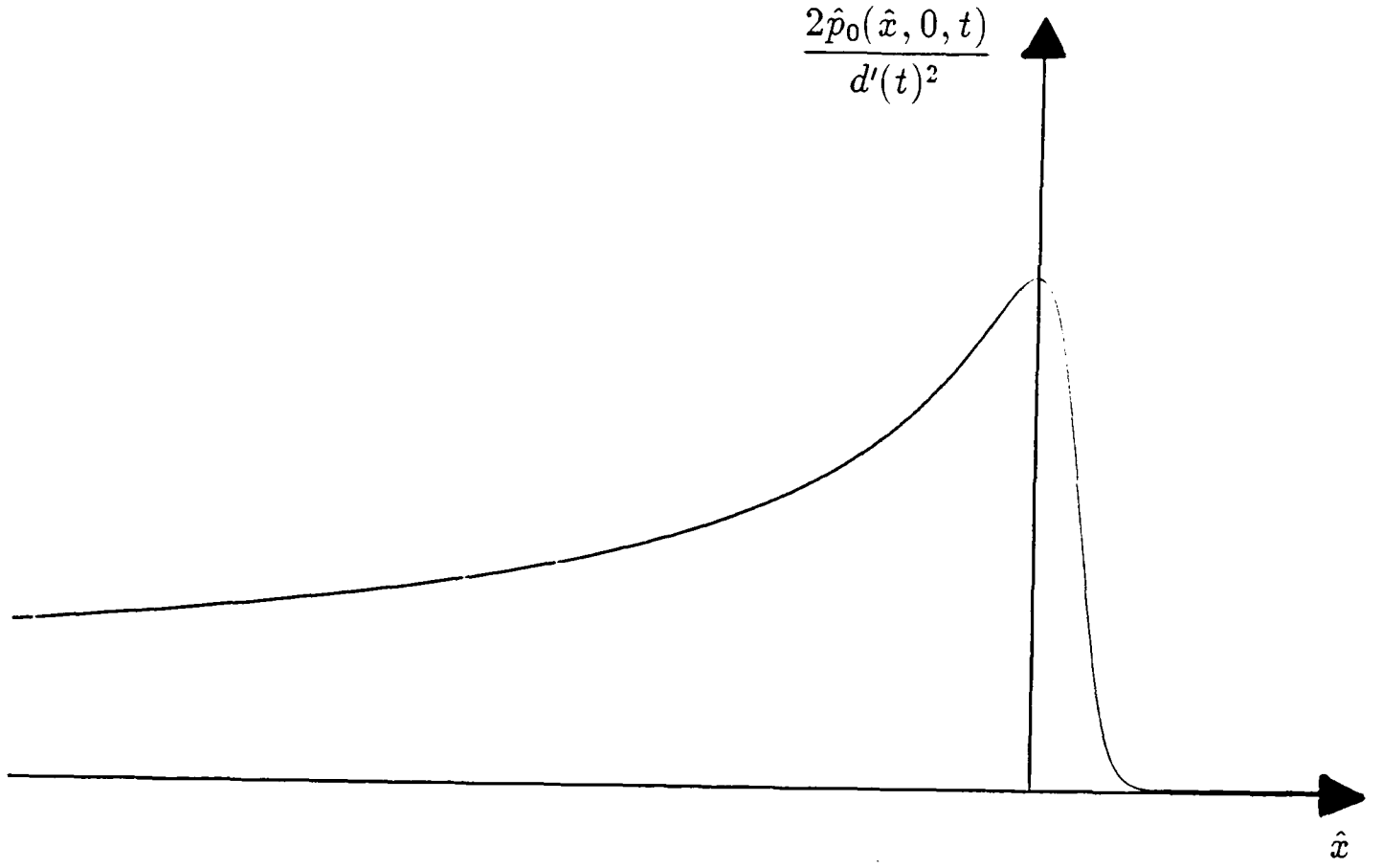

Figure 2.10: The leading order inner pressure distribution on the body.

2.8 The Jet Problem

The remaining region of the flow to be considered is that of the jet. We expect the jet to be a long, thin stream of fluid partially attached to the body and emanating from the inner region. The most appropriate coordinate system in which to investigate the jet will therefore be one conforming to the shape of the body and moving with it, as described in Milne-Thomson (1968). We choose curvilinear coordinates $(\bar{x},\bar{y})$ with $\bar{x}$ measured along the body and $\bar{y}$ measured normal it, as shown in Figure (2.11). Let the normal to the body passing through the point P, with coordinates $(\bar{x},\bar{y})$, meet the body at M, where the curvature of the body is $\kappa(\bar{x})$. C is the centre of curvature and PM is the perpendicular to the adjacent radius which passes through P' at $(\bar{x}+\delta\bar{x},\bar{y}+\delta\bar{y})$. If we measure $\bar{x}$ along the body from an origin at O, then $OM=\bar{x}$, $MM'=\delta\bar{x}$, $MP=\bar{y}$ and $NP'=\delta\bar{y}$. Hence,

$$\frac{PN}{\delta\bar{x}}=\frac{1/\kappa+\bar{y}}{1/\kappa}=1+\kappa\bar{y},$$

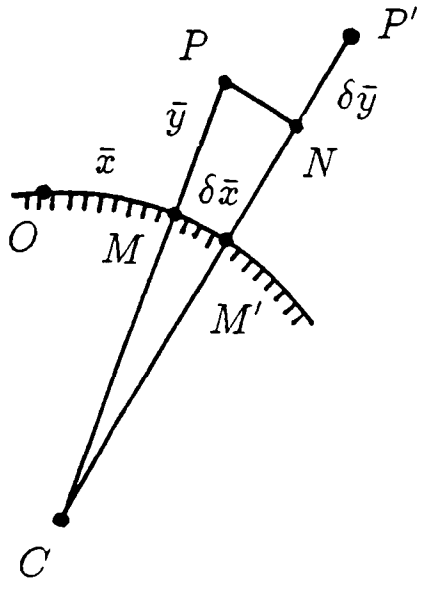

Figure 2.11: Curvilinear jet coordinate system.

and so $PN = (1 + \kappa\bar{y})\delta\bar{x}$. The appropriate scale factors h_1 and h_2 for this coordinate system are, therefore,

$$h_1 = 1 + \kappa\bar{y}, \qquad h_2 = 1.$$

In the new coordinates, the body is given by $\bar{y} = 0$ and, since from the scaling in the inner problem we expect the jet thickness to be $O(\epsilon)$, we write the free surface profile as $\bar{y} = \epsilon h(\bar{x}, t)$. In this coordinate system Laplace's equation (2.3) becomes

$$\frac{\kappa'\bar{y}}{(1+\kappa\bar{y})^2}\frac{\partial\phi}{\partial\bar{x}} + \frac{1}{1+\kappa\bar{y}}\frac{\partial^2\phi}{\partial\bar{x}^2} + \kappa\frac{\partial\phi}{\partial\bar{y}} + (1+\kappa\bar{y})\frac{\partial^2\phi}{\partial\bar{y}^2} = 0, \tag{2.76}$$

where κ' denotes $d\kappa/d\bar{x}$. The boundary condition on the body, $\bar{y} = 0$, is continuity of normal velocity between the body and the fluid and, therefore,

$$\frac{\partial\phi}{\partial\bar{y}} = 0 \quad \text{on} \quad \bar{y} = 0 \tag{2.77}$$

in the moving system. On the free surface $\bar{y} = \epsilon h(\bar{x}, t)$ we have the usual kinematic condition

$$\epsilon\left[\frac{\partial h}{\partial t} + \frac{1}{1+\kappa\bar{y}}\frac{\partial\phi}{\partial\bar{x}}\frac{\partial h}{\partial\bar{x}}\right] - \frac{\partial\phi}{\partial\bar{y}} = 0, \tag{2.78}$$

and pressure matching condition

$$\frac{\partial\phi}{\partial t} + \frac{1}{2}\left[\frac{1}{(1+\kappa\bar{y})^2}\left(\frac{\partial\phi}{\partial\bar{x}}\right)^2 + \left(\frac{\partial\phi}{\partial\bar{y}}\right)^2\right] = 0. \tag{2.79}$$

Motivated by the arc length conservation property in the case of wedge impacts, we expect the length of the jet to be $O(1/\epsilon)$ and, from the inner problem, to be of thickness $O(\epsilon)$. We therefore introduce scaled *jet variables* $\tilde{x}$ and $\tilde{y}$ defined by

$$\tilde{x} = \epsilon\bar{x}, \qquad \tilde{y} = \frac{\bar{y}}{\epsilon},$$

and, because the velocity of fluid flowing into the jet from the inner region is $O(1/\epsilon)$, define a scaled jet velocity potential, $\tilde{\phi}(\tilde{x}, \tilde{y}, t)$, by

$$\tilde{\phi} = \epsilon^2\phi.$$

The body is described in original variables by $y = f(\epsilon x)$ and so the curvature $\kappa(x)$ is

$$\kappa(x) = \frac{y''}{(1+y'^2)^{\frac{3}{2}}} = \frac{\epsilon^2 f''(\epsilon x)}{(1+\epsilon^2 f'(\epsilon x)^2)^{\frac{3}{2}}},$$

which is evidently $O(\epsilon^2)$. Therefore we introduce a new scaled jet curvature $\tilde{\kappa}(\tilde{x})$ so that

$$\kappa = \frac{\tilde{\kappa}}{\epsilon^2}.$$

Writing the equation (2.76) and the boundary conditions (2.77), (2.78) and (2.79) in jet variables we obtain the full jet problem, which has governing equation,

$$\frac{\epsilon^3\tilde{\kappa}'\tilde{y}}{(1+\epsilon^3\tilde{\kappa}\tilde{y})^2}\frac{\partial\tilde{\phi}}{\partial\tilde{x}} + \frac{1}{1+\epsilon^3\tilde{\kappa}\tilde{y}}\frac{\partial^2\tilde{\phi}}{\partial\tilde{x}^2} + \frac{\kappa}{\epsilon}\frac{\partial\tilde{\phi}}{\partial\tilde{y}} + \frac{(1+\epsilon^3\tilde{\kappa}\tilde{y})}{\epsilon^4}\frac{\partial^2\tilde{\phi}}{\partial\tilde{y}^2} = 0, \tag{2.80}$$

subject to the boundary conditions,

$$\frac{\partial\tilde{\phi}}{\partial\tilde{y}} = 0 \quad \text{on} \quad \tilde{y} = 0, \tag{2.81}$$

$$\epsilon^4\left[\frac{\partial\tilde{h}}{\partial t} + \frac{1}{1+\epsilon^3\tilde{\kappa}\tilde{y}}\frac{\partial\tilde{\phi}}{\partial\tilde{x}}\frac{\partial\tilde{h}}{\partial\tilde{x}}\right] - \frac{\partial\tilde{\phi}}{\partial\tilde{y}} = 0 \quad \text{on} \quad \tilde{y} = \tilde{h}(\tilde{x}, t), \tag{2.82}$$

$$\frac{\partial\tilde{\phi}}{\partial t} + \frac{1}{2}\left[\frac{1}{(1+\epsilon^3\tilde{\kappa}\tilde{y})^2}\left(\frac{\partial\tilde{\phi}}{\partial\tilde{x}}\right)^2 + \frac{1}{\epsilon^4}\left(\frac{\partial\tilde{\phi}}{\partial\tilde{y}}\right)^2\right] = 0 \quad \text{on} \quad \tilde{y} = \tilde{h}(\tilde{x}, t). \tag{2.83}$$

We now seek solutions for $\tilde{\phi}$ and $\tilde{h}$ as asymptotic series in powers of ϵ, in the form

$$\tilde{\phi} = \tilde{\phi}_0 + \epsilon\tilde{\phi}_1 + \epsilon^2\tilde{\phi}_2 + O(\epsilon^3),$$
$$\tilde{h} = \tilde{h}_0 + \epsilon\tilde{h}_1 + \epsilon^2\tilde{h}_2 + O(\epsilon^3).$$

Substituting into Laplace's equation (2.80), we obtain the leading order terms

$$\begin{aligned}
O(1) \qquad & \frac{\partial^2 \tilde{\phi}_0}{\partial \tilde{y}^2} = 0, \\
O(\epsilon) \qquad & \frac{\partial^2 \tilde{\phi}_1}{\partial \tilde{y}^2} = 0, \\
O(\epsilon^2) \qquad & \frac{\partial^2 \tilde{\phi}_2}{\partial \tilde{y}^2} = 0, \\
O(\epsilon^3) \qquad & \frac{\partial^2 \tilde{\phi}_3}{\partial \tilde{y}^2} + \tilde{\kappa}\tilde{y}\frac{\partial^2 \tilde{\phi}_0}{\partial \tilde{y}^2} + \tilde{\kappa}\frac{\partial \tilde{\phi}_0}{\partial \tilde{y}} = 0, \\
O(\epsilon^4) \qquad & \frac{\partial^2 \tilde{\phi}_4}{\partial \tilde{y}^2} + \tilde{\kappa}\tilde{y}\frac{\partial^2 \tilde{\phi}_1}{\partial \tilde{y}^2} + \tilde{\kappa}\frac{\partial \tilde{\phi}_1}{\partial \tilde{y}} + \frac{\partial^2 \tilde{\phi}_0}{\partial \tilde{x}^2} = 0.
\end{aligned}$$

Similarly, substituting into equation (2.77), the boundary condition the body $\tilde{y} = 0$, gives

$$\begin{aligned}
O(1) \qquad & \frac{\partial \tilde{\phi}_0}{\partial \tilde{y}} = 0, \\
O(\epsilon) \qquad & \frac{\partial \tilde{\phi}_1}{\partial \tilde{y}} = 0, \\
O(\epsilon^2) \qquad & \frac{\partial \tilde{\phi}_2}{\partial \tilde{y}} = 0, \\
O(\epsilon^3) \qquad & \frac{\partial \tilde{\phi}_3}{\partial \tilde{y}} = 0.
\end{aligned}$$

By integrating the governing equations and applying the boundary condition we deduce that $\tilde{\phi}_0$, $\tilde{\phi}_1$, $\tilde{\phi}_2$ and $\tilde{\phi}_3$ are independent of $\tilde{y}$, and that $\tilde{\phi}_4$ is given by

$$\tilde{\phi}_4(\tilde{x}, \tilde{y}, t) = -\frac{1}{2}\frac{\partial^2 \tilde{\phi}_0}{\partial \tilde{x}^2}\tilde{y}^2 + \beta_4(\tilde{x}, t),$$

where the function $\beta_4(\tilde{x}, t)$ is unknown. The leading order non-zero term in the expansion of the kinematic boundary condition (2.78) is, therefore,

$$\frac{\partial \tilde{h}_0}{\partial t} + \frac{\partial \tilde{\phi}_0}{\partial \tilde{x}}\frac{\partial \tilde{h}_0}{\partial \tilde{x}} - \frac{\partial \tilde{\phi}_4}{\partial \tilde{y}} = 0 \quad \text{on} \quad \tilde{y} = \tilde{h}_0(\tilde{x}, t)$$

and from the pressure condition (2.79) we obtain

$$\begin{aligned}
O(1) \qquad & \frac{\partial \tilde{\phi}_0}{\partial t} + \frac{1}{2}\left(\frac{\partial \tilde{\phi}_0}{\partial \tilde{x}}\right)^2 = 0, \\
O(\epsilon) \qquad & \frac{\partial \tilde{\phi}_1}{\partial t} + \frac{\partial \tilde{\phi}_0}{\partial \tilde{x}}\frac{\partial \tilde{\phi}_1}{\partial \tilde{x}} = 0, \\
O(\epsilon) \qquad & \frac{\partial \tilde{\phi}_2}{\partial t} + \frac{\partial \tilde{\phi}_0}{\partial \tilde{x}}\frac{\partial \tilde{\phi}_2}{\partial \tilde{x}} + \frac{1}{2}\left(\frac{\partial \tilde{\phi}_1}{\partial \tilde{x}}\right)^2 = 0, \\
O(\epsilon^2) \qquad & \frac{\partial \tilde{\phi}_3}{\partial t} + \frac{\partial \tilde{\phi}_0}{\partial \tilde{x}}\frac{\partial \tilde{\phi}_3}{\partial \tilde{x}} + \frac{\partial \tilde{\phi}_1}{\partial \tilde{x}}\frac{\partial \tilde{\phi}_2}{\partial \tilde{x}} + \tilde{\kappa}\tilde{h}_0\left(\frac{\partial \tilde{\phi}_0}{\partial \tilde{x}}\right)^2 = 0.
\end{aligned}$$

Substituting the solution for $\tilde{\phi}_4(\tilde{x}, \tilde{y}, t)$ into these equations we obtain two partial differential equations for the leading order velocity potential $\tilde{\phi}_0(\tilde{x}, t)$ and free surface profile $\tilde{h}_0(\tilde{x}, t)$,

$$\frac{\partial \tilde{h}_0}{\partial t} + \frac{\partial}{\partial \tilde{x}}\left(\tilde{h}_0 \frac{\partial \tilde{\phi}_0}{\partial \tilde{x}}\right) = 0, \tag{2.84}$$

$$\frac{\partial \tilde{\phi}_0}{\partial t} + \frac{1}{2}\left(\frac{\partial \tilde{\phi}_0}{\partial \tilde{x}}\right)^2 = 0. \tag{2.85}$$

If we introduce the leading order horizontal velocity $\tilde{u}_0(\tilde{x}, t)$, where $\tilde{u}_0(\tilde{x}, t) = \partial \tilde{\phi}_0 / \partial \tilde{x}$, and differentiate (2.85) once with respect to $\tilde{x}$, then we obtain the shallow water equations in the absence of gravity,

$$\frac{\partial \tilde{h}_0}{\partial t} + \frac{\partial}{\partial \tilde{x}}\left(\tilde{h}_0 \tilde{u}_0\right) = 0, \tag{2.86}$$

$$\frac{\partial \tilde{u}_0}{\partial t} + \tilde{u}_0 \frac{\partial \tilde{u}_0}{\partial \tilde{x}} = 0, \tag{2.87}$$

which is as we would expect, since they represent statements of conservation of mass and of momentum in a thin layer of fluid.

The appropriate boundary conditions on the velocity and free surface elevation are specified at the exit from the inner region $\tilde{x} = d(t)$, where both take their asymptotic values from the inner solution, and so

$$\tilde{u}_0(d(t), t) = 2d'(t), \qquad \tilde{h}_0(d(t), t) = h(t) = \frac{\pi}{8}\frac{d(t)}{d'(t)^2}.$$

The factor of two arises in the velocity condition to account for the motion of the entire inner region with velocity $d'(t)$ as well as the asymptotic value of the fluid velocity far down the jet in the inner problem, also $d'(t)$. The position of the jet tip is identified as the smallest value of $\tilde{x} > d(t)$ at which $\tilde{h}_0(\tilde{x}, t) = 0$. The leading order jet problem is summarised in Figure (2.12).

2.8.1 Solution of the Leading Order Jet Problem

Equations (2.86) and (2.87) are two first order quasi-linear hyperbolic equations and can therefore be solved using the method of characteristics as described, for example, in Ockendon & Tayler (1985). Equation (2.87) is a kinematic wave

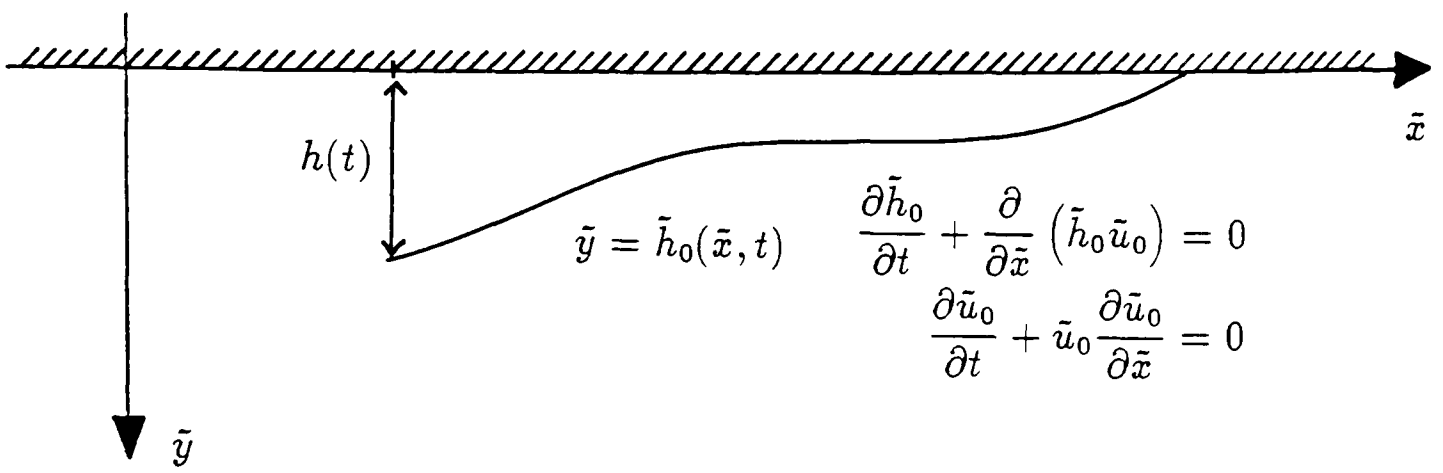

Figure 2.12: Leading order jet problem.

equation, and since it is independent of $\tilde{h}_0(\tilde{x}, t)$, it can be solved directly for $\tilde{u}_0(\tilde{x}, t)$. First we parameterize the boundary conditions by $\alpha \geq 0$ so that

$$\tilde{x} = d(\alpha), \quad t = \alpha, \quad \tilde{u}_0 = 2d'(\alpha), \quad \tilde{h}_0 = h(\alpha).$$

The characteristics can be parameterized by $\beta \geq 0$, and the characteristic equations of (2.86) are

$$\frac{\partial \tilde{x}}{\partial \beta} = \tilde{u}_0, \quad \frac{\partial t}{\partial \beta} = 1, \quad \frac{\partial \tilde{u}_0}{\partial \beta} = 0.$$

These equations can be readily integrated to give the solution implicitly, viz.

$$\tilde{x} = 2d'(\alpha)\beta + d(\alpha), \quad t = \alpha + \beta, \quad \tilde{u}_0 = 2d'(\alpha).$$

For any particular function $d(\cdot)$ we can attempt to eliminate α and β to obtain $\tilde{u}_0(\tilde{x}, t)$ explicitly. The result can then be substituted into equation (2.87), which can be solved for $\tilde{h}_0(\tilde{x}, t)$ in a similar manner, but we defer doing this until we consider specific body shapes later in the Chapter.

If we specify boundary data on $\tilde{x} = d(t)$ for all $t \geq 0$, then we expect to obtain a well defined solution for $\tilde{u}_0(\tilde{x}, t)$ in some region of $\tilde{x} \geq d(t)$. The domain of definition of the solution is limited by the curve on which the Jacobian $\partial(\tilde{x}, t)/\partial(\alpha, \beta)$ vanishes, corresponding to the locus of points where the inversion of $\tilde{x} = \tilde{x}(\alpha, \beta)$ and $t = t(\alpha, \beta)$ for $\alpha(\tilde{x}, t)$ and $\beta(\tilde{x}, t)$ fails. In the present problem, this statement yields the condition

$$d'(\alpha) - 2d''(\alpha)\beta = 0. \tag{2.88}$$

In particular, if the equivalent plate is expanding, $d'(t) > 0$, then shocks cannot occur in the solution for $\tilde{u}_0(\tilde{x}, t)$ if $d''(t) < 0$. If there is a curve in $\tilde{x} \geq d(t)$ on which equation (2.88) holds, then the earliest time, t^*, at which the solution fails is of interest. Differentiating (2.88) with respect to $\tilde{x}$ and setting the result equal to zero gives

$$[d''(\alpha) - 2d'''(\alpha)\beta] \frac{\partial \alpha}{\partial \tilde{x}} - 2d''(\alpha) \frac{\partial \beta}{\partial \tilde{x}} = 0.$$

Furthermore, since at any turning point of (2.88) $dt/d\tilde{x} = 0$, consequently,

$$\frac{dt}{d\tilde{x}} = \frac{\partial t}{\partial \alpha} \frac{\partial \alpha}{\partial \tilde{x}} + \frac{\partial t}{\partial \beta} \frac{\partial \beta}{\partial \tilde{x}} = \frac{\partial \alpha}{\partial \tilde{x}} + \frac{\partial \beta}{\partial \tilde{x}} = 0.$$

Eliminating either $\partial\alpha/\partial\tilde{x}$ or $\partial\beta/\partial\tilde{x}$ between these equations another relation between α and β can be obtained, namely

$$3d''(\alpha) - 2d'''(\alpha)\beta = 0. \tag{2.89}$$

Equations (2.88) and (2.89) can now be solved for α and β, and hence for $\tilde{x}^*$, the position of the first shock and t^*, the time when it occurs. Physically, the shock where the solution fails is a zero gravity hydraulic jump.

Finally, since there is a flow with speed $d'(t)/\epsilon$ from the inner region with asymptotic thickness $\epsilon h(t)$ into the jet, the volume flux is $h(t)d'(t)$, and so at time t the volume of fluid in the jet is

$$\int_0^t h(s)d'(s)\,\mathrm{d}s = \frac{\pi}{8} \int_0^t \frac{d(s)}{d'(s)}\,\mathrm{d}s. \tag{2.90}$$

Evidently the volume of fluid in the jet is $O(1)$, which is small compared with the $O(1/\epsilon)$ volume of fluid displaced by the body. This justifies our earlier assumption that led to the matching condition (2.45).

2.8.2 The Pressure in the Jet Region

Once the solution in the jet is known we can evaluate the leading order pressure in the jet $\tilde{p}(\tilde{x}, \tilde{y}, t)$ from Bernoulli's equation (2.4). Written in jet variables we have

$$\frac{\partial \tilde{\phi}}{\partial t} + \frac{1}{2}\left[\frac{1}{(1+\epsilon^3\tilde{\kappa}\tilde{y})^2}\left(\frac{\partial \tilde{\phi}}{\partial \tilde{x}}\right)^2 + \frac{1}{\epsilon^4}\left(\frac{\partial \tilde{\phi}}{\partial \tilde{y}}\right)^2\right] + \epsilon^2 \tilde{p} = 0,$$

and so, if we seek a solution for $\tilde{p}$ as an asymptotic series in powers of ϵ in the form

$$\tilde{p} = \frac{1}{\epsilon^2}\tilde{p}_0 + \frac{1}{\epsilon}\tilde{p}_1 + \tilde{p}_2 + \epsilon\tilde{p}_3 + O(\epsilon^2),$$

then the leading order pressures are given by

$$\begin{aligned}
-\tilde{p}_0 &= \frac{\partial\tilde{\phi}_0}{\partial t} + \frac{1}{2}\left(\frac{\partial\tilde{\phi}_0}{\partial\tilde{x}}\right)^2, \\
-\tilde{p}_1 &= \frac{\partial\tilde{\phi}_1}{\partial t} + \frac{\partial\tilde{\phi}_0}{\partial\tilde{x}}\frac{\partial\tilde{\phi}_1}{\partial\tilde{x}}, \\
-\tilde{p}_2 &= \frac{\partial\tilde{\phi}_2}{\partial t} + \frac{\partial\tilde{\phi}_0}{\partial\tilde{x}}\frac{\partial\tilde{\phi}_2}{\partial\tilde{x}} + \frac{1}{2}\left(\frac{\partial\tilde{\phi}_1}{\partial\tilde{x}}\right)^2, \\
-\tilde{p}_3 &= \frac{\partial\tilde{\phi}_3}{\partial t} + \frac{\partial\tilde{\phi}_0}{\partial\tilde{x}}\frac{\partial\tilde{\phi}_3}{\partial\tilde{x}} + \frac{\partial\tilde{\phi}_1}{\partial\tilde{x}}\frac{\partial\tilde{\phi}_2}{\partial\tilde{x}} + \tilde{\kappa}\tilde{y}\left(\frac{\partial\tilde{\phi}_0}{\partial\tilde{x}}\right)^2.
\end{aligned}$$

Referring to the pressure matching condition (2.79), we deduce that since $\tilde{p}_0$, $\tilde{p}_1$ and $\tilde{p}_2$ are functions of $\tilde{x}$ only they must be identically zero, and so the zero pressure on the free surface is impressed through the jet to at least $O(\epsilon)$. If the curvature $\tilde{\kappa}(\tilde{x})$ is everywhere zero then so is the pressure to all orders. Otherwise the leading order non-zero term is

$$\tilde{p}_3 = \tilde{\kappa}(\tilde{x})\tilde{u}_0(\tilde{x},t)^2\left(\tilde{h}_0(\tilde{x},t) - \tilde{y}\right),$$

which is precisely the pressure required to balance the centrifugal effect of flow around a curved body. In particular, the pressure on the body is

$$\tilde{p} = \epsilon\tilde{\kappa}(\tilde{x})\tilde{u}_0(\tilde{x},t)^2\tilde{h}_0(\tilde{x},t) + O(\epsilon^2), \tag{2.91}$$

which is evidently $O(\epsilon)$ compared to a pressure of $O(1/\epsilon)$ in the outer region and of $O(1/\epsilon^2)$ in the inner region. The sign of the pressure depends on the sign of the curvature. In particular, if the body is convex then $\tilde{\kappa} < 0$, and so the leading order pressure on the body will be negative, suggesting that, in the absence of surface effects, the jet will separate from the body. In a recent paper Vanden-Broeck & Keller (1989) have shown that even small amounts of surface tension can be the crucial in determining the position of separation points in inviscid flow, and so the naïve statement that the jet will separate where the pressure becomes negative should be treated with caution. Once separation has occurred the jet becomes a thin stream of fluid falling under gravity, and since

this problem has been addressed by Keller & Geer (1973) and Vanden-Broeck and Keller (1982) we shall not pursue it further here.

2.9 Construction of the Composite Expansion

Once the leading order inner, outer and jet solutions have been obtained we can construct a uniformly valid composite expansion. Construction of the composite expansion can be carried out in a number of different ways, and since such expansions are not unique they may yield different answers, but they will all be equivalent to the order of accuracy retained. Van Dyke (1975) discusses a number of methods but the simplest is *additive composition* where the sum of the outer and inner expansions is corrected by subtracting their common part. In the natural notation, where $f_i^{(M)}$ denotes the M-term inner expansion, and so on, the rule for additive composition is

$$f_c^{(M,N)} = f_i^{(M)} + f_o^{(N)} - \left[f_o^{(N)}\right]_i^{(M)} = f_o^{(N)} + f_i^{(M)} - \left[f_i^{(M)}\right]_o^{(N)}.$$

Since the inner potential is unknown we cannot construct the composite potential, but fortunately we can determine the composite expansion of the pressure on the body. Adopting the notation of the previous paragraph, the leading order term of the outer pressure on the body from equation (2.44) is

$$p_o^{(1)} = \frac{1}{\epsilon} \frac{d(t)d'(t)}{(d(t)^2 - X^2)^{\frac{1}{2}}} \quad \text{for} \quad X < d(t).$$

The leading order term of the inner pressure on the body is given in equation (2.75) to be

$$p_i^{(1)} = \frac{d'(t)^2}{2\epsilon^2} \left[1 - (\xi \pm (\xi^2 - 1)^{\frac{1}{2}})^2\right],$$

where we take the plus sign for $\xi \leq -1$ and the minus sign for $\xi \geq 1$, and $\hat{x}$ is given in terms of ξ by equation (2.71). The leading order pressure due to the jet is

$$p_j^{(1)} = \epsilon \tilde{\kappa}(\tilde{x}) \tilde{h}_0(\tilde{x}, t) \tilde{u}_0(\tilde{x}, t)^2 \quad \text{for} \quad \tilde{x} > d(t).$$

On the portion of the wetted body surface corresponding to the equivalent plate in the outer solution $|x| \leq d(t)/\epsilon$ the total pressure is due to the pressure in the inner and the outer solutions. Their common part is easily calculated by taking

the one term inner expansion of the one term outer pressure. Written in inner variables this is

$$\frac{1}{\epsilon}\frac{d(t)d'(t)}{(d(t)^2-(d(t)+\epsilon^2\hat{x})^2)^{\frac{1}{2}}},$$

and so, expanding for small ϵ, this gives

$$\left[p_o^{(1)}\right]_i^{(1)} = \frac{1}{\epsilon^2}\frac{d(t)^{\frac{1}{2}}d'(t)}{(-2\hat{x})^{\frac{1}{2}}},$$

and the composite pressure on $|x| \leq d(t)/\epsilon$ is therefore

$$p_c^{(1,1)} = p_i^{(1)} + p_o^{(1)} - \left[p_o^{(1)}\right]_i^{(1)}. \tag{2.92}$$

On the remainder of the wetted body surface, corresponding to the jet in $|x| \geq d(t)/\epsilon$, the total pressure in due to the pressure in the inner and the jet solutions. The composite pressure is therefore

$$p_c^{(1,1)} = p_i^{(1)} + p_j^{(1)} - \left[p_j^{(1)}\right]_i^{(1)}, \tag{2.93}$$

where the form of $\left[p_j^{(1)}\right]_i^{(1)}$ will be calculated for specific body shapes later in the chapter.

2.10 The Total Force on the Body

The total force per unit width exerted on the impacting body can be evaluated by integrating the composite pressure distribution over the body. The leading order term in the outer pressure is of order $O(1/\epsilon)$ and, since it acts over a length of $O(1/\epsilon)$, it produces a force of $O(1/\epsilon^2)$. The leading term in the expansion of the inner pressure despite being $O(1/\epsilon^2)$ acts over a $O(\epsilon)$ length producing a $O(1/\epsilon)$ force and consequently makes no contribution to the force at leading order. Similarly the pressure due to the jet is $O(\epsilon)$ acting over a $O(1/\epsilon)$ length and so the resulting force is only $O(1)$, and its contribution to the expression for the force enters at third order.

If we write the total force, $F(t)$, as an asymptotic series in powers of ϵ in the form

$$F(t) = \frac{1}{\epsilon^2}F_0(t) + \frac{1}{\epsilon}F_1(t) + F_2(t) + O(\epsilon),$$

then the leading order term is due solely to the outer solution. The force on the equivalent plate in the outer solution is evaluated by integrating $P_0(X,t)$ from $X=-d(t)$ to $X=d(t)$ to give

$$F_0(t)=\int_{-d(t)}^{d(t)}P_0(X,t)\,\mathrm{d}X=d(t)d'(t)\int_{-d(t)}^{d(t)}\frac{\mathrm{d}X}{(d(t)^2-X^2)^{\frac{1}{2}}}=\pi d(t)d'(t). \quad (2.94)$$

Wagner (1932) neglected the pressure in the jet and the inner region and calculated this formula directly from the flat plate solution without comment.

2.11 Examples of Impacting Bodies

In this section we calculate the leading order solution in the outer and jet regions for a number of simple body shapes and construct the resulting composite pressure distributions. In each case the procedure is the same. First, we identify the small parameter ϵ in terms of the constants defining the body shape by writing the body in the form $y=f(\epsilon x)$, and insisting for definiteness that $f(1)=1$. Then we determine the function $d(t)$, describing the width of the equivalent plate, by substituting for $f(\cdot)$ into the solution of the integral equation (2.47). The solution of the jet problem can be obtained by solving equations (2.86) and (2.87), and finally the composite pressure distribution on the body can be evaluated from equations (2.92) and (2.93).

2.11.1 Wedge

The simplest impacting body is a *wedge*, $y=m|x|$. We can write the profile in the form $y=f(\epsilon x)$ by choosing $f(x)=|x|$ and defining the small parameter ϵ so that $\epsilon=m$. The theory is therefore applicable to wedges with small deadrise angle such that $m\ll 1$. Substituting $f(\cdot)$ into the solution of the integral equation arising from the free surface matching condition (2.47), we obtain

$$t(d)=\frac{2}{\pi}\int_0^d\frac{\xi}{(d^2-\xi^2)^{\frac{1}{2}}}\,\mathrm{d}\xi=\frac{2d}{\pi},$$

which gives Wagner's (1932) result that

$$d(t)=\frac{\pi t}{2}. \quad (2.95)$$

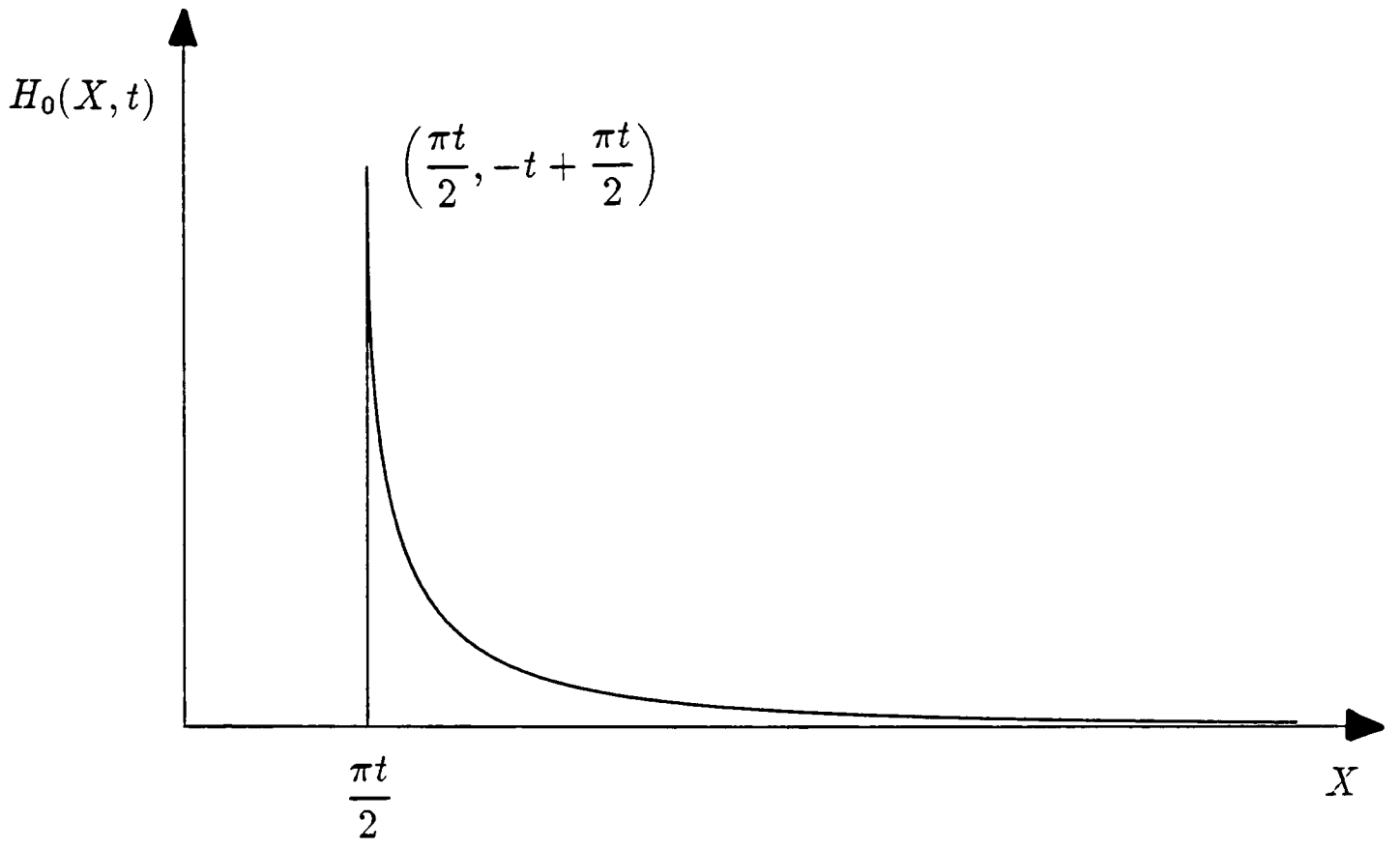

Figure 2.13: Leading order outer free surface elevation for a wedge shaped body.

Notice that $d(t)$ is linearly dependent on t, in accordance with the self-similarity of the wedge impact problem. Since the maximum pressure occurs at the point $x = d(t)/\epsilon$, it will always be a factor of $\pi/2 \simeq 1.571$ further from $x = 0$ than the point of intersection between the body and the level of the undisturbed fluid surface.

We can now evaluate the leading order shape of the outer free surface using equation (2.38) to be

$$H_0(X,t) = -t + \frac{2X}{\pi}\int_0^{\frac{\pi t}{2}} \frac{\mathrm{d}\tau}{(X^2-\tau^2)^{\frac{1}{2}}} = -t + \frac{2X}{\pi}\sin^{-1}\left(\frac{\pi t}{2X}\right), \qquad (2.96)$$

which is shown is Figure (2.13). From (2.63) the asymptotic jet thickness in the inner region is

$$h(t) = \frac{\pi}{8}\frac{d(t)}{d'(t)^2} = \frac{t}{4}.$$

In the leading order jet problem, equation (2.87) has parametric solution

$$\tilde{x}(\alpha,\beta) = \frac{\pi}{2}(2\alpha+\beta), \quad t(\alpha,\beta) = \alpha+\beta, \quad \tilde{u}_0(\alpha,\beta) = \pi,$$

and so equation (2.86) takes the form

$$\frac{\partial \tilde{h}_0}{\partial t} + \pi\frac{\partial \tilde{h}_0}{\partial \tilde{x}} = 0,$$

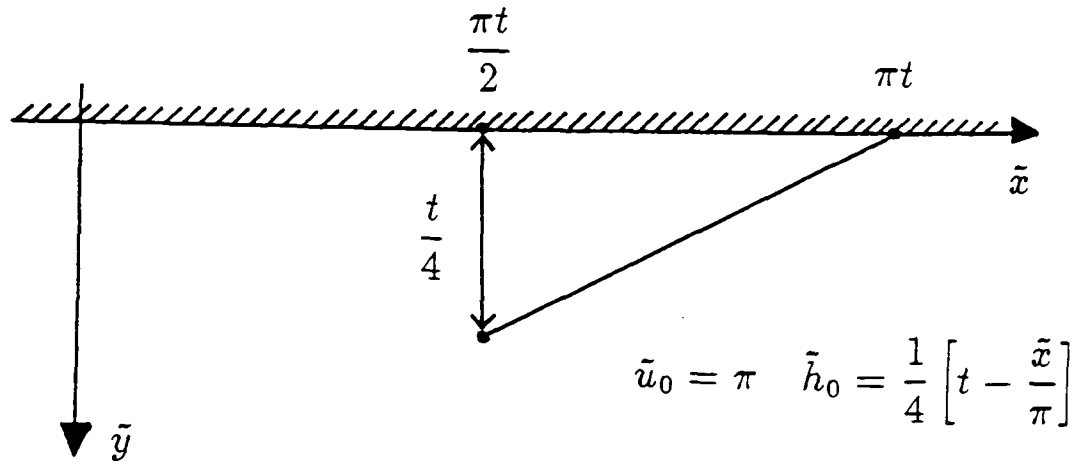

Figure 2.14: Leading order jet solution for a wedge shaped body.

which has characteristic equations

$$\frac{\partial \tilde{x}}{\partial \gamma} = \pi, \quad \frac{\partial t}{\partial \gamma} = 1, \quad \frac{\partial \tilde{h}_0}{\partial \gamma} = 0.$$

Subject to the boundary conditions

$$\tilde{x}(0,\delta) = \frac{\pi\delta}{2}, \quad t(0,\delta) = \delta, \quad \tilde{h}_0(0,\delta) = \frac{\delta}{4} \quad \text{for} \quad \delta \geq 0,$$

the parametric solution is

$$\tilde{x}(\gamma,\delta) = \frac{\pi}{2}(2\gamma + \delta), \quad t(\gamma,\delta) = \gamma + \delta, \quad \tilde{h}_0(\gamma,\delta) = \frac{\delta}{4},$$

which can be written explicitly as

$$\tilde{u}_0(\tilde{x},t) = \pi, \quad \tilde{h}_0(\tilde{x},t) = \frac{1}{4}\left[t - \frac{\tilde{x}}{\pi}\right], \tag{2.97}$$

as shown in Figure (2.14). (A simple check on the algebra is to verify by direct integration that the mass of fluid in the jet is equal to the value of $\pi t^2/16$ predicted by equation (2.90).) The tip of the jet is evidently at $\tilde{x} = \pi t$, and so the arc length of the jet surface is $\pi t/2\epsilon + O(1)$, in agreement with the arc length conservation property for wedge impacts. The condition for shocks to form in the solution for $\tilde{h}_0(\tilde{x},t)$ is that the Jacobian $\partial(\tilde{x},t)/\partial(\gamma,\delta)$ should vanish. This never occurs, and so both $\tilde{u}_0(\tilde{x},t)$ and $\tilde{h}_0(\tilde{x},t)$ are well defined for $t \geq 0$.

Since the surface of the body is flat there are no curvature terms in the Bernoulli equation (2.79), and so the zero pressure on the free surface of the jet is impressed through to all orders, and the pressure on the wedge in the jet

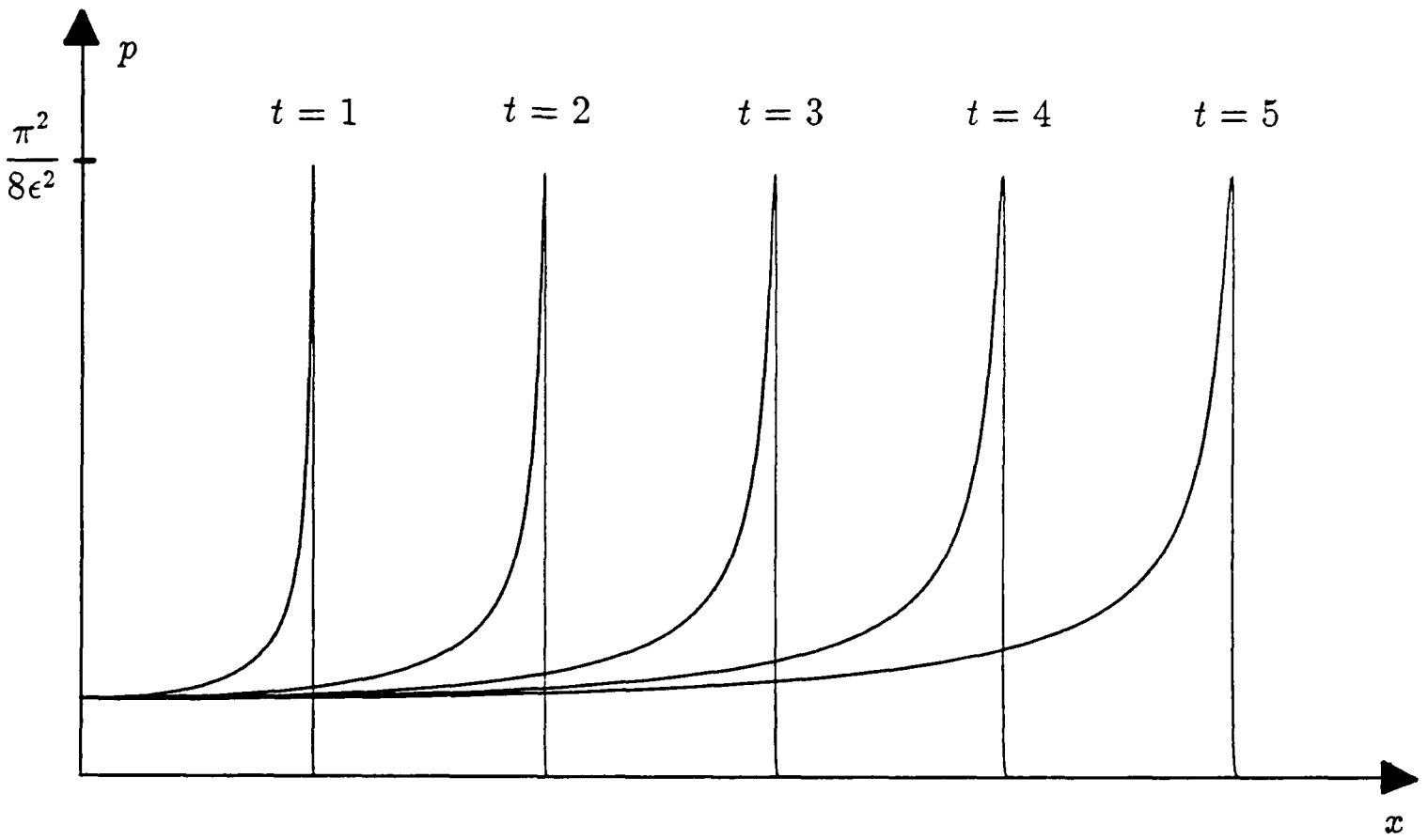

Figure 2.15: Leading order composite pressure distributions on a wedge.

region is identically zero.[1] The composite pressure distribution on the wedge can therefore be evaluated using equations (2.92) and (2.93), after taking

$$p_j^{(1)} = \left[p_j^{(1)}\right]_i^{(1)} = 0.$$

Figure (2.15) shows a sequence of pressure distributions at different times, and Figure (2.16) shows a typical set of pressure histories measured at equally spaced points on the wedge face. Since the maximum pressure is $d'(t)^2/2\epsilon^2 = \pi^2/8\epsilon^2$, which is a constant, all the peaks are of equal height, and as $t \to 0^+$ the pressure at $x = 0$ has a discontinuity of this magnitude. Also, in accordance with the self-similarity of the problem, the pressure history graphs are the same curve subjected to a translation in the t-direction proportional to distance away from the wedge vertex. The leading order force on the body is given by $\pi d(t)d'(t)/\epsilon^2 = \pi^3 t/4\epsilon^2$.

[1]The zero pressure in the jet region explains why the inevitable errors in the numerical calculations of Greenhow (1987) led to a small negative pressure on the upper part of the wedge face, which suggested, in violation of the self-similarity property, that the jet would separate.

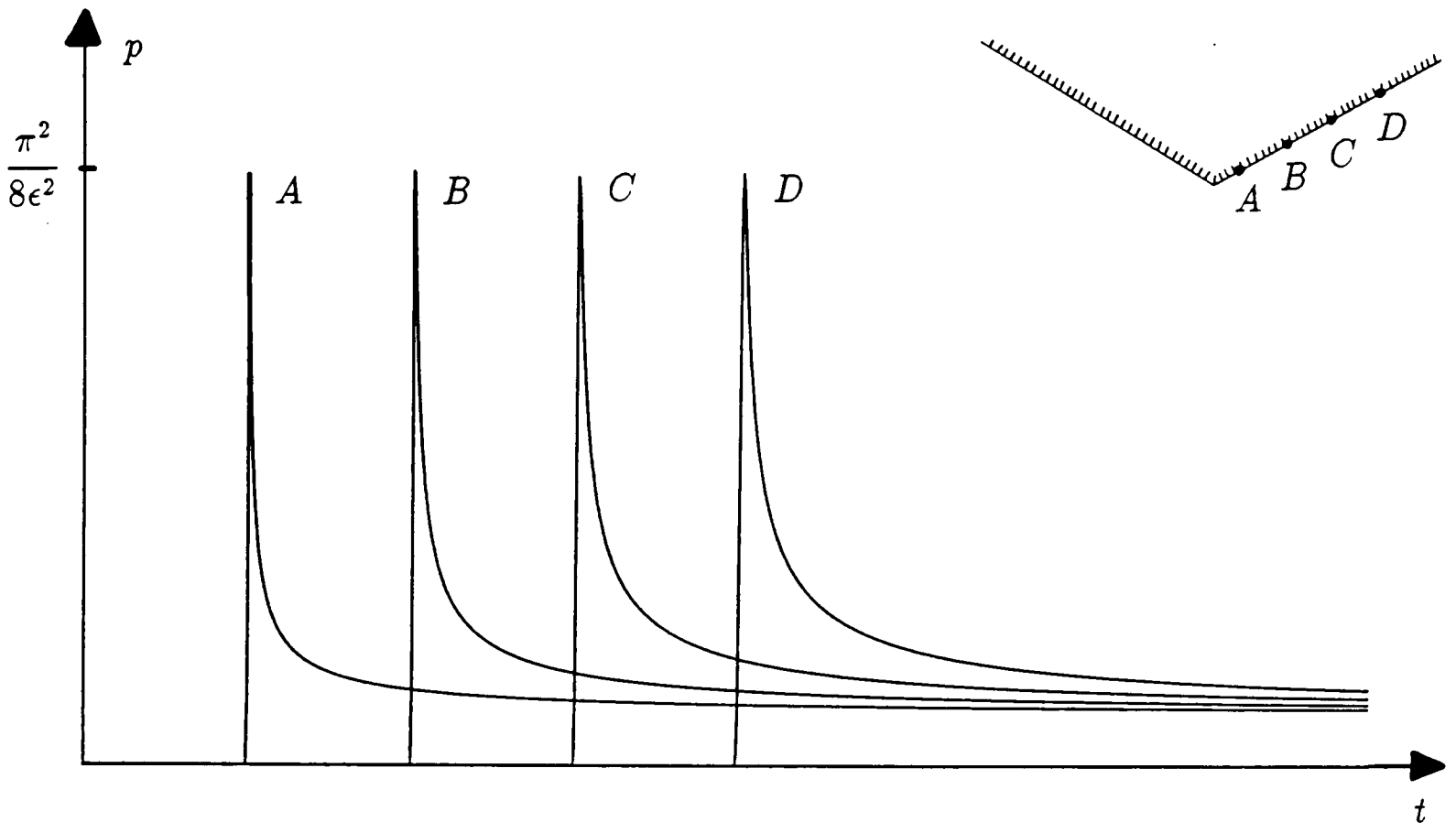

Figure 2.16: Leading order composite pressure histories for a wedge.

2.11.2 Parabola

We now consider the impact of a *parabolic* body, $y = mx^2$. We can write the profile in the form $y = f(\epsilon x)$ by choosing $f(x) = x^2$ and defining the small parameter ϵ so that $\epsilon = m^{\frac{1}{2}}$. The theory is therefore applicable to parabolic bodies whose deadrise angle is everywhere small such that $m^{\frac{1}{2}} \ll 1$. Substituting $f(\cdot)$ into the solution of the integral equation (2.47) we obtain

$$t(d) = \frac{2}{\pi}\int_0^d \frac{\xi^2}{(d^2-\xi^2)^{\frac{1}{2}}}\,\mathrm{d}\xi = \frac{d^2}{2},$$

and so inverting gives

$$d(t) = (2t)^{\frac{1}{2}}. \tag{2.98}$$

The maximum pressure occurs at the point $x = d(t)/\epsilon$, and so it will always be a factor of $\sqrt{2} \simeq 1.414$ further from $x = 0$ than the point of intersection between the body and the level of the undisturbed fluid surface.

We can now evaluate the leading order shape of the outer free surface us-

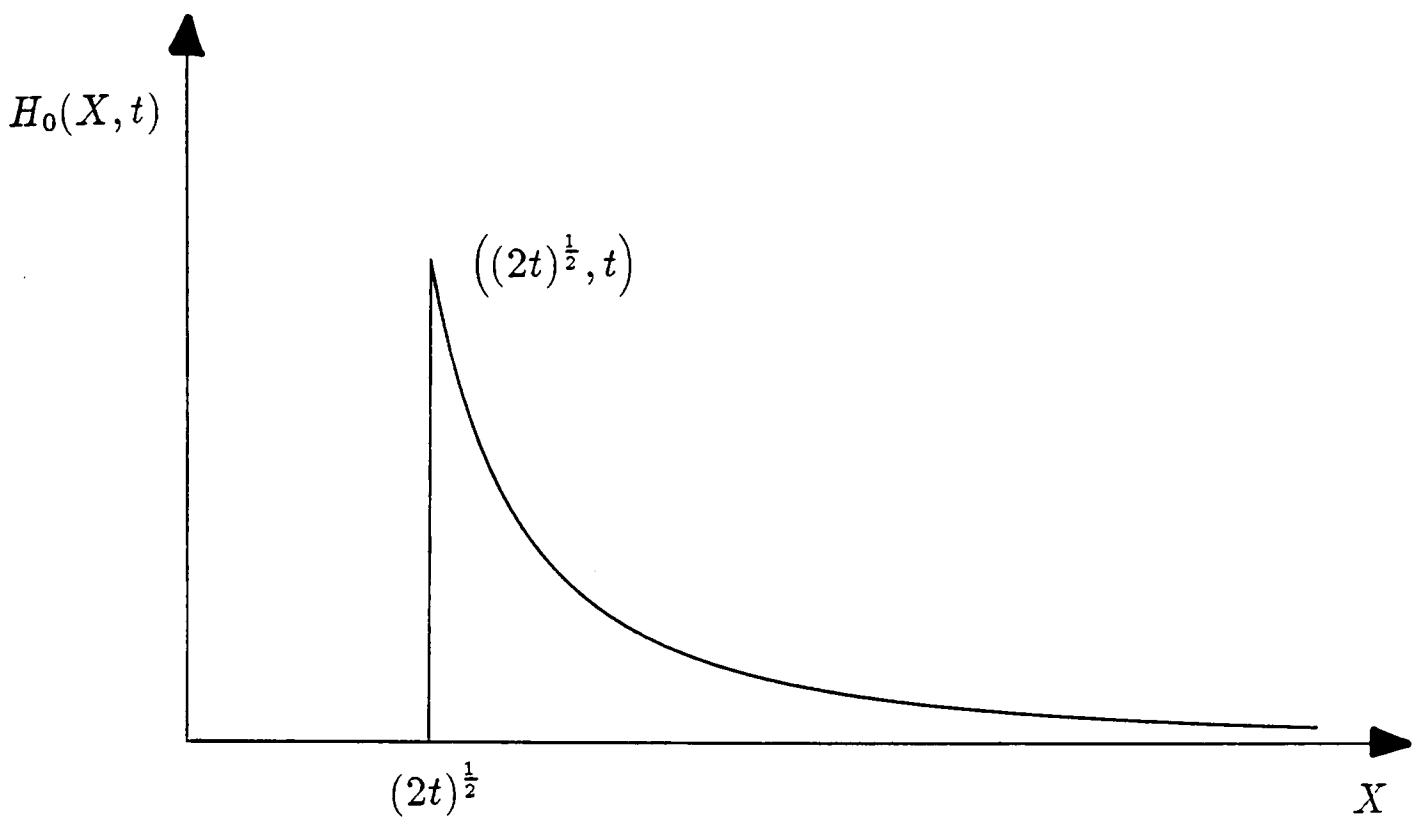

Figure 2.17: Leading order free surface elevation for a parabolic body.

ing (2.38) to be

$$H_0(X,t) = -t + \frac{2X}{\pi}\int_0^t \frac{\mathrm{d}\tau}{(X^2-2\tau)^{\frac{1}{2}}} = -t - X(X^2-2t)^{\frac{1}{2}} + X^2 \qquad (2.99)$$

which is shown is Figure (2.17). From (2.63) the asymptotic jet thickness in the inner region is

$$h(t) = \frac{\pi}{8}\frac{d(t)}{d'(t)^2} = \frac{\pi t^{\frac{3}{2}}}{2\sqrt{2}}.$$

In the leading order jet problem, equation (2.87) has parametric solution

$$\tilde{x}(\alpha,\beta) = \sqrt{2}\left(\beta\alpha^{-\frac{1}{2}} + \alpha^{\frac{1}{2}}\right), \quad t(\alpha,\beta) = \alpha+\beta, \quad \tilde{u}_0(\alpha,\beta) = \sqrt{2}\alpha^{-\frac{1}{2}},$$

which can be written explicitly as $\tilde{u}_0(\tilde{x},t) = \tilde{x}/t$. Equation (2.86) now takes the form

$$t\frac{\partial \tilde{h}_0}{\partial t} + \tilde{x}\frac{\partial \tilde{h}_0}{\partial \tilde{x}} + \tilde{h}_0 = 0,$$

which has characteristic equations

$$\frac{\partial \tilde{x}}{\partial \gamma} = \tilde{x}, \quad \frac{\partial t}{\partial \gamma} = t, \quad \frac{\partial \tilde{h}_0}{\partial \gamma} = -\tilde{h}_0.$$

Subject to the boundary conditions

$$\tilde{x}(0,\delta) = \sqrt{2}\delta^{\frac{1}{2}}, \quad t(0,\delta) = \delta, \quad \tilde{h}_0(0,\delta) = \frac{\pi\delta^{\frac{3}{2}}}{2\sqrt{2}}, \quad \text{for} \quad \delta \geq 0,$$

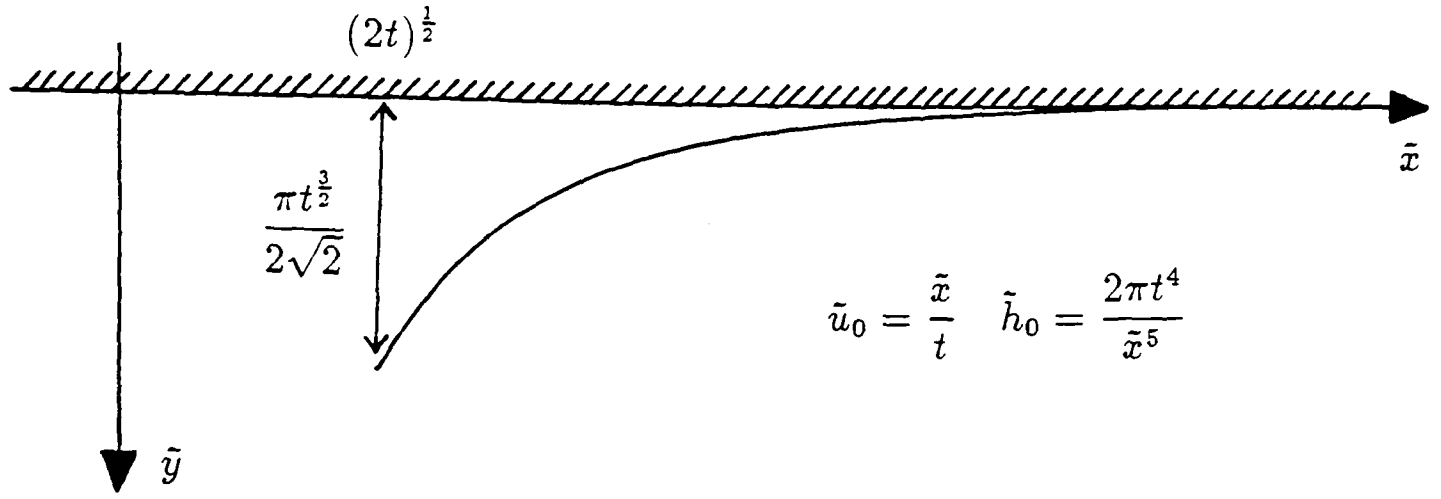

Figure 2.18: Leading order jet solution for a parabolic body.

the parametric solution is

$$\tilde{x}(\gamma,\delta) = \sqrt{2}\delta^{\frac{1}{2}}e^{\gamma}, \quad t(\gamma,\delta) = \delta e^{\gamma}, \quad \tilde{h}_0(\gamma,\delta) = \frac{\pi\delta^{\frac{3}{2}}}{2\sqrt{2}}e^{-\gamma},$$

which can be written explicitly as

$$\tilde{u}_0(\tilde{x},t) = \frac{\tilde{x}}{t}, \quad \tilde{h}_0(\tilde{x},t) = 2\pi\frac{t^4}{\tilde{x}^5}, \tag{2.100}$$

as shown in Figure (2.18). (Again we can verify by direct integration that the mass of fluid in the jet is equal to the value of $\pi t^2/8$ predicted by equation (2.90).) The tip of the jet is evidently at $\tilde{x} = +\infty$ in contrast to the case of a wedge impact where it is at $\tilde{x} = \pi t$. The condition for shocks to form in the solution for $\tilde{u}_0(\tilde{x},t)$, from equation (2.88), is never satisfied. The condition for shocks to form in $\tilde{h}_0(\tilde{x},t)$ is that the Jacobian $\partial(\tilde{x},t)/\partial(\gamma,\delta)$ vanishes, which is only satisfied at $\delta = 0$ (corresponding to the instant of impact). Hence both $\tilde{u}_0(\tilde{x},t)$ and $\tilde{h}_0(\tilde{x},t)$ are well defined for $t \geq 0$.

The curvature of the body, $\tilde{\kappa}(\tilde{x})$, is equal to -2 everywhere, and so we can evaluate the leading order term of the pressure in the jet from equation (2.91) to be

$$\tilde{p}_3 = -4\pi\frac{t^2}{\tilde{x}^3},$$

and a typical pressure distribution on the body in the jet region is shown in Figure (2.19). The composite pressure distribution on the body can now be evaluated using equations (2.92) and (2.93), by taking

$$p_j^{(1)} = -4\epsilon\pi\frac{t^2}{\tilde{x}^3}, \quad \left[p_j^{(1)}\right]_i^{(1)} = -4\epsilon\pi\frac{t^2}{d(t)^3} = \sqrt{2}\epsilon\pi t^{\frac{1}{2}},$$

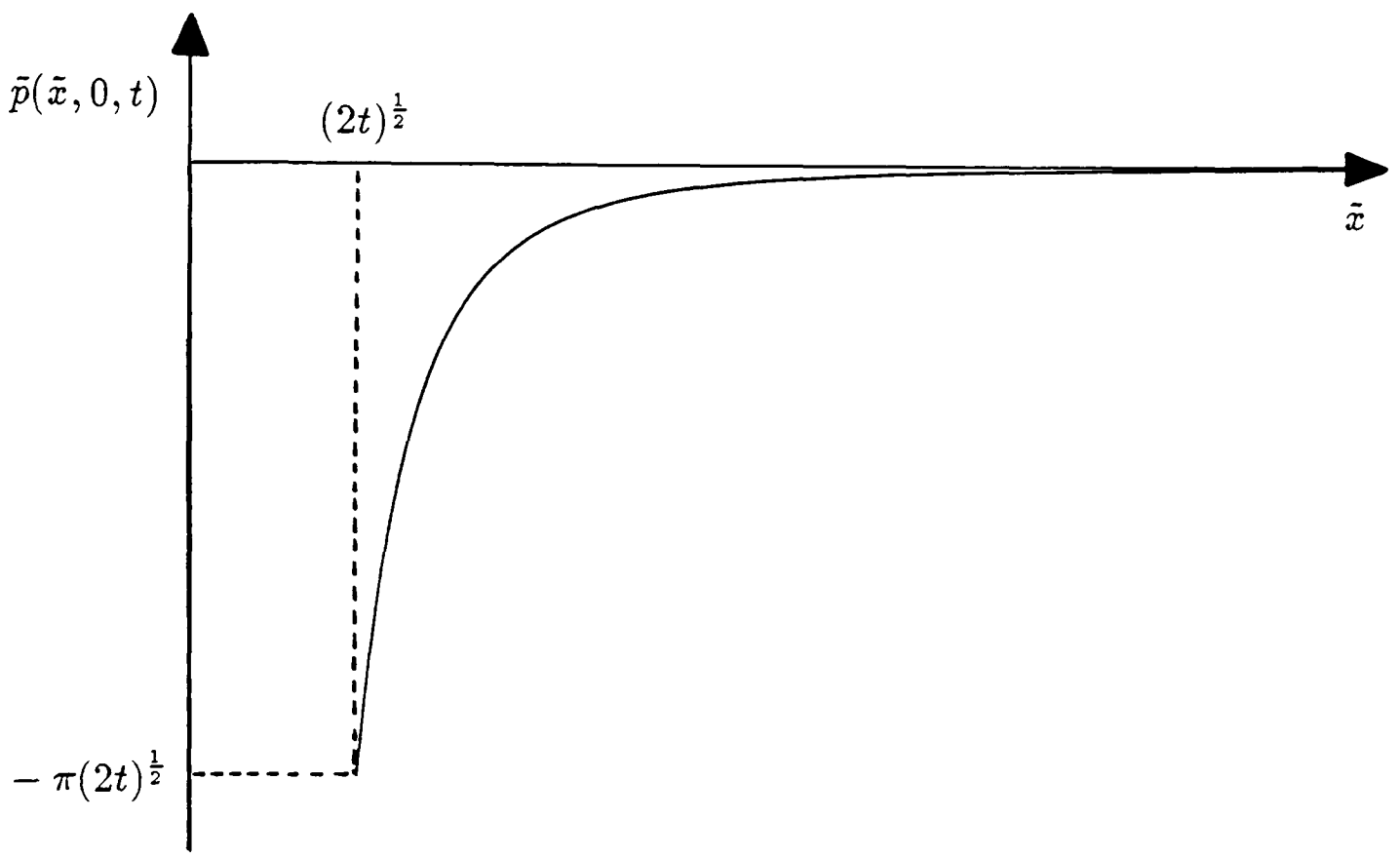

Figure 2.19: Typical leading order pressure distribution in the jet region for a parabolic body.

and since the pressure in the jet region is negative we expect the jet to separate from the body at the point where the composite pressure $p_c^{(1,1)}$ vanishes. Figure (2.20) shows a sequence of pressure distributions at different times, and Figure (2.21) shows a typical set of pressure histories measured at equally spaced points on the body. The maximum pressure on the body is $d'(t)^2/2\epsilon^2 = 1/4t\epsilon^2$, and so as $t \to 0^+$ the pressure at $x = 0$ has a $1/t$ singularity. Since $d(t) = (2t)^{\frac{1}{2}}$ the magnitude of the pressure peaks decrease like $1/x^2$ with distance x, and the leading order force on the body is constant, given by $\pi d(t)d'(t)/\epsilon^2 = \pi/\epsilon^2$.

2.11.3 Flat-Bottomed Wedge

With the main aim of comparing our results with the experimental data of Driscoll & Lloyd (1982), we consider the impact of a *flat-bottomed wedge* with semi-base width a whose profile is described by

$$y = \begin{cases} 0 & \text{if } |x| < a \\ m(x-a) & \text{if } |x| \geq a. \end{cases}$$

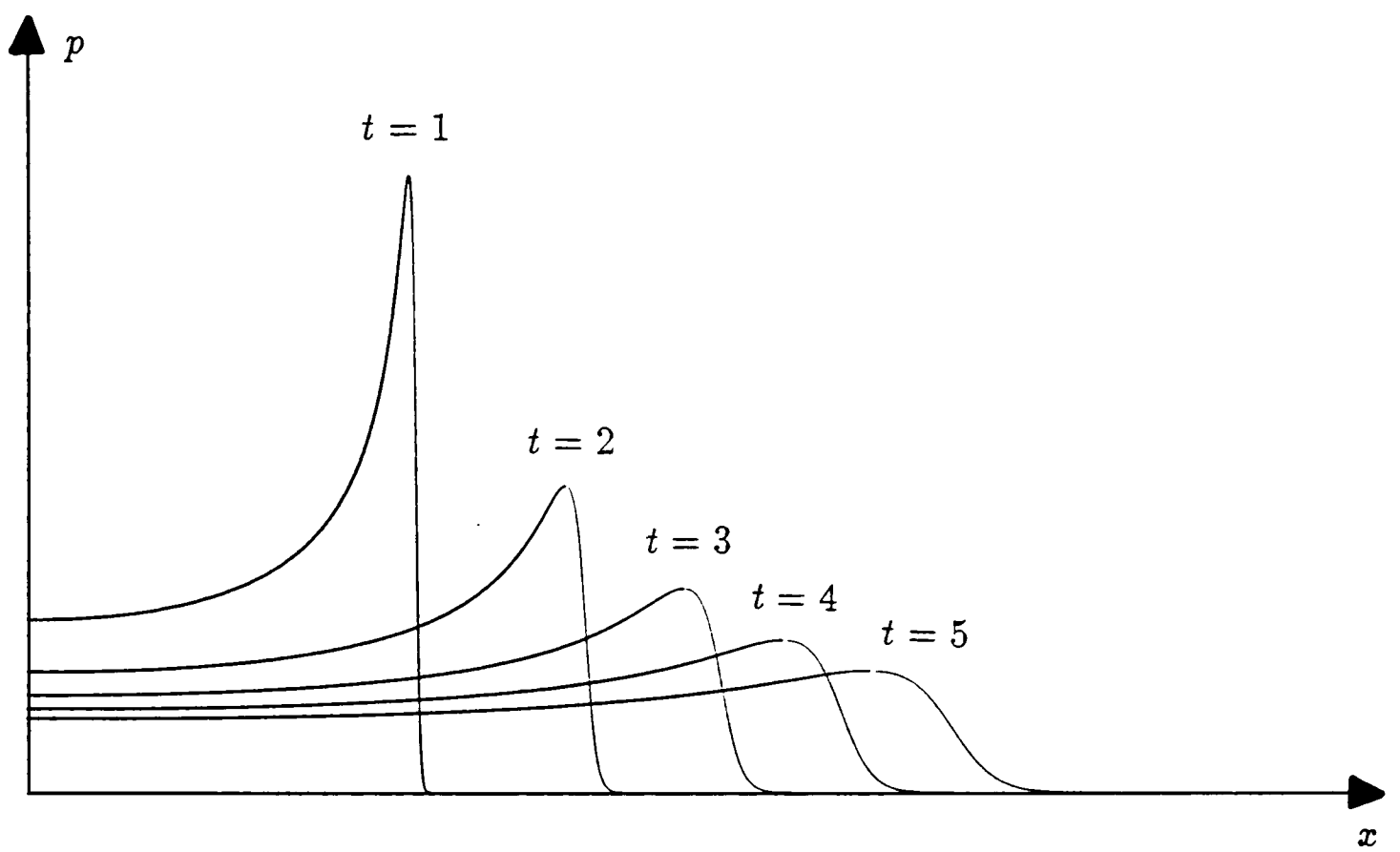

Figure 2.20: Leading order composite pressure distributions for a parabolic body.

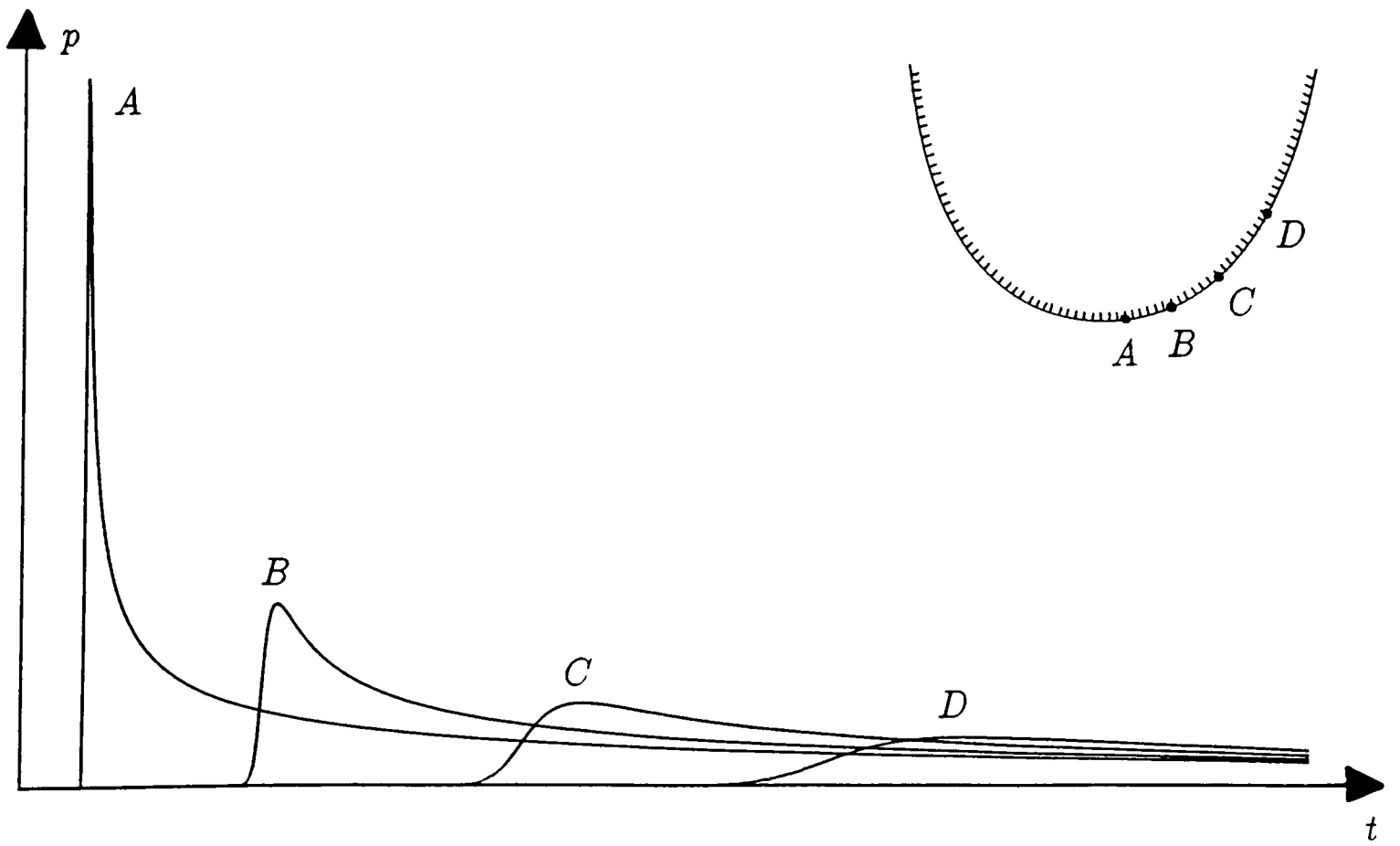

Figure 2.21: Leading order composite pressure histories for a parabolic body.

We can write the profile in the form $y = f(\epsilon x)$ by choosing $f(x)$ to be

$$f(x) = \begin{cases} 0 & \text{if } |x| < a \\ x - a & \text{if } |x| \geq a, \end{cases}$$

and defining the small parameter $\epsilon = m$. The theory is therefore applicable to wedges with small deadrise angle such that $m \ll 1$. Substituting $f(\cdot)$ into the solution of the integral equation (2.47) we obtain

$$t(d) = \frac{2}{\pi} \int_a^d \frac{\xi - a}{(d^2 - \xi^2)^{\frac{1}{2}}} \, \mathrm{d}\xi = \frac{2}{\pi} \left[a \sin^{-1} \left(\frac{a}{d} \right) + \left(d^2 - a^2 \right)^{\frac{1}{2}} - \frac{\pi a}{2} \right]$$

which gives an algebraic relation between t and $d(t)$,

$$a \sin^{-1} \left(\frac{a}{d} \right) + \left(d^2 - a^2 \right)^{\frac{1}{2}} - \frac{\pi}{2} (t + a) = 0, \tag{2.101}$$

which can be solved for $d(t)$ with a simple iterative numerical scheme. Differentiating (2.101) with respect to t we obtain an expression for $d'(t)$,

$$d'(t) = \frac{\pi}{2} \frac{d(t)}{(d(t)^2 - a^2)^{\frac{1}{2}}},$$

which can be readily evaluated once $d(t)$ is known. Notice that $d(0) = a$, and that as $t \to \infty$, $d'(t) \to \pi/2$ just as for normal wedge impacts. Figure (2.22) shows the computed solution for $d(t)$ for a particular choice of a. Since $d(t)$ is only known numerically, we could evaluate the leading order surface shape by performing a numerical integration of equation (2.38). Similarly, the jet solution could be obtained by numerically integrating the pair of first order hyperbolic equations (2.86) and (2.87) governing the leading order solution, as described, for example, in Morton (1986a). Since the curvature of the wedge face is zero, the pressure in the jet is identically zero, just as for wedge impacts.

The composite pressure distribution on the wedge can now be evaluated using equations (2.92) and (2.93), by taking

$$p_j^{(1)} = \left[p_j^{(1)} \right]_i^{(1)} = 0,$$

and Figure (2.23) shows a sequence of pressure distributions at different times. Figure (2.24) shows a typical set of pressure histories measured at equally spaced points on the body. At the instant $t = 0$ the pressure is infinite over $|x| \leq d(t)/\epsilon$,

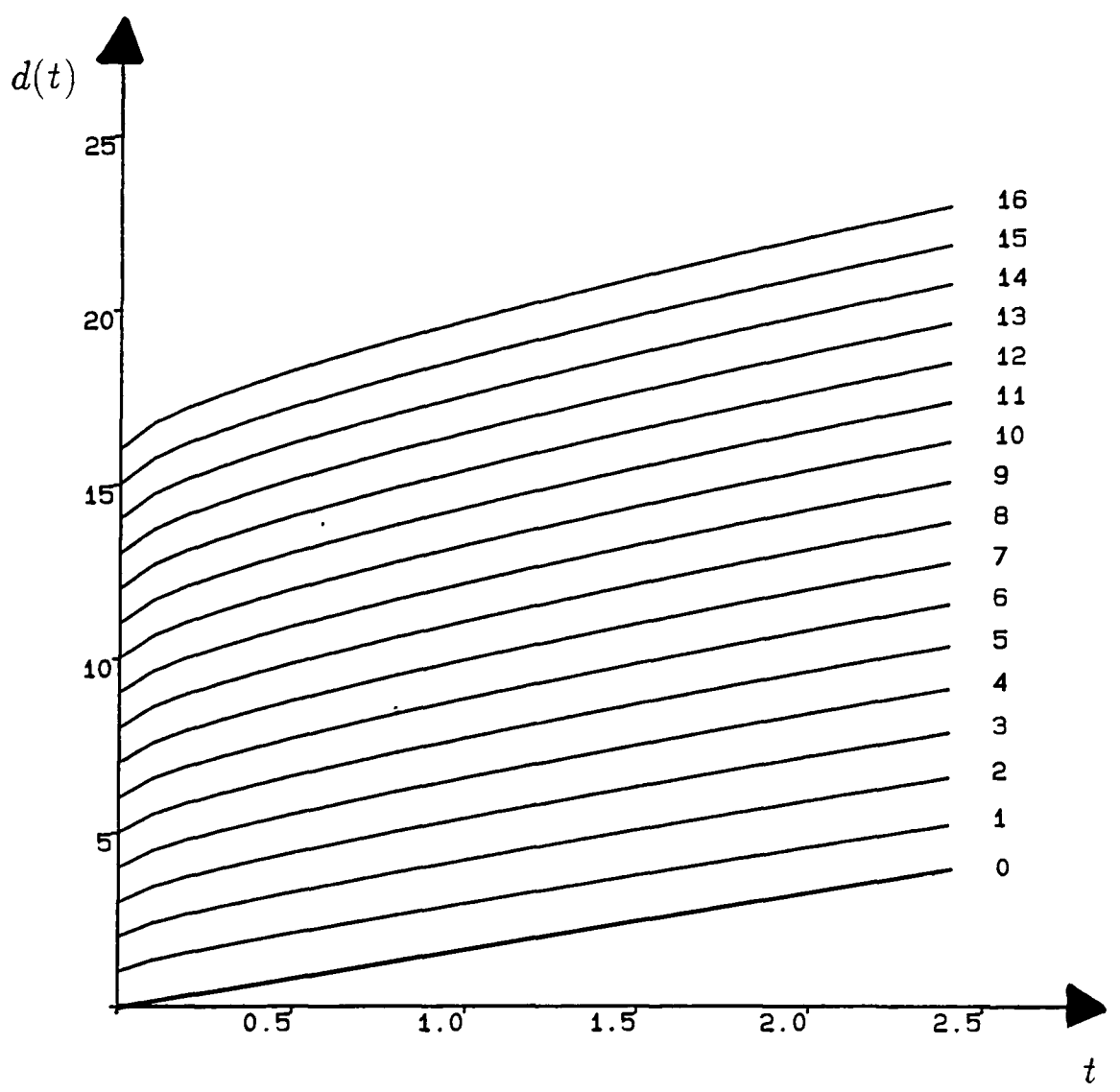

Figure 2.22: Computed values of $d(t)$ for flat-bottomed wedges for various values of the keel width.

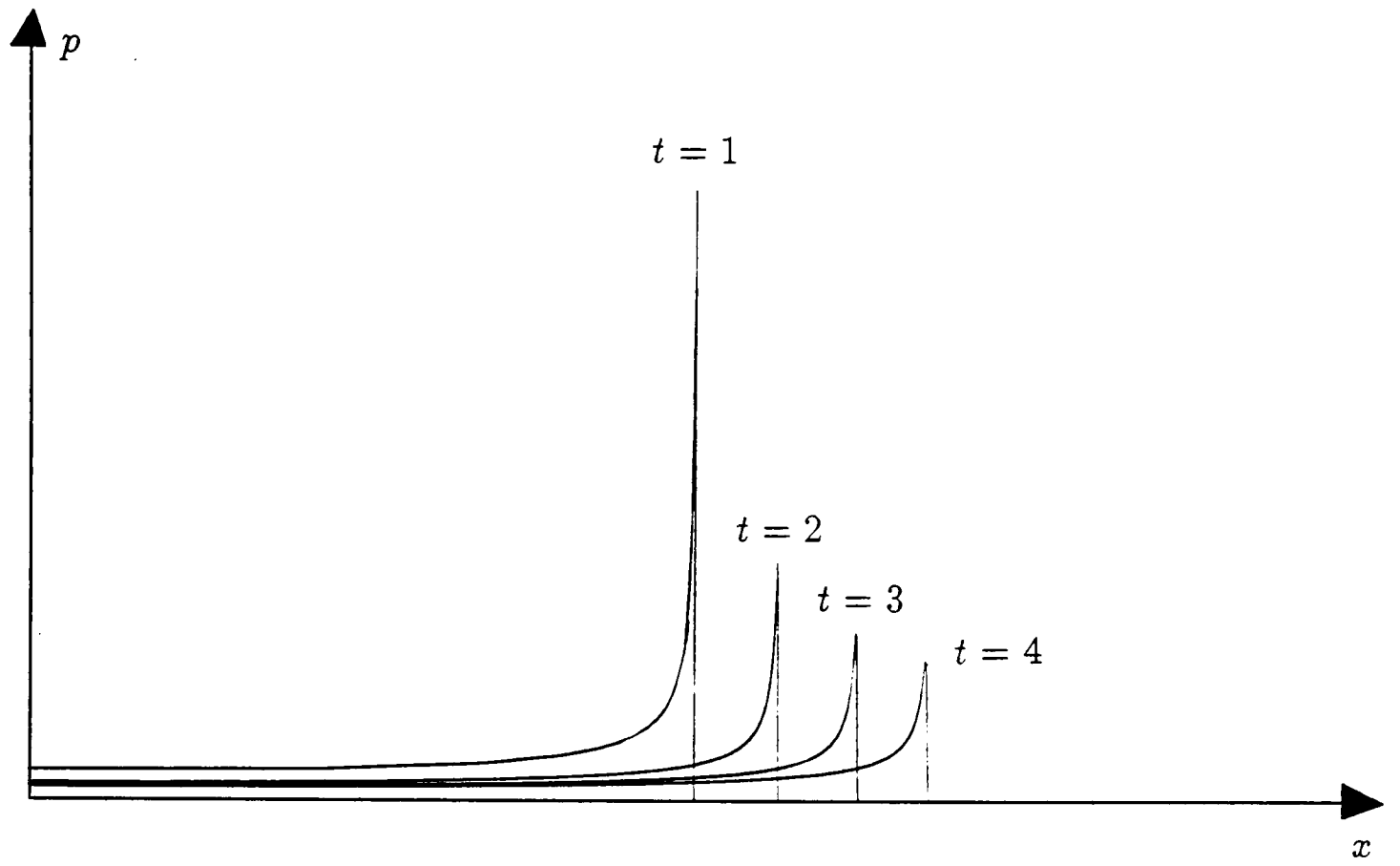

Figure 2.23: Leading order composite pressure distributions for a wedge with a flat keel.

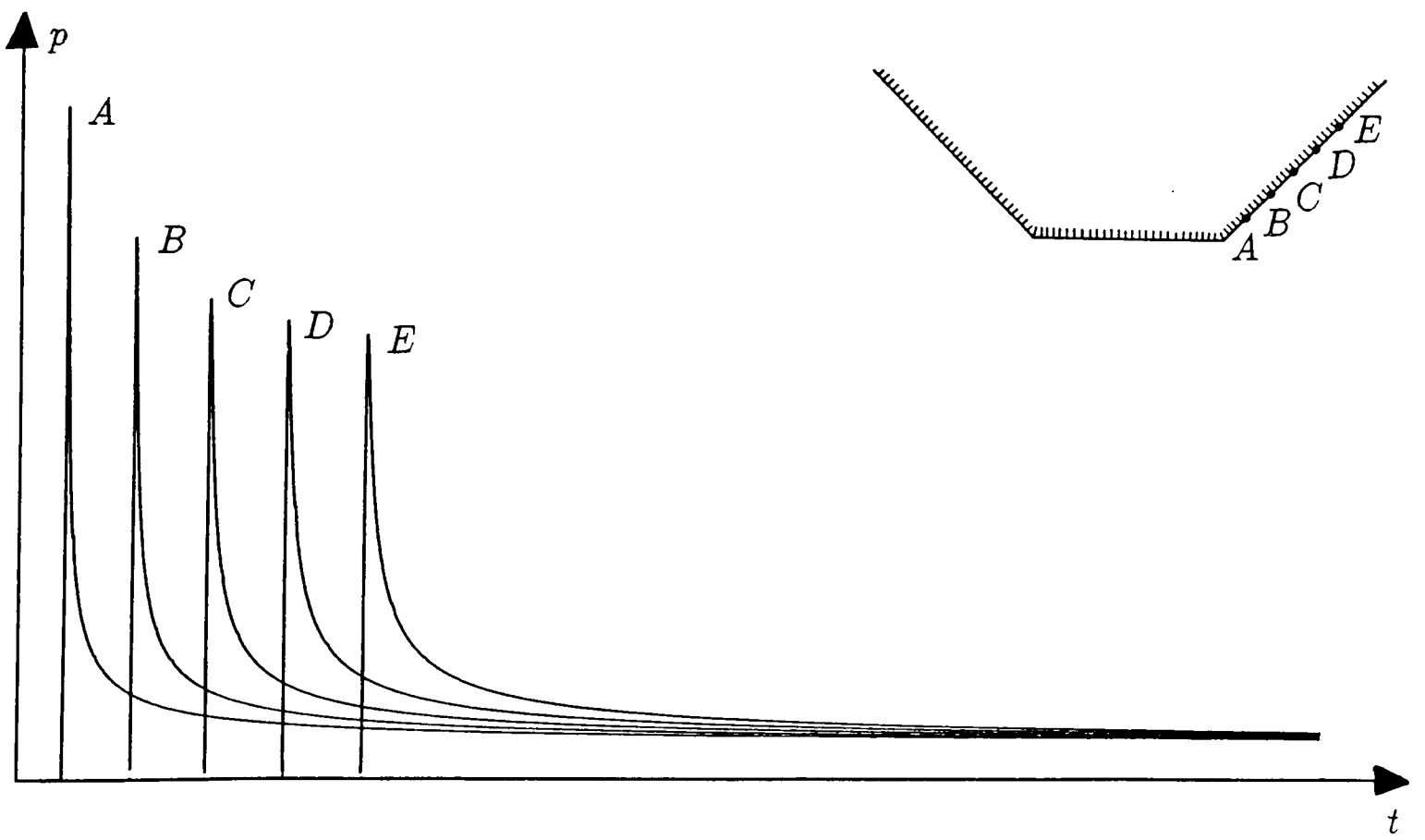

Figure 2.24: Leading order composite pressure histories for a wedge with a flat keel.

and the maximum pressure is

$$\frac{d'(t)^2}{2\epsilon^2} = \frac{\pi^2}{8\epsilon^2}\frac{d(t)^2}{(d(t)^2 - a^2)},$$

which decreases from an infinite value at $t = 0$ and tends to the wedge limit of $\pi^2/8\epsilon^2$ as $t \to \infty$. The nature of the singularity in the pressure at $x = 0$ as $t \to 0^+$ can be determined by writing $d(t) = a + \delta$ for $\delta \ll 1$. Expanding the expression for $d(t)$ for small δ we obtain

$$\delta^{\frac{1}{2}} \sim \frac{\pi t}{2(2a)^{\frac{1}{2}}} \text{as} \quad t \to 0^+,$$

and expanding the expression for $d'(t)$ gives

$$d'(t) \sim \frac{\pi}{2}\left(\frac{a}{2\delta}\right)^{\frac{1}{2}} \text{as} \quad \delta \to 0^+.$$

Substituting these asymptotic forms into the formula for the maximum pressure we deduce that

$$\frac{d'(t)^2}{2\epsilon^2} \sim \frac{a}{t} \quad \text{as} \quad t \to 0^+,$$

and so the pressure at $x = 0$ has a $1/t$ singularity as $t \to 0^+$.

2.12 More Complicated Impact Models

The model described in this chapter can be extended to include a number of the effects that were neglected on physical grounds in Section 2.1. In fact, we shall show that the inclusion of most of these phenomena only alters the solution at second order or lower, thus providing a theoretical justification for our procedure.

2.12.1 The Effect of Gravity

Including the effect of gravity has the result of introducing a non-zero body force term, $\Omega = gy$, into Bernoulli's equation (2.4), so that in dimensional variables the pressure matching condition in the full impact problem (2.14) becomes

$$\frac{\partial \phi}{\partial t} + \frac{1}{2}\left[\left(\frac{\partial \phi}{\partial x}\right)^2 + \left(\frac{\partial \phi}{\partial y}\right)^2\right] + gh = 0 \quad \text{on} \quad y = h(x,t).$$

After non-dimensionalizing, the coefficient of the additional term is the reciprocal of the Froude number squared, $1/\mathrm{F}_r^2 = gl/V^2$, which we denote by $\hat{g}$. We observe

that our previous neglect of gravity for large Froude number corresponded to setting $\hat{g} = 0$.

If $\hat{g}$ is $O(1)$, then the pressure condition in the outer problem (2.20) is modified by gravity to give

$$\frac{\partial \Phi}{\partial t} + \frac{\epsilon}{2}\left[\left(\frac{\partial \Phi}{\partial X}\right)^2 + \left(\frac{\partial \Phi}{\partial Y}\right)^2\right] + \epsilon \hat{g} H = 0,$$

and so the leading order problem is unchanged and the second order problem is the same except for equation (2.33), which becomes

$$\frac{\partial \Phi_1}{\partial t} + H_0 \frac{\partial^2 \Phi_0}{\partial t \partial Y} + \frac{1}{2}\left[\left(\frac{\partial \Phi_0}{\partial X}\right)^2 + \left(\frac{\partial \Phi_0}{\partial Y}\right)^2\right] + \hat{g} H_0 = 0.$$

The leading order pressure is unaltered but the second order term becomes

$$-P_1 = \frac{1}{2}\left[\left(\frac{\partial \Phi_0}{\partial X}\right)^2 + \left(\frac{\partial \Phi_0}{\partial Y}\right)^2\right] + \frac{\partial \Phi_1}{\partial t} + \hat{g} Y.$$

The inner problem is modified by the addition of the term $\hat{g}\left[\epsilon \hat{h}(\hat{x}, t) - f(d(t)) + t\right]$, to the pressure matching condition (2.50), and consequently gravity only enters the problem at third order.

In order to investigate the rôle of gravity in the jet region we recall that the gravitational potential Ω is defined so that the body force is given by $\mathbf{F} = -\nabla\Omega$, and so in the curvilinear coordinate system $(\bar{x}, \bar{y})$ we have

$$\frac{1}{1 + \kappa \bar{y}} \frac{\partial \Omega}{\partial \bar{x}} = -\frac{\epsilon \hat{g} f'(\epsilon x(\bar{x}))}{(1 + \epsilon^2 f'(\epsilon x(\bar{x}))^2)^{\frac{1}{2}}}, \quad \frac{\partial \Omega}{\partial \bar{y}} = -\frac{\hat{g}}{(1 + \epsilon^2 f'(\epsilon x(\bar{x}))^2)^{\frac{1}{2}}},$$

where x and y are the coordinates in the original cartesian system. Since $d\bar{x}/dx = (1 + \epsilon^2 f'(\epsilon x(\bar{x}))^2)^{\frac{1}{2}}$ we can integrate these relations to obtain

$$\Omega = -\hat{g}\left[f(\epsilon x(\bar{x})) + \frac{\bar{y}}{(1 + \epsilon^2 f'(\epsilon x(\bar{x}))^2)^{\frac{1}{2}}}\right].$$

Furthermore $x(\bar{x}) = \bar{x} + O(\epsilon^2)$, and so when we introduce the scaled jet variables and expand Ω in powers of ϵ we obtain the leading order terms

$$\Omega = -\hat{g}\left[f(\tilde{x}) + \epsilon \tilde{y} + O(\epsilon^2)\right].$$

Substituting this expression into the Bernoulli condition (2.79), we alter its third order term to give

$$\frac{\partial\tilde{\phi}_2}{\partial t} + \frac{\partial\tilde{\phi}_0}{\partial\tilde{x}}\frac{\partial\tilde{\phi}_2}{\partial\tilde{x}} + \frac{1}{2}\left(\frac{\partial\tilde{\phi}_1}{\partial\tilde{x}}\right)^2 - \hat{g}f(\tilde{x}) = 0,$$

and its fourth order term yields

$$\frac{\partial\tilde{\phi}_3}{\partial t} + \frac{\partial\tilde{\phi}_0}{\partial\tilde{x}}\frac{\partial\tilde{\phi}_3}{\partial\tilde{x}} + \frac{\partial\tilde{\phi}_1}{\partial\tilde{x}}\frac{\partial\tilde{\phi}_2}{\partial\tilde{x}} + \tilde{\kappa}\tilde{y}\left(\frac{\partial\tilde{\phi}_0}{\partial\tilde{x}}\right)^2 - \hat{g}\tilde{y} = 0.$$

Since the third order term is only a function of $\tilde{x}$ it is identically zero, and so the first non-zero term in the expansion of the pressure remains the fourth term. Hence, the leading order solution is unaffected and the leading order pressure becomes

$$\tilde{p}_3 = \left[\tilde{\kappa}(\tilde{x})\tilde{u}_0(\tilde{x},t)^2 - \hat{g}\right]\left(\tilde{h}_0(\tilde{x},t) - \tilde{y}\right),$$

as we might expect. For wedge impacts this means that instead of being zero to all orders there is now a negative $O(\epsilon)$ pressure due to gravity on the body,

$$\tilde{p} = -\frac{\epsilon\hat{g}}{4}\left[t - \frac{\tilde{x}}{\pi}\right] + O(\epsilon^2),$$

indicating that the jet may now separate from the wedge. This conclusion agrees qualitatively with the evidence of the photographs as Greenhow (1987), one of which is reproduced in Figure (1.6), which clearly show the jet 'falling off' the wedge face. For parabolic impacts the situation is similar and the effect of gravity is to make the magnitude of the negative leading order jet pressure larger,

$$\tilde{p} = -\frac{2\pi t^4\epsilon}{\tilde{x}^5}\left[2\frac{\tilde{x}^2}{t^2} + \hat{g}\right] + O(\epsilon^2)$$

and hence encourage earlier separation.

2.12.2 The Effect of a Variable Impact Speed

If we let the dimensional impact speed $V(t)$ vary with time t on an $O(1)$ time scale then, in dimensionless variables, the position of the body is given by

$$y = f(\epsilon x) - \int_0^t v(\tau)\,\mathrm{d}\tau,$$

where $v(t)$ is the dimensionless speed. Hence, in the full impact problem the velocity matching condition (2.12) becomes

$$\epsilon f'(\epsilon x)\frac{\partial \phi}{\partial x} - \frac{\partial \phi}{\partial y} = v(t).$$

The outer problem is modified through the kinematic condition, and equation (2.18) becomes

$$\epsilon f'(X)\frac{\partial \Phi}{\partial X} - \frac{\partial \Phi}{\partial Y} = v(t) \quad \text{on} \quad Y = \epsilon(f(X) - t),$$

and so in the leading order outer problem equation (2.24) is replaced by

$$\frac{\partial \Phi_0}{\partial Y} = -v(t) \quad \text{on} \quad Y = 0, \quad |X| < d(t).$$

The solution of the leading order problem is now

$$\Phi_0(X, Y, t) = -v(t)\left[Y + \Re(d(t)^2 - Z^2)^{\frac{1}{2}}\right], \tag{2.102}$$

so the leading order free surface elevation is given by

$$H_0(X, t) = -\int_0^t v(\tau)\,\mathrm{d}\tau + X\int_0^t \frac{v(\tau)}{(X^2 - d(\tau)^2)^{\frac{1}{2}}}\,\mathrm{d}\tau,$$

and the leading order mass conservation matching condition to determine $d(t)$, equation (2.46), now takes the form

$$d(t)\int_0^t \frac{v(\tau)}{(d(t)^2 - d(\tau)^2)^{\frac{1}{2}}}\,\mathrm{d}\tau = f(d(t)).$$

This integral equation can again be solved by writing t as a function of d and introducing a new integration variable σ by $\tau = t(\sigma)$ so that $d\tau = t'(\sigma)d\sigma$. The equation becomes

$$\int_0^d \frac{v(t(\sigma))}{(d^2 - \sigma^2)^{\frac{1}{2}}}\,\mathrm{d}\sigma = \frac{f(d)}{d},$$

which is an Abel integral equation which has the solution

$$v(t(\sigma))t'(\sigma) = \frac{2}{\pi}\frac{d}{d\sigma}\int_0^\sigma \frac{f(\xi)}{(\sigma^2 - \xi^2)^{\frac{1}{2}}}\,\mathrm{d}\xi,$$

provided that the integral exists. Integrating this expression with respect to σ we obtain

$$\int_0^t v(\tau)\,\mathrm{d}\tau = \frac{2}{\pi}\int_0^d \frac{f(\xi)}{(d^2 - \xi^2)^{\frac{1}{2}}}\,\mathrm{d}\xi, \tag{2.103}$$

which is a generalisation of our previous solution (2.47), and again given any body shape $f(\cdot)$ we can evaluate the corresponding $d(t)$. The leading order pressure on the plate is still given by equation (2.42) and, substituting in the solution (2.102), it takes the form

$$P_0(X,0,t) = \frac{v(t)d(t)d'(t)}{(d(t)^2 - X^2)^{\frac{1}{2}}} + v'(t)(d(t)^2 - X^2)^{\frac{1}{2}}. \tag{2.104}$$

A simple example is a wedge $f(X) = |X|$ impacting with speed given by $v(t) = t^n$ for $n \geq 0$. Substituting into (2.103) we obtain $t^{n+1}/(n+1) = 2d/\pi$, and hence

$$d(t) = \frac{\pi t^{n+1}}{2(n+1)},$$

in accordance with the self-similarity property for power law impact velocities.

Both the inner and the jet problem were formulated in coordinate systems moving with the body, and so we must take account of the acceleration of the frame of reference due to the change in velocity. If $\mathbf{j}$ denotes the unit vector in the vertical direction then the statement of conservation of momentum (2.2) now takes the form

$$\frac{d\mathbf{u}}{dt} = -\nabla p + \mathbf{F} - v'(t)\mathbf{j}, \tag{2.105}$$

where the additional term is the force due to the acceleration of the body, relative to which the local coordinate system is fixed. $\mathbf{u}$ is measured relative to the moving frame. Integrating this equation once, we obtain the Bernoulli equation for the problem,

$$\frac{\partial \phi}{\partial t} + \frac{1}{2}|\nabla \phi|^2 + p - v'(t)y = 0. \tag{2.106}$$

In the inner problem the pressure condition (2.30) is modified by the addition of a term $v'(t)\left[\epsilon h(x,t) - f(d(t)) + t\right]$, which affects the third order and higher terms of the equation. The velocity matching condition on the body (2.50) becomes

$$f'(d(t) + \epsilon^2 \hat{x})\left[d'(t) + \frac{\partial \hat{\phi}}{\partial \hat{x}}\right] - \frac{1}{\epsilon}\frac{\partial \hat{\phi}}{\partial \hat{y}} = v(t) \quad \text{on} \quad y = 0,$$

and so the leading order problem is unaltered and the impact speed first enters the second order problem. The matching procedure is as before, except that the asymptotic thickness of the jet is now

$$h(t) = \frac{\pi}{8}\frac{v(t)^2 d(t)}{d'(t)^2}. \tag{2.107}$$

In order to solve the problem in the jet region we recall that the cartesian co-ordinate y can be expressed in terms of the curvilinear coordinate system $(\bar{x}, \bar{y})$ by

$$y = f(\epsilon x(\bar{x})) - \frac{\bar{y}}{(1 + \epsilon^2 f'(\epsilon x(\bar{x}))^2)^{\frac{1}{2}}},$$

and that $x(\bar{x}) = \bar{x} + O(\epsilon^2)$. When we introduce scaled jet variables and expand in powers of ϵ, the third order term of the Bernoulli equation gives

$$\frac{\partial \tilde{\phi}_2}{\partial t} + \frac{\partial \tilde{\phi}_0}{\partial \tilde{x}} \frac{\partial \tilde{\phi}_2}{\partial \tilde{x}} + \frac{1}{2} \left(\frac{\partial \tilde{\phi}_1}{\partial \tilde{x}} \right)^2 - v'(t) f(\tilde{x}) = 0,$$

and the fourth order term gives

$$\frac{\partial \tilde{\phi}_3}{\partial t} + \frac{\partial \tilde{\phi}_0}{\partial \tilde{x}} \frac{\partial \tilde{\phi}_3}{\partial \tilde{x}} + \frac{\partial \tilde{\phi}_1}{\partial \tilde{x}} \frac{\partial \tilde{\phi}_2}{\partial \tilde{x}} + \tilde{\kappa} \tilde{y} \frac{1}{2} \left(\frac{\partial \tilde{\phi}_0}{\partial \tilde{x}} \right)^2 + v'(t) \tilde{y} = 0.$$

The third order term is independent of $\tilde{y}$ and is therefore identically zero, and so the first non-zero term in the pressure is the fourth term. The leading order solution is unaltered and the leading order pressure becomes

$$p_3 = \left[\tilde{\kappa}(\tilde{x}) \tilde{u}_0(\tilde{x}, t)^2 + v'(t) \right] \left(\tilde{h}_0(\tilde{x}, t) - \tilde{y} \right).$$

As we would expect, when the body is accelerated so that $v'(t) > 0$ the pressure on the body is increased and therefore separation is discouraged. Decelerating the body so that $v'(t) < 0$ has the opposite effect.

In the simple case of a wedge impacting with a power law speed $v(t) = t^n$ the pressure due to the jet is

$$\tilde{p} = \frac{\epsilon n t^{n-1}}{4} \left[t - \frac{\tilde{x}}{\pi} \right] + O(\epsilon^2),$$

over the region of the jet $\pi t/2 \leq \tilde{x} \leq \pi t$.

Figures (2.25) and (2.26) show the composite pressure distribution on a wedge shaped body impacting with a speed linear in t, so that $v(t) = t$, and a typical set of composite pressure histories respectively.

2.12.3 The Effect of Surface Tension

The effect of surface tension in the fluid surface can also be included in the model. If the pressures are $p_1(x, y, t)$ and $p_2(x, y, t)$ either side of an interface, then

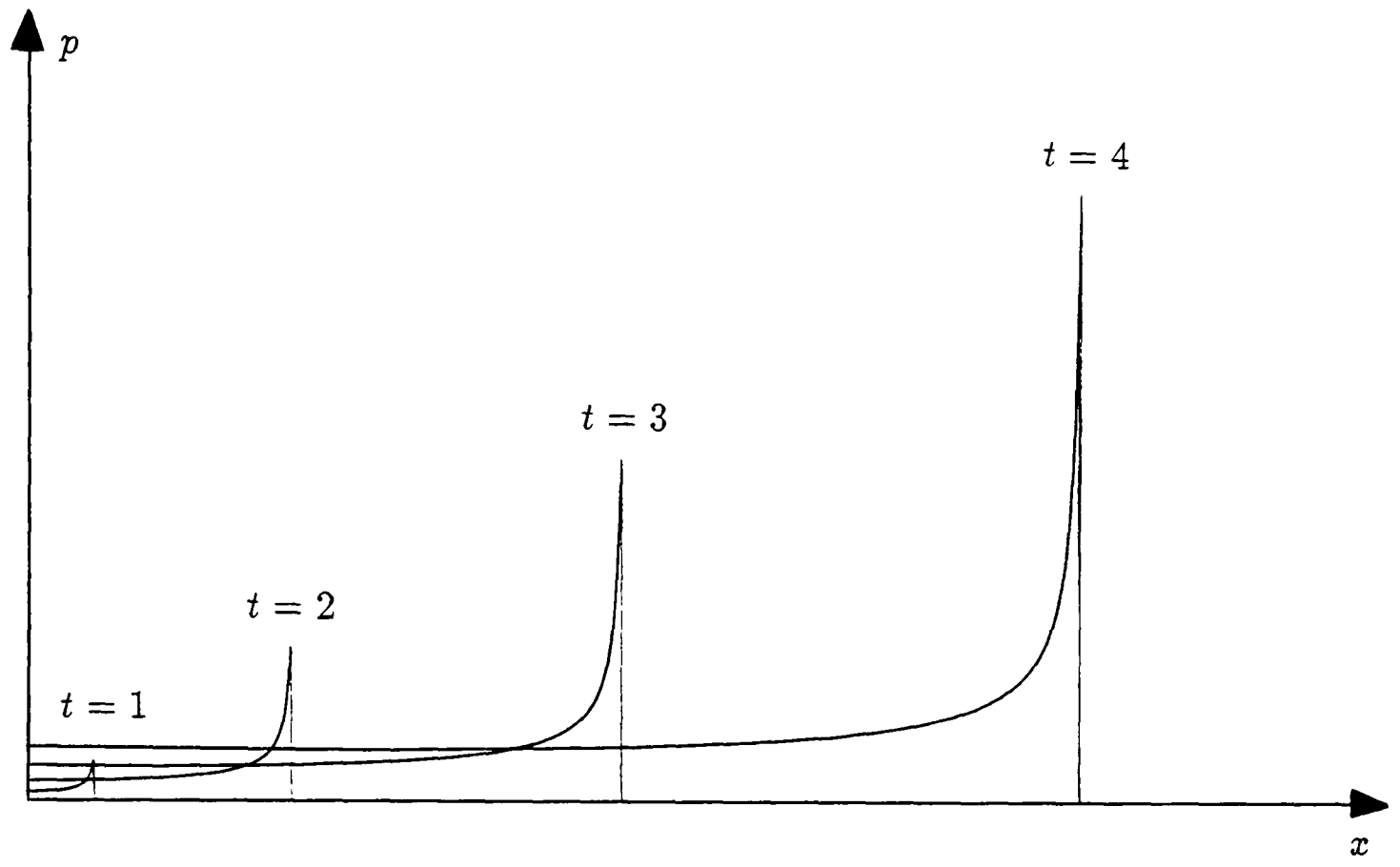

Figure 2.25: Leading order composite pressure distributions on a wedge shaped body with $v(t) = t$.

a simple force balance argument, as presented for example in Milne-Thomson (1968), gives the relation

$$p_1 - p_2 = \kappa\gamma$$

at each point of the interface, where γ is the surface tension and κ is the local curvature, whose sign is chosen so that the contribution of the term $\kappa\gamma$ is directed towards the local centre of curvature. Using this pressure matching condition at the free surface and non-dimensionalizing, the coefficient of the new term becomes $\gamma/\rho l V^2$, the reciprocal of the Weber number, which we denote by $\hat{\gamma}$. The pressure matching condition in the full problem (2.14) therefore becomes

$$\frac{\partial\phi}{\partial t} + \frac{1}{2}\left[\left(\frac{\partial\phi}{\partial x}\right)^2 + \left(\frac{\partial\phi}{\partial y}\right)^2\right] + \hat{\gamma}\frac{\partial^2 h}{\partial x^2}\left[1 + \left(\frac{\partial h}{\partial x}\right)^2\right]^{-\frac{3}{2}} = 0.$$

Assuming that $\hat{\gamma}$ is $O(1)$, the additional term is $O(\epsilon^2)$ in the outer problem, and so its effect is only felt at third order, while in the inner problem it is $O(\epsilon)$ and so it only affects the fourth order problem. In the jet region away form the tip the new term enters the pressure condition at $O(\epsilon^7)$ and so appears first in the

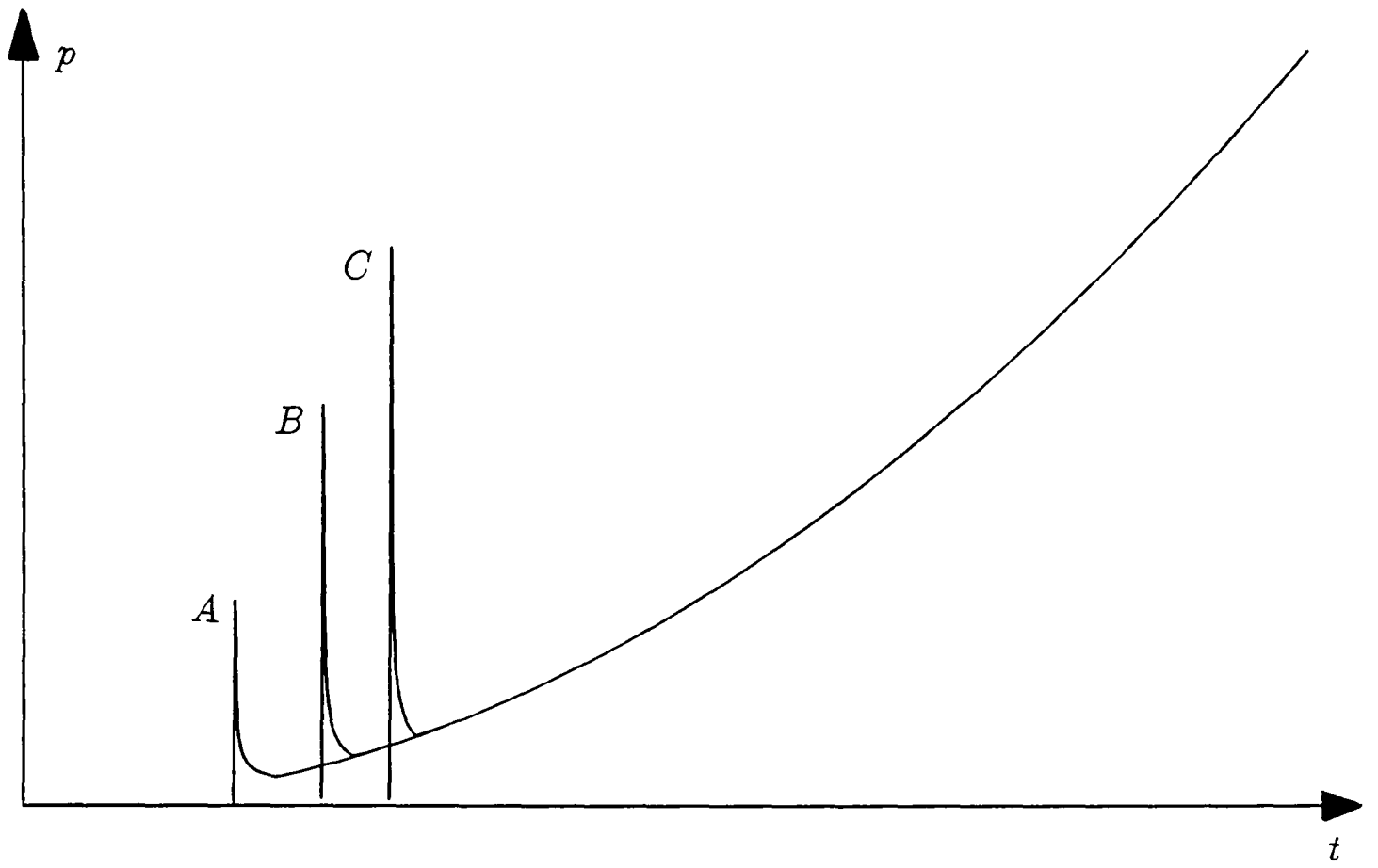

Figure 2.26: Leading order composite pressure histories on a wedge shaped body with $v(t) = t$.

seventh order problem. Thus, our earlier neglect of surface tension which was made because the Weber number was large is in fact valid to leading order for any Weber number that satisfies $\hat{\gamma} = O(1/\epsilon)$. We remark again, however, that even minute amounts of surface tension can have a dominant effect on the solution in the region of the jet tip and where the jet separates from the body.

2.12.4 Non-Planar Initial Free Surface

The model can be extended to include impacts onto fluids with a non-planar initial free surface, provided that the initial deformation is not too great. If we denote the initial free surface shape by $H_0(X, 0) = \eta(X)$, then the outer problem is unaltered apart from the expression for the leading order free surface (2.38), which becomes

$$H_0(X,t) = -t + \eta(X) + \int_0^t \frac{X}{(X^2 - d(\tau)^2)^{\frac{1}{2}}}\,\mathrm{d}\tau,$$

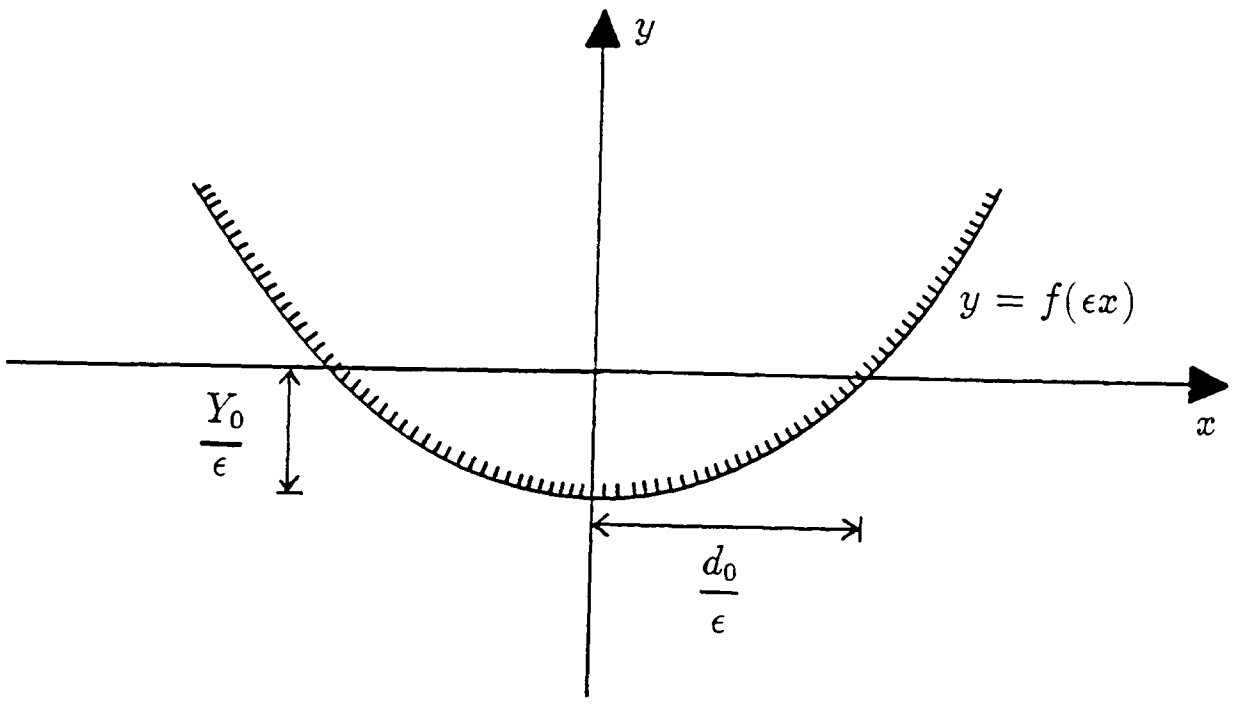

Figure 2.27: Geometry of an initially submerged body at $t = 0$.

for $X \geq d(t)$. Applying the matching condition (2.45) and inverting the resulting integral equation, gives the new expression for $t(d)$, namely

$$t(d) = \frac{2}{\pi} \int_0^d \frac{f(\xi) - \eta(\xi)}{(d^2 - \xi^2)^{\frac{1}{2}}},$$

provided that the integral exists. Evidently altering the initial free surface shape has the consequence of altering the effective body shape. The leading order inner and jet problems are only altered through the change in $d(t)$.

For example, if the impacting body and the initial free surface are both wedge shaped, so that $f(X) = \alpha|X|$ and $\eta(X) = -\beta|X|$ then we obtain

$$d(t) = \frac{\pi t}{2(\alpha + \beta)}.$$

2.12.5 Bodies Initially in Contact with the Fluid

The theory can also be applied to the situation where the impacting body is initially submerged in the half-space of quiescent fluid to a depth $Y_0/\epsilon = f(d_0)$, so that the initial plate width is d_0/ϵ, as shown in Figure (2.27).

The outer problem is unaltered apart from the matching condition (2.45), which becomes

$$H_0(d(t), t) = f(d(t)) - t - Y_0,$$

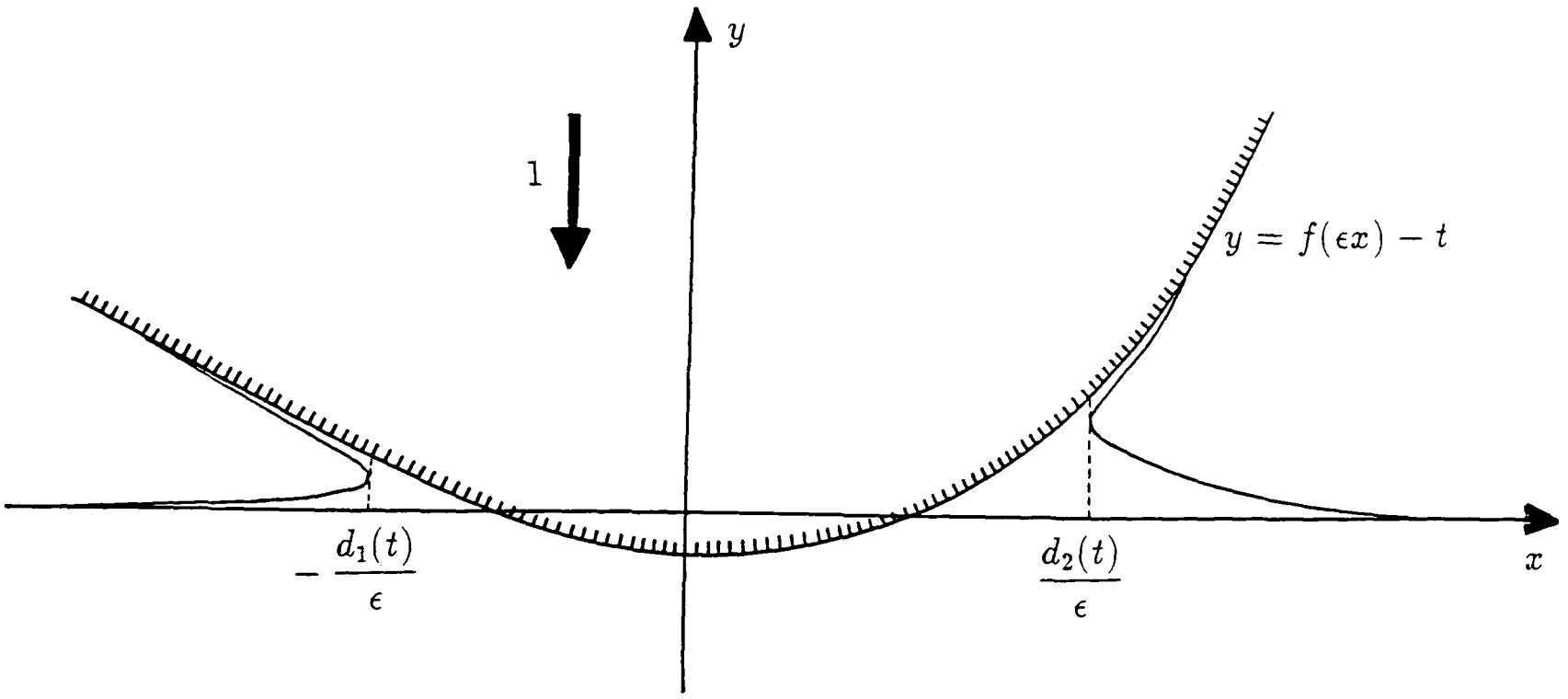

Figure 2.28: Impact of a non-symmetric body with small deadrise angle.

and so $t(d)$ is given by

$$t(d) = \frac{2}{\pi}\left[\int_{d_0}^{d} \frac{f(\xi)}{(d^2-\xi^2)^{\frac{1}{2}}}\,\mathrm{d}\xi - Y_0 \cos^{-1}\left(\frac{d_0}{d}\right)\right].$$

Again, since no initial conditions are imposed on the leading order inner and jet problems, they are only altered through the change in $d(t)$.

For example, when the impacting body is a parabola, $Y = X^2$, we obtain

$$\left(d^2 - 2d_0^2\right)\cos^{-1}\left(\frac{d_0}{d}\right) + d_0\left(d^2 - d_0^2\right)^{\frac{1}{2}} - \pi t = 0,$$

and $d(t) \to (2t)^{\frac{1}{2}}$ as $t \to \infty$ as we expect.

2.12.6 Non-Symmetric Bodies

Thus far only symmetric bodies have been considered, but the theory easily extends to non-symmetric impacting bodies. In this case, transferring the boundary conditions in the outer problem gives rise to two unknown points at the edges of the equivalent plate. Using the subscripts $1, 2$ to indicate quantities in $x < 0$ and $x > 0$ respectively, we denote these points by $-d_1(t)/\epsilon$ and $d_2(t)/\epsilon$, as shown in Figure (2.28). We can make the outer problem symmetric by defining the new space variable $X^* = X - (d_2(t) - d_1(t))/2$, and considering a plate whose semi-width, $d^*(t)$, is given by $d^*(t) = (d_1(t) + d_2(t))/2$. The solution to the leading

order outer problem is, therefore,

$$\Phi_0(X,Y,t) = -\left[Y + \Re\left(d^*(t)^2 - Z^{*2}\right)^{\frac{1}{2}}\right],$$

where $Z^* = X^* + iY$. The matching condition (2.45), applied at the edges of the plate, now takes the form

$$H_0^i((-1)^i d_i(t), t) = f((-1)^i d_i(t)) - t \quad \text{for} \quad i = 1, 2,$$

and so $d_1(\cdot)$ and $d_2(\cdot)$ are determined by

$$(-1)^i d^*(t) \int_0^t \frac{\mathrm{d}\tau}{(d^*(t)^2 - d^*(\tau))^{\frac{1}{2}}} = f((-1)^i d_i(t)) \quad \text{for} \quad i = 1, 2.$$

The leading order term in the expansion of the total force is $F_0(t) = \pi d^*(t) d^{*\prime}(t)$. The leading order inner and jet problems are only altered through the change in the appropriate function $d_i(t)$ for $i = 1, 2$.

For example, if the body is a non-symmetric wedge described by $f(x) = -\alpha x$ for $x < 0$ and $f(x) = \beta x$ for $x > 0$, then $d_1(t) = \pi/2\alpha$ and $d_2(t) = \pi/2\beta$, and a typical spatial pressure distribution is shown in Figure (2.29) in the case $\beta = \sqrt{2}\alpha$.

2.12.7 Fluid Compressibility

The inclusion of fluid compressibility presents substantial additional difficulties, as outlined in Section 1.4.1(c), and no attempt has been made to do this in the present work. We remark, however, that for ship slamming problems the time scale over which compressible effects are significant is much shorter than the typical duration of a slam. To demonstrate this, consider a parabolic body, $y = x^2/2l$, with radius of curvature l, impacting with speed V. The speed of the edge of the equivalent plate is $d'(t)/\epsilon = (Vl/t)^{\frac{1}{2}}$, which is of the same order as the sound speed in the water, c_w, when t is $O(lV/c_w^2)$. Taking the typical dimensions of a ship from Section 2.1, this means that the time scale during which compressibility is important is of order 10^{-4} seconds, which is only one thousandth of the typical duration of a slam.

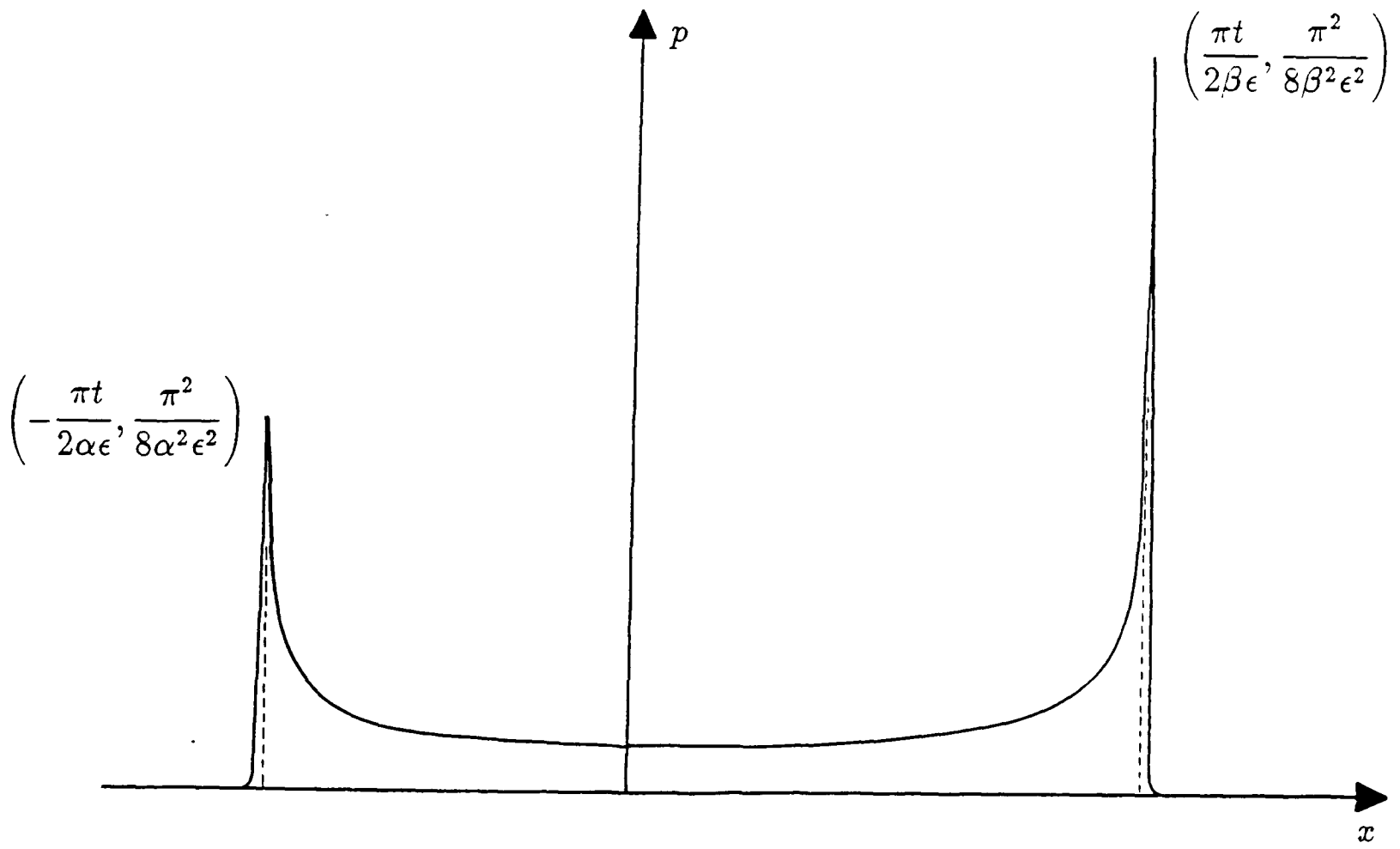

Figure 2.29: Typical spatial pressure distribution on a non-symmetric wedge given by $f(x) = -\alpha x$ for $x < 0$ and $f(x) = \beta x$ for $x > 0$.

2.12.8 Elastic Properties of the Body

No real ship hull is perfectly rigid and so a more detailed description of ship slamming would involve a consideration of the effect of the elastic properties of an impacting body on the solution. A number of numerical studies have been performed, but theoretical approaches so far are restricted to considering the effect of a prescribed fluid loading on an elastic shell, as described by Korobkin (1983).

2.13 Comparison of Theory and Experiment

It was originally intended that the present theoretical work would be accompanied by a series of drop tests using scaled ship hull models, to be performed by the Admiralty at their Rosslaire site. Unfortunately, the Admiralty have not yet performed these experiments and so we will compare our theory with experimental data available in the open literature.

Figure (2.30) shows a series of pressure histories recorded during the impact of a 2m wide model with a 5m radius of curvature onto water reproduced from Hagiwara & Yuhara (1974a,b). The theoretical predictions of the value and the position of the maximum pressure for the same body are given for comparison in Figure (2.31). Evidently the latter is in excellent agreement while the former is substantially over predicted in the early stages of the impact. This over prediction may be due to the effects of air cushioning or possibly the difficulties of resolving the sharp, fast-moving pressure maximum in a small scale experiment.

Figure (2.32) shows a typical set of pressure histories for an approximately parabolic two-dimensional hull section, reproduced from Nethercote *et al.* (1984) and Figure (2.33) shows the corresponding theoretical values for a parabolic body of similar dimensions. The large variations of the pressure on the keel are due to air entrapment, and are not represented by our theory which predicts an infinite pressure there at the instant of impact, but away from the keel the agreement is good.

The experiments of Driscoll & Lloyd (1982) permit comparison with our theory for flat-bottomed wedges. Two typical pressure histories are shown in Figure (2.34). On the flat keel they show a primary pressure peak followed by a shallow

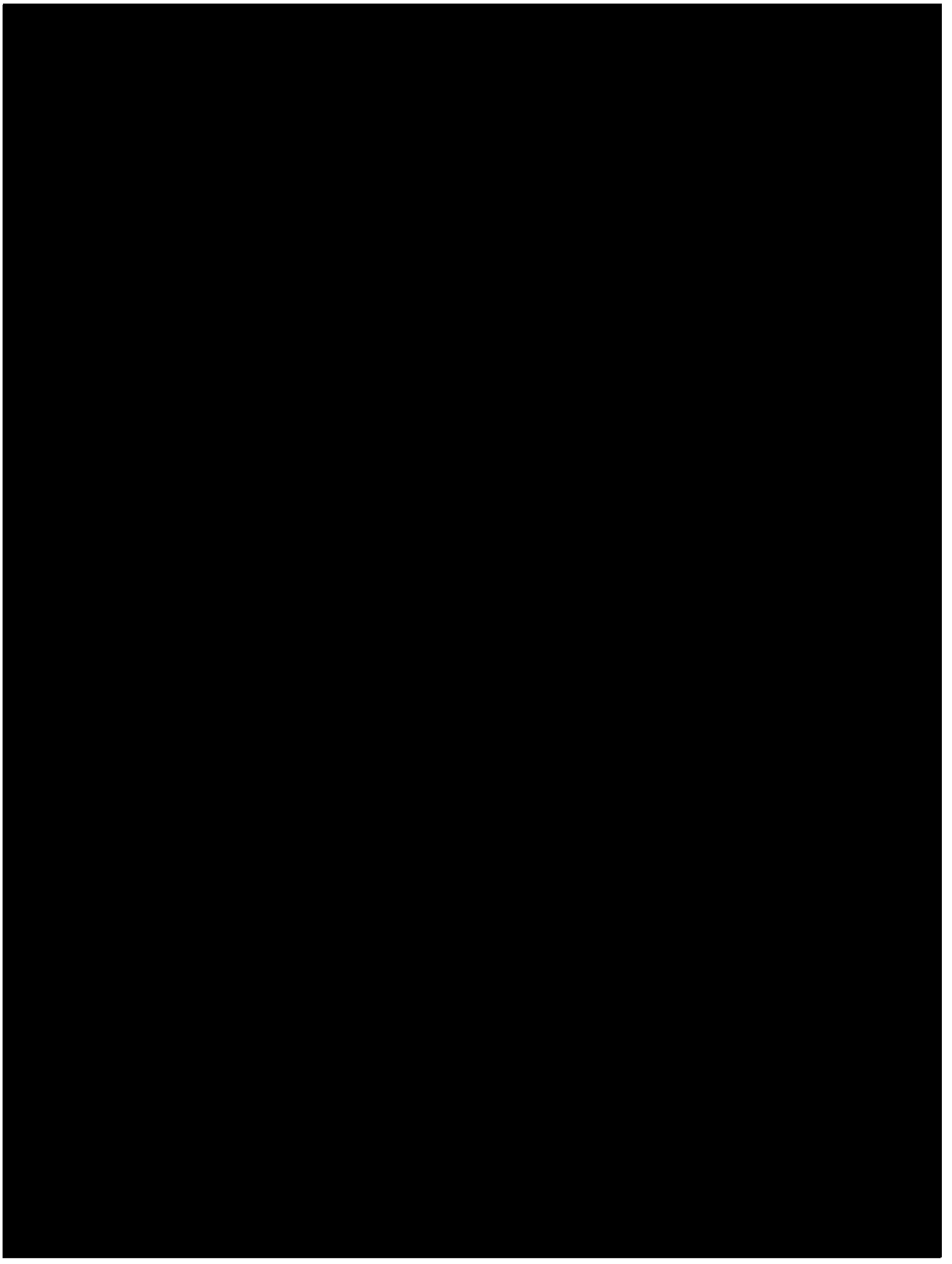

Figure 2.30: Experimental pressure histories for a 2m wide parabolic model with a radius of curvature of 5m. Reproduced from Hagiwara & Yuhara (1974a,b).

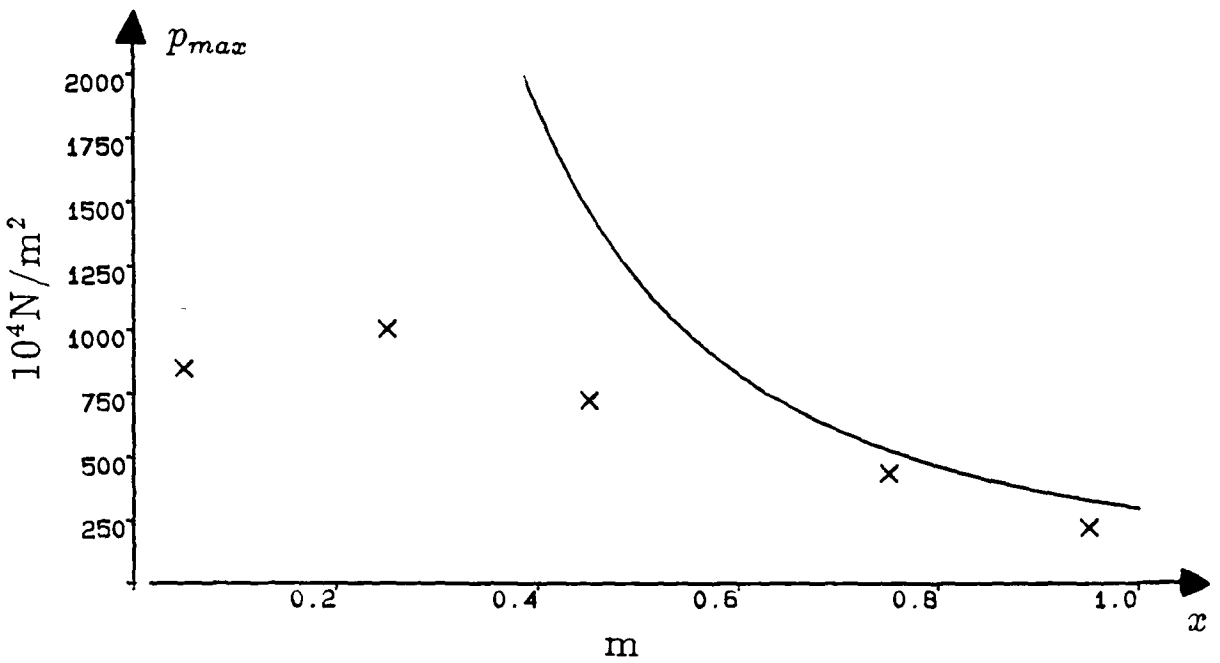

(a)

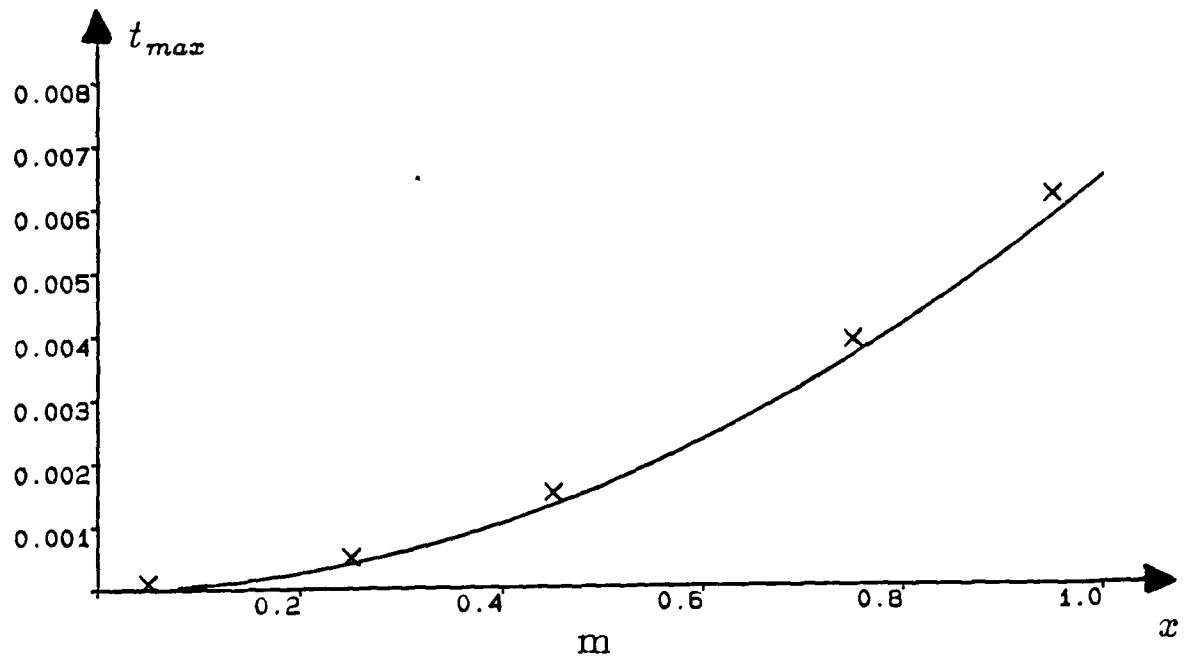

(b)

Figure 2.31: Comparison between experimental data and theory. (a) Maximum pressure in $10 kN/m^2$ and (b) Time to maximum pressure in seconds versus distance from the centerline in m.

Figure 2.32: Typical pressure histories for an approximately parabolic model. Reproduced from Nethercote *et al.* (1984).

secondary peak, while on the deadrise there is a single, sharp pressure maximum. The secondary peak on the keel is apparently due to air entrapment, and was more marked for models with larger keels. Figure (2.35) compares the experimentally observed magnitude and position of the maximum pressure pulse with the corresponding theoretical values. The predicted size of the maximum pressure is in rough agreement with the experimental data, and the position of the pressure maximum, calculated from equation (2.101), is well represented.

2.14 Comparison with other Theories

The present theory subsumes and extends the intuitive ideas of Wagner (1932). The outer solution formally reproduces the flat plate approximation for bodies with small deadrise angle, and justifies the inclusion of Wagner's 'splash-up' factor to determine the width of the plate. The inner solution is formally derived and its correct scale obtained by matching. The jet solution and composite pressure distribution are new. The entire theory, including the expression for the

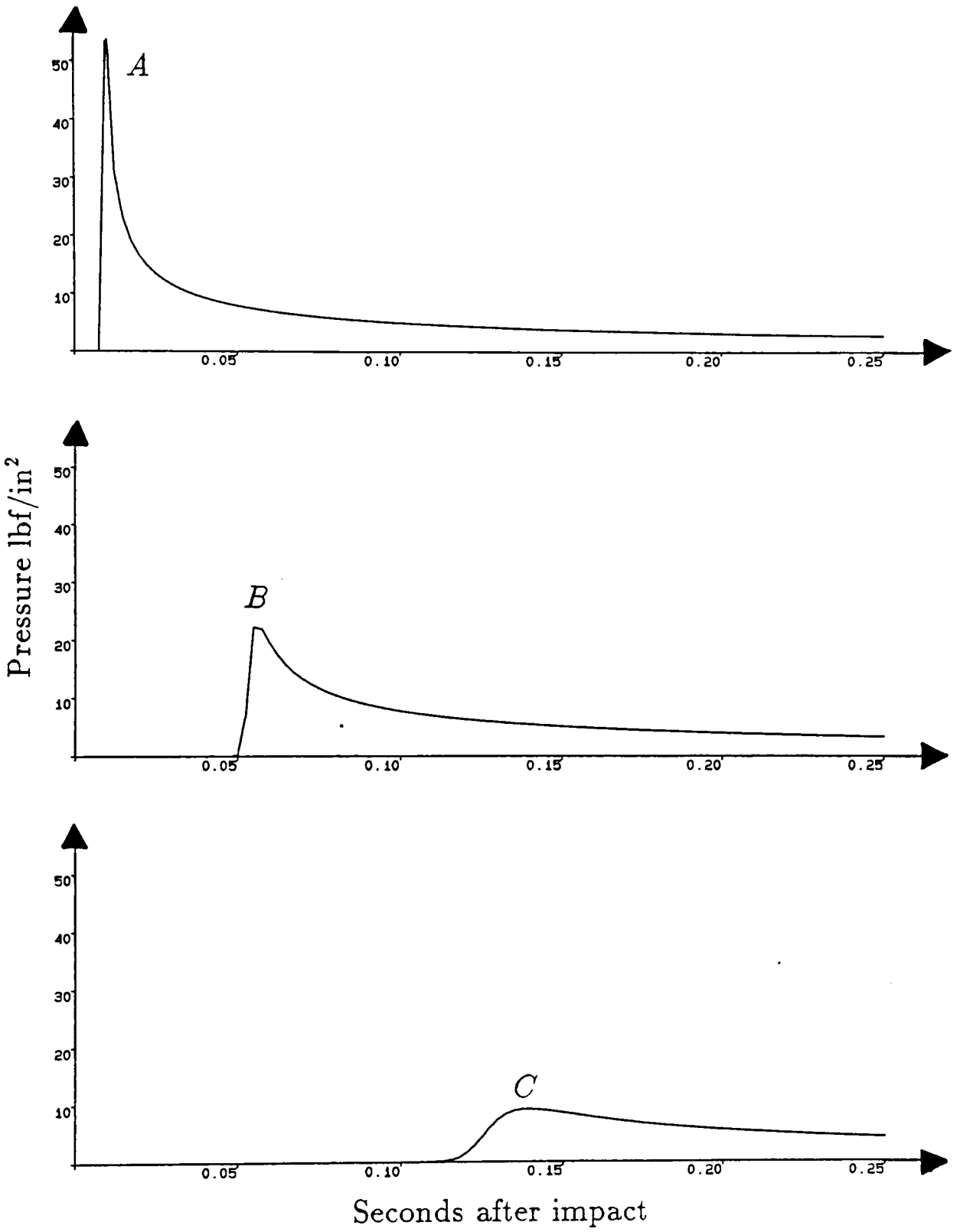

Figure 2.33: Theoretically predicted pressure histories for a parabolic body impacting at 20fps.

Figure 2.34: Typical pressure histories for a flat-bottomed wedge measured (a) on the flat keel (b) on the deadrise. Reproduced from Driscoll & Lloyd (1982).

total force, is generalized to arbitrary bodies with small deadrise angle, and an explicit solution of the integral equation to determine the plate width has been pointed out.

Our leading order pressure calculations can be used to correct the approximations made by Borg (1959), made using geometrical arguments for small deadrise wedges. His value of the pressure on the keel of $1/\epsilon$ should be $\pi/2\epsilon \simeq 1.571/\epsilon$, and his value for the maximum pressure of $1.125/\epsilon^2$ should be $\pi^2/8\epsilon^2 \simeq 1.233/\epsilon^2$.

An interesting comparison can be made with the asymptotic theory of Pukhnachov & Korobkin (1981) and Korobkin & Pukhnachov (1985), which applies to the initial stages of the impact of blunt bodies with arbitrary deadrise angle, and which uses time as the small parameter. Their analysis of the impact of a two-dimensional parabolic body, $y = mx^2$, at constant speed predicts a maximum non-dimensional pressure of

$$\frac{\Pi_{max}}{mt} \quad \text{for} \quad t \ll 1,$$

where $\Pi_{max} \simeq 0.47$, compared to the leading order term in the present small deadrise approximation of

$$\frac{d'(t)^2}{2\epsilon^2} = \frac{1}{2}\frac{1}{mt} \quad \text{for} \quad m \ll 1.$$

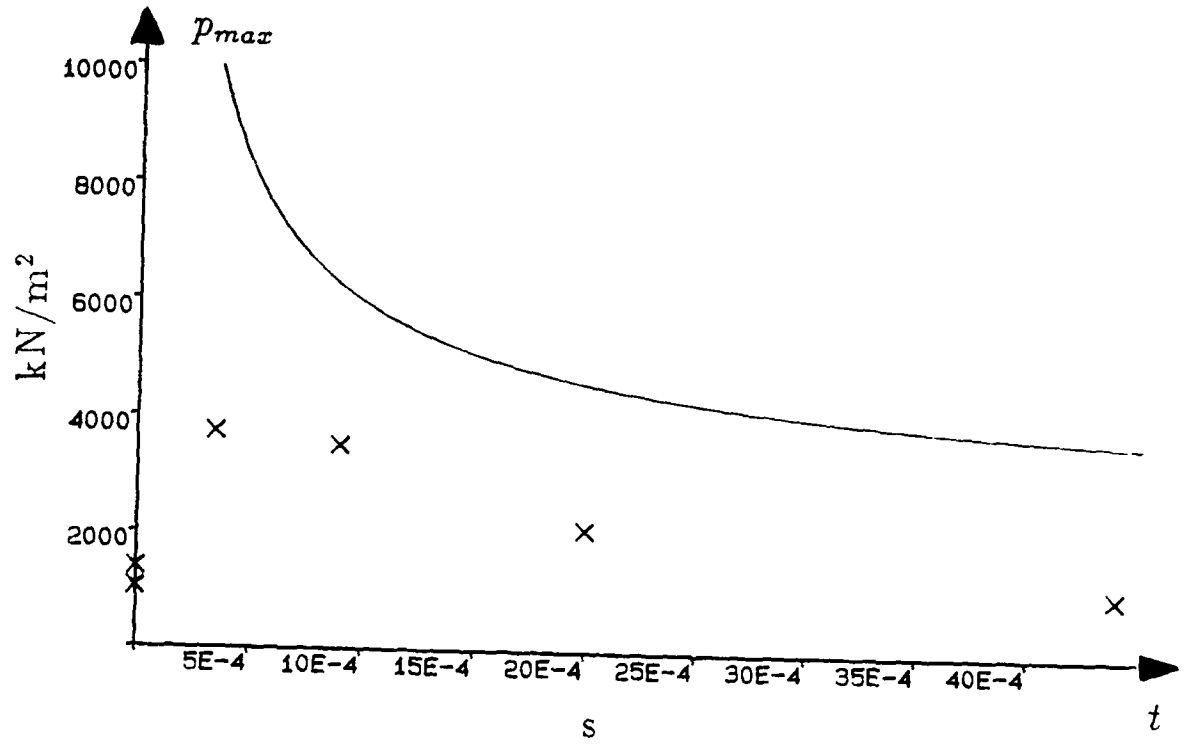

(a)

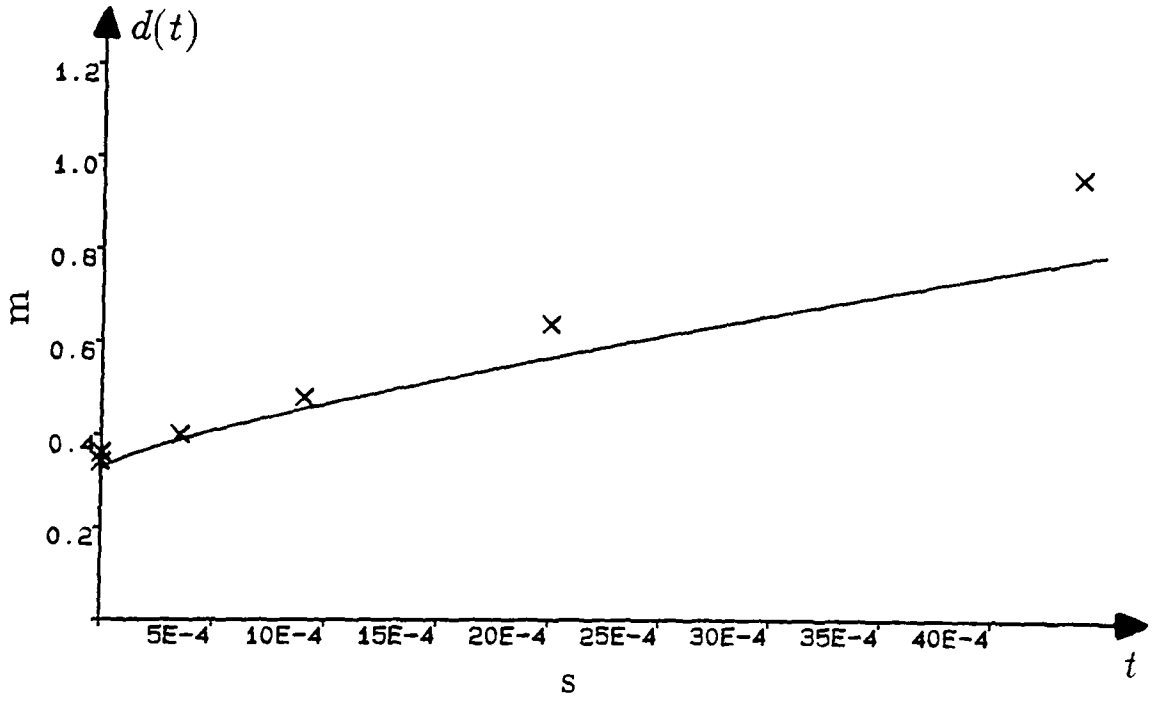

(b)

Figure 2.35: Comparison between experimental data and theory. (a) Maximum pressure in kN/m^2 and (b) position of maximum pressure in m versus time after first impact in seconds.

Unfortunately, the other properties of their solution are not so easy to compare and the exact relation between the two theories remains unclear.

Chapter 3

Three-Dimensional Fluid Impact Problems

In this chapter we generalize the procedure described in Chapter 2 to three-dimensional bodies with small deadrise angle. Less analytic progress is possible but we can obtain solutions to the leading order outer problem in some simple geometries. A variational formulation of the problem is derived, valid in two or three dimensions, leading to a fixed domain computational scheme, which can be implemented using finite elements. Finally, the method is extended to fluid-solid and fluid-fluid impact problems.

3.1 Problem Formulation

We consider the three-dimensional impact of a rigid body onto a half-space of quiescent, inviscid and incompressible fluid. We take cartesian coordinates (x, y, z) with the y-axis vertically upwards and the x and z-axes in the plane of the undisturbed fluid surface. Fluid initially fills $y \leq 0$ and $y > 0$ is assumed to be a vacuum. The effects of surface tension and gravity are again ignored. The impacting body has shape $y = f(x, z)$, where $f(0, 0) = 0$ and $f(x, z) > 0$ for $|x|, |z| > 0$ and moves vertically downwards with constant speed V. The instant $t = 0$ corresponds to the first moment of impact, and so the position of the body at time t is given by

$$y = f(x, z) - Vt.$$

The fluid velocity $\mathbf{u}(x, y, z, t)$ and pressure $p(x, y, z, t)$ satisfy Euler's equations (2.1) and (2.2). The flow is irrotational and so we introduce a velocity potential

$\phi(x, y, z, t)$, where $\mathbf{u} = \nabla\phi$. The governing equation is again Laplace's equation (2.3) and the pressure is determined from Bernoulli's equation (2.4). On the wetted body surface $y = f(x, z) - Vt$ the condition representing continuity of normal velocity now takes the form

$$\frac{\partial f}{\partial x}\frac{\partial \phi}{\partial x} + \frac{\partial f}{\partial z}\frac{\partial \phi}{\partial z} - \frac{\partial \phi}{\partial y} = V. \tag{3.1}$$

On the free surface $y = h(x, z, t)$ we have the kinematic condition

$$\frac{\partial h}{\partial t} + \frac{\partial h}{\partial x}\frac{\partial \phi}{\partial x} + \frac{\partial h}{\partial z}\frac{\partial \phi}{\partial z} - \frac{\partial \phi}{\partial y} = 0, \tag{3.2}$$

and from Bernoulli's equation the requirement of zero pressure gives the relation

$$\frac{\partial \phi}{\partial t} + \frac{1}{2}\left[\left(\frac{\partial \phi}{\partial x}\right)^2 + \left(\frac{\partial \phi}{\partial y}\right)^2 + \left(\frac{\partial \phi}{\partial z}\right)^2\right] = 0. \tag{3.3}$$

The initial conditions and far-field condition are the same as in two dimensions, viz.

$$\phi(x, y, z, 0) = 0, \quad h(x, z, 0) = 0, \tag{3.4}$$

together with

$$|\nabla\phi(x, y, z, t)| \to 0 \quad \text{as} \quad (x^2 + y^2 + z^2)^{\frac{1}{2}} \to \infty. \tag{3.5}$$

3.2 Bodies with Small Deadrise Angle

Once again in order to make progress we restrict our attention to bodies whose deadrise angle is everywhere small. First, we non-dimensionalize as we did in Section 2.3 and define the dimensionless z-coordinate, z^*, by

$$z^* = \frac{z}{l},$$

and immediately drop the starred notation for dimensionless variables. The position of the impacting body is now given by

$$y = f(\epsilon x, \epsilon z) - t,$$

and non-dimensionalizing the equations we obtain the full three-dimensional impact problem,

$$\frac{\partial^2\phi}{\partial x^2}+\frac{\partial^2\phi}{\partial y^2}+\frac{\partial^2\phi}{\partial z^2} = 0 \quad \text{in the fluid,} \tag{3.6}$$

$$\epsilon\left[\frac{\partial f}{\partial x}\frac{\partial\phi}{\partial x}+\frac{\partial f}{\partial z}\frac{\partial\phi}{\partial z}\right]-\frac{\partial\phi}{\partial y} = 1 \quad \text{on} \quad y=f(\epsilon x,\epsilon z)-t, \tag{3.7}$$

$$\frac{\partial h}{\partial t}+\frac{\partial h}{\partial x}\frac{\partial\phi}{\partial x}+\frac{\partial h}{\partial z}\frac{\partial\phi}{\partial z}-\frac{\partial\phi}{\partial y} = 0 \quad \text{on} \quad y=h(x,z,t), \tag{3.8}$$

$$\frac{\partial\phi}{\partial t}+\frac{1}{2}\left[\left(\frac{\partial\phi}{\partial x}\right)^2+\left(\frac{\partial\phi}{\partial y}\right)^2+\left(\frac{\partial\phi}{\partial z}\right)^2\right] = 0 \quad \text{on} \quad y=h(x,z,t). \tag{3.9}$$

The problem is subject to the initial conditions

$$\phi(x,y,z,0)=0, \quad h(x,z,0)=0, \tag{3.10}$$

and far-field condition

$$|\nabla\phi(x,y,z,t)|\to 0 \quad \text{as} \quad (x^2+y^2+z^2)^{\frac{1}{2}}\to\infty. \tag{3.11}$$

3.3 Outer Problem

Following closely the analysis used for the two-dimensional problem in Section 2.4, we investigate the problem in the outer region by introducing scaled outer variables, with the addition of

$$Z=\epsilon z,$$

and obtain the full outer problem,

$$\frac{\partial^2\Phi}{\partial X^2}+\frac{\partial^2\Phi}{\partial Y^2}+\frac{\partial^2\Phi}{\partial Z^2} = 0 \quad \text{in the fluid,} \tag{3.12}$$

$$\epsilon\left[\frac{\partial f}{\partial X}\frac{\partial\Phi}{\partial X}+\frac{\partial f}{\partial Z}\frac{\partial\Phi}{\partial Z}\right]-\frac{\partial\Phi}{\partial Y} = 1 \quad \text{on} \quad Y=\epsilon(f(X,Z)-t), \tag{3.13}$$

$$\frac{\partial H}{\partial t}+\frac{\partial H}{\partial X}\frac{\partial\Phi}{\partial X}+\frac{\partial H}{\partial Z}\frac{\partial\Phi}{\partial Z}-\frac{\partial\Phi}{\partial Y} = 0 \quad \text{on} \quad Y=\epsilon H(X,Z,t), \tag{3.14}$$

$$\frac{\partial\Phi}{\partial t}+\frac{\epsilon}{2}\left[\left(\frac{\partial\Phi}{\partial X}\right)^2+\left(\frac{\partial\Phi}{\partial Y}\right)^2+\left(\frac{\partial\Phi}{\partial Z}\right)^2\right] = 0 \quad \text{on} \quad Y=\epsilon H(X,Z,t), \tag{3.15}$$

together with the initial conditions

$$\Phi(X,Y,Z,0)=0, \quad H(X,Z,0)=0, \tag{3.16}$$

and far-field condition

$$|\nabla\Phi(X,Y,Z,t)| \to 0 \quad \text{as} \quad (X^2+Y^2+Z^2)^{\frac{1}{2}} \to \infty. \tag{3.17}$$

We now perform Taylor series expansions of the boundary conditions about $Y=0$ in order to express them in terms of quantities evaluated on the position of the undisturbed free surface. As before, this procedure presents no difficulties provided that the free surface remains single valued, but if it turns over as we expect then we must once again choose to neglect the thin, fast-moving jet (now more properly termed a *spray sheet*) that forms close to the body. Performing this linearization in two dimensions gives rise to a single unknown point $X = d(t)$ where the change of boundary conditions occurred; in three dimensions the geometry is more complicated and it will produce an unknown plane *curve* in $Y=0$, denoted by $t=\omega(X,Z)$, representing the boundary of the equivalent flat plate.

If we now seek regular perturbation solutions for Φ and H as asymptotic series in powers of ϵ, then the leading order outer problem is

$$\frac{\partial^2\Phi_0}{\partial X^2}+\frac{\partial^2\Phi_0}{\partial Y^2}+\frac{\partial^2\Phi_0}{\partial Z^2} = 0 \quad \text{in the fluid,} \tag{3.18}$$

$$\frac{\partial\Phi_0}{\partial Y} = -1 \quad \text{on} \quad Y=0, \quad t>\omega(X,Z), \tag{3.19}$$

$$\frac{\partial\Phi_0}{\partial Y} = \frac{\partial H_0}{\partial t} \quad \text{on} \quad Y=0, \quad t<\omega(X,Z), \tag{3.20}$$

$$\frac{\partial\Phi_0}{\partial t} = 0 \quad \text{on} \quad Y=0, \quad t<\omega(X,Z), \tag{3.21}$$

with the initial conditions

$$\Phi_0(X,Y,Z,0)=0, \quad H_0(X,Z,0)=0, \tag{3.22}$$

and far-field condition

$$|\nabla\Phi_0(X,Y,Z,t)| \to 0 \quad \text{as} \quad (X^2+Y^2+Z^2)^{\frac{1}{2}} \to \infty. \tag{3.23}$$

If we integrate (3.21) and use the initial condition for Φ_0 (3.22a), then we obtain

$$\Phi_0 = 0 \quad \text{on} \quad Y=0, \quad t<\omega(X,Z). \tag{3.24}$$

The leading order outer problem is summarised in Figure (3.1). Once Φ_0 has

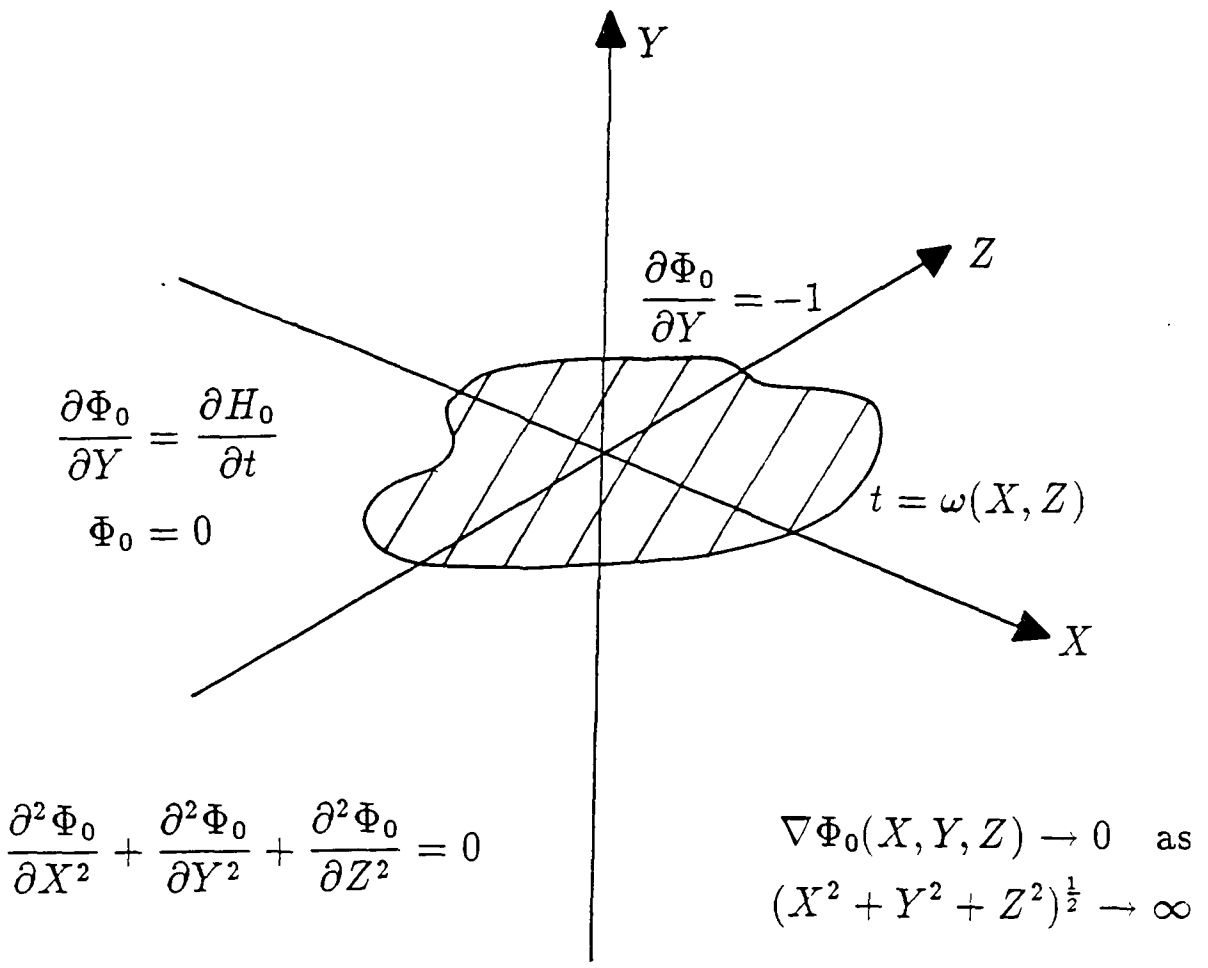

Figure 3.1: Leading order outer problem.

been determined the leading order free surface elevation can be calculated from equation (3.20),

$$H_0(X, Z, t) = \int_0^t \frac{\partial \Phi_0}{\partial Y}(X, 0, Z, \tau)\, \mathrm{d}\tau \quad \text{for} \quad t < \omega(X, Z). \tag{3.25}$$

3.4 Matching Condition to Determine $\omega(X, Z)$

By extending the argument presented in Appendix B to three dimensions it is easy to show that, on the assumption that the volume of fluid in the spray sheet is small compared to a typical volume based on the outer length scale, the matching condition to determine the boundary of the equivalent flat plate, $t = \omega(X, Z)$, remains

$$H_0(X, Z, t) = f(X, Z) - t \quad \text{on} \quad t = \omega(X, Z). \tag{3.26}$$

Using equation (3.25), this gives the matching condition

$$\int_0^t \frac{\partial \Phi_0}{\partial Y}(X, 0, Z, \tau)\, \mathrm{d}\tau = f(X, Z) - t \quad \text{on} \quad t = \omega(X, Z). \tag{3.27}$$

3.5 Variational Formulation of the Problem

Except in the special case of rotationally symmetric bodies, obtaining a general solution of the leading order outer problem in three dimensions is too difficult. A great mathematical simplification can be made, in both two and three dimensions, by formulating the problem as a *variational inequality*. The solution of this variational formulation can be associated with the minimiser of a variational integral, providing information about the existence, uniqueness and smoothness of the solution. This approach also leads to an efficient numerical procedure for calculating solutions for arbitrary bodies in either two or three dimensions. Details of the theory of variational inequalities and examples of their application to free and moving boundary problems are contained in Elliott & Ockendon (1982).

In order to write a free boundary problem with a second order field equation as a variational inequality, we require continuity of the first derivative of the dependent variable. In the present problem $\partial\Phi_0/\partial Y$ is discontinuous across the curve $t = \omega(X, Z)$ and so, as it stands, the problem cannot be so written. The techniques employed to transform such problems into ones having solutions with continuous first derivatives are usually termed *Baiocchi Transformations*, and have been the source of interest in the literature, even before the pioneering work by C. Baiocchi from whom they take their name. Fortunately, the smoothing transformation that was suggested by Korobkin (1982) for the Lagrangian formulation of the impact of a blunt body can be applied successfully to the present problem. Instead of working with the velocity potential $\Phi_0(X, Y, Z, t)$, we introduce a *displacement potential*, $\Psi_0(X, Y, Z, t)$, defined by

$$\Psi_0(X, Y, Z, t) = -\int_0^t \Phi_0(X, Y, Z, \tau)\,\mathrm{d}\tau, \tag{3.28}$$

and since Φ_0 satisfies Laplace's equation (3.18) then so does Ψ_0,

$$\nabla^2\Psi_0 = 0 \quad \text{in} \quad Y < 0. \tag{3.29}$$

On the boundary $Y = 0$ when $t < \omega(X, Z)$ the conditions (3.20) and (3.24) mean that

$$\frac{\partial\Psi_0}{\partial Y}(X, 0, Z, t) = -H_0(X, Z, t), \tag{3.30}$$

$$\Psi_0(X, 0, Z, t) = 0. \tag{3.31}$$

When $t > \omega(X, Z)$ equation (3.19) also holds, and so

$$\begin{aligned}
\frac{\partial \Psi_0}{\partial Y}(X, 0, Z, t) &= -\int_0^t \frac{\partial \Phi_0}{\partial Y}(X, Z, \tau)\, \mathrm{d}\tau \\
&= -\int_0^\omega \frac{\partial H_0}{\partial \tau}(X, Z, \tau)\, \mathrm{d}\tau + \int_\omega^t \mathrm{d}\tau \\
&= -H_0(X, Z, \omega) + (t - \omega) \\
&= t - f(X, Z). \qquad (3.32)
\end{aligned}$$

The great advantage of this transformation is that, since the matching condition (3.26) holds, the first derivative of the new dependent variable, $\partial \Psi_0 / \partial Y$, is continuous across $t = \omega(X, Z)$. Ψ_0 satisfies the *linear complementarity problem*,

$$\begin{aligned}
\nabla^2 \Psi_0 = 0 \quad &\text{in} \quad Y < 0, \\
\Psi_0 \left(\frac{\partial \Psi_0}{\partial Y} - t + f(X, Z) \right) = 0 \quad &\text{on} \quad Y = 0,
\end{aligned}$$

with

$$\Psi_0 \geq 0, \quad \left(\frac{\partial \Psi_0}{\partial Y} - t + f(X, Z) \right) \geq 0 \quad \text{on} \quad Y = 0.$$

We can now write the problem as a variational inequality. First we introduce the real Sobolev space $\mathcal{H}^1$, with inner product $(\cdot, \cdot)$ and associated norm $\| \cdot \|$. Then we define the *symmetric continuous bilinear form* $a : \mathcal{H}^1 \times \mathcal{H}^1 \to \Re$ by

$$a(u, v) = \iiint_{Y<0} \nabla u \cdot \nabla v \, \mathrm{d}X \, \mathrm{d}Y \, \mathrm{d}Z,$$

and the *continuous linear mapping* $\ell : \mathcal{H}^1 \to \Re$ by

$$\ell(u) = \iint_{Y=0} g(X, Z, t) u \, \mathrm{d}X \, \mathrm{d}Z,$$

where $g(X, Z, t) = t - f(X, Z)$ and the boundary values are defined in the usual way by the trace operator $\mathrm{T}_r : \mathcal{H}^1 \to L^2(Y = 0)$. $\mathcal{V}$ denotes the set of all $v \in \mathcal{H}^1$ such that $v \geq 0$ in $Y < 0$. Now for any $v \in \mathcal{V}$ consider

$$a(\Psi_0, v - \Psi_0) = \iiint_{Y<0} \nabla \Psi_0 \cdot \nabla (v - \Psi_0) \, \mathrm{d}X \, \mathrm{d}Y \, \mathrm{d}Z.$$

Applying Green's Theorem shows that this is equal to

$$\iint_{Y=0} (v - \Psi_0) \nabla \Psi_0 \cdot \mathbf{n} \, \mathrm{d}X \, \mathrm{d}Z,$$

where $\mathbf{n}$ is the outward unit normal to $Y = 0$. Furthermore,

$$\nabla\Psi_0 \cdot \mathbf{n} = \frac{\partial \Psi_0}{\partial Y} \geq g(X, Z, t),$$

and so we deduce that Ψ_0 satisfies the variational inequality

$$a(\Psi_0, v - \Psi_0) \geq \ell(v - \Psi_0) \quad \text{for all} \quad v \in \mathcal{V}. \tag{3.33}$$

Since $a(\cdot, \cdot)$ is symmetric it can be shown that the variational inequality is equivalent to a *constrained minimisation*,

$$J(\Psi_0) \leq J(v) \quad \text{for all} \quad v \in \mathcal{V}, \quad \text{where} \quad J(v) = \frac{1}{2}a(v, v) - \ell(v). \tag{3.34}$$

If $a(\cdot, \cdot)$ is coercive, viz. there exists an $\alpha > 0$ such that $a(v, v) \geq \alpha \parallel v \parallel^2$ for all $v \in \mathcal{H}^1$, then the Hilbert space projection theorem proves that the solution to (3.33) exists and is unique in $\mathcal{V}$. $a(\cdot, \cdot)$ is coercive when the region occupied by fluid is bounded, but the question of its coercivity in an unbounded domain remains open. However, since all our computations are necessarily made in a finite domain, we shall not need to pursue the point further.

3.6 Computational Approach

The variational formulation of the problem lends itself to a computational approach based on finite elements. Details of the computational schemes employed are given in Appendix C, but the basic approach is outlined below. The solution domain $Y \leq 0$ is divided into subregions called *finite elements*. Each of the n *nodes* are shared by a number of different elements, thereby connecting them together to form a *mesh*. A function $v \in \mathcal{V}$ is approximated in terms of its values at the nodes, which are written in vector form as

$$\mathbf{v} = (v_1, v_2, \ldots, v_n)^t.$$

The variation of v within an element is determined by the values of v at the nodes of the element;

$$\mathbf{v}^e = (w_i, w_j, \ldots, w_p)^t,$$

where $i, j, \ldots, p$ denote the nodes of the element, and takes the form

$$\mathbf{v} = (N_i, N_j, \ldots, N_p)\,(v_i, v_j, \ldots, v_p)^t,$$

where $N_i, N_j, \ldots, N_p$ are the *element basis functions.* Inserting this approximation for v into equation (3.34) yields

$$J(\Psi_0) = \min_{v_1, v_2, \ldots, v_n} \left[\frac{1}{2} \mathbf{v}^t K \mathbf{v} - \mathbf{v}^t \mathbf{F} \right],$$

where K is the $n \times n$ *stiffness matrix* whose entries are given by

$$K_{ij} = a(N_i, N_j) \quad \text{for} \quad i, j = 1, 2, \ldots, n,$$

and $\mathbf{F}$ is the $n \times 1$ *load vector* whose entries are

$$F_i = \ell(N_i) \quad \text{for} \quad i = 1, 2, \ldots, n.$$

Minimising over the coefficients $v_1, v_2, \ldots, v_n$ we obtain n equations for the unknown vector

$$\Psi_0 = (w_1, w_2, \ldots, w_n),$$

namely

$$\frac{\partial J(\Psi_0)}{\partial w_i} = 0 \quad \text{for} \quad i = 1, 2, \ldots, n,$$

from which we obtain the linear algebraic equation

$$K \Psi_0 = \mathbf{F}. \tag{3.35}$$

This system of equations for $w_1, w_2, \ldots, w_n$ can be solved by the well-known iterative method of projected successive over relaxation (SOR), as described in Crank (1984) and Morton (1986b). Once the solution for Ψ_0 is known, Φ_0 can be recovered by numerical differentiation, and the free surface elevation H_0 can be evaluated numerically from equation (3.20).

In the following examples, we used the piecewise linear basis functions described in Appendix C to approximate the solution. Figure (3.2) shows the computed free surface for a two-dimensional wedge $Y = \epsilon |X|$. It is evidently in good agreement with the exact solution which is available from equation (2.96). The method can equally well be applied in three dimensions, and Figure (3.3) shows the computed free surface for the impact of a three-dimensional cone $Y = \epsilon R$ at two different times. The unfortunate lack of circular symmetry is an inevitable result of plotting the solution on a rectangular rather than a radially symmetric grid.

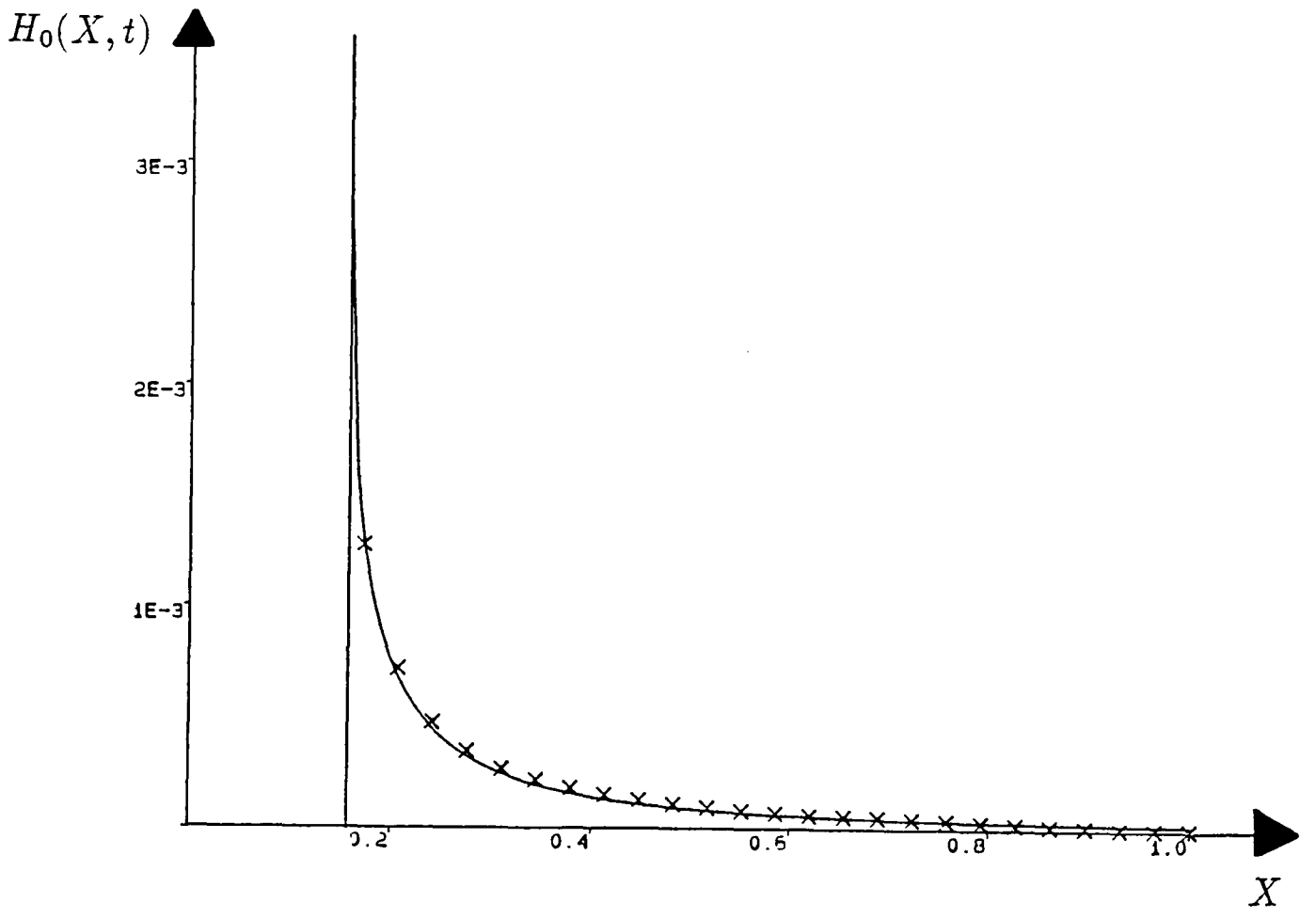

Figure 3.2: Comparison between exact and computed outer free surface elevation for a two-dimensional wedge $Y = \epsilon|X|$ at $t = 0.1$.

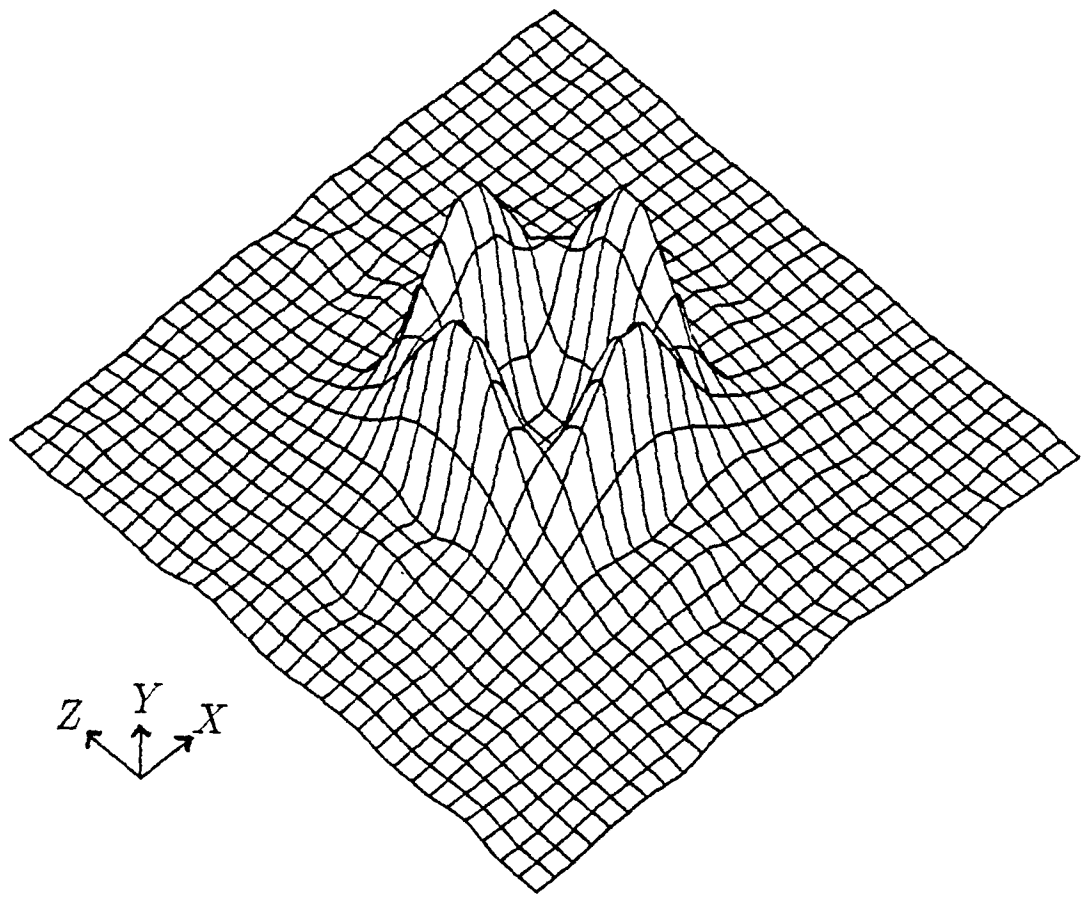

Figure 3.3: Computed free surface elevation for a three-dimensional cone $Y = \epsilon R$ at $t = 0.25$ and $t = 0.5$.

3.7 Solution of the Outer Problem

Unfortunately the complex variable techniques we employed to solve the leading order outer problem in two dimensions do not work in three dimensions. The situation is further complicated by the unknown curve $t = \omega(X, Z)$ and, consequently, no general closed form solution can be obtained. We can, however, construct solutions for some special cases where the geometry is simple enough to allow us to proceed.

3.7.1 Body with Rotational Symmetry

An explicit solution can be obtained if the impacting body is rotationally symmetric about the vertical axis. We introduce cylindrical polar coordinates denoted by (R, Θ, Y), in which the profile of the body is described by $Y = \epsilon f(R)$. The solution is independent of Θ, and so the boundary of the equivalent plate must be a circle of unknown radius $R = c(t)$. Writing the leading order outer problem in these coordinates we obtain

$$\frac{1}{R}\frac{\partial}{\partial R}\left(R\frac{\partial \Phi_0}{\partial R}\right) + \frac{\partial^2 \Phi_0}{\partial Y^2} = 0 \quad \text{in} \quad Y < 0, \tag{3.36}$$

$$\frac{\partial \Phi_0}{\partial Y} = -1 \quad \text{on} \quad Y = 0, \quad R < c(t), \tag{3.37}$$

$$\frac{\partial \Phi_0}{\partial Y} = \frac{\partial H_0}{\partial t} \quad \text{on} \quad Y = 0, \quad R > c(t), \tag{3.38}$$

$$\Phi_0 = 0 \quad \text{on} \quad Y = 0, \quad R > c(t). \tag{3.39}$$

If we first seek a solution separable in R and Y, then we can deduce that the general axisymmetric solution of Laplace's equation in $Y \leq 0$ is given by

$$\Phi_0(R, Y, t) = \int_0^\infty A(k) e^{-k|Y|} J_0(kR)\, \mathrm{d}k, \tag{3.40}$$

where $J_0(\cdot)$ is a Bessel Function of the first kind of order zero and the function $A(\cdot)$ is determined by the boundary conditions. Substituting this expression into the boundary conditions we obtain a pair of integral equations for $A(\cdot)$,

$$\left.\begin{aligned} \int_0^\infty k A(k) J_0(kR)\, \mathrm{d}k &= -1 \quad \text{for} \quad R < c(t) \\ \int_0^\infty A(k) J_0(kR)\, \mathrm{d}k &= 0 \quad \text{for} \quad R > c(t) \end{aligned}\right\}.$$

Sneddon (1966) discusses dual integral equations of this kind and, by considering the properties of the *Weber-Schafheitlin integral*,

$$\int_0^\infty t^{-\lambda} J_\mu(at) J_\nu(at)\,\mathrm{d}t,$$

shows that the present problem has solution

$$A(k) = -\frac{2c^2}{\pi} j_1(kr), \tag{3.41}$$

where $j_i(\cdot)$ denotes a spherical Bessel function of order i. Since

$$j_1(kr) = -\left(\frac{\pi}{2kc}\right)^{\frac{1}{2}} J_{\frac{3}{2}}(kc) = \left[\frac{\sin(kc)}{k^2c^2} - \frac{\cos(kc)}{kc}\right],$$

the solution for $\Phi_0(R, Y, t)$ is

$$\Phi_0(R, Y, t) = -\left(\frac{2c^3}{\pi}\right)^{\frac{1}{2}} \int_0^\infty \frac{e^{-k|Y|}}{k^{\frac{1}{2}}} J_{\frac{3}{2}}(kr) J_0(kR)\,\mathrm{d}k, \tag{3.42}$$

which decays like $1/\rho^2$ as $|\rho| \to \infty$ where $\rho = (R^2 + Y^2)^{\frac{1}{2}}$. In particular, we can evaluate the value of the potential on $Y = 0$ to be

$$\Phi_0(R, 0, t) = -\frac{2}{\pi}\left(c(t)^2 - R^2\right)^{\frac{1}{2}} \quad \text{for} \quad R \le c(t). \tag{3.43}$$

From equation (3.20) the free surface elevation $H_0(R, t)$ is given by

$$H_0(R, t) = \int_0^t \frac{\partial \Phi_0}{\partial Y}(R, 0, \tau)\,\mathrm{d}\tau,$$

where

$$\frac{\partial \Phi_0}{\partial Y}(R, 0, t) = -\left(\frac{2c^3}{\pi}\right)^{\frac{1}{2}} \int_0^\infty k^{\frac{1}{2}} J_{\frac{3}{2}}(kc) J_0(kR)\,\mathrm{d}k.$$

Evaluating this integral we obtain

$$\frac{\partial \Phi_0}{\partial Y}(R, 0, t) = \frac{2}{\pi}\left[\frac{c(t)}{(R^2 - c(t)^2)^{\frac{1}{2}}} - \sin^{-1}\left(\frac{c(t)}{R}\right)\right],$$

and so

$$H_0(R, t) = \frac{2}{\pi}\int_0^t \left[\frac{c(\tau)}{(R^2 - c(\tau)^2)^{\frac{1}{2}}} - \sin^{-1}\left(\frac{c(\tau)}{R}\right)\right]\mathrm{d}\tau. \tag{3.44}$$

The matching condition (3.27) to determine $c(t)$ is, therefore,

$$f(c(t)) - t = \frac{2}{\pi}\int_0^t \left[\frac{c(\tau)}{(c(t)^2 - c(\tau)^2)^{\frac{1}{2}}} - \sin^{-1}\left(\frac{c(\tau)}{c(t)}\right)\right]\mathrm{d}\tau. \tag{3.45}$$

We can solve the integral equation by writing t as a function of c, and introducing the new integration variable σ so that $\tau = t(\sigma)$ and hence $d\tau = t'(\sigma)d\sigma$. The equation then becomes

$$f(c) - t = \frac{2}{\pi}\int_0^c \left[\frac{\sigma}{(c^2-\sigma^2)^{\frac{1}{2}}} - \sin^{-1}\left(\frac{\sigma}{c}\right)\right] t'(\sigma)\,\mathrm{d}\sigma,$$

and, after integrating the second term by parts, we obtain

$$f(c) = \frac{2}{\pi}\int_0^c \frac{\sigma t'(\sigma) + t(\sigma)}{(c^2-\sigma^2)^{\frac{1}{2}}}\,\mathrm{d}\sigma.$$

This is now an Abel integral equation and has the solution

$$\sigma t'(\sigma) + t(\sigma) = \frac{d}{d\sigma}\int_0^\sigma \frac{\xi f(\xi)}{(\sigma^2-\xi^2)^{\frac{1}{2}}}\,\mathrm{d}\xi,$$

provided that the integral exists. Integrating this expression once with respect to σ gives a formula for $t(c)$,

$$t(c) = \frac{1}{c}\int_0^c \frac{\xi f(\xi)}{(c^2-\xi^2)^{\frac{1}{2}}}\,\mathrm{d}\xi. \tag{3.46}$$

If, more generally, the impacting body moves with non-dimensional speed $v(t)$, then we can extend the above analysis to obtain the solution

$$\int_0^{t(c)} v(\tau)\,\mathrm{d}\tau = \frac{1}{c}\int_0^c \frac{\xi f(\xi)}{(c^2-\xi^2)^{\frac{1}{2}}}\,\mathrm{d}\xi. \tag{3.47}$$

Schmieden (1953) solved the same integral equation in a similar way.

When the impacting body is a *cone* so that $f(R) = \alpha R$, the problem is self-similar and has solution

$$c(t) = \frac{4t}{\alpha\pi}, \tag{3.48}$$

which agrees with the calculations of Shiffman & Spencer (1957), and we observe that the ratio of the radius of the cross-section of the body at $Y = 0$ to the radius of $t = \omega(X, Z)$ is $4/\pi \simeq 1.273$. When the impacting body is a *paraboloid*, $f(R) = \alpha R^2$, we obtain the solution

$$c(t) = \left(\frac{3t}{2\alpha}\right)^{\frac{1}{2}}, \tag{3.49}$$

which predicts that effective radius of the cross-section of the body at $Y = 0$ is $(3/2)^{\frac{1}{2}} \simeq 1.225$ times the actual one. Similarly, when the body is a semi-circle

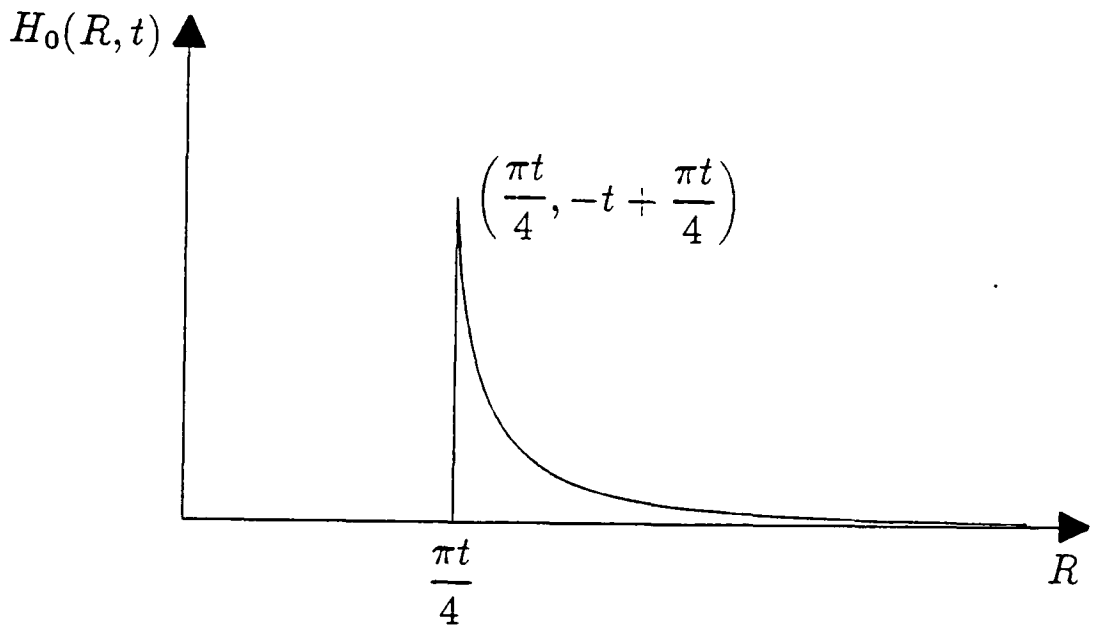

Figure 3.4: Leading order outer free surface elevation for a cone $Y = \epsilon R$.

of unit radius, $f(R) = 1 - (1 - R^2)^{\frac{1}{2}}$ for $R \leq 1$, we obtain an algebraic relation between t and $c(t)$,

$$t + \frac{1 - c^2}{4c} \log \left| \frac{1 + c}{1 - c} \right| - \frac{1}{2} = 0,$$

which can be solved numerically for $c(t)$ with a simple iterative scheme. A two-dimensional plot of the leading order free surface elevation for a cone, calculated from equation (3.44), is shown in Figure (3.4).

Following the same approach as in the plane case, we can obtain the $O(1/\epsilon)$ leading order outer pressure on the disc, $R \leq r(t)$, to be

$$P_0(R, 0, t) = \frac{\partial \Phi_0}{\partial t}(R, 0, t) = \frac{2}{\pi} \frac{c(t)c'(t)}{(c(t)^2 - R^2)^{\frac{1}{2}}}, \tag{3.50}$$

and integrating this expression over the disc gives an expression for the $O(1/\epsilon^2)$ leading order term in the expansion of the force,

$$F_0(t) = 4c'(t)c(t)^2. \tag{3.51}$$

For a cone, the leading order force is quadratic in t and equal to $(16t)^2/\pi^3$, while for a paraboloid it is proportional to $t^{\frac{1}{2}}$ and equal to $3(3t/2)^{\frac{1}{2}}$.

The experimental results of Moghisi & Squire (1981) demonstrate that, in the initial stages of the impact of a hemisphere with constant speed, the total force on the body, $F(t)$, is proportional to the square root of the depth of submergence.

Written in dimensionless variables, they obtained the expression

$$F(t) = \frac{a\pi}{2} t^{\frac{1}{2}}$$

where the constant a was found to be approximately equal to 5.22. The present theory applied to a parabolic body with unit radius of curvature impacting at constant speed, predicts that the force is

$$F(t) = \frac{3\sqrt{3}}{\epsilon^2} t^{\frac{1}{2}} + O\left(\frac{1}{\epsilon}\right) \quad \text{where} \quad \epsilon = \frac{1}{\sqrt{2}}.$$

The square root dependence of the force on depth is in agreement with the experimental results, and the constant is approximately equal to 10.39, which is in fair agreement with the experimental value of about 8.20.

3.7.2 Body with Elliptic Cross-Section

Korobkin (1985) has obtained an exact solution when the impacting body is an *elliptic paraboloid*, and his approach is repeated here for completeness. We introduce an *elliptic coordinate system* (ρ, μ, ν) which is connected to the cartesian system (X, Y, Z) by the relations

$$X^2 = \frac{\rho^2 \mu^2 \nu^2}{h^2 k^2} \tag{3.52}$$

$$Y^2 = \frac{(\rho^2 - k^2)(k^2 - \mu^2)(k^2 - \nu^2)}{h^2(k^2 - h^2)} \tag{3.53}$$

$$Z^2 = \frac{(\rho^2 - h^2)(\mu^2 - h^2)(h^2 - \nu^2)}{h^2(k^2 - h^2)} \tag{3.54}$$

where

$$k^2 \leq \rho^2 < \infty, \qquad h^2 \leq \mu^2 \leq k^2, \qquad 0 \leq \nu^2 \leq h^2,$$

and h and k are numbers such that $k > h > 0$. The surfaces $\rho =$ constant, $\mu =$ constant and $\nu =$ constant form a confocal system of ellipsoids, hyperboloids of one sheet and hyperboloids of two sheets respectively. When ρ has the value k the ellipsoid is flattened down to the focal ellipse with semi-major axis k and eccentricity h given by

$$\frac{X^2}{k^2} + \frac{Z^2}{k^2 - h^2} = 1, \qquad Y = 0. \tag{3.55}$$

The plane $Y = 0$ outside the elliptic disc is given by $\mu = h$, with ρ varying from k to infinity. Laplace's equation separates in ellipsoidal coordinates, and the general form of a harmonic external to the ellipsoid $\rho = \rho_1$ and vanishing at infinity is given by

$$\sum_{n=0}^{\infty} \sum_{m=1}^{2n+1} \frac{F_n^m(\rho)}{F_n^m(\rho_1)} E_n^m(\mu) E_n^m(\nu),$$

where $E(\cdot)$ and $F(\cdot)$ denote Lamé functions of the first and second kind respectively. A full description of the theory of ellipsoidal harmonics can be found in the famous books by Whittaker & Watson (1962) and Hobson (1965).

The position of the impacting body is described by

$$Z = \frac{X^2}{a^2} + \frac{Z^2}{b^2} - t,$$

and the eccentricity of a cross-section $Z =$ constant is given by $\epsilon = (1 - b^2/a^2)^{\frac{1}{2}}$. The curve $t = \omega(X, Z)$ will be a confocal ellipsoid, whose semi-major axis we denote by $a_0\sqrt{t}$ and eccentricity by e. The problem admits a similarity solution, in terms of the similarity variables $\hat{X}$, $\hat{Z}$ and $\hat{\Phi}_0$ defined by

$$\hat{X} = \frac{X}{a_0 t^{\frac{1}{2}}}, \qquad \hat{Z} = \frac{Z}{a_0 t^{\frac{1}{2}}}, \qquad \hat{\Phi}_0 = \frac{\Phi_0}{a_0 t^{\frac{3}{2}}}.$$

In the new variables, the boundary of the equivalent plate is

$$\hat{X}^2 + \frac{\hat{Z}^2}{1 - e^2} = 1, \qquad Y = 0$$

which we identify with the elliptic disc given by equation (3.55) by choosing $k = 1$ and $h = e$.

Solving the problem directly for $\hat{\Phi}_0$ leads to analytical difficulties when applying the matching condition, so it is easier to consider the problem for the displacement potential, $\hat{\Psi}_0$, given by $\hat{\Phi}_0 = \partial\hat{\Psi}_0/\partial t$. Furthermore, rather than solve the problem in the half-space $Y \leq 0$, it is convenient to continue $\hat{\Psi}_0$ in an *odd* way into the upper half-space, and seek a solution harmonic everywhere outside the ellipsoid. Finally, we introduce

$$\widehat{W}_0(\hat{X}, Y, \hat{Z}, t) = \frac{\partial\hat{\Psi}_0}{\partial Y}(\hat{X}, Y, \hat{Z}, t).$$

If the solution for $\widehat{W}_0$ is restricted to be *even* in Y, then $\hat{\Psi}_0$ is *odd* in Y, and so the condition $\hat{\Psi}_0(\hat{X}, 0, \hat{Z}, t) = 0$ outside the ellipsoid is satisfied automatically. The boundary value problem satisfied by $\widehat{W}_0(\hat{X}, Y, \hat{Z})$ is, therefore,

$$\nabla^2 \widehat{W}_0 = 0 \quad \text{in} \quad \rho \geq 1, \tag{3.56}$$

$$\widehat{W}_0 = \frac{\hat{X}^2}{a^2} + \frac{\hat{Z}^2}{b^2} - \frac{1}{a_0^2} \quad \text{on} \quad \rho = 1, \tag{3.57}$$

$$\widehat{W}_0 = H_0, \quad \text{on} \quad \mu = 1 \tag{3.58}$$

$$\widehat{W}_0 \to 0 \quad \text{as} \quad |\rho| \to \infty. \tag{3.59}$$

We can obtain a closed form solution to this problem by recalling that only Lamé functions of the first species are even in $\hat{X}$, Y and $\hat{Z}$, and that to reproduce quadratic terms in $\hat{X}$ and $\hat{Z}$ on the ellipse $\rho = 1$ we further restrict ourselves to those of second order. There are only two functions that fulfil both these requirements, and so the general solution is given by

$$\widehat{W}_0 = A\left\{\frac{\hat{X}^2}{\alpha_1^2} + \frac{Y^2}{\alpha_1^2 - e^2} + \frac{\hat{Z}^2}{\alpha_1^2 - 1}\right\}\frac{\sigma_1(\rho)}{\sigma_1(1)}$$

$$+B\left\{\frac{\hat{X}^2}{\alpha_2^2} + \frac{Y^2}{\alpha_2^2 - e^2} + \frac{\hat{Z}^2}{\alpha_2^2 - 1}\right\}\frac{\sigma_2(\rho)}{\sigma_2(1)}, \tag{3.60}$$

where

$$\alpha_1^2 = \frac{1}{3}(1 + e^2 + (1 + e^4 - e^2)^{\frac{1}{2}}), \qquad \alpha_2^2 = \frac{1}{3}(1 + e^2 - (1 + e^4 - e^2)^{\frac{1}{2}}),$$

and the Lamé functions of the second kind are given by

$$\sigma_n(\rho) = \int_\rho^\infty \frac{\mathrm{d}\xi}{(\xi^2 - \alpha_n^2)^2(\xi^2 - e^2)^{\frac{1}{2}}(\xi^2 - 1)^{\frac{1}{2}}}, \quad \text{for} \quad n = 1, 2.$$

From the boundary conditions on the disc we obtain

$$A = m\left(\frac{1 - \epsilon^2}{b^2}\right), \qquad B = \alpha_1\left(\frac{1 - \epsilon^2}{b^2}\right)\left(\frac{1}{a^2} + \frac{m}{\alpha_2}\right),$$

where

$$m = \frac{\alpha_2}{e^2}\frac{\alpha_2 - e^2}{\alpha_1 - \alpha_2}\frac{\epsilon^2\alpha_1 - e^2}{1 - \epsilon^2}.$$

Furthermore, by equating coefficients of the constant term, we obtain an expression for the semi-major axis,

$$a_0^2 = \frac{3b^2}{(2 - e^2 - \epsilon^2)}.$$

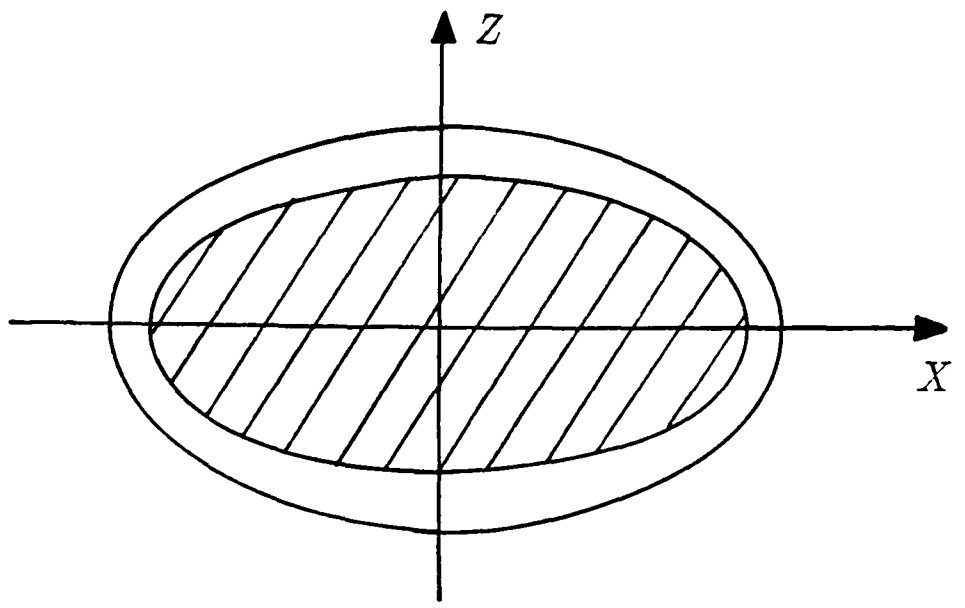

Figure 3.5: Relative arrangement of the contact line $t = \omega(X, Z)$ and the section $Y = 0$ during the impact of an elliptic paraboloid.

From the far-field condition we deduce that $m(e, \epsilon) = 0$, and so the eccentricities e and ϵ are related by

$$e = \epsilon \left(\frac{2 - \epsilon^2}{3 - 2\epsilon^2} \right)^{\frac{1}{2}} .$$

Figures (3.5) and (3.6) are reproduced from Korobkin & Pukhnachov (1988). The first shows the relative arrangement of the boundary of the equivalent plate and the body cross-section at $Y = 0$, and the second is a plot of the function $e = e(\epsilon)$. Notice that in the limiting case $a = b = 1$ (a parabolic body of revolution) we recover the result $r(t) = (3t/2)^{\frac{1}{2}}$ obtained in Section 3.7.1, and in the case $b \to 0$, $\epsilon \to 1$ (a two-dimensional parabola) we reproduce the result $d(t) = (2t)^{\frac{1}{2}}$ obtained in the Chapter 2.

Unfortunately, this approach cannot be easily generalized to other bodies with elliptic cross-section, since the boundary conditions on the disc do not, in general, permit such a straightforward expansion in terms of the external harmonics. [1] Working directly for the velocity potential leads to a easier boundary value problem, but the resulting integration in time required to impose the matching condition can only, in general, be performed numerically.

[1] Hauptman & Miloh (1986) have followed a similar approach for the related problem of an elliptic wing with some success.

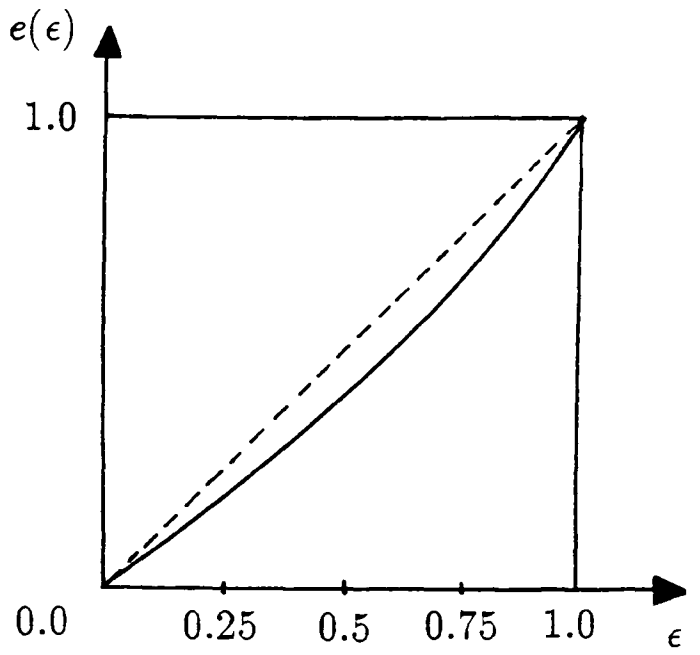

Figure 3.6: Plot of the function $e = e(\epsilon)$.

3.8 Inner and Spray Sheet Problems

3.8.1 Inner Problem

As in the two-dimensional case, we seek to correct the singularity in the leading order outer problem by obtaining the appropriate inner problem near the boundary of the equivalent plate, $t = \omega(\epsilon x, \epsilon z)$.

To investigate the inner region we introduce $O(1)$ curvilinear coordinates ξ and η to describe the (x, z)-plane, as shown in Figure (3.7). The new coordinates are defined so that $\xi = 0$ is the curve $t = \omega(\epsilon x, \epsilon z)$, which has curvature $\kappa(\epsilon\eta, t)$. Written in the coordinates ξ, η and y, Laplace's equation becomes

$$\begin{aligned} \epsilon\frac{\partial\kappa}{\partial\eta}(\epsilon\eta,t)\frac{\xi}{(1+\kappa(\epsilon\eta,t)\xi)^2}\frac{\partial\phi}{\partial\eta} + \frac{1}{(1+\kappa(\epsilon\eta,t)\xi)}\frac{\partial^2\phi}{\partial\eta^2} \\ + \kappa(\epsilon\eta,t)\frac{\partial\phi}{\partial\xi} + (1+\kappa(\epsilon\eta,t)\xi)\frac{\partial^2\phi}{\partial\xi^2} + \frac{\partial^2\phi}{\partial y^2} = 0 \end{aligned} \tag{3.61}$$

and the boundary conditions take the form

$$\left[\alpha'(t) + \epsilon\frac{\partial\phi}{\partial\xi}\right]\frac{\partial f}{\partial\xi} + \left[\beta'(t) + \frac{\epsilon}{(1+\kappa(\epsilon\eta,t)\xi)}\frac{\partial\phi}{\partial\eta}\right]\frac{1}{(1+\kappa(\epsilon\eta,t)\xi)}\frac{\partial f}{\partial\eta} - \frac{\partial\phi}{\partial y} = 1$$
$$\text{on} \quad y = f(\epsilon x, \epsilon z) - t, \tag{3.62}$$

$$\begin{aligned} \frac{\partial h}{\partial t} - \frac{\alpha'(t)}{\epsilon}\frac{\partial h}{\partial\xi} - \frac{\beta'(t)}{\epsilon(1+\kappa(\epsilon\eta,t)\xi)}\frac{\partial h}{\partial\eta} + \frac{1}{(1+\kappa(\epsilon\eta,t)\xi)^2}\frac{\partial\phi}{\partial\eta}\frac{\partial h}{\partial\eta} \\ + \frac{\partial\phi}{\partial\xi}\frac{\partial h}{\partial\xi} - \frac{\partial\phi}{\partial y} = 0 \quad \text{on} \quad y = h(x,z,t), \end{aligned} \tag{3.63}$$

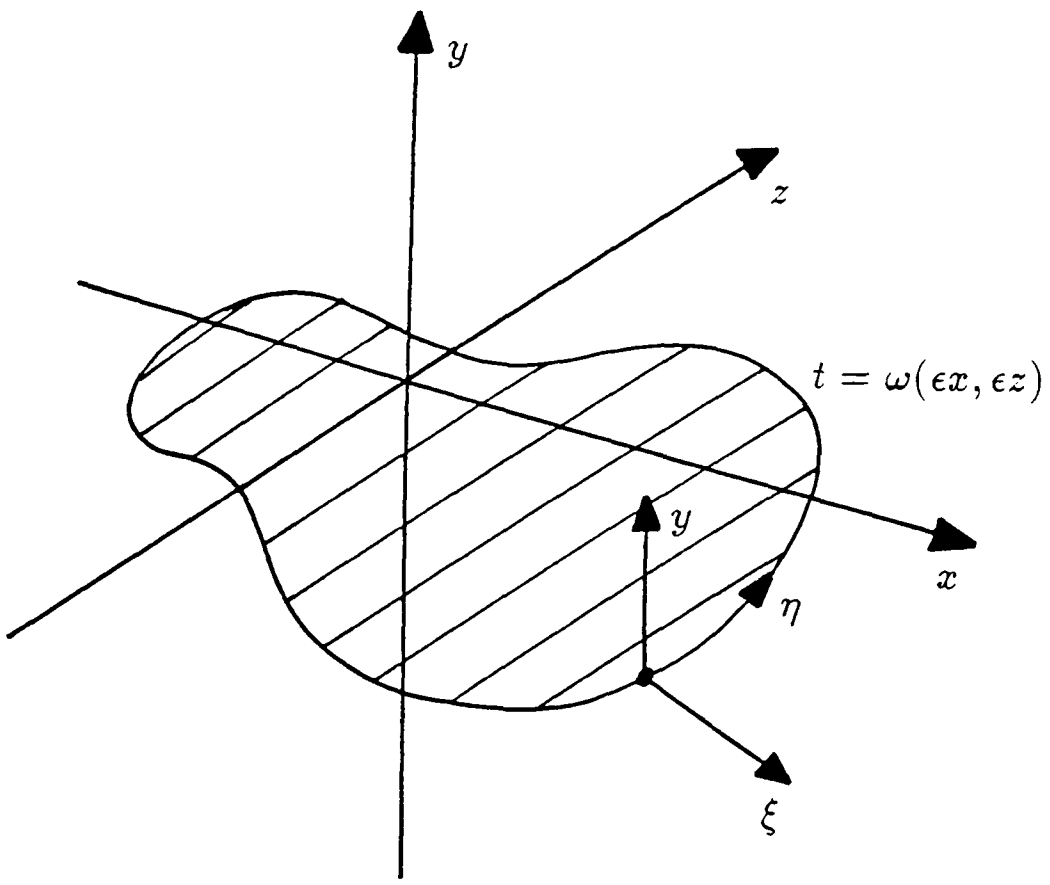

Figure 3.7: Curvilinear coordinate system for the inner problem.

$$\frac{1}{2}\left[\frac{1}{(1+\kappa(\epsilon\eta,t.)\xi)^2}\left(\frac{\partial\phi}{\partial\eta}\right)^2+\left(\frac{\partial\phi}{\partial\xi}\right)^2+\left(\frac{\partial\phi}{\partial y}\right)^2\right] + \frac{\partial\phi}{\partial t}-\frac{\alpha'(t)}{\epsilon}\frac{\partial\phi}{\partial\xi}-\frac{\beta'(t)}{\epsilon(1+\kappa(\epsilon\eta,t)\xi)}\frac{\partial\phi}{\partial\eta}=0 \quad \text{on} \quad y=h(x,z,t), \tag{3.64}$$

where $(\alpha(t)/\epsilon, \beta(t)/\epsilon)$ is the velocity of the point $\xi = 0$, $\eta = 0$ in terms of the directions associated with the curvilinear coordinates ξ and η. Following the analysis of the two-dimensional case, we denote the unknown scale of the inner region by $n > -1$ and define inner variables $\hat{\xi}$, $\hat{\eta}$ and $\hat{y}$ so that

$$\xi = \epsilon^n\hat{\xi}, \quad \eta = \frac{\hat{\eta}}{\epsilon}, \quad \hat{y} = \lambda(0,0,t) - t + \epsilon^n\hat{y},$$

where $\lambda(\xi,\eta,t)$ is the value of the function $f(\epsilon x, \epsilon z)$ at the point with coordinates (ξ,η). [2] Since the fluid velocity must be $O(1/\epsilon)$ in the inner region, the scaled inner velocity potential, $\hat{\phi}(\hat{\xi},\hat{y},\hat{\eta},t)$, is defined by

$$\phi(\xi,y,\eta,t) = \epsilon^{n-1}\hat{\phi}(\hat{\xi},\hat{y},\hat{\eta},t).$$

In the inner variables, the inner free surface elevation is $O(1)$ and the position of the body is $O(\epsilon)$, and so we introduce the notations $\hat{y} = \hat{h}(\hat{\xi},\hat{\eta},t)$ and $\hat{y} =$

[2] In the two-dimensional case $\lambda(\hat{x},t) = f(d(t) + \epsilon^{n+1}\hat{x})$.

$\epsilon\hat{f}(\hat{\xi},\hat{\eta},t)$ respectively for them. Writing the full impact problem in these inner variables, Laplace's equation becomes

$$\begin{aligned}&\frac{\partial\kappa(\hat{\eta},t)}{\partial\hat{\eta}}\frac{\epsilon^{2n}\hat{\xi}}{(1+\epsilon^n\kappa(\hat{\eta},t)\hat{\xi})^2}\frac{\partial\hat{\phi}}{\partial\hat{\eta}}+\frac{\epsilon^{n+1}}{(1+\epsilon^n\kappa(\hat{\eta},t)\hat{\xi})}\frac{\partial^2\hat{\phi}}{\partial\hat{\eta}^2}\\&+\frac{\kappa(\hat{\eta},t)}{\epsilon}\frac{\partial\hat{\phi}}{\partial\hat{\xi}}+\epsilon^{-(n+1)}(1+\epsilon^n\kappa(\hat{\eta},t)\hat{\xi})\frac{\partial^2\hat{\phi}}{\partial\hat{\xi}^2}+\epsilon^{-(n+1)}\frac{\partial^2\hat{\phi}}{\partial\hat{y}^2}=0\end{aligned}\tag{3.65}$$

together with the boundary conditions

$$\left[\alpha'(t)+\frac{\partial\hat{\phi}}{\partial\hat{\xi}}\right]\frac{\partial\lambda}{\partial\xi}+\left[\beta'(t)+\frac{\epsilon^{n+1}}{(1+\epsilon^n\kappa(\hat{\eta},t)\hat{\xi})}\frac{\partial\hat{\phi}}{\partial\hat{\eta}}\right]\frac{1}{(1+\epsilon^n\kappa(\hat{\eta},t)\hat{\xi})}\frac{\partial\lambda}{\partial\eta}-\frac{1}{\epsilon}\frac{\partial\hat{\phi}}{\partial\hat{y}}=1$$
$$\text{on}\quad y=f(\epsilon x,\epsilon z)-t,\tag{3.66}$$

$$\begin{aligned}&\frac{\partial\lambda}{\partial t}(0,0,t)-1+\epsilon^n\frac{\partial\hat{h}}{\partial t}-\frac{\alpha'(t)}{\epsilon}\frac{\partial\hat{h}}{\partial\hat{\xi}}-\frac{\epsilon^n\beta'(t)}{(1+\epsilon^n\kappa(\hat{\eta},t)\hat{\xi})}\frac{\partial\hat{h}}{\partial\hat{\eta}}\\&+\frac{\epsilon^{2n+1}}{(1+\epsilon^n\kappa(\hat{\eta},t)\hat{\xi})^2}\frac{\partial\hat{\phi}}{\partial\hat{\eta}}\frac{\partial\hat{h}}{\partial\hat{\eta}}+\frac{1}{\epsilon}\frac{\partial\hat{\phi}}{\partial\hat{\xi}}\frac{\partial\hat{h}}{\partial\hat{\xi}}-\frac{1}{\epsilon}\frac{\partial\hat{\phi}}{\partial\hat{y}}=0\quad\text{on}\quad\hat{y}=\hat{h}(\hat{\xi},\hat{\eta},t),\end{aligned}\tag{3.67}$$

$$\begin{aligned}&\frac{1}{2}\left[\frac{\epsilon^{2n}}{(1+\epsilon^n\kappa(\hat{\eta},t)\hat{\xi})^2}\left(\frac{\partial\hat{\phi}}{\partial\hat{\eta}}\right)^2+\frac{1}{\epsilon^2}\left(\frac{\partial\hat{\phi}}{\partial\hat{\xi}}\right)^2+\frac{1}{\epsilon^2}\left(\frac{\partial\hat{\phi}}{\partial\hat{y}}\right)^2\right]+\epsilon^{n-1}\frac{\partial\hat{\phi}}{\partial t}\\&+\left(1-\frac{\partial\lambda}{\partial t}(0,0,t)\right)\frac{1}{\epsilon}\frac{\partial\hat{\phi}}{\partial\hat{y}}-\frac{\alpha'(t)}{\epsilon^2}\frac{\partial\hat{\phi}}{\partial\hat{\xi}}-\frac{\epsilon^{n-1}\beta'(t)}{(1+\epsilon^n\kappa(\hat{\eta},t)\hat{\xi})}\frac{\partial\hat{\phi}}{\partial\hat{\eta}}\quad\text{on}\quad\hat{y}=\hat{h}(\hat{\xi},\hat{\eta},t).\end{aligned}\tag{3.68}$$

Expanding $\hat{\phi}$ and $\hat{h}$ as asymptotic series in powers of ϵ in the usual way, and writing

$$\hat{\phi}_0(\hat{\xi},\hat{\eta},\hat{y},t)=\alpha'(t)\hat{\xi}+\hat{\phi}_0^*(\hat{\xi},\hat{\eta},\hat{y},t),$$

the leading order inner problem is

$$\frac{\partial^2\hat{\phi}_0^*}{\partial\hat{\xi}^2}+\frac{\partial^2\hat{\phi}_0^*}{\partial\hat{y}^2}=0\quad\text{in the fluid,}\tag{3.69}$$

$$\frac{\partial\hat{\phi}_0^*}{\partial\hat{y}}=0\quad\text{on}\quad\hat{y}=0,\tag{3.70}$$

$$\frac{\partial\hat{\phi}_0^*}{\partial\hat{\xi}}\frac{\partial\hat{\phi}_0^*}{\partial\hat{\xi}}-\frac{\partial\hat{\phi}_0^*}{\partial\hat{y}}=0\quad\text{on}\quad\hat{y}=0,\tag{3.71}$$

$$\left(\frac{\partial\hat{\phi}_0^*}{\partial\hat{\xi}}\right)^2+\left(\frac{\partial\hat{\phi}_0^*}{\partial\hat{y}}\right)^2=\alpha'(t)^2\quad\text{on}\quad\hat{y}=0.\tag{3.72}$$

This is exactly the same problem as that obtained for the two dimensional case in Section 2.6, with $\hat{x}$ replaced by $\hat{\xi}$ and the velocity of the edge of the plate $d'(t)/\epsilon$

replaced by $\alpha'(t)/\epsilon$, the normal velocity of the curve $t = \omega(\epsilon x, \epsilon x)$. Thus, we can solve it in the same way and matching with local form of the outer solution again requires that $n = 1$.

3.8.2 Spray Sheet Problem

The spray sheet region can be analysed in a similar way, and this leads to a two-dimensional version of the jet problem described in Section 2.7. The leading order problem is now that of a thin two-dimensional sheet rather than a thin one-dimensional jet. The problem is described in terms of curvilinear coordinates $\bar{\xi}$, $\bar{\eta}$ and $\bar{y}$ conforming to the shape of the body. Introducing scaled spray sheet variables $\tilde{\xi}$, $\tilde{\eta}$ and $\tilde{y}$, defined by

$$\tilde{\xi} = \epsilon\bar{\xi}, \quad \tilde{\eta} = \epsilon\bar{\eta}, \quad \tilde{y} = \frac{\bar{y}}{\epsilon},$$

the leading order expression for the thickness of the spray sheet $\tilde{y} = \tilde{h}_0(\tilde{\xi}, \tilde{\eta}, t)$, and the $\tilde{\xi}$ and $\tilde{\eta}$ components of the leading order velocity $\tilde{u}_0(\tilde{\xi}, \tilde{\eta}, t)$ and $\tilde{v}_0(\tilde{\xi}, \tilde{\eta}, t)$ satisfy the equations

$$\frac{\partial \tilde{h}_0}{\partial t} + \frac{1}{(1+\kappa(\tilde{\eta},t)\tilde{\xi})}\frac{\partial}{\partial \tilde{\xi}}\left((1+\kappa(\tilde{\eta},t)\tilde{\xi})\tilde{h}_0\tilde{u}_0\right) + \frac{1}{(1+\kappa(\tilde{\eta},t)\tilde{\xi})}\frac{\partial}{\partial \tilde{\eta}}\left(\tilde{h}_0\tilde{v}_0\right) = 0 \tag{3.73}$$

$$\frac{\partial \tilde{u}_0}{\partial t} + \tilde{u}_0\frac{\partial \tilde{u}_0}{\partial \tilde{\xi}} + \frac{\tilde{v}_0}{(1+\kappa(\tilde{\eta},t)\tilde{\xi})}\frac{\partial \tilde{u}_0}{\partial \tilde{\eta}} = 0 \tag{3.74}$$

$$\frac{\partial \tilde{v}_0}{\partial t} + \tilde{u}_0\frac{\partial \tilde{v}_0}{\partial \tilde{\xi}} + \frac{\tilde{v}_0}{(1+\kappa(\tilde{\eta},t)\tilde{\xi})}\frac{\partial \tilde{v}_0}{\partial \tilde{\eta}} = 0 \tag{3.75}$$

The geometry of the leading order spray sheet problem is shown in Figure (3.8). The pressure on the body is again $O(\epsilon)$.

3.9 Extension to Fluid-Solid Impact Problems

The impact of a fluid on a solid is identical to the impact of a solid on a fluid, and so the present work can be applied immediately to the situation where a body of water strikes a solid surface, provided that both have small deadrise angle. A recent review of theoretical and experimental work on the impact of a fluid

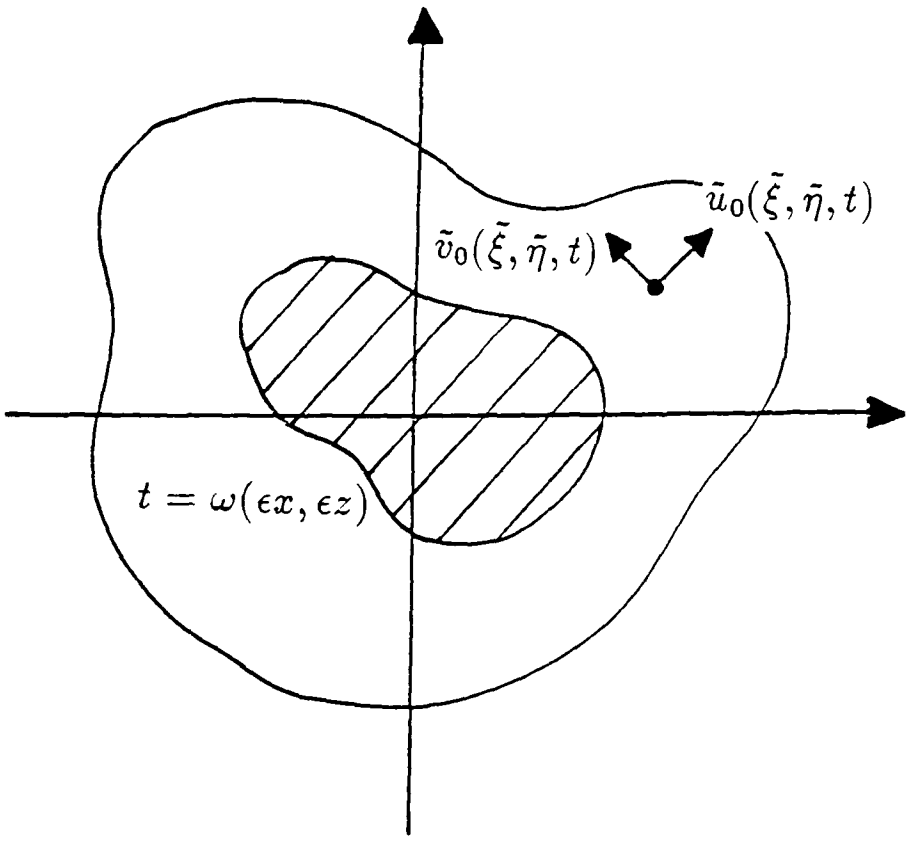

Figure 3.8: Leading order spray sheet problem.

onto solid boundary is due to Lesser & Field (1983), who concentrate mainly on approximate theories for the earliest stages of the impact when compressibility effects are significant. Unfortunately, a comparison with the work of Cumberbatch (1960), who studied the impact of a wedge of incompressible fluid on a plane wall, is not possible since he only investigated wedges with semi-opening angle less than $\pi/4$.

3.10 Extension to Fluid-Fluid Impact Problems

The ideas of the previous two chapters can be generalised to the impact of two bodies of immiscible fluid, provided both bodies have small deadrise angle, and the geometry of such an impact is shown in Figure (3.9). We denote the shape of the upper fluid, which is moving vertically downwards with non-dimensional speed $v^{(1)}$, by $y = f^{(1)}(\epsilon x, \epsilon z)$, and the lower fluid, which is moving vertically upwards with non-dimensional speed $v^{(2)}$, by $y = -f^{(2)}(\epsilon x, \epsilon z)$. $f^{(1)}(\cdot,\cdot)$ and $f^{(2)}(\cdot,\cdot)$ are defined so that the first contact is made at $x = 0$, $z = 0$ at time $t = 0$. The velocity potentials in the upper and lower fluids are denoted by

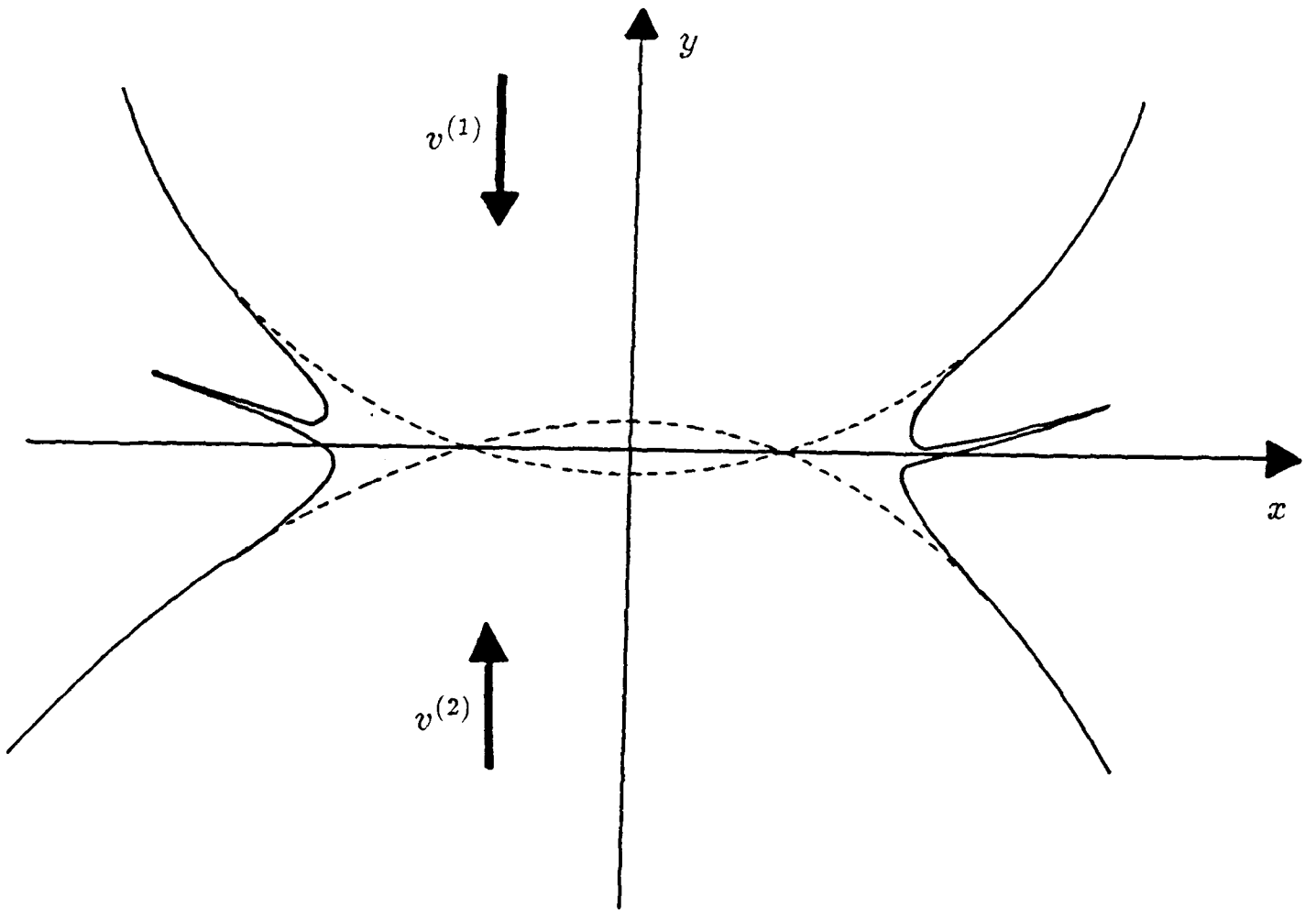

Figure 3.9: Fluid-fluid impact geometry. The dashed curves denote the position each fluid would have reached in the absence of the other.

$\phi^{(1)}(x,y,z,t)$ and $\phi^{(2)}(x,y,z,t)$ respectively, $h^{(1)}(x,z,t)$ and $h^{(2)}(x,z,t)$ are the profiles of the upper and lower free surfaces and the interface between the fluids is $y=\eta(x,z,t)$. The governing equation and boundary conditions are as described in Section 3.1 for solid-fluid impacts, with a normal velocity matching condition at the interface between the fluids replacing the condition on the rigid body, and, since $\eta(x,z,t)$ is unknown, an additional pressure matching condition. In this simple model we neglect the effects of gravity and surface tension between the fluids and consider only the case when the fluids have the same density. The full impact problem, for initial fluid profiles with small deadrise angle, is given by

$$\frac{\partial^2\phi^{(i)}}{\partial x^2}+\frac{\partial^2\phi^{(i)}}{\partial y^2}+\frac{\partial^2\phi^{(i)}}{\partial z^2}=0 \quad \text{in the fluids} \quad i=1,2, \tag{3.76}$$

with the boundary conditions

$$\frac{\partial\eta}{\partial t}+\epsilon\left[\frac{\partial\eta}{\partial x}\frac{\partial\phi^{(i)}}{\partial x}+\frac{\partial\eta}{\partial z}\frac{\partial\phi^{(i)}}{\partial z}\right]-\frac{\partial\phi^{(i)}}{\partial y}=0 \tag{3.77}$$
$$\text{on} \quad y=\eta(x,z,t) \quad \text{for} \quad i=1,2,$$

$$\frac{\partial\phi^{(1)}}{\partial t}+\frac{1}{2}\left[\left(\frac{\partial\phi^{(1)}}{\partial x}\right)^2+\left(\frac{\partial\phi^{(1)}}{\partial y}\right)^2+\left(\frac{\partial\phi^{(1)}}{\partial z}\right)^2\right]=\frac{\partial\phi^{(2)}}{\partial t}$$
$$+\frac{1}{2}\left[\left(\frac{\partial\phi^{(2)}}{\partial x}\right)^2+\left(\frac{\partial\phi^{(2)}}{\partial y}\right)^2+\left(\frac{\partial\phi^{(2)}}{\partial z}\right)^2\right] \quad \text{on} \quad y=\eta(x,z,t), \tag{3.78}$$

$$\frac{\partial h^{(i)}}{\partial t}+\epsilon\left[\frac{\partial h^{(i)}}{\partial x}\frac{\partial\phi^{(i)}}{\partial x}+\frac{\partial h^{(i)}}{\partial z}\frac{\partial\phi^{(i)}}{\partial z}\right]-\frac{\partial\phi^{(i)}}{\partial y}=0 \tag{3.79}$$
$$\text{on} \quad y=h^{(i)}(x,z,t) \quad \text{for} \quad i=1,2,$$

$$\frac{\partial\phi^{(i)}}{\partial t}+\frac{1}{2}\left[\left(\frac{\partial\phi^{(i)}}{\partial x}\right)^2+\left(\frac{\partial\phi^{(i)}}{\partial y}\right)^2+\left(\frac{\partial\phi^{(i)}}{\partial z}\right)^2\right]=0 \tag{3.80}$$
$$\text{on} \quad y=h^{(i)}(x,z,t) \quad \text{for} \quad i=1,2.$$

The initial conditions are

$$\phi^{(i)}(x,y,z,0)=0, \quad h^{(i)}(x,z,0)=f^{(i)}(x,z) \quad \text{for} \quad i=1,2, \tag{3.81}$$

and the appropriate far-field conditions are

$$\begin{aligned}\nabla\phi^{(1)} &\to (0,-v^{(1)},0) \quad \text{as} \quad y\to+\infty,\\ \nabla\phi^{(2)} &\to (0,v^{(2)},0) \quad \text{as} \quad y\to-\infty.\end{aligned} \tag{3.82}$$

3.10.1 Outer Problem

To obtain the outer problem, we proceed as in Section 3.3, with addition of an outer interface profile, $E(X,Z,t)$, defined by $E(X,Z,t) = \eta(x,z,t)$. Expanding the dependent variables as asymptotic series in powers of ϵ, we obtain the leading order outer problem, which has governing equation

$$\frac{\partial^2 \Phi_0^{(i)}}{\partial X^2} + \frac{\partial^2 \Phi_0^{(i)}}{\partial Y^2} + \frac{\partial^2 \Phi_0^{(i)}}{\partial Z^2} = 0 \quad \text{in the fluids} \quad i = 1,2, \tag{3.83}$$

and boundary conditions

$$\frac{\partial E_0}{\partial t} = \frac{\partial \Phi_0^{(i)}}{\partial Y} \quad \text{on} \quad Y = 0, \quad t < \omega(X,Z), \quad \text{for} \quad i = 1,2, \tag{3.84}$$

$$\frac{\partial \Phi_0^{(1)}}{\partial t} = \frac{\partial \Phi_0^{(2)}}{\partial t} \quad \text{on} \quad Y = 0, \quad t < \omega(X,Z), \tag{3.85}$$

$$\frac{\partial H_0^{(i)}}{\partial t} = \frac{\partial \Phi_0^{(i)}}{\partial Y} \quad \text{on} \quad Y = 0, \quad t > \omega(X,Z), \quad \text{for} \quad i = 1,2, \tag{3.86}$$

$$\frac{\partial \Phi_0^{(i)}}{\partial t} = 0 \quad \text{on} \quad Y = 0, \quad t > \omega(X,Z), \quad \text{for} \quad i = 1,2, \tag{3.87}$$

and is subject to the initial conditions

$$\Phi_0^{(i)}(X,Y,Z,0) = 0, \quad H_0^{(i)}(X,Z,0) = f^{(i)}(X,Z) \quad \text{for} \quad i = 1,2, \tag{3.88}$$

and the far-field conditions

$$\begin{aligned} \nabla \Phi_0^{(1)} &\to (0, -v^{(1)}, 0) \quad \text{as} \quad y \to +\infty, \\ \nabla \Phi_0^{(2)} &\to (0, v^{(2)}, 0) \quad \text{as} \quad y \to -\infty. \end{aligned} \tag{3.89}$$

Integrating equation (3.85) with respect to time and using the initial condition (3.88a) we deduce that

$$\Phi_0^{(1)} = \Phi_0^{(2)} \quad \text{on} \quad Y = 0, \quad t < \omega(X,Z). \tag{3.90}$$

$\Phi_0^{(1)}$ is harmonic in $Y > 0$ and $\Phi_0^{(2)}$ is harmonic in $Y < 0$, and from equations (3.84) and (3.90) we deduce that the derivatives $\partial \Phi_0^{(i)}/\partial X$, $\partial \Phi_0^{(i)}/\partial Y$ and $\partial \Phi_0^{(i)}/\partial Z$ for $i = 1,2$ are continuous across $Y = 0$ for $t > \omega(X,Z)$. The solution, denoted by $\Phi_0(X,Y,Z,t)$, is, therefore, harmonic everywhere, apart from the region of the plane $Y = 0$ on which $t > \omega(X,Z)$.

In the two-dimensional case we seek a solution harmonic in the cut (X,Y)-plane, with the cuts taken between $(-\infty,0)$ and $(-d(t),0)$ and between $(d(t),0)$ and $(\infty,0)$. The solution for Φ_0 is, therefore,

$$\Phi_0(X,Y,t) = \alpha Y + \beta \Re\left(d(t)^2 - Z^2\right)^{\frac{1}{2}}, \tag{3.91}$$

where now $Z = X + iY$, and α and β are determined from the far-field conditions,

$$\alpha = \frac{1}{2}(v^{(2)} - v^{(1)}), \quad \beta = -\frac{1}{2}(v^{(1)} + v^{(2)}).$$

Substituting Φ_0 into equation (3.84) and integrating once we obtain a simple linear expression for the interface between the fluids,

$$E_0(X,t) = \alpha t.$$

Similarly, integrating equation (3.86) and using the initial condition (3.88b) gives expressions for the leading order free surface shapes similar to that in the previous chapter,

$$H_0^{(1)}(X,t) = f^{(1)}(X) + \alpha t - \beta X \int_0^t \frac{\mathrm{d}\tau}{(X^2 - d(\tau)^2)^{\frac{1}{2}}}, \tag{3.92}$$

$$H_0^{(2)}(X,t) = -f^{(2)}(X) + \alpha t + \beta X \int_0^t \frac{\mathrm{d}\tau}{(X^2 - d(\tau)^2)^{\frac{1}{2}}}. \tag{3.93}$$

The analogue of the matching condition (2.45) is that the leading order free surfaces should meet at $X = d(t)$, viz.

$$H_0^{(1)}(d(t),t) = H_0^{(2)}(d(t),t), \tag{3.94}$$

and so

$$\frac{1}{2}\left(f^{(1)}(d(t)) + f^{(2)}(d(t))\right) = \beta d(t) \int_0^t \frac{\mathrm{d}\tau}{(d(t)^2 - d(\tau)^2)^{\frac{1}{2}}}.$$

This is another Abel integral equation, and has the solution

$$t(d) = \frac{1}{\pi\beta} \int_0^d \frac{f^{(1)}(\xi) + f^{(2)}(\xi)}{(d^2 - \xi^2)^{\frac{1}{2}}}\,\mathrm{d}\tau, \tag{3.95}$$

provided that the integral exists.

3.10.2 Inner and Jet Solutions

Expanding in the inner region centred on $x = d(t)/\epsilon$ and $y = \alpha t$ we obtain exactly the same leading order inner problem as in the case of solid-fluid impacts. Unless $\alpha = 0$, the jet makes a non-zero $O(\epsilon)$ angle to the x-axis. To leading order the jet problem is unaltered and the jet angle can only be obtained by carrying out a second order analysis in the inner region. This has not been performed.

For example, consider the impact of a fluid wedge, $f^{(1)}(x) = m_1|x|$, and a fluid parabola, $f^{(2)}(x) = m_2 x^2$. Substituting into equation (3.95) we obtain

$$d(t) = \frac{2}{\pi m_2}\left[-m_1 + \left(m_1^2 + m_2\pi^2\beta t\right)^{\frac{1}{2}}\right],$$

which reproduces our earlier results for parabolic and wedge shaped bodies in the special cases $m_1 = 0$ and $m_2 = 0$ respectively. Figure (3.10) shows a typical set of composite pressure histories for the impact of a fluid wedge with a fluid parabola in the case $m_1 = m_2 = 1$.

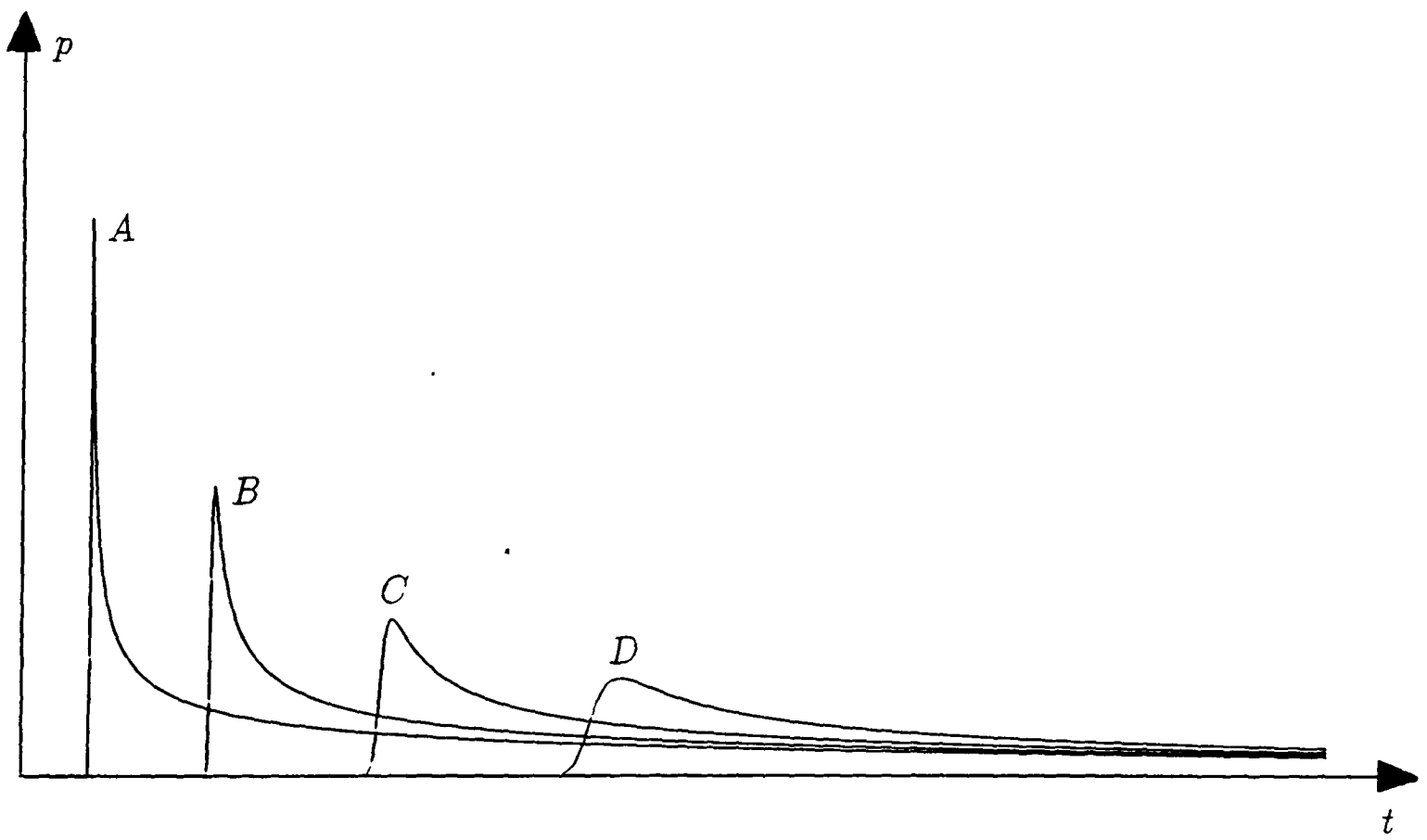

Figure 3.10: Typical composite pressure histories for the impact of a fluid wedge with a fluid parabola in the case $m_1 = m_2 = 1$.

Chapter 4

Stability and Exit Problems

In this chapter we describe a partial linear stability analysis of the leading order outer problem. The results lead to a discussion of the essential differences between entry and exit problems.

4.1 Stability Analysis

A linear analysis of the stability of the leading order outer solution to perturbations in the Z-direction is possible.

Expanding the solution to the full two-dimensional problem near the edge of the equivalent plate, $X = d(t)$, locally in both space and time leads to a perturbed problem of a semi-infinite plate $Y = 0$, $X < d(t)$ that is difficult to analyse. Instead we proceed as in classical gas dynamics and take as our basic, unperturbed problem a simpler 'travelling wave' problem on an infinite domain. The solution for the leading order outer problem, Φ_0, has a square root singularity at the free boundary $X = d(t)$, which means that we can neglect the impact speed but not $\partial H_0/\partial t$ compared with $\partial \Phi_0/\partial Y$. Dropping the zero subscripts for clarity, the approximate local model is therefore

$$\frac{\partial^2 \Phi}{\partial X^2} + \frac{\partial^2 \Phi}{\partial Y^2} + \frac{\partial^2 \Phi}{\partial Z^2} = 0 \quad \text{in} \quad Y < 0, \tag{4.1}$$

$$\frac{\partial \Phi}{\partial Y} = 0 \quad \text{on} \quad Y = 0, \quad X < d(t), \tag{4.2}$$

$$\frac{\partial \Phi}{\partial Y} = \frac{\partial H}{\partial t} \quad \text{on} \quad Y = 0, \quad X > d(t), \tag{4.3}$$

$$\Phi = 0 \quad \text{on} \quad Y = 0, \quad X > d(t), \tag{4.4}$$

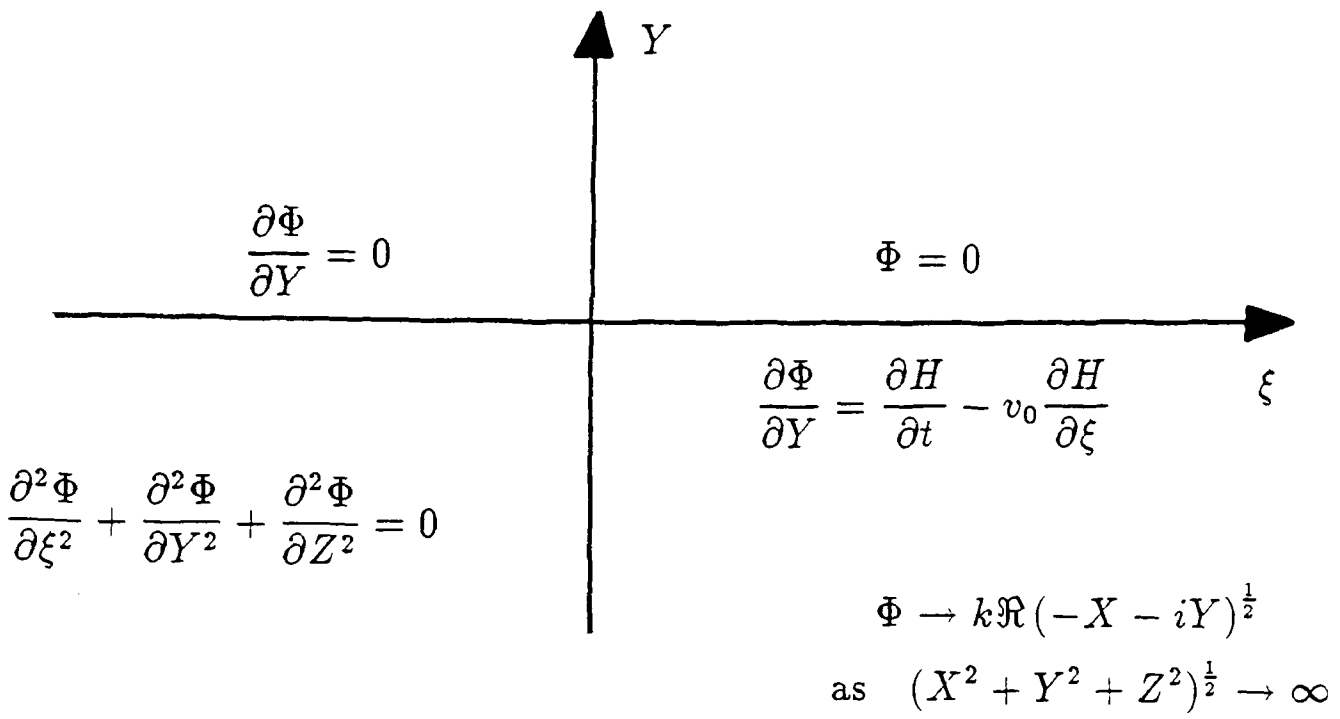

Figure 4.1: Approximate travelling wave problem.

with the matching condition

$$H(X,t) \to 0 \quad \text{as} \quad X \to d(t)^+. \tag{4.5}$$

In order to match with the two-dimensional solution, the far-field behaviour of this local solution must be such that

$$\Phi \to k\Re(-X - iY)^{\frac{1}{2}} \quad \text{as} \quad (X^2 + Y^2 + Z^2)^{\frac{1}{2}} \to \infty, \tag{4.6}$$

where, because we are only considering variations on a short time scale, k is a constant. Introducing the travelling wave variable $\xi = X - v_0 t$, where v_0 is the constant speed of the wave, the problem becomes

$$\frac{\partial^2 \Phi}{\partial \xi^2} + \frac{\partial^2 \Phi}{\partial Y^2} + \frac{\partial^2 \Phi}{\partial Z^2} = 0 \quad \text{in} \quad Y < 0, \tag{4.7}$$

$$\frac{\partial \Phi}{\partial Y} = 0 \quad \text{on} \quad Y = 0, \quad \xi < 0, \tag{4.8}$$

$$\frac{\partial \Phi}{\partial Y} = \frac{\partial H}{\partial t} - v_0 \frac{\partial H}{\partial \xi} \quad \text{on} \quad Y = 0, \quad \xi > 0, \tag{4.9}$$

$$\Phi = 0 \quad \text{on} \quad Y = 0, \quad \xi > 0, \tag{4.10}$$

which is summarised in Figure (4.1). This problem has an exact travelling wave solution which is independent of Z, viz.

$$\Phi = k\Re(-\xi - iY,)^{\frac{1}{2}}, \qquad H = -\frac{k\xi^{\frac{1}{2}}}{v_0} \quad \text{for} \quad \xi > 0.$$

Both k and v_0 are determined by matching with the solution to the full problem and will be related in any particular problem. The precise nature of this relationship is, however, unimportant, and it is sufficient to observe that k and v_0 must have the same sign. The cases $v_0 > 0$ and $v_0 < 0$ correspond to entry and exit problems respectively.

We wish to investigate the stability of the solution to a small harmonic perturbation in the Z-direction. Following the approach described by Ockendon (1980) we write the new free boundary as

$$\xi = \delta \cos(nZ)\, e^{\sigma t} + O(\delta^2), \tag{4.11}$$

where $\delta \ll 1$ and $n > 0$ are given real constants, and the temporal exponent σ is to be determined.

We now seek solutions for $\Phi(\xi, Y, Z, t)$ and $H(\xi, Z, t)$ as asymptotic series in powers of δ, in the form

$$\Phi = \Phi_0 + \delta \cos(nZ)\, e^{\sigma t} \Phi_1 + O(\delta^2), \tag{4.12}$$

$$H = H_0 + \delta \cos(nZ)\, e^{\sigma t} H_1 + O(\delta^2). \tag{4.13}$$

Substituting these expressions into equations (4.7), (4.8), (4.9) and (4.10) and expanding in powers of δ, the leading order problem is exactly the unperturbed one, and so the leading order terms are

$$\Phi_0 = kR^{\frac{1}{2}} \cos\left(\frac{\Theta}{2}\right), \qquad H_0 = -\frac{k\xi^{\frac{1}{2}}}{v_0} \quad \text{for} \quad \xi > 0,$$

where $R = (\xi^2 + Y^2)^{\frac{1}{2}}$ and Θ are local plane polar coordinates with the ξ-axis as the polar axis. The second order problem has governing equation

$$\frac{\partial^2 \Phi_1}{\partial \xi^2} + \frac{\partial^2 \Phi_1}{\partial Y^2} - n^2 \Phi_1 = 0 \quad \text{in} \quad Y < 0, \tag{4.14}$$

and boundary conditions

$$\frac{\partial \Phi_1}{\partial Y} = 0 \quad \text{on} \quad Y = 0, \quad \xi < 0, \tag{4.15}$$

$$\frac{\partial \Phi_1}{\partial Y} = \sigma H_1(\xi) - v_0 H_1'(\xi) \quad \text{on} \quad Y = 0, \quad \xi > 0, \tag{4.16}$$

$$\Phi_1 = 0 \quad \text{on} \quad Y = 0, \quad \xi > 0. \tag{4.17}$$

We can satisfy the boundary conditions (4.15) and (4.17) by seeking a solution for Φ_1 in the form

$$\Phi_1 = f(R)\cos\left(\frac{\Theta}{2}\right),$$

where, from equation (4.14), the function $f(R)$ satisfies the second order ordinary differential equation

$$f''(R) + \frac{f'(R)}{R} - \left(\frac{1}{4R^2} + n^2\right) f(R) = 0. \tag{4.18}$$

From the far-field condition (4.6), we deduce that $\Phi_1 = o(R^{\frac{1}{2}})$ as $R \to \infty$ and $H_1 = o(\xi^{\frac{1}{2}})$ as $\xi \to \infty$, and so both Φ_1 and H_1 can have no worse than square root singularities at the origin. The appropriate solution for $f(R)$ is therefore $e^{-nR}/R^{\frac{1}{2}}$, and so the solution for Φ_1 is

$$\Phi_1 = \frac{me^{-nR}}{R^{\frac{1}{2}}}\cos\left(\frac{\Theta}{2}\right),$$

where the constant m is undetermined. The differential equation satisfied by $H_1(\xi)$ is obtained by substituting for Φ_1 into equation (4.16), which gives

$$v_0 H_1'(\xi) - \sigma H_1(\xi) = -\frac{me^{-n\xi}}{2\xi^{\frac{3}{2}}}. \tag{4.19}$$

Equation (4.19) can be integrated directly and, after one integration by parts, has the solution

$$H_1(\xi) = \frac{me^{\sigma\xi/v_0}}{v_0}\left[\frac{e^{-(n+\sigma/v_0)\xi}}{\xi^{\frac{1}{2}}} + (n+\sigma/v_0)\int_0^{\xi}\frac{e^{-(n+\sigma/v_0)s}}{s^{\frac{1}{2}}}\,\mathrm{d}s + c\right], \tag{4.20}$$

where c is another undetermined constant. If $\sigma/v_0 > 0$ then the condition that $H_1(\xi) = o(\xi^{\frac{1}{2}})$ as $\xi \to \infty$ we can only be satisfied if

$$c = -\int_0^{\infty}\frac{e^{-(n+\sigma/v_0)s}}{s^{\frac{1}{2}}}\,\mathrm{d}s = -(n+\sigma/v_0)^{\frac{1}{2}}\sqrt{\pi}, \tag{4.21}$$

whereas if $\sigma/v_0 < 0$ the condition is satisfied regardless of the value of c.

The expansions (4.12) and (4.13) are invalid near the perturbed free boundary where $R = O(\delta)$, and so to correct the outer expansion we seek an inner expansion in the neighbourhood of $R = 0$. The appropriate inner variables $\hat{\xi}$, $\hat{Y}$, $\hat{\Phi}(\hat{\xi}, \hat{Y}, Z, t)$ and $\hat{H}(\hat{\xi}, Z, t)$ are defined by

$$\xi = \delta\hat{\xi}, \quad Y = \delta\hat{Y},$$

and

$$\Phi(X,Y,Z,t) = \delta^{\frac{1}{2}}\hat{\Phi}(\hat{\xi},\hat{Y},Z,t), \quad H(X,Z,t) = \delta^{\frac{1}{2}}\hat{H}(\hat{\xi},Z,t).$$

The inner problem is governed by the equation

$$\frac{\partial^2\hat{\Phi}}{\partial\hat{\xi}^2} + \frac{\partial^2\hat{\Phi}}{\partial\hat{Y}^2} + \frac{\partial^2\hat{\Phi}}{\partial Z^2} = 0 \quad \text{in} \quad \hat{Y} < 0, \tag{4.22}$$

together with the boundary conditions

$$\frac{\partial\hat{\Phi}}{\partial\hat{Y}} = 0 \quad \text{on} \quad \hat{Y} = 0, \quad \hat{\xi} < \cos(nZ)\,e^{\sigma t} + O(\delta), \tag{4.23}$$

$$\frac{\partial\hat{\Phi}}{\partial\hat{Y}} = \delta\frac{\partial\hat{H}}{\partial t} - v_0\frac{\partial\hat{H}}{\partial\hat{\xi}} \quad \text{on} \quad \hat{Y} = 0, \quad \hat{\xi} > \cos(nZ)\,e^{\sigma t} + O(\delta), \tag{4.24}$$

$$\hat{\Phi} = 0 \quad \text{on} \quad \hat{Y} = 0, \quad \hat{\xi} > \cos(nZ)\,e^{\sigma t} + O(\delta). \tag{4.25}$$

Expanding the dependent variables $\hat{\Phi}$ and $\hat{H}$ in powers of δ, in the form

$$\hat{\Phi} = \hat{\Phi}_0 + \delta\hat{\Phi}_1 + O(\delta^2),$$

$$\hat{H} = \hat{H}_0 + \delta\hat{H}_1 + O(\delta^2),$$

the leading order inner problem has the governing equation

$$\frac{\partial^2\hat{\Phi}_0}{\partial\hat{\xi}^2} + \frac{\partial^2\hat{\Phi}_0}{\partial\hat{Y}^2} + \frac{\partial^2\hat{\Phi}_0}{\partial Z^2} = 0 \quad \text{in} \quad \hat{Y} < 0, \tag{4.26}$$

together with the boundary conditions

$$\frac{\partial\hat{\Phi}_0}{\partial\hat{Y}} = 0 \quad \text{on} \quad \hat{Y} = 0, \quad \hat{\xi} < \cos(nZ)\,e^{\sigma t}, \tag{4.27}$$

$$\frac{\partial\hat{\Phi}_0}{\partial\hat{Y}} = -v_0\frac{\partial\hat{H}_0}{\partial\hat{\xi}} \quad \text{on} \quad \hat{Y} = 0, \quad \hat{\xi} > \cos(nZ)\,e^{\sigma t}, \tag{4.28}$$

$$\hat{\Phi}_0 = 0 \quad \text{on} \quad \hat{Y} = 0, \quad \hat{\xi} > \cos(nZ)\,e^{\sigma t}. \tag{4.29}$$

The solution of the leading order inner problem is, therefore,

$$\hat{\Phi}_0 = k\Re\left(\cos(nZ)e^{\sigma t} - \hat{\xi} - i\hat{Y}\right)^{\frac{1}{2}}, \tag{4.30}$$

$$\hat{H}_0 = -\frac{k}{v_0}\left(\hat{\xi} - \cos(nZ)e^{\sigma t}\right)^{\frac{1}{2}} \quad \text{for} \quad \hat{\xi} > \cos(nZ)\,e^{\sigma t}, \tag{4.31}$$

plus any terms generated by matching with the outer expansion.[1]

[1]The inner expansion is itself invalid near $\hat{\xi} = 0$, $\hat{Y} = 0$ and repeated inner expansions would be needed to determine higher order terms in the free boundary position in equation (4.11).

The one term outer expansion of the inner potential $\hat{\Phi}$ automatically matches with the one term inner expansion of the outer potential Φ, but matching the two-term outer expansion with the one-term inner expansion requires that

$$m = \frac{k}{2}.$$

The two-term inner expansion of the free surface elevation $H_1(\xi)$, given by equation (4.20), is

$$\frac{k}{2v_0}\left(\frac{1}{\delta^{\frac{1}{2}}\hat{\xi}^{\frac{1}{2}}} + c\right) + O(\delta^{\frac{1}{2}}). \tag{4.32}$$

The first term automatically matches the term of $O(1/\hat{\xi}^{\frac{1}{2}})$ in the expansion of equation (4.31) as $\hat{\xi} \to \infty$. However, the second term produces a constant of $\delta^{\frac{1}{2}}kc/2v_0$ which the next term in the expansion of equation (4.31) has to match. This would lead to a potential problem for the second term in the expansion for $\hat{\Phi}$ which would have to satisfy homogenous Neumann data on $\hat{Y} = 0$ and homogenous Dirichlet data on $\hat{\xi} = 0$ and be such that the Neumann data on $\hat{\xi} > 0$ had a finite integral. The boundary conditions mean that such a function would have to be a linear combination of square roots of $\hat{\xi} + iY$, and there is no such function with the required finite integral. We conclude that the term $kc/2v_0$ in (4.32) is actually zero, and so $c = 0$.

In the case $\sigma/v_0 > 0$ then equation (4.21) implies that $\sigma/v_0 + n = 0$ but, since $n > 0$, this is impossible. Thus, $\sigma/v_0 < 0$ is the only possibility and therefore σ and v_0 must have *opposite* signs. This observation suggests that an impact problem in which the equivalent flat plate expands and $v_0 > 0$ is *stable*, but that an exit problem in which the equivalent flat plate contracts and $v_0 < 0$ is *unstable* to small perturbations in the Z-direction. We are, however, unable to obtain a dispersion relation between σ and n.

4.2 Some Remarks Concerning Exit Problems

The stability analysis suggests that there is a fundamental difference between entry and exit problems at small deadrise angle.

Firstly, even though any solution of our expanding plate model can be reversed in time to give the solution of an exit problem, with the same initial conditions as

those encountered in the evolution of an entry problem, this tells us little about the evolution of an exit problem for arbitrary initial data. In addition to the stability argument, the differences between the two situations are emphasised by the fact that reversing the sign of time in an entry problem reverses the sign of the leading order outer pressure, given by equation (2.44). Hence, large negative pressures are predicted on the body, which are likely to invalidate the model by causing the boundary of the contracting plate to break up.

Secondly, although the smoothing transformation (3.28) can still be applied to an exit problem, we can no longer derive the matching condition (2.45) in the region traversed by $t = \omega(X, Z)$. This difficulty prevents us from writing down an integral equation to determine the plate width corresponding to (2.46) without making additional physical assumptions about the shape of the free surface in this region.

Finally, we note that a solution to any exit problem in the absence of viscosity, gravity and surface tension is that the body loses contact with the fluid instantaneously and $h(x, z, t) = h(x, z, 0)$. This suggests that including the effects of viscosity, gravity or surface effects may be crucial to understanding exit problems.

There are very few mathematical papers dealing with exit problems. Greenhow (1988) performed numerical calculations using a boundary integral method for the exit of a circular cylinder at constant velocity from an inviscid fluid. He obtained a variety of flows but experienced numerical difficulties when the fluid particles on the free surface became too spread out. However, for a range of exit speeds he found that the solution broke down regardless of the particle spacing. The reason appeared to be physical rather than solely numerical and to be connected with the formation of a sizeable region of large negative pressure on the cylinder. Figure (4.2) is reproduced from his paper and shows how the free surface is drawn under the cylinder during exit, as well as giving the pressure distribution on body just before numerical breakdown occurred. Greenhow (1988) also included photographs of small scale experiments, which showed a spontaneous break up of the free surface.

The exit problem is still open, as yet no mathematical theory exists to describe the experimental and numerical observations.

Figure 4.2: Numerically calculated free surface and pressure distribution during the exit of a cylinder, just before numerical breakdown. The pressures of $\rho V^2/2$ and $\rho g a$ are shown for reference, and the hydrostatic pressure is marked with a dot. Reproduced from Greenhow (1988).

Chapter 5

The Effect of an Air Layer on Fluid Impact

In this chapter we formulate a mathematical model for the impact of a rigid body onto a fluid in the presence on a cushioning fluid layer between them. Some numerical and analytical solutions are obtained in appropriate asymptotic limits, and numerical solutions are obtained to the full leading order problem. Finally, we compare our results with the earlier work of other authors.

5.1 Physical Motivation

The impact models described in the previous two chapters neglect several mechanisms that may be important in practical problems. Apart from those already discussed, the most likely explanation for the discrepancy between the pressure readings on the keel of a roughly parabolic body shown in Figure (2.34) and the corresponding analytical solution, shown in Figure (2.35), is that the pressure in the air between the solid and the liquid before the impact occurs is not negligible, and so the free surface deforms before the impact and a cushioning pocket of air is trapped. In order to discuss this mechanism, we derive a model which incorporates the air flow before an impact.

Following the argument in Section 2.1, the Reynolds number in the water is large and the Mach number in the water is small, and so again we model the water as an incompressible, inviscid fluid. Thus, we consider the impact of a two-dimensional, rigid, symmetric body onto an quiescent half-space of inviscid and incompressible fluid. Taking cartesian axes (x, y) as before, and working

in dimensional variables, the position of the body is given by $y = f(x) + a(t)$. Initially air fills the space between the body and the undisturbed water surface. Taking the same typical values of width and velocity as in Chapter Two, we can evaluate the relevant non-dimensional parameters in the air. Since the kinematic viscosity of air, ν, is roughly $10^{-5}\mathrm{m}^2\mathrm{s}^{-1}$, the *Reynolds number*, R_e, for the flow in the air is

$$\mathrm{R}_e = \frac{Vl}{\nu} \sim 10^7.$$

The speed of sound in air, c_a, is approximately $330\mathrm{ms}^{-1}$, and so the *Mach number in the air*, M_a, is

$$\mathrm{M}_a = \frac{V}{c_a} \sim 10^{-1}.$$

Since $\mathrm{R}_e \gg 1$ and $\mathrm{M}_a \ll 1$ we shall model the air as an inviscid and incompressible fluid. We note, however, that air compressibility effects will become important whenever the speeds in the air become comparable with the local sound speed, and that this is most likely to occur as the air-gap narrows just before the body first touches the water surface. Since the Froude number, $\mathrm{F}_r \gg 1$, and the Weber number, $\mathrm{W}_e \gg 1$, are both large we will again neglect the effects of gravity and surface tension at the free surface. For simplicity we have referred to the two fluids in the model as air and water, but obviously the model is more general, and can be applied to any two inviscid, incompressible and immiscible fluids.

5.2 Problem Formulation

The flows in the air and in the water are both irrotational, and so we can define velocity potentials ϕ_1 in the air and ϕ_2 in the water. It is sometimes more convenient to work directly with the x and y-components of velocity, and so we denote these by $u_i(x,y,t) = \partial\phi_i/\partial x$ and $v_i(x,y,t) = \partial\phi_i/\partial y$ respectively, where $i = 1$ for quantities in the air and $i = 2$ for those in the water. The governing equations in both fluids are Euler's equations (2.1) and (2.2);

$$\frac{\partial u_i}{\partial x} + \frac{\partial v_i}{\partial y} = 0, \tag{5.1}$$

$$\frac{\partial u_i}{\partial t} + u_i\frac{\partial u_i}{\partial x} + v_i\frac{\partial u_i}{\partial y} = -\frac{1}{\rho_i}\frac{\partial p_i}{\partial x}, \tag{5.2}$$

$$\frac{\partial v_i}{\partial t} + u_i\frac{\partial v_i}{\partial x} + v_i\frac{\partial v_i}{\partial y} = -\frac{1}{\rho_i}\frac{\partial p_i}{\partial y}, \tag{5.3}$$

for $i = 1, 2$. Extending our notation, $p_1(x, y, t)$, $p_2(x, y, t)$ are the pressure in the air and the water and ρ_1, ρ_2 denote the density of the air and of the water respectively.

At the surface of the body we require continuity of normal velocity between the body and the air,

$$u_1 f'(x) - v_1 = -a'(t) \quad \text{on} \quad y = f(x) + a(t). \tag{5.4}$$

At the free boundary between the air and the water, denoted by $y = h(x, t)$, the kinematic condition applied to each fluid gives

$$\frac{\partial h}{\partial t} + u_1 \frac{\partial h}{\partial x} - v_1 = 0, \quad \text{and} \quad \frac{\partial h}{\partial t} + u_2 \frac{\partial h}{\partial x} - v_2 = 0 \quad \text{on} \quad y = h(x, t). \tag{5.5}$$

In the absence of gravity and surface tension, the air and water pressures must be equal at the free surface, and so from Bernoulli's equation (2.4) we have

$$\rho_1 \left(\frac{\partial \phi_1}{\partial t} + \frac{1}{2} |\nabla \phi_1|^2 \right) = \rho_2 \left(\frac{\partial \phi_2}{\partial t} + \frac{1}{2} |\nabla \phi_2|^2 \right) \quad \text{on} \quad y = h(x, t). \tag{5.6}$$

At time $t = 0$ we impose the initial conditions

$$h(x, 0) = 0, \quad \phi_i(x, y, 0) = 0 \quad \text{for} \quad i = 1, 2, \tag{5.7}$$

and the problem has the far-field condition

$$|\nabla \phi_i| \to \mathbf{0} \quad \text{as} \quad (x^2 + y^2 + z^2)^{\frac{1}{2}} \to \infty \quad \text{for} \quad i = 1, 2. \tag{5.8}$$

5.3 Non-dimensionalization

First we non-dimensionalize the problem by scaling the variables with the typical horizontal length, l, and typical air-gap thickness, λ. We scale the vertical air velocity with V, which is a typical vertical speed of the body. From the mass conservation condition (5.1), the typical horizontal speed in the air is Vl/λ. The length scale in the water is l, but the velocity scale, denoted by U, has to be determined. The free surface elevation scales with $\lambda \rho_1 / \rho_2$. From the Euler equations, we see that the air pressure is of order $\rho_1 V^2 l^2 / \lambda^2$ whilst the water pressure is of order $\rho_2 U V l / \lambda$. Since the pressure is continuous across the free boundary, the pressures in the air and in the water must be comparable, and

this determines an appropriate value of U to be $V\rho_1 l/\rho_2\lambda$. On substituting the new scaled variables into the equations and boundary conditions, we find that two non-dimensional groups of parameters arise naturally. These are the *initial aspect ratio of the gap*, which we denote by

$$\varepsilon = \frac{\lambda}{l},$$

and the *ratio of the density of air to the density of water*, which we denote by

$$\delta = \frac{\rho_1}{\rho_2} \simeq 10^{-3}.$$

The experiments of Lewison (1970) suggest that the water surface only responds to the approaching body when it is very close to it, and so we will investigate solutions to our model when both these parameters are small, viz. $\varepsilon \ll 1$ and $\delta \ll 1$.

5.3.1 The Water Problem

In the water problem the non-dimensionalization takes the form

$$x^* = \frac{x}{l}, \qquad y^* = \frac{y}{l}, \qquad t^* = \frac{Vt}{l},$$

with

$$u_2^* = \frac{u_2}{U}, \qquad v_2^* = \frac{v_2}{U}, \qquad \phi_2^*(x^*, y^*, t^*) = \frac{1}{Ul}\phi_2(x, y, t),$$

and

$$p_2^*(x^*, y^*, t^*) = \frac{\varepsilon^2}{\rho_1 V^2} p_2(x, y, t), \qquad h^*(x^*, t^*) = \frac{1}{\delta\lambda} h(x, t).$$

Dropping the starred notation for dimensionless quantities, the governing equations in the water are

$$\frac{\partial u_2}{\partial x} + \frac{\partial v_2}{\partial y} = 0, \tag{5.9}$$

$$\frac{\partial u_2}{\partial t} + \delta\left[u_2\frac{\partial u_2}{\partial x} + v_2\frac{\partial u_2}{\partial y}\right] = -\frac{\partial p_2}{\partial x}, \tag{5.10}$$

$$\frac{\partial v_2}{\partial t} + \delta\left[u_2\frac{\partial v_2}{\partial x} + v_2\frac{\partial v_2}{\partial y}\right] = -\frac{\partial p_2}{\partial y}, \tag{5.11}$$

with the statement that the flow is irrotational, $\nabla \times \mathbf{u}_2 = 0$, taking the form

$$\frac{\partial u_2}{\partial y} - \frac{\partial v_2}{\partial x} = 0. \tag{5.12}$$

The boundary condition on the free surface is

$$\frac{\partial h}{\partial t} + \delta u_2 \frac{\partial h}{\partial x} - v_2 = 0 \quad \text{on} \quad y = \delta h(x,t), \tag{5.13}$$

and from Bernoulli's equation the water pressure is

$$p_2 = -\left[\frac{\partial \phi_2}{\partial t} + \frac{\delta}{2}\left(u_2^2 + v_2^2\right)^{\frac{1}{2}}\right]. \tag{5.14}$$

The initial conditions are

$$h(x,0) = 0, \quad \phi_2(x,y,0) = 0, \tag{5.15}$$

and the far field-condition is

$$\frac{\partial \phi_2}{\partial x}, \quad \frac{\partial \phi_2}{\partial y} \to 0 \quad \text{as} \quad (x^2+y^2+z^2)^{\frac{1}{2}} \to \infty. \tag{5.16}$$

5.3.2 The Air Problem

In the air problem the non-dimensionalization takes the form

$$x^* = \frac{x}{l}, \qquad y^* = \frac{y}{\lambda}, \qquad t^* = \frac{Vt}{l},$$

with

$$u_1^* = \frac{u_1 \lambda}{Vl}, \qquad v_2^* = \frac{v_2}{V}, \qquad \phi_1^*(x^*,y^*,t^*) = \frac{1}{Vl}\phi_1(x,y,t),$$

and

$$p_1^*(x^*,y^*,t^*) = \frac{\varepsilon^2}{\rho_1 V^2} p_1(x,y,t), \qquad h^*(x^*,t^*) = \frac{1}{\delta\lambda} h(x,t),$$

$$f^*(x^*) = \frac{1}{\lambda} f(x), \qquad a^*(t^*) = \frac{1}{\lambda} a(t).$$

Dropping the starred notation for dimensionless quantities, the air problem is given by the equations

$$\frac{\partial u_1}{\partial x} + \frac{\partial v_1}{\partial y} = 0, \tag{5.17}$$

$$\frac{\partial u_1}{\partial t} + u_1 \frac{\partial u_1}{\partial x} + v_1 \frac{\partial u_1}{\partial y} = -\frac{\partial p_1}{\partial x}, \tag{5.18}$$

$$\varepsilon^2 \left[\frac{\partial v_1}{\partial t} + u_1 \frac{\partial v_1}{\partial x} + v_1 \frac{\partial v_1}{\partial y}\right] = -\frac{\partial p_1}{\partial y}, \tag{5.19}$$

with the statement that the flow is irrotational, $\nabla \times \mathbf{u}_1 = 0$, taking the form

$$\frac{\partial u_1}{\partial x} - \varepsilon^2 \frac{\partial v_1}{\partial y} = 0. \tag{5.20}$$

The boundary conditions on the body and the free surface are

$$u_1 f'(x) - v_1 = -a'(t) \quad \text{on} \quad y = f(x) + a(t), \tag{5.21}$$

$$\frac{\delta}{\varepsilon}\left[\frac{\partial h}{\partial t} + u_1 \frac{\partial h}{\partial x}\right] - v_1 = 0 \quad \text{on} \quad y = \frac{\delta}{\varepsilon} h(x,t), \tag{5.22}$$

and from Bernoulli's equation the air pressure is

$$p_1 = -\left[\frac{\partial \phi_1}{\partial t} + \frac{1}{2}\left(u_1^2 + \varepsilon^2 v_1^2\right)^{\frac{1}{2}}\right]. \tag{5.23}$$

The initial conditions are

$$h(x,0) = 0, \quad \phi_1(x,y,0) = 0, \tag{5.24}$$

and the far field-condition is

$$\frac{\partial \phi_1}{\partial x}, \quad \frac{\partial \phi_1}{\partial y} \to 0 \quad \text{as} \quad (x^2 + y^2 + z^2)^{\frac{1}{2}} \to \infty. \tag{5.25}$$

5.4 The Leading Order Water Problem

If we seek a solution for ϕ_2 (and hence u_2 and v_2) as an asymptotic series in δ, in the form

$$\phi_2 = (\phi_2)_0 + \delta(\phi_2)_1 + O(\delta^2),$$

then, dropping the clumsy subscript notation and dealing with leading order quantities unless otherwise stated, the leading order problem is given by the acoustic equations

$$\frac{\partial u_2}{\partial x} + \frac{\partial v_2}{\partial y} = 0, \tag{5.26}$$

$$\frac{\partial u_2}{\partial t} = -\frac{\partial p_2}{\partial x}, \tag{5.27}$$

$$\frac{\partial v_2}{\partial t} = -\frac{\partial p_2}{\partial y}, \tag{5.28}$$

with the condition of irrotational flow

$$\frac{\partial u_2}{\partial y} - \frac{\partial v_2}{\partial x} = 0. \tag{5.29}$$

The boundary conditions on the free surface are

$$\frac{\partial h}{\partial t} = v_2, \quad p_1 = p_2 \quad \text{on} \quad y = 0. \tag{5.30}$$

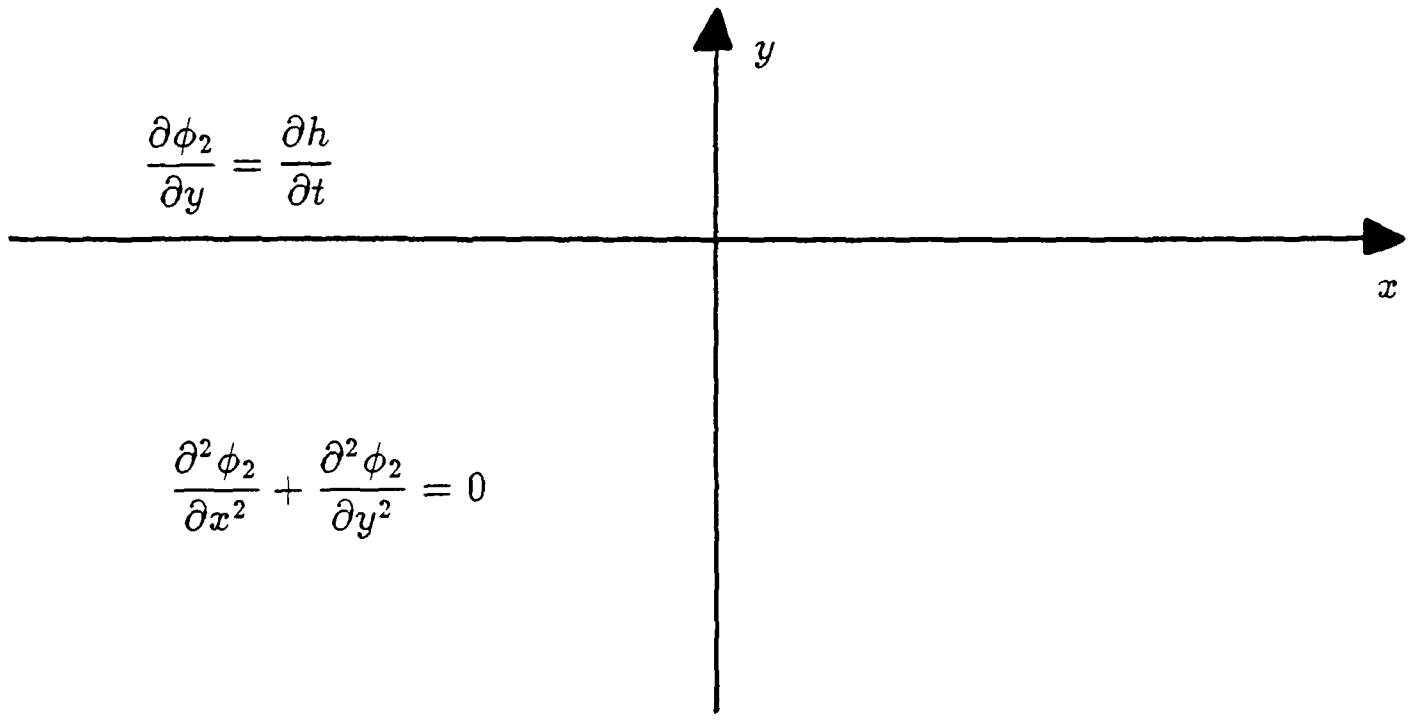

Figure 5.1: The leading order water problem.

The leading order water problem is shown in Figure (5.1). If we regard $h(x,t)$ as being determined from the air problem then it is easiest to treat the problem as a boundary value problem for the velocity potential. Since, to leading order,

$$\frac{\partial \phi_2}{\partial y} = \frac{\partial h}{\partial t} \quad \text{on} \quad y = 0,$$

the solution for $\partial\phi_2/\partial y$, harmonic in $y \leq 0$ and satisfying the boundary condition and the far-field condition (5.16) is obtained by using the appropriate Green's function;

$$\frac{\partial \phi_2}{\partial y}(x,y,t) = \frac{y}{\pi}\int_{-\infty}^{+\infty} \frac{\partial h}{\partial t}(\xi,t)\frac{\mathrm{d}\xi}{(\xi-x)^2+y^2}. \tag{5.31}$$

Hence, the velocity potential ϕ_2 is given by

$$\phi_2(x,y,t) = \frac{1}{2\pi}\int_{-\infty}^{+\infty} -\frac{\partial h}{\partial t}(\xi,t)\log\left((\xi-x)^2+y^2\right)\,\mathrm{d}\xi. \tag{5.32}$$

Furthermore,

$$\frac{\partial \phi_2}{\partial x}(x,0,t) = \frac{1}{\pi}\int_{-\infty}^{+\infty} \frac{\partial h}{\partial t}(\xi,t)\frac{\mathrm{d}\xi}{\xi-x} = \mathcal{H}\left(\frac{\partial h}{\partial t}\right), \tag{5.33}$$

where $\mathcal{H}(\cdot)$ denotes a *Hilbert Transform*. From equation (5.28) we deduce that

$$-\frac{\partial p_2}{\partial x} = \frac{\partial}{\partial t}\mathcal{H}\left(\frac{\partial h}{\partial t}\right),$$

and therefore the pressure is determined in terms of the free surface elevation to be

$$\frac{\partial p_2}{\partial x} = -\mathcal{H}\left(\frac{\partial^2 h}{\partial t^2}\right). \tag{5.34}$$

5.5 The Leading Order Air Problem

The solution of the air problem is dependent on the ratio δ/ε, and so we introduce the new parameter, ϑ, defined by

$$\vartheta = \frac{\delta}{\varepsilon}.$$

If we seek solutions for u_1 and v_1 as an asymptotic series in ε^2, in the form

$$u_1 = (u_1)_0 + \varepsilon^2(u_1)_1 + O(\varepsilon^4), \qquad v_1 = (v_1)_0 + \varepsilon^2(v_1)_1 + O(\varepsilon^4),$$

and again drop the subscripts, then the leading order problem is given by the equations

$$\frac{\partial u_1}{\partial x} + \frac{\partial v_1}{\partial y} = 0, \tag{5.35}$$

$$\frac{\partial u_1}{\partial t} + u_1\frac{\partial u_1}{\partial x} + v_1\frac{\partial u_1}{\partial y} = -\frac{\partial p_1}{\partial x}, \tag{5.36}$$

$$0 = -\frac{\partial p_1}{\partial y}, \tag{5.37}$$

with the statement that the flow is irrotational

$$\frac{\partial u_1}{\partial y} = 0. \tag{5.38}$$

The boundary condition on the body is

$$u_1 f'(x) - v_1 = -a'(t) \quad \text{on} \quad y = f(x) + a(t), \tag{5.39}$$

and those on the free surface are

$$\vartheta\left[\frac{\partial h}{\partial t} + u_1\frac{\partial h}{\partial x}\right] - v_1 = 0, \quad p_1 = p_2 \quad \text{on} \quad y = \vartheta h(x,t). \tag{5.40}$$

The geometry of the leading order air problem is shown in Figure (5.2). From equation (5.38), we deduce that u_1 is a function of x and t only, and so we can integrate equation (5.36) with respect to y to obtain

$$v_1 = -\frac{\partial u_1}{\partial x}y + \alpha(x,t),$$

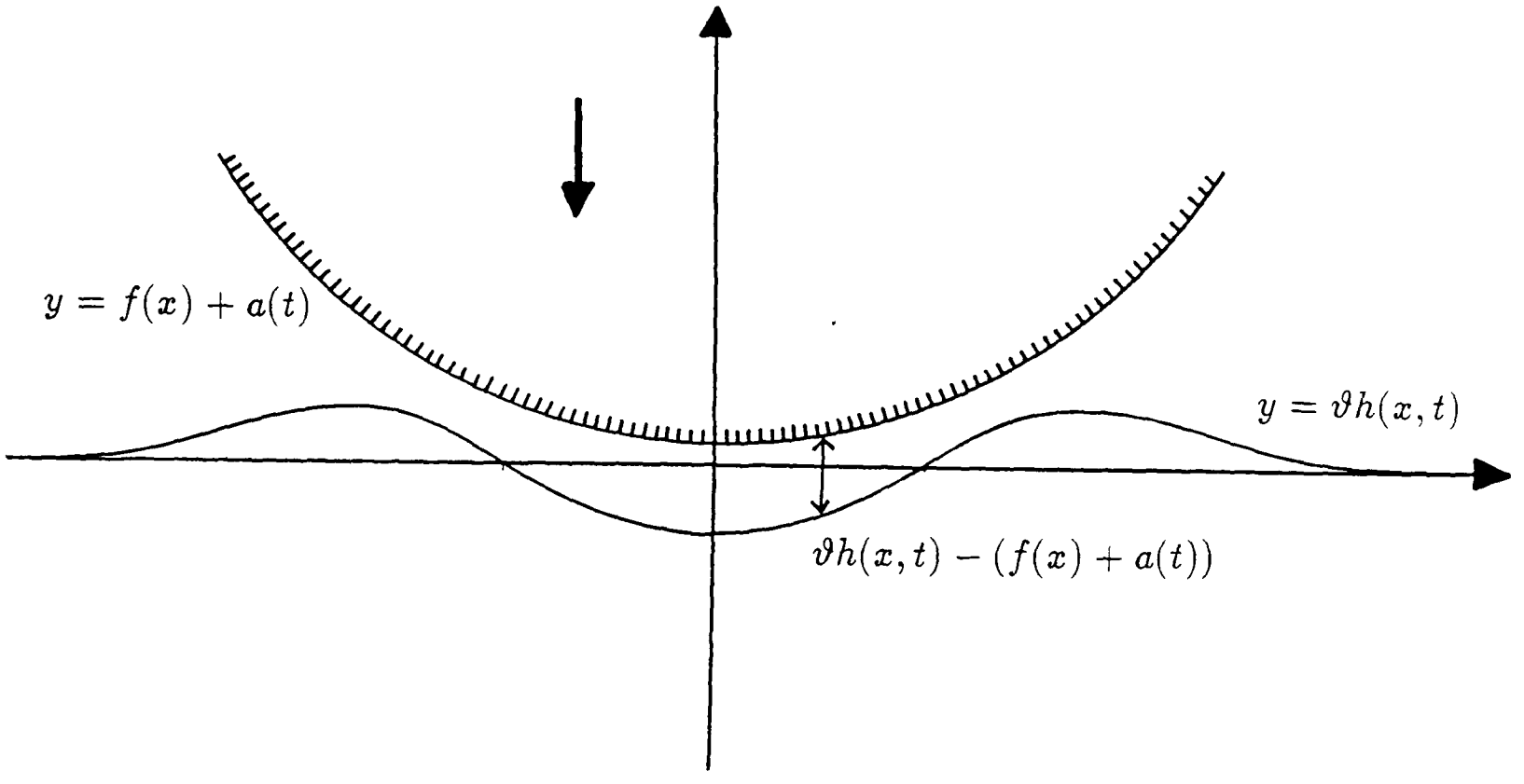

Figure 5.2: Geometry of the leading order air problem.

where $\alpha(x,t)$ is an unknown function of x and t. Substituting into the boundary conditions (5.39) and (5.40a) and eliminating $\alpha(x,t)$ gives

$$\frac{\partial}{\partial t}\left\{\vartheta h(x,t) - (a(t) + f(x))\right\} + \frac{\partial}{\partial x}\left[\left\{\vartheta h(x,t) - (a(t) + f(x))\right\} u_0\right] = 0. \quad (5.41)$$

Since $\vartheta h(x,t) - (a(t) + f(x))$ is the thickness of the air-gap, this is just a statement of conservation of mass in the air. From equation (5.36),

$$-\frac{\partial p_1}{\partial x} = \frac{\partial u_1}{\partial t} + u_1 \frac{\partial u_1}{\partial x},$$

and so using equation (5.34) we can eliminate the pressure and obtain an integral equation for $h(x,t)$, namely,

$$\mathcal{H}\left(\frac{\partial^2 h}{\partial t^2}\right) = \frac{\partial u_1}{\partial t} + u_1 \frac{\partial u_1}{\partial x}. \quad (5.42)$$

Equations (5.41) and (5.42) are a coupled pair of integral and differential equations for the leading order free surface elevation, $h(x,t)$, and the leading order horizontal air velocity, $u_1(x,t)$. Once they have been solved the solution in the water can be evaluated by substituting $h(x,t)$ into equation (5.34), and the problem therefore reduces to solving this coupled pair of equations.

5.6 Asymptotic Solutions

The coupled equations (5.41) and (5.42) are analytically intractable, but progress can be made by seeking solutions in appropriate asymptotic limits before resorting to numerical calculations. For clarity, we drop the subscript one and denote the leading order air velocity simply by $u(x,t)$.

5.6.1 Small Time Asymptotic Behaviour

If we take $a(t) = 1-t$ then we can investigate the small time asymptotic behaviour of the solution by seeking solutions for $h(x,t)$ and $u(x,t)$ as power series in time t for $t \ll 1$, in the form

$$u(x,t) = \sum_{n=0}^{\infty} u_n(x)t^n, \qquad h(x,t) = \sum_{n=0}^{\infty} h_n(x)t^n.$$

Substituting into equation (5.41) and equating coefficients of t, we obtain the leading order terms

$$\begin{aligned} O(1) \qquad & \vartheta h_1(x) + 1 + \frac{\partial}{\partial x}\left[\{\vartheta h_0 - (1+f(x))\}\, u_0(x)\right] = 0, \\ O(t) \quad & 2\vartheta h_2(x) + \frac{\partial}{\partial x}\left[(\vartheta h_1 + 1)u_0(x)\right] + \frac{\partial}{\partial x}\left[\{\vartheta h_0 - (1+f(x))\}\, u_1(x)\right] = 0, \end{aligned} \tag{5.43}$$

and from equation (5.42) the leading order terms

$$\begin{aligned} O(1) \qquad & \mathcal{H}(2h_2(x)) = u_1(x) + u_0(x)\frac{\partial u_0}{\partial x}, \\ O(t) \quad & \mathcal{H}(6h_3(x)) = 2u_2(x) + \frac{\partial}{\partial x}\left(u_0(x)u_1(x)\right). \end{aligned} \tag{5.44}$$

We observe that this perturbation scheme is singular, and it is not now possible to satisfy all the initial conditions. If we choose to satisfy

$$h(x,0) = 0, \qquad u(x,0) = 0,$$

then $h_0(x) \equiv 0$ and $u_0(x) \equiv 0$ and from (5.43a) we deduce that $h_1(x) = -1/\vartheta$ and hence $u_1(x) = 0$. Continuing the expansions to higher orders it is not hard to show that $u(x,t) \equiv 0$, which is physically meaningless. We can, however, impose the initial conditions

$$h(x,0) = 0, \qquad \frac{\partial h}{\partial t}(x,0) = 0,$$

then $h_0(x) \equiv 0$ and $h_1(x) \equiv 0$. Integrating equation (5.43a) gives a simple expression for the leading order velocity, viz.

$$u_0(x) = \frac{x}{1+f(x)}, \tag{5.45}$$

and equation (5.43b) gives a formula for the first non-zero term in the free surface elevation,

$$h_2(x) = \frac{1}{2\vartheta}\frac{\partial}{\partial x}\left[(1+f(x))u_1(x) - u_0(x)\right]. \tag{5.46}$$

Substituting both these expressions into (5.44a), inverting the Hilbert Transform, and integrating with respect to x gives an integral equation for the second order term in the expansion of the velocity,

$$u_1(x) = g(x) + \frac{\vartheta}{1+f(x)}\frac{1}{\pi}\int_{-\infty}^{+\infty} u_1(\xi)\log\left|1-\frac{x}{\xi}\right| \mathrm{d}\xi, \tag{5.47}$$

where the function $g(x)$ is given by

$$g(x) = \frac{x}{(1+f(x))^2} + \frac{\vartheta}{1+f(x)}\frac{1}{\pi}\int_{-\infty}^{+\infty} \xi\left\{\frac{1+f(\xi)-\xi f'(\xi)}{(1+f(\xi))^3}\right\}\log\left|1-\frac{x}{\xi}\right| \mathrm{d}\xi.$$

This singular integral equation can, with care, be solved numerically by the method of successive approximations. An initial guess for $u_1(x)$ is substituted into the right hand side of equation (5.47), and the resulting integrations performed numerically. The result is a revised approximation for $u_1(x)$, and this procedure is repeated until the desired convergence is obtained. Figures (5.3) and (5.4) show the first two terms in the expansion of the horizontal air velocity and the leading order non-zero term in the expansion of the free surface elevation for bodies with profile $y = x^2$ and $y = x^6$ respectively. Notice how in each case the free surface is forced down under the centre of the body and up at its sides, potentially causing a cushion of air to be caught between the body and the water. Care should be taken in interpreting these results too glibly since, of course, they only are only a good approximation to the behaviour of the solution during the initial stages of the motion when $t \ll 1$.

5.6.2 Weak Coupling Behaviour

The equations can also be investigated asymptotically when $\vartheta \ll 1$, corresponding to the case when the aspect ratio of the air-gap is large compared to the

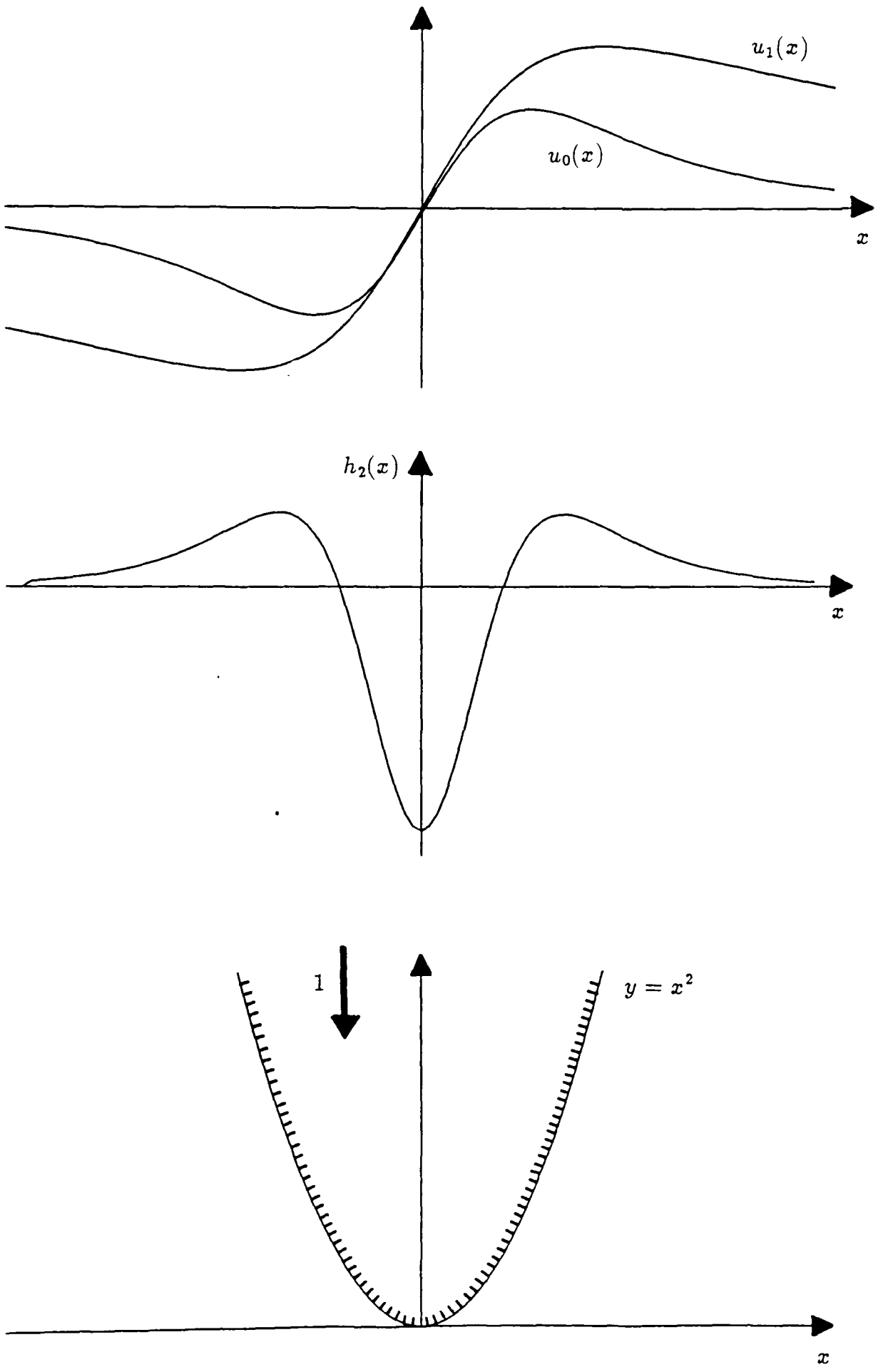

Figure 5.3: Leading order terms in the small time expansion of the velocity and free surface elevation for a body with profile $y = x^2$.

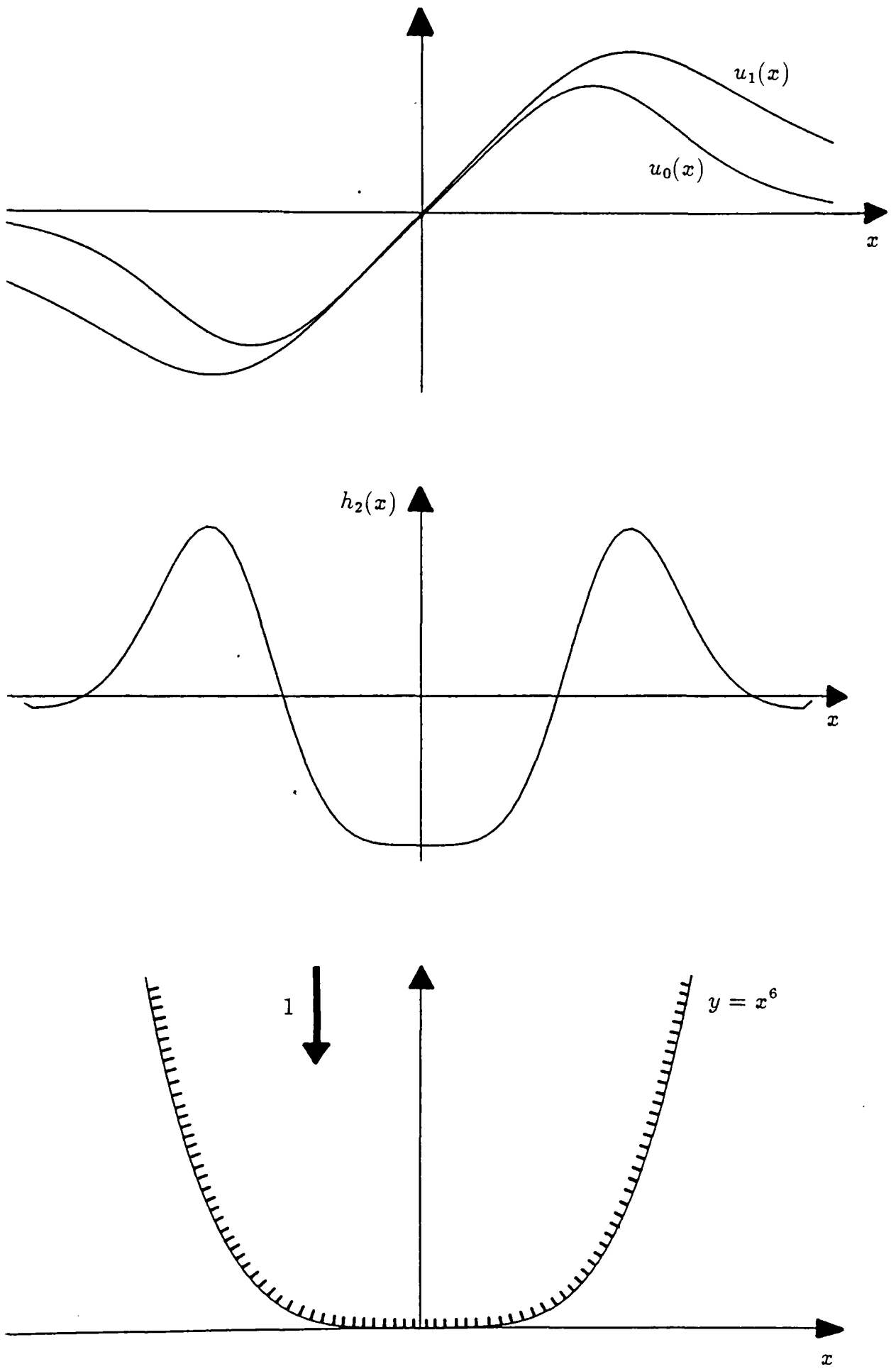

Figure 5.4: Leading order terms in the small time expansion of the velocity and free surface elevation for a body with profile $y = x^6$.

density ratio, and so the coupling between the air and the water problems is weak. We seek formal solutions for $u(x,t)$ and $h(x,t)$ as power series in ϑ in the form

$$u = u_0 + \vartheta u_1 + \vartheta^2 u_2 + O(\vartheta^3), \qquad h = h_0 + \vartheta h_1 + \vartheta^2 h_2 + O(\vartheta^3).$$

Substituting into equation (5.41) and equating coefficients of ϑ, we obtain the leading order terms

$$\begin{aligned} O(1) \quad & \frac{\partial}{\partial t}(a(t)+f(x)) + \frac{\partial}{\partial x}\left[(a(t)+f(x))u_0(x,t)\right] = 0, \\ O(\vartheta) \quad & \frac{\partial h_0}{\partial t}(x,t) + \frac{\partial}{\partial x}\left[h_0(x,t)u_0(x,t) - (a(t)+f(x))u_1(x,t)\right] = 0, \end{aligned} \tag{5.48}$$

and from equation (5.41)

$$\begin{aligned} O(1) \quad & \mathcal{H}\left(\frac{\partial^2 h_0}{\partial t^2}\right) = \frac{\partial u_0}{\partial t} + u_0(x)\frac{\partial u_0}{\partial x}, \\ O(\vartheta) \quad & \mathcal{H}\left(\frac{\partial^2 h_1}{\partial t^2}\right) = \frac{\partial u_1}{\partial t} + \frac{\partial}{\partial x}\left(u_0(x)u_1(x)\right). \end{aligned} \tag{5.49}$$

Equation (5.48a) can be integrated directly to give

$$u_0(x,t) = -\frac{a'(t)x}{a(t)+f(x)}, \tag{5.50}$$

and then $h_0(x,t)$ can be calculated by inverting the Hilbert Transform in equation (5.49a), yielding

$$\begin{aligned} \frac{\partial^2 h_0}{\partial t^2} = \frac{1}{\pi}\int_{-\infty}^{+\infty} \Bigg[& \frac{\xi}{(a(t)+f(\xi))^2}\left\{(a(t)+f(\xi))a''(t) - a'(t)^2\right\} \\ & - \frac{a'(t)^2\xi}{(a(t)+f(\xi))^3}\left\{a(t)+f(\xi)-\xi f'(\xi)\right\}\Bigg]\frac{\mathrm{d}\xi}{\xi - x}. \end{aligned} \tag{5.51}$$

In general, this must be evaluated numerically. We can, however, obtain a closed form solution in the special case when the body shape is a *finite flat plate*, so that $f(x) \equiv 0$ for $|x| \leq 1$. From equation (5.50) we obtain $u_0(x,t) = -a'(t)x/a(t)$, and hence $v_0(x,t) = a'(t)y/a(t)$ in $|x| \leq 1$. If we insist that there is zero pressure at the ends of the air-gap, $|x| = 1$, then the corresponding pressure distribution on $y = 0$ is

$$p_0(x,0,t) = \frac{a'(t)}{a(t)}(1-x^2) \quad \text{for} \quad |x| \leq 1, \tag{5.52}$$

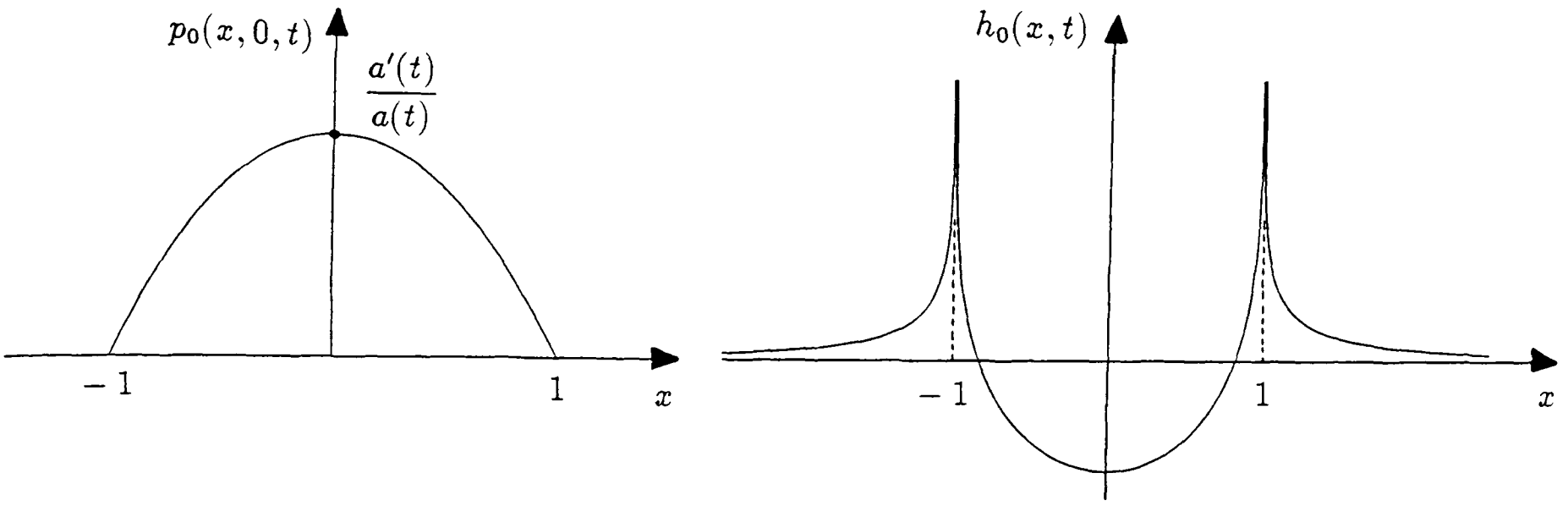

Figure 5.5: Leading order pressure and free surface elevation in the case $\vartheta = 0$ for a flat body.

as sketched in Figure (5.5). Evaluating, the integral in equation (5.51) gives an explicit formula for the leading order shape of the free surface, namely

$$h_0(x,t) = \frac{2}{\pi} \log|a(t)| \left[2 + x \log\left|\frac{1-x}{1+x}\right| \right], \tag{5.53}$$

which is also plotted in Figure (5.5). Evidently $h_0(x,t) \to \infty$ as $|x| \to 1$, and the discontinuity in the pressure gradient at the edges of the plate gives rise to an infinite free surface elevation at $|x| = 1$. This limiting case (the weak coupling means that the water surface has been treated as a rigid, flat boundary in the air problem) has appeared in the literature on a number of occasions, for example in papers by Verhagen (1967), Lewison (1970) and Asryan (1972) and is the crudest possible model of air entrapment.

The Hilbert Transform in equation (5.51) can be evaluated numerically by using the appropriate NAG routine, D01AQF, and the results agree with those computed for the full problem as $\vartheta \to 0$.

5.7 Numerical Calculations

Integrating equation (5.41) with respect to x gives an expression for $u(x,t)$ in terms of the unknown function $h(x,t)$,

$$u(x,t) = -\frac{1}{\vartheta h(x,t) - (a(t) + f(x))} \frac{\partial}{\partial t} \left[\int_0^x \vartheta h(\xi,t) - (a(t) + f(\xi))\, \mathrm{d}\xi \right],$$

which can be written more conveniently as

$$u(x,t) = \frac{1}{\vartheta h(x,t) - (a(t) + f(x))} \left[a'(t)x - \vartheta \frac{\partial F}{\partial t}(x,t) \right], \tag{5.54}$$

where

$$F(x,t) = \int_0^x h(\xi,t)\,\mathrm{d}\xi.$$

The free surface elevation is now determined from equation (5.42). Inverting the Hilbert Transform gives

$$\frac{\partial^2 h}{\partial t^2} = -\frac{1}{\pi} \int_0^x \left[\frac{\partial u}{\partial t}(\xi,t) + u(\xi,t) \frac{\partial u}{\partial x}(\xi,t) \right] \frac{\mathrm{d}\xi}{\xi - x}. \tag{5.55}$$

The numerical procedure employed to solve these equations (5.54) and (5.55) is again an iterative one, beginning with an initial guess for the free surface elevation $h(x,t)$, which is expressed as a sequence of values at a n equally spaced points, $x_1, x_2, \ldots, x_n$. Using these values the function $F(x,t)$ can be evaluated at each of the points x_i for $i = 1, 2, \ldots, n$ by using one of the standard techniques for numerical quadrature. Next, the corresponding values of $u(x_i,t)$ are obtained by a using equation (5.54) and performing a numerical differentiation with respect to t, resulting in the values of the first iteration for the horizontal air velocity. These values are then used to evaluate the singular integral in equation (5.55). Particular care is taken to split up the range of integration in order to remove the weak logarithmic singularity at the point $\xi = x$; the contribution from the neighbourhood of that point being approximated by expanding the integrand in a Taylor series and evaluating the resulting Cauchy Principal Value integral analytically. Finally, the result of this quadrature is integrated twice with respect to time by making use of the famous formula,

$$\int_0^t \int_0^{t'} g(t'')\,\mathrm{d}t''\,\mathrm{d}t' = \int_0^t (t - \xi) g(\xi)\,\mathrm{d}\xi,$$

and the next iteration for $h(x,t)$ is obtained. The process is repeated until a suitable criterion for convergence is satisfied, and the resulting expressions were plotted graphically.

Figure (5.6) shows the computed values of the horizontal air velocity and free surface elevation for a parabolic body, $y = x^2$, approaching the water at

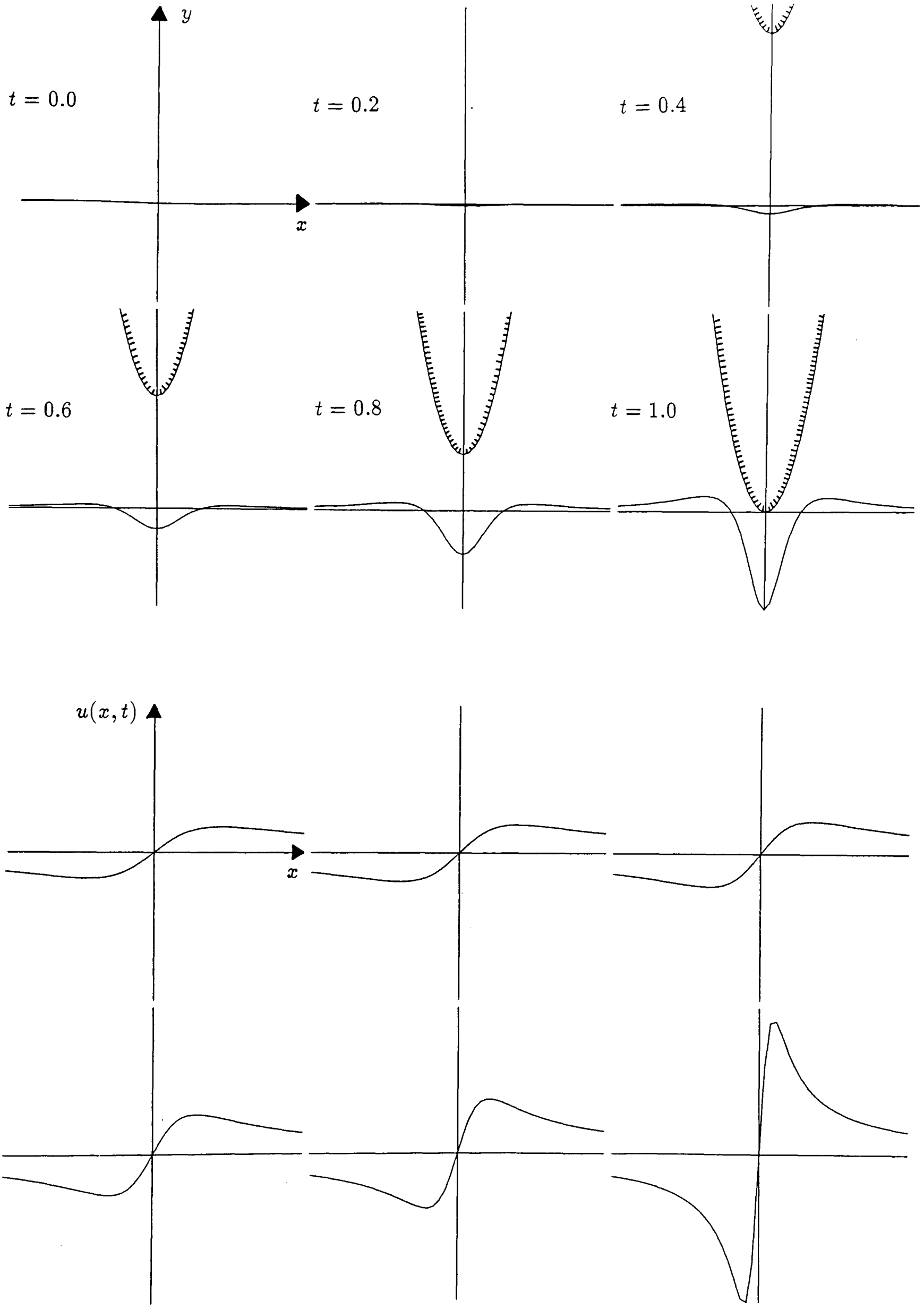

Figure 5.6: Computed free surface elevation and air velocity for a quadratic body $y = x^2$.

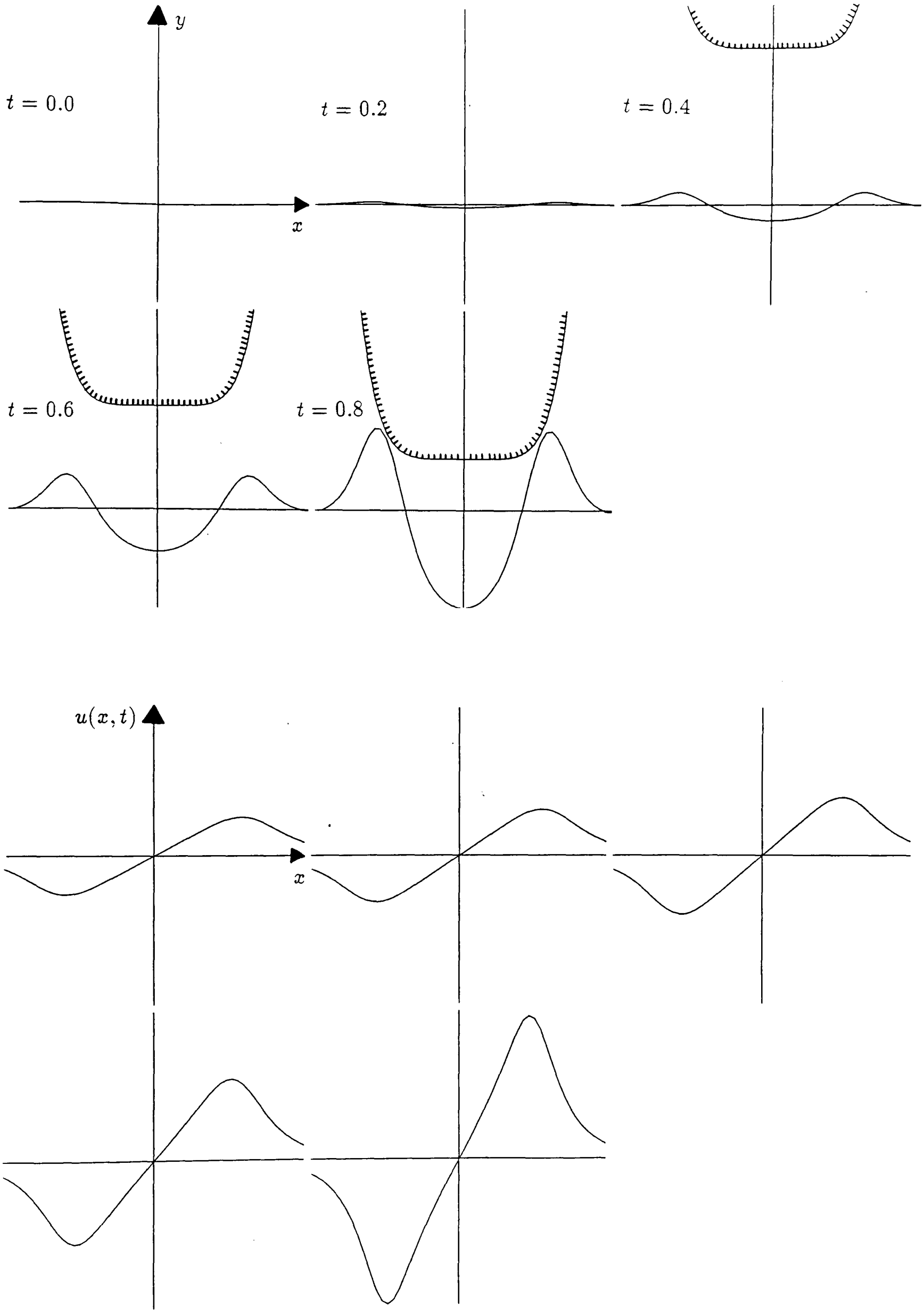

Figure 5.7: Computed free surface elevation and air velocity for a body with profile $y = x^6$.

constant speed at various values of the non-dimensional time t, with the function $a(t)$ defined so that $a(0) = 1$. Figure (5.7) shows the same quantities for a body with profile $y = x^6$. Again, we notice that how a cushion of air forms between the body and the water in each case. These calculations can be continued until the water surface and the body touch for the first time, but as the air-gap narrows the horizontal air velocity, given by equation (5.54), tends to infinity. This unbounded growth is physically unacceptable since when the air speed becomes comparable with the sound speed in the air the neglected effect of air compressibility becomes significant, invalidating the incompressible model.

5.8 Comparison with other Research

The results presented in this chapter predict the formation of an air pocket during the initial stages of impact in the presence of an air layer. Direct experimental observations of the thin air gap and the free surface during the impact are difficult, and the author is unaware of any quantitative experimental data for the air velocity and free surface deformation. However, the pressure histories presented by Driscoll & Lloyd (1982) for flat-bottomed wedges show that the first contact between the body and the water is usually made at the junction of the keel and the sloping face of the wedge, suggesting that even the simplest model, leading to equations (5.52) and (5.53), describes the basic process. However, no satisfactory method for predicting the size of the entrapped air bubble has been obtained.

The present work justifies most of the ad hoc approximations made by Verhagen (1967), Lewison (1970) and Asryan (1972) during the initial stages of the motion when compressibility effects in the air are negligible. However, no justification has been found for their treatment of the compressibility effects, for which all of these authors applied the ideas of classical steady nozzle flow to an intrinsically unsteady problem. Their results must therefore be treated with caution.

After impact has occurred the experimental results of Verhagen (1967) and Lewison (1970) indicate that the trapped air cushion breaks up into bubbles at its edges, which expand into the centre of the pocket at a speed comparable to the sound speed.

Chapter 6

Conclusions and Further Work

In this thesis, we have discussed a number of models for solid-fluid impacts which are relevant to ship slamming.

The two-dimensional problem of the impact of a rigid body onto an inviscid, incompressible fluid is a difficult free boundary problem even in the absence of gravity and surface tension. Despite progress by a number of authors, no exact solutions to the problem are known. However, in the case of bodies which have *small deadrise angle* we have shown that the flow field may be analysed in three distinct regions; an *outer region* in which the leading order problem is equivalent to the impact of a flat plate of unknown width, a high pressure *inner region* in which the free surface turns over and a low pressure *jet* partially attached to the body and emanating from the inner region. In each region the leading order problem has been formulated and the leading order pressure and total force on the body obtained. The size of the plate and the scale of the inner region were determined by matching the inner and outer solutions. The leading order composite pressure distribution on the body was calculated for some simple body shapes, and the results were found to be in agreement with some experimental observations.

The approach was extended to three dimensional bodies with small deadrise angle. Less analytical progress was possible, but a complete leading order solution was obtained for bodies with axial symmetry. A variational formulation of the leading order outer problem was derived, leading to a fixed domain numerical method for calculating solutions and a simple finite element code was written to implement it.

The major discrepancy between the present theory and experimental observations is due to the effect of air caught between the body and the fluid surface. A coupled model for the flow in the air and the fluid was derived and, in an appropriate asymptotic limit, reduced to a coupled pair of integro-differential equations. These equations were investigated in various limits and a numerical solution was obtained which predicted the formation of an air pocket between the body and the fluid to cushion the impact.

6.1 Further Work

6.1.1 Two-Dimensional Bodies

The solution in two dimensions would be improved by calculating higher order terms in the three regions. The most straightforward second order problem is that in the outer region, which is of Weiner-Hopf type, and should be amenable to solution by conventional methods. This would also be the most useful second order solution, since it would then permit the calculation of the second order term in the expansion in the total force.

The effect of surface tension should also be more carefully examined in the neighbourhood of the jet tip and the point where the jet separates from the body. The work of Vanden-Broeck & Keller (1989) suggests that surface tension effects may play the dominant rôle in these regions, even when the Weber number is large.

6.1.2 Three-Dimensional Bodies

There is much scope for further work in obtaining solutions to the leading order outer problem in different three-dimensional geometries, such as when the equivalent plate is a semi-infinite wedge whose angle would be determined by matching. As similar mixed boundary value problems arise in many different contexts, such as electrostatics, it is possible that such problems have already been investigated.

6.1.3 Neglected Effects

The neglect of water compressibility was justified for ship slamming problems in Section 2.12.7. However, compressibility can be more important in other physical situations, for example during the initial stages of the impact of a fluid drop onto a solid surface. Despite the work of a number of authors no satisfactory understanding of impact onto a fully compressible fluid has yet been reached.

The influence of the elastic properties of the body on the solution has not been investigated. The first effort should be to model the body as a thin elastic plate or shell and, assuming that the deformation of the body from its initial shape is small, and calculate the effect of the pressure predicted by the present theory on it. The full problem, in which the fluid flow is coupled back to the deformation of the body, presents substantial additional difficulties and may have to be studied numerically.

6.1.4 Air Cushioning

In the present model for a cushioning air layer between the body and the fluid surface the air is assumed to be incompressible, and as a consequence the model is invalid when the air speed in the narrowing gap approaches the sound speed. Hence, the model cannot properly be used to predict the size of the entrapped air pocket. The models presented by other authors which attempt to represent the effects of compressibility are unsatisfactory, and a compressible version of the theory is required. Unfortunately, the compressibility effects occur just as the free surface effects are most significant and the problem is therefore a difficult one. In addition, as the gap narrows the fragmentation of the free surface into spray may be significant and should be investigated. Once the gap has closed is should be possible to model the resulting oscillations of pressure in the trapped air bubble using the classical theory of shocks in one-dimensional unsteady gas dynamics.

6.1.5 Exit Problems

Mathematically, perhaps the most fascinating open problem is that of the exit of a rigid body from a fluid, which was discussed in Chapter 4. Viscosity, sur-

face tension and the surface roughness of the body may all play a rôle and, to the author's knowledge, no satisfactory theory to describe fluid exit phenomena exists. The literature on the subject is small and the problem deserves further analytical and numerical investigation.

Appendix A

Proof of the Arc Length Property

In this appendix we prove that during the entry of a semi-infinite wedge into an inviscid, incompressible fluid, the arc length measured along the free surface between any two fluid particles remains constant. This property was first demonstrated by Wagner (1932) and subsequently verified by Garabedian (1953) using complex variable techniques. If we consider a wedge with arbitrary deadrise angle, $f(x) = m|x|$, moving with constant speed V, then the problem is given by Laplace's equation (2.3) together with the boundary conditions (2.5), (2.6), (2.7), the initial conditions (2.8), (2.9) and the far-field condition (2.10).

At time t, the arc length, $s(t)$, between two free surface particles at positions $x = x_0(t)$ and $x = x_1(t)$ is

$$s(t) = \int_{x_0(t)}^{x_1(t)} \left(1 + h_x^2\right)^{\frac{1}{2}} \, \mathrm{d}x,$$

and so,

$$\frac{ds}{dt} = \int_{x_0(t)}^{x_1(t)} \frac{h_x h_{xt}}{\left(1 + h_x^2\right)^{\frac{1}{2}}} \, \mathrm{d}x + \left[\left(1 + h_x^2\right)^{\frac{1}{2}} \frac{dx}{dt}\right]_{x_0(t)}^{x_1(t)},$$

where subscripts denote partial derivatives in the usual way. To establish the arc length conservation property, it is sufficient to show that

$$\frac{ds}{dt} = \frac{h_x h_{xt}}{\left(1 + h_x^2\right)^{\frac{1}{2}}} - \frac{d}{dx}\left[\left(1 + h_x^2\right)^{\frac{1}{2}} \frac{\partial \phi}{\partial x}\right] = 0, \tag{A.1}$$

where, in order to measure the arc length between the *same* fluid particles throughout the motion, we have chosen $dx/dt = \partial\phi/\partial x$. In the absence of gravity and surface tension, there is no length scale in the problem, and so we

can reduce the number of independent variables from three to two by introducing similarity variables X and Y, defined by

$$X = \frac{x}{Vt}, \qquad Y = \frac{y}{Vt}.$$

We define a new velocity potential $\Phi(X,Y)$ so that

$$\phi(x,y,t) = V^2 t \Phi(X,Y),$$

and a new free surface elevation $H(X)$ by

$$h(x,t) = VtH(X),$$

so that, in the similarity variables, the surface is given by $Y = H(X)$. The analysis is further simplified by introducing a reduced velocity potential, $\chi(X,Y)$, defined by

$$\chi(X,Y) = \Phi(X,Y) - \frac{1}{2}(X^2 + Y^2),$$

In these new variables, the governing equation in the fluid becomes

$$\frac{\partial^2 \chi}{\partial X^2} + \frac{\partial^2 \chi}{\partial X^2} = -2, \tag{A.2}$$

and the boundary conditions on the free surface $Y = H(X)$ are

$$H'(X)\frac{\partial \chi}{\partial X} - \frac{\partial \chi}{\partial Y} = 0, \tag{A.3}$$

$$\left(\frac{\partial \chi}{\partial X}\right)^2 + \left(\frac{\partial \chi}{\partial X}\right)^2 + 2\chi = 0. \tag{A.4}$$

Eliminating $\partial\chi/\partial Y$ between (A.3) and (A.4) gives a relation for $\partial\chi/\partial X$ on the free surface, namely

$$\left(\frac{\partial \chi}{\partial X}\right)^2 \left(1 + H'(X)^2\right) + 2\chi = 0. \tag{A.5}$$

Written in the similarity variables, equation (A.1) becomes

$$\frac{XH'(X)H''(X)}{(1+H'(X)^2)^{\frac{1}{2}}} = \frac{d}{dX}\left[\left(1 + H'(X)^2\right)^{\frac{1}{2}} \frac{\partial \Phi}{\partial X}\right]. \tag{A.6}$$

The right hand side of equation (A.6) is equal to

$$\frac{XH'(X)H''(X)}{(1+H'(X)^2)^{\frac{1}{2}}} + \left(1 + H'(X)^2\right)^{\frac{1}{2}} + \frac{d}{dX}\left[\frac{\partial \chi}{\partial X}\left(1 + H'(X)^2\right)^{\frac{1}{2}}\right].$$

Using the chain rule and the relation (A.5) gives

$$\frac{d}{dX}\left[\frac{\partial\chi}{\partial X}\left(1+H'(X)^2\right)^{\frac{1}{2}}\right]=\left(\frac{\partial}{\partial X}+H'(X)\frac{\partial}{\partial Y}\right)\left[(-2\chi)^{\frac{1}{2}}\right]=-\left(1+H'(X)^2\right)^{\frac{1}{2}},$$

and hence the right hand side of equation (A.6) is identically equal to the left hand side. Thus, the result is proved. We note that exactly the same analysis can be applied to the three dimensional problem of the impact of a cone to show that the arc length on the free surface, measured along the section cut by any plane though the axis of symmetry, is also preserved.

Appendix B

The Matching Condition to Determine $d(t)$

In two-dimensions the proposed matching condition to determine the plate semi-width, $d(t)$, is

$$H_0(d(t),t) = f(d(t)) - t \quad \text{for all} \quad t \geq 0.$$

We wish to show that this condition can be deduced from the assumption that the volume of fluid in the jet is small compared to a typical volume of fluid on the outer length scale, meaning that to leading order in ϵ, the volume of fluid displaced by the body is equal to the volume of fluid above the original undisturbed waterline $Y = 0$ in the outer solution. We denote the position of the intersection of the body profile with the undisturbed fluid surface by $X = c(t)$. The volume of fluid displaced by the body is, therefore,

$$\int_0^{c(t)} (f(X) - t)\,\mathrm{d}X.$$

The displaced fluid is divided into three parts, the fluid under the body for $c(t) < X < d(t)$ which has volume

$$\int_{c(t)}^{d(t)} (f(X) - t)\,\mathrm{d}X,$$

the fluid between the undisturbed surface and the free surface for $X > d(t)$ which to leading order in ϵ has volume

$$\int_{d(t)}^{\infty} H_0(X,t)\,\mathrm{d}X,$$

and the fluid in the jet, the volume of which we assume is negligible at leading order. Equating these expressions then differentiating with respect to t we obtain

$$d'(t)f(d(t)) - d(t) - td'(t) - d'(t)H_0(d(t),t) + \int_{d(t)}^{\infty} \frac{\partial H_0}{\partial t}(X,t)\,\mathrm{d}X = 0.$$

We now observe that, by global conservation of mass,

$$\int_0^{\infty} \frac{\partial \Phi_0}{\partial Y}(X,0,t)\,\mathrm{d}X = -d(t) + \int_{d(t)}^{\infty} \frac{\partial H_0}{\partial t}(X,t)\,\mathrm{d}X \equiv 0.$$

On substituting this expression for the integral term into the previous relation, we obtain

$$d'(t)\left[f(d(t)) - t - H_0(d(t),t)\right] = 0 \quad \text{for all} \quad t \geq 0,$$

and therefore if $d'(t) \neq 0$ then $d(t)$ satisfies the proposed matching condition

$$H_0(d(t),t) = f(d(t)) - t \quad \text{for all} \quad t \geq 0.$$

A similar analysis can be performed in three dimensions.

Appendix C

Details of the Finite Element Computations

C.1 Two-Dimensions

In two dimensions we use piecewise linear elements with the corresponding element basis functions N_1, N_2 and N_3, which, when written in terms of the local coordinates $\xi, \eta \in [-1, 1]$, have the forms

$$\begin{aligned} N_1(\xi,\eta) &= (1-\xi-\eta), \\ N_2(\xi,\eta) &= \xi, \\ N_3(\xi,\eta) &= \eta. \end{aligned}$$

The simplest mesh is one made up of triangular elements with the nodes spaced in a square array at distances ΔX and ΔY apart in the X and Y-directions respectively, as shown in Figure (C.1). The elements of the local stiffness matrix, K^e, from which the global stiffness matrix is constructed, can easily be found to be

$$K^e = \frac{1}{2}\begin{pmatrix} 2 & -1 & -1 \\ -1 & 1 & 0 \\ -1 & 0 & 1 \end{pmatrix},$$

and the entries in the load vector $\mathbf{F}$ are obtained by straightforward numerical integration.

C.2 Three-Dimensions

In three dimensions we again use piecewise linear basis functions, with the corresponding element basis functions $N_1, N_2, \ldots, N_8$ defined in terms of the local

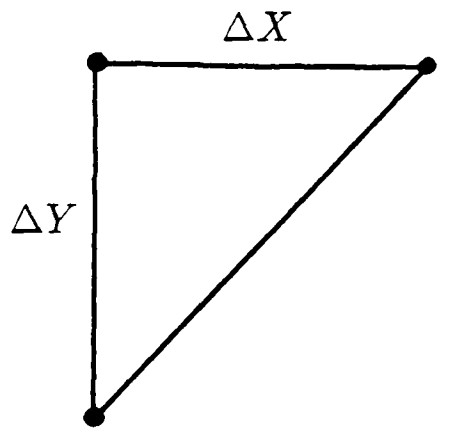

Figure C.1: Two-dimensional triangular finite element.

coordinates $\xi, \eta, \rho \in [-1, 1]$ by

$$\begin{aligned}
N_1(\xi,\eta,\rho) &= \frac{1}{8}(1+\xi)(1+\eta)(1+\rho), \\
N_2(\xi,\eta,\rho) &= \frac{1}{8}(1-\xi)(1+\eta)(1+\rho), \\
N_3(\xi,\eta,\rho) &= \frac{1}{8}(1-\xi)(1-\eta)(1+\rho), \\
N_4(\xi,\eta,\rho) &= \frac{1}{8}(1+\xi)(1-\eta)(1+\rho), \\
N_5(\xi,\eta,\rho) &= \frac{1}{8}(1+\xi)(1+\eta)(1-\rho), \\
N_6(\xi,\eta,\rho) &= \frac{1}{8}(1-\xi)(1+\eta)(1-\rho), \\
N_7(\xi,\eta,\rho) &= \frac{1}{8}(1-\xi)(1-\eta)(1-\rho), \\
N_8(\xi,\eta,\rho) &= \frac{1}{8}(1+\xi)(1-\eta)(1-\rho),
\end{aligned}$$

where

$$\xi = \frac{2(X - X_c)}{\Delta X}, \quad \eta = \frac{2(Y - Y_c)}{\Delta Y}, \quad \rho = \frac{2(Z - Z_c)}{\Delta Z}.$$

(X_c, Y_c, Z_c) denotes the position of the centroid of the element and $\Delta X, \Delta Y$ and ΔZ are the distances between the nodes in the X, Y and Z directions respectively. The nodes are arranged in the three dimensional rectangular array. Figure (C.2) shows a typical finite element which is the rectangular prism formed by the twenty-six nodes adjoining any interior node. Following the notation of Caffrey & Bruch (1979), who solved the problem of seepage through a homogenous dam

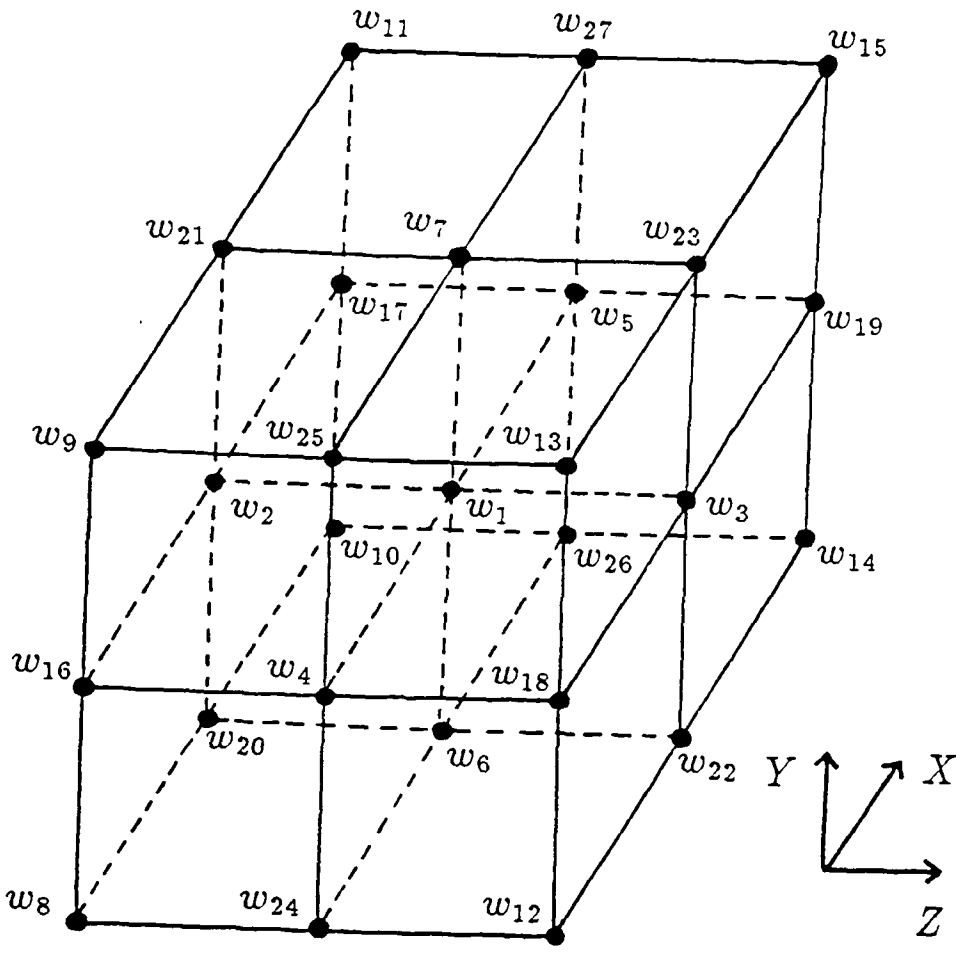

Figure C.2: Three-dimensional finite element.

by a similar variational minimisation, we define $w_{i,j,k} = w_1$, $w_{i-1,j,k} = w_2$ and $w_{i-1,j-1,k-1} = w_3$ etc. and introduce the notation

$$a = \frac{2}{\Delta X}, \quad b = \frac{2}{\Delta Y}, \quad c = \frac{2}{\Delta Z}, \quad \frac{1}{V} = 18abc,$$

with

$$\begin{aligned}
E_1 &= -(a^2 + b^2 + c^2)V, \\
E_2 &= (-4a^2 - 4b^2 + 2c^2)V, \\
E_3 &= (-4a^2 + 2b^2 - 4c^2)V, \\
E_4 &= (2a^2 - 4b^2 - 4c^2)V, \\
E_5 &= (-16a^2 + 8b^2 + 8c^2)V, \\
E_6 &= (8a^2 - 16b^2 + 8c^2)V, \\
E_7 &= (8a^2 + 8b^2 - 16c^2)V, \\
E_8 &= -32E_1.
\end{aligned}$$

The SOR scheme with projection can now be written

$$w_1^{(n+\frac{1}{2})} = -E_8 \left\{ E_1 \left[w_8^{(n)} + w_9^{(n)} + w_{10}^{(n)} + w_{11}^{(n+1)} + w_{12}^{(n)} + w_{13}^{(n+1)} + w_{14}^{(n)} + w_{15}^{(n+1)} \right] \right.$$
$$+ E_2 \left[w_{16}^{(n)} + w_{17}^{(n+1)} + w_{18}^{(n+1)} + w_{19}^{(n)} \right] + E_3 \left[w_{20}^{(n)} + w_{21}^{(n+1)} + w_{22}^{(n)} + w_{23}^{(n+1)} \right]$$
$$+ E_4 \left[w_{24}^{(n)} + w_{25}^{(n+1)} + w_{26}^{(n+1)} + w_{27}^{(n)} \right] + E_5 \left[w_2^{(n)} + w_3^{(n+1)} \right]$$
$$\left. + E_6 \left[w_4^{(n)} + w_5^{(n+1)} \right] + E_7 \left[w_6^{(n)} + w_7^{(n+1)} \right] \right\},$$

$$w_{i,j,k}^{(n+1)} = \max \left[0, w_{i,j,k}^{(n)} + \omega (w_{i,j,k}^{(n+\frac{1}{2})} - w_{i,j,k}^{(n)}) \right],$$

where $w_{i,j,k}^{(n)}$ denotes the value of the solution at (i,j,k)th node at the nth iteration, and constant $\omega \in [0,2]$ is called the *relaxation parameter.*

In both two and three dimensions the computation must of course be carried out on a domain of finite size, and so on the boundary a zero flux condition is imposed in the usual way by eliminating fictitious points outside the domain. The code is written in FORTRAN 77 and implemented on a Digital VAX 11/785. Typically fifty iterations are made to obtain each solution, and this takes roughly five minutes of CPU time.

References

Asryan, N.G. 1972 Solid plate impact on surface of incompressible fluid in the presence of a gas layer between them. *Izv. Akad. Nauk Arm. SSR Mekh.* **25** : 32-49

Belick, Ö., Bishop, R.E.D., Price, W.G. 1987 Influence of bottom and flare slamming on structural responses. R.I.N.A. W5 (1987) : 1-14

Birkhoff, G., Zarantonello, E.H. 1957 *Jets, Wakes and Cavities.* Academic Press, New York.

Bishop, R.E.D., Clarke, J.D., Price, W.G. 1984 Comparison of full scale and predicted responses of two frigates in a severe weather trial. *Trans. R.I.N.A.* **126** : 153-166

Bishop, R.E.D., Price, W.G., Wu, Y. 1986 A general linear hydroelasticity theory of floating structures moving in a seaway. *Phil. Trans. R. Soc. Lond.* A **316** : 375-426

Borg, S.F. 1959 The maximum pressures and total force on straight-sided wedges with small deadrise. *J. Am. Soc. Naval Engrs* **71** (3) : 559-561

Caffrey, J., Bruch Jr., J.C. 1979 Three-dimensional seepage through a homogeneous dam. *Adv. in Water Res.* **2** : 167-176

Chu, W.-H., Abramson, H.N. 1961 Hydrodynamic Theories of Ship Slamming - Review and Extension. *J. Ship Res.* **4** (4) : 9-21

Chuang, S.-L. 1967 Experiments on slamming of wedge shaped bodies. *J. Ship Res.* **11** (3) : 190-198

Crank, J. 1984 *Free and Moving Boundary Problems.* Oxford University Press. 425pp

Cumberbatch, E. 1969 The impact of a water wedge on a wall. *J. Fluid Mech.* **7** : 353-374

Dobrovol'skaya, Z.N. 1969 On some problems of similarity flow of fluid with a free surface. *J. Fluid Mech.* **36** (4) : 805-829

Driscoll, A., Lloyd, A. 1982 *Slamming Experiments - Description of Facilities and Details of Impact Pressure Results.* A.M.T.E.(H) Report R82002

Elliott, C.M., Ockendon, J.R. 1982 *Weak and Variational Methods for Moving Boundary Problems.* Pitman Research Notes in Mathematics **59** 213pp

Eroshin, V.A., Romanenkov, N.I., Serebryakov, I.V., Yakimov, Yu.L. 1980 Hydrodynamic forces at blunt body impact on a compressible fluid surface. *Izv. Akad. Nauk SSSR Mekh. Zhidk. Gaza* **6** : 44-51

Eroshin, V.A., Plyusnin, A.V., Romanenkov, N.I., Sozonenko, Yu.A., Yakimov, Yu.L. 1984 Atmosphere influence on hydrodynamic forces at a plane disc impact on a compressible fluid surface. *Izv. Akad. Nauk SSSR Mekh. Zhidk. Gaza* **3** : 15-20

Fabula, A.G. 1957 Ellipse-fitting approximation of two-dimensional normal sym-

metric impact of rigid bodies on water. *Proc. 5th Mid-Western Conf. Fluid Mech.* 299-315

Ferdinande, M.S. 1966 Theoretical considerations on the penetration of a wedge into the water. *International Shipbuilding Progress* **13** : 102-116

Fraenkel, L.E. 1958 On the vertical water entry of a slender cone. A.R.D.E. Fort Halstead Memo.(B) 22/58

Garabedian, P.R. 1953 Oblique water entry of a wedge. *Comm. Pure Appl. Math.* **6** : 157-165

Garabedian, P.R. 1965 Asymptotic description of a free boundary at the point of separation. *Proc. Symp. Appl. Math.* **17** : 111-117

Gonor, A.L. 1986 Thin wedge penetration into liquid. *Dokl. Akad. Nauk SSSR* **290** : 1068-1072

Graham, R. 1988 Slamming experiments with a radio-controlled SWATH model. *Proc. Int. Conf. on SWATH Ships and Advanced Multi-Hulled Vessels.* London, November 1988. Paper 9

Greenhow, M. 1987 Wedge entry into initially calm water. *Appl. Ocean Res.* **9** (4) : 214-223

Greenhow, M., Yanbao, Li 1987 Added masses for circular cylinders near or penetrating fluid boundaries - review, extension and application to water-entry, -exit and slamming. *Ocean Engng.* **14** (4) : 325-348

Greenhow, M. 1988 Water-entry and -exit of a horizontal circular cylinder. *Appl. Ocean Res.* **10** (4) : 191-199

Hagiwara, K., Yuhara, T. 1974a Fundamental Study of Wave Impact Load on a Ship Bow. *J. Soc. Nav. Arch. Japan* **135** : 181-189

Hagiwara, K., Yuhara, T. 1974b Fundamental Study of Wave Impact Load on a Ship Bow. *J. Soc. Nav. Arch. Japan* **137**

Hauptman, A., Miloh, T. 1986 On the exact solution of the linearized lifting surface problem of an elliptic wing. *Q. Jl Mech. appl. Math.* **39** (1) : 41-66

Hobson, E.W. 1965 *The Theory of Spherical and Ellipsoidal Harmonics.* Chelsea, New York.

Hughes, O.F. 1972 Solution of the wedge entry problem by numerical conformal mapping. *J. Fluid Mech.* **56** (1) : 173-192

Johnstone E.A., Mackie, A.G. 1973 The use of Lagrangian coordinates in the water entry and related problems. *Proc. Camb. Phil. Soc.* **74** : 529-538

Keller, J.B., Geer, J. 1973 Flows of thin streams with free boundaries. *J. Fluid Mech.* **59** (3) : 417-432

Kreps, R.L. 1943 Experimental investigation of impact in landing. *N.A.C.A. T.M. 1046*

Korobkin, A.A. 1982 Formulation of penetration problem as a variational inequality. *Din. Sploshnoi Sredy* **58** : 73-79

Korobkin, A.A. 1983 Penetration of elastic shells in ideal liquid. *Din. Sploshnoi Sredy* **63** : 84-93

Korobkin, A.A. 1984 Penetration of a blunt body in weakly compressible fluid.

Zh. Prikl. Mekh. Tekh. Fiz. **5** : 104-110

Korobkin, A.A. 1985 Initial asymptotics of solution of three-dimensional problem on a blunt body penetration in ideal liquid. *Dokl. Akad. Nauk SSSR* **283** : 838-842

Korobkin, A.A., Pukhnachov, V.V. 1985 Initial asymptotics in contact hydrodynamics problems. Int. Conf. Numer. Ship Hydrodyn., 4th, ed. J.H. McCarthy. Bethesda, Md: David W. Taylor Nav. Ship Res. Dev. Cent. : 138-151

Korobkin, A.A., Pukhnachov, V.V. 1988 Initial stage of water impact. *Ann. Rev. Fluid Mech.* **20** : 159-185

Lesser, M.B. 1981 Analytic solutions of liquid-drop impact problems. *Proc. R. Soc. Lond.* A **377** : 289-308

Lesser, M.B., Field, J.E. 1983 The impact of compressible fluids. *Ann. Rev. Fluid Mech.* **15** : 97-122

Lewison, G.R.G., Maclean, W.M. 1968 On the cushioning of water impact by entrapped air. *J. Ship Res.* **12** : 116-130

Lewison, G.R.G. 1970 On the Reduction of Slamming Pressures. *Trans. R.I.N.A.* **112** : 285-306

Mackie, A.G. 1962 A linearized theory of the water entry problem. *Q. Jl Mech. appl. Math.* **15** (2) : 137-151

Mayo, W.L. 1943 Analysis and modification of theory for impact of seaplanes on water. *N.A.C.A. T.M. 1008*

Milne-Thomson, L.M. 1968 *Theoretical Hydrodynamics*, 5th ed. Macmillan, London. 743pp

Moghisi, M., Squire, P.T. 1981 An experimental investigation of the initial force of impact on a sphere striking a liquid surface. *J. Fluid Mech.* **108** : 133-146

Moran, J.P. 1961 The Vertical Water-Exit and -Entry of Slender Symmetric Bodies. *J. Aero. Sci.* **28** (10) : 803-812

Moran, J.P. 1965 On the hydrodynamic theory of water-exit and -entry. *TAR-TR 6501*, Therm Advanced Research Inc., Ithaca, New York.

Morton, K.W. 1986a *Numerical Solution of Partial Differential Equations.* Oxford University Computing Laboratory Lecture Notes, Michaelmas Term 1986. 151pp

Morton, K.W. 1986b *Finite Element Methods.* Oxford University Computing Laboratory Lecture Notes, Michaelmas Term 1986. 132pp

Nethercote, W.C.E., Mackay, M., Menon, B. 1986 *Some Warship Slamming Investigations.* D.R.E.A. Technical Memorandum 86/206

Ockendon, J.R. 1980 Linear and nonlinear stability of a class of moving boundary problems. *Free Boundary Problems* (2 vols.), ed. E. Magenes. Proceedings Pavia Bimestre (1979), 1st. Naz. Alta Matem. Francesco Severi, Rome. Vol 2 : 443-478.

Ockendon, J.R., Tayler, A.B. 1985 *Partial Differential Equations.* Oxford University Mathematical Institute Lecture Notes, May 1985.

Pabst , W. 1931 Landing impact of seaplanes. *N.A.C.A. T.M. 624*

Payne, P.R. 1981 The vertical impact of a wedge on a fluid. *Ocean Engng* **8** (4) : 421-436

Pierson, J.D. 1950 The penetration of a fluid surface by a wedge. Stevens Inst. Tech. Exp. Towing Tank Report 381

Pierson, J.D. 1951 On the virtual mass of water associated with an immersing wedge. *J. Aero. Sci.* June 1951 : 430-431

Pukhnachov, V.V. 1979 Linear approximation in the problem on a blunt body entry in water. *Din. Sploshnoi Sredy* **38** : 143-150

Pukhnachov, V.V., Korobkin, A.A. 1981 Initial asymptotics in problem of blunt body entrance into liquid. Int. Conf. Numer. Ship Hydrodyn, 3rd, ed. J.-G. Dern, H.J. Hassling. Paris: Bassin d'Essais des Carès : 579-591.

Schmieden, C. 1953 Der Aufschlang von Rotations-körpen auf eine Wasseroberfläche. *Z.A.M.M.* **33** (4) : 147-151

Shiffman, M., Spencer, D.C. 1951 The Force of Impact on a Cone Striking a Water Surface (Vertical Entry). *Comm. Pure Appl. Math.* **4** : 379-417

Sneddon, I.N. 1966 *Mixed Boundary Value Problems in Potential Theory.* North-Holland, Amsterdam. 283pp

Tayler, A.B. 1972 Singularities at flow separation points. *Q. Jl Mech. appl. Math.* **26** (2) : 153-172

Van Dyke, M. 1975 *Perturbation Methods in Fluid Mechanics*, Annotated Edition. Parabolic. 271pp.

Vanden-Broeck, J.-M., Keller, J.B. 1982 Jets rising and falling under gravity. *J. Fluid Mech.* **124** : 335-345

Vanden-Broeck, J.-M., Keller, J.B. 1989 Pouring flows with separation. *Phys. Fluids* A **1** (1) : 156-159

Verhagen, J.H.G. 1967 The Impact of a Flat Plate on a Water Surface. *J. Ship Res.* **11** : 211-223

Von Kármán, T. 1929 The impact on seaplane floats during landing. *N.A.C.A. T.N. No. 321*

Wagner, H. 1931 Landing of seaplanes. *N.A.C.A. T.N. No. 622*

Wagner, H. 1932 Uber Stoß- und Gleitvorgänge an der Oberfläche von Flüssigkeiten. *Z.A.M.M.* **12** (4) : 193-215 (Translated into English as Phenomena associated with Impacts and Sliding on liquid surfaces. N.A.C.A. Translation 1366)

Watanabe, I. 1986 Analytical Expression of Hydrodynamic Impact Pressure By Matched Asymptotic Expansion Technique. *Trans. West Japan Soc. Naval Arch.* **71** : 77-85

Whittaker, E.T., Watson, G.N. 1962 *A Course in Modern Analysis*, 4th ed. Cambridge University Press.

Yim, B. 1985 Numerical solution of two-dimensional wedge slamming with a nonlinear free surface condition. Int. Conf. Numer. Ship Hydrodyn, 4th, ed. J.H. McCarthy. Bethesda, Md: David W. Taylor Nav. Ship Res. Dev. Cent. : 107-115